Hassan, Kazi Iqbal (2015) “MEMORY STRESS”: Physical and mathematical modelling of the influence of water-working on sediment entrainment and transport. PhD thesis.

http://theses.gla.ac.uk/6707/

Copyright and moral rights for this thesis are retained by the author

A copy can be downloaded for personal non-commercial research or study, without prior permission or charge

This thesis cannot be reproduced or quoted extensively from without first obtaining permission in writing from the Author

The content must not be changed in any way or sold commercially in any format or medium without the formal permission of the Author

When referring to this work, full bibliographic details including the author, title, awarding institution and date of the thesis must be given.

Glasgow Theses Service
http://theses.gla.ac.uk/
theses@gla.ac.uk

“MEMORY STRESS”:
Physical and mathematical modelling of the influence of water-working on sediment entrainment and transport

By

Kazi Iqbal Hassan

MSc BEng

Submitted in fulfilment of the requirements for the Degree of Doctor of Philosophy

SCHOOL OF ENGINEERING

UNIVERSITY OF GLASGOW

April, 2015

Abstract

Recent research has indicated that variability of antecedent flows is a fundamental control on the entrainment and transport of sediment in river systems. Specifically, the low flows between successive floods appear to have a far greater influence on the stability of a river bed than previously assumed. Increased durations of low flows increase sand-gravel bed stability so as to delay entrainment and significantly reduce transport. Although a degree of quantification of "memory stress" effects has been attempted by previous researchers, their applied methodology precludes development of appropriate mathematical relationships implicit to correcting existing sediment transport equations. The overall aim of this thesis is therefore to address this deficiency via robust physical and mathematical modelling.

In total, 84 flume experiments were carried out in a flume. Two poorly sorted ($\sigma_g \geq 1.6$) sand-gravel mixtures of unimodal and bimodal distribution were compared and contrasted for sensitivity of modality to memory effects upon bedload and entrainment threshold. Five memory timescales (10, 30, 60, 120 and 240 minutes) were tested and contrasted with baseline data obtained for runs performed without any memory. Experiments employed a stepped discharge hydrograph covering sub-threshold to fully mobile conditions. A reference transport based approach was employed to determine entrainment threshold, and to develop mathematical descriptors of memory effects.

Results show that increasing memory timescales up to 240 minutes increases entrainment thresholds (τ^*_{c50}) by up to 49% whilst subsequent transport decreases by up to 97%. The memory effect prevails non-linearly for the range of low flows of non-dimensional transport (q^*) between 10^{-6} *to* 10^{-1}. Using these flume data, novel mathematical functions for bedload are developed to account for the influence of memory timescales. Here, memory is described via rising exponents of the function to quantify degree of non-linearity of transport to shear stress, and changes in the structure of the bed due to memory are represented within a lumped coefficient. Trends in the suite of exponents and coefficients indicate that changes in bed structure are of greater importance than the shift in non-linearity of bedload. Hence, the first framework for correcting existing graded sediment formulae for memory stress has been effectively developed using a scaling of the granular scale roughness parameter, A_n. Predicted results are calibrated and validated against available memory stress datasets from both field and laboratory based studies. Results show that without memory correction, over 80% of estimates fail to predict measured bedload effectively; once A_n based correction is applied, 100% of data are predicted effectively.

Key words: Memory stress, entrainment threshold, graded sediment, fractional transports

Table of Contents

List of Tables

List of Figures

List of Accompanying Material

Appendix A: Unimodal bed experimental programme in baseline and memory stress

Appendix B: Bimodal bed experimental programme in baseline and memory stress

Appendix C: Prediction of bed load for memory affected transports: calculation sheets

Appendix D: Experimental data on bedload transport from Unimodal and bimodal bed experiments in different memory time scales

Acknowledgement

I would like to express my special thanks to my supervisor, Dr. Heather Haynes. You have been truly inspirational. Your guidance and mentoring were exceptional and have allowed me to grow as a research scientist. Through numerous meetings, discussions and emails with you I have been able to learn in depth of the complexities of sediment dynamics. Dr. Haynes you ensured all technical support I needed, yet, at the same time you never forgot to allow me time to support my family. Your careful review of my experimental set-up, my results and my draft thesis was exceptional. From your methods and style I have learnt that there is a logical chronology of writing a technical report and how to tackle the complexities it brings to light. Your vision is very wide and far reaching for your researchers, and at the same time very supportive; you arranged additional collaboration opportunities for me, and allowed me to visit other centres of excellence at Heriot Watt University (Professor Gareth Pender), the University of Urbana-Champaign, Illinois (Professor Gary Parker) and the University of Mississippi (Professor Weiming Wu, now at Clarkson University). Your support at the final stage of my thesis submission was really critical towards completion of my research; thank you.

I am greatly indebted to Professor Gareth Pender who permitted me visiting researcher access to flumes, technical support, facilities and staff at Heriot-Watt during my main experimental programme. In your very busy schedules, you offered me fortnightly progress meeting schedules, uninterrupted and unchanged for over a year; those routine progress meetings were instrumental and forceful towards completion of my experiments. I express my deepest gratitude towards your exceptional caring support to your researchers.

Professor William Sloan your prompt review during my yearly progression reporting gave me early direction to my research, particularly selecting methodology and measurement technique for my experiments. I thank you very much for your support. Professor Chris Pears, I am very thankful for the meeting with you; you wanted to make sure my research progresses smoothly.

I had the opportunity to work in two hydraulic laboratories; in the University of Glasgow and in Heriot-Watt University. Stuart, Bobby, Tim and Ian you have always been very supportive. Stuart I want to thank you so much for assistance

and advice setting up the experimental apparatus for me, so many times. Tim and Bobby I will not forget your watchful and routine H&S checks during my lone working hours in the laboratory. In Heriot-Watt - Alastair, Tom, Dave, Graham and James – I want to thank you all for your continued support. You made me feel very welcome, making Heriot-Watt my home. My sincere thanks to you all for your support.

Special thanks to Professor Parker and Professor Wu for their support in learning computational techniques for the fractional transport approaches presented in this thesis. Professor Parker your patience amazed me; you showed me step-by-step the computational technique of transport in heterogeneous sediment; I would probably never have learnt to such depth this knowledge had I not visited your hydraulic centre. Professor Wu you were very prompt to offer me unparalleled guidance and unwavering support to help me build my own algorithm and programme of calculating fractional transport in your formula. Your follow-up emails, discussions and your words of support while visiting my experimental set-up at Heriot Watt was inspirational.

I thank Dr Ockelford for your patience in addressing fully my queries; you were very caring and prompt to answer my many emails, clarifying my doubt and helping me set up my experiments. Dr Vignaga your daily help and hands on teaching of experimental methods was the pathway for me to set-up my flume correctly; thank you so much for supplying me many of the technical documents and manuals related to flume experiments. I want to thank the young researchers with whom I shared the work space in the University of Glasgow; Stephanie, Siding, Melani, Sarah, Ben, Marni and Gellian - thank you to all of you for your support in our many different daily routines.

I would like to express my deep gratitude to The Natural Environment Research Council (NERC) for funding this research.

Finally special thanks to my family, my wife and my two sons; you were always there to support me this novel cause.

Kazi Iqbal Hassan
April 2015

Author's Declaration

I, Kazi Iqbal Hassan, declare that this thesis, the primary dataset presented and all other work are my own and have been generated by me as the result of my own original research.

I confirm that:

This work was done wholly or mainly while in candidature for a research degree at this University;

Where any part of this thesis has previously been submitted for a degree or any other qualification at this University or any other institution, this has been clearly stated;

Where I have consulted the published work of others, this is always clearly attributed;

Where I have quoted from the work of others, the source is always given. With the exception of such quotations, this thesis is entirely my own work;

I have acknowledged all main sources of help;

Where the thesis is based on work done by myself jointly with others, I have made clear exactly what was done by others and what I have contributed myself;

Either none of this work has been published before submission, or parts of this work have been published.

Kazi Iqbal Hassan
April 2015

Definitions/Abbreviations

Symbol/ abbreviation	Description	Dimension
A, A_1, A_2	Area	L^2
A_n	Roughness parameter related to bed-material size composition	-
ASCE	American Society of Civil Engineers	-
*A**	Coefficient in Einstein bedload function	-
a	Mobility parameter in Shvidchenko bedload transport relation	-
a_1	Coefficient of proportionality; depends on grain shape and packing	-
a_2	Coefficient of proportionality; depends on fluid flow, pressure and viscous force	-
b	Exponent in regression relations	-
*B**	Coefficient in Einstein bedload function	-
BM	Bimodal sediment mixture	-
BM_SH_10	Bimodal mixture experiment in memory condition for 10 minutes memory duration (other memory experiment notations for 30, 60, 120 and 240 minute follow same format for notation)	-
C	Constant	-
c	Coefficient term in regression relations	-
C_D	Drag force coefficient	-
C_L	Lift force coefficient	-
c_1	Coefficient to account for particle shape	-
c_2	Coefficient to account for geometry and packing of the grains	-
D, D_i, D_j, D_1, D_2, D_m	Particle's diameter; and same for size class i, j, 1, 2, and mean (arithmetic) respectively	L
Dr	A reference size class	L
D_{16}	Grain size, by weight 16% finer than this size in a distribution	L
D_{35}	Grain size, by weight 35% finer than this size in a distribution	L
D_{50}	Median grain size, by weight 50% finer than this size in a distribution	L
D_{60}	Grain size, by weight 60% finer than this size in a distribution	L
D_{84}	Grain size, by weight 84% finer than this size in a distribution	L
D_c, D_f	Particle size of the coarse and fine modes in bimodal mixture respectively	L
D^*	Dimensionless particle number	-
e	Dimensionless in Ackers and White's reference transport number, which varies according to grain size	
EC	European Commission	-
EF	Efficiency Factor: ratio of predicted and	-

	observed bedload	
EPSRC	The Engineering and Physical Sciences Research Council	-
FRMRC 1	Flood-Risk Management Research Consortium, phase 1	-
FRMRC 2	Flood-Risk Management Research Consortium, phase 2	-
F_D	Fluid drag force	$M\,LT^{-2}$
F_G	Gravity force	$M\,LT^{-2}$
f_i	Fractional proportion of the i*th* subrange in mixture	-
f_j	Fractional proportion of the j*th* subrange in mixture	-
f_{a1}, f_{a2}	Fractional proportion for a particular fraction from area 1 and 2	-
f_{ai}	Fractional proportion for size class i	-
g	Acceleration due to gravity	LT^{-2}
G_{gr}	Ackers and White reference transport parameter	-
P_{ei} *and* $P_{hi,}$	Exposure and hiding probability for i*th* grain class	-
F_i	Fractional proportion for i*th* size class in bulk mix	-
Fr	Dimensionless Froude number for representing flow regime for sub-critical, critical and super-critical flow	-
LWEC	Living with Environmental Change	-
m	Exponent in hiding function	-
MPM	Meyer-Peter and Muller	-
NERC	The Natural Environment Research Council	-
N	Total number of grain classes in Wu's hiding function	-
n, n_b, n_w	Manning's roughness coefficient, same for bed and wall	$L^{-1/3}T$
n'	Manning's roughness coefficient for grain's skin	$L^{-1/3}T$
n''	Manning's roughness coefficient for bed form	$L^{-1/3}T$
P, P_b, P_w	Hydraulic radius; same of bed and wall	L
p_i	Fractional proportion for i*th* size class in bedload samples	-
P_{ei}	Exposure probability of grain class i	-
P_{hi}	Hiding probability of grain class i	-
p_m	Fractional proportion of the two modes in bimodal mixture	-
P(τ)	Probability density function of bed shear stress (τ)	-
Q	Rate of water flow/discharge	L^3T^{-1}
q_{ci}, q_{cr}	Unit discharge for size class I and reference size class r	L^2T^{-1}
q_b	Volumetric bedload per unit width	L^2T^{-1}
q_i^*	Non-dimensional bedload transports per unit width for i*th* size class, also called Einstein bedload parameter	-

q^*	Non-dimensional bedload transports per unit width, also called Einstein bedload parameter	-
R, R_b	Hydraulic radius; same for bed	L
R_{e^*}, R_{e^*c}	Dimensionless boundary or Shear Reynolds number	-
R^2	Coefficient of determination	-
R_{ep}	Dimensionless Particle Reynolds number	-
R_{ep50}	Dimensionless Particle Reynolds number for median size (D_{50}) class of sediment	-
RP	Return Period, for use of extreme flood event	-
S	Flume bed slope	-
s	Submerged specific gravity of sediment	-
SH	Stress history; used as a prefix to memory time scales	-
T	Memory time	T
T_b	*D*imensionless bedload transport function	-
t	Sediment counting time period in Yalin's visual approach	T
t_1, t_2	Sediment counting time period in visual approach for area 1 and area 2 respectively	T
u	Flow velocity	LT^{-1}
UK	United Kingdom	-
UKCIP	United Kingdom Climate Impacts Programme	-
UM	Unimodal sediment mixture	-
UM_SH_10	Unimodal mixture experiment in memory condition for 10 minutes memory duration (other memory experiment notations for 30, 60, 120 and 240 minutes follow same format for notation)	-
u_* , u_c^*	Shear velocity and critical shear velocity respectively	LT^{-1}
*W**	Dimensionless bedload transport	-
W_i^*	Dimensionless bedload transport for *i*th grain size subrange	-
X	Used to represent return period for extreme flood event; e.g., 2 and 100 represents 1 in 2 year and 1 in 100 year return period flood event respectively	-
x	Number of particles in motion in general	-
x_1, x_2	Number of particles in motion in general from area 1 and 2 respectively	-
x_i	Number of particles in motion for i*th* size class	-
z	Water depth above bed	L
z_0	Roughness height (height above bed where velocity becomes zero)	L
α	Particle's pivot angle	Degree
γ	Unit weight of water	$ML^{-2}T^{-2}$
γ_s	Unit weight of sediment	$ML^{-2}T^{-2}$
σ_g	Sorting coefficient of sediment mixture	-
θ	Bed slope angle	Degree
μ	Dynamic viscosity of fluid	$ML^{-1}T^{-1}$

ν	Kinematic viscosity of fluid	L^2T^{-1}
ε_i	Hiding function ($\varepsilon_i = \tau^*_{ri} / \tau^*_{50}$)	-
κ	von Karman's constant, dimensionless	-
ρ	Density of water	ML^{-3}
ρ_s	Density of sediment	ML^{-3}
τ	Bed shear stress	$ML^{-1}T^{-2}$
τ_{c50}	Bed shear stress at critical condition of sediment motion for median (D_{50}) size class	$ML^{-1}T^{-2}$
τ_c , τ_{ci}	Bed shear stress at critical condition of sediment motion; same at critical condition for i*th* size class	$ML^{-1}T^{-2}$
τ_{ri}, τ_{r50}	Reference bed shear stress for i*th* size class and median size class (D_{50}) respectively	$ML^{-1}T^{-2}$
τ_W	Instantaneous bed shear stress	$ML^{-1}T^{-2}$
τ_{WC}	Instantaneous bed shear stress required to put the particle in motion (equal to the resisting force)	$ML^{-1}T^{-2}$
τ^*	Dimensionless bed shear stress, also known as Shields parameter	-
τ^*_c	Dimensionless bed shear stress at threshold motion of sediment	-
τ^*_{c50}	Dimensionless bed shear stress at threshold motion of sediment for median grain size (D_{50})	-
τ^*_{ci}	Dimensionless bed shear stress at threshold motion of sediment for i*th* grain size subrange	-
τ^*_i	Dimensionless bed shear stress for i*th* grain size subrange	-
τ^*_{cm}	Dimensionless bed shear stress at threshold motion of sediment for mean (arithmetic) size class	-
τ^*_{ri}	Dimensionless reference bed shear stress for i*th* grain size subrange	-
τ^*_{r50}	Dimensionless reference bed shear stress for median size class (D_{50})	-
Length = L; Mass = M; Time = T; Force = F; Angle=Degree		

Chapter 1: Introduction of the Research

1.1 Introduction

This research thesis focuses upon graded sediment dynamics in unidirectional flow. Although the threshold motion of sediment (from stable to transported, and vice versa) is the most important parameter for understanding of the discipline, both its definition and method of determination remain a major challenge for the scientific community. This is due to complex process interactions between flow and the granular boundary, whose poor description and incomplete understanding has led to notable scatter and uncertainty in research datasets specific to entrainment threshold and bedload prediction. In seeking to address these problems, there is an emerging science dedicated to the temporal dependency of flow-sediment process interactions and their controls on entrainment and transport. This purports that, even if subjected to flow lower than the threshold condition, a non-cohesive sediment bed can build "memory stress" in a manner which stabilises the bed and increases its resistance to entrainment. It is to the advance of knowledge regarding the "memory stress" concept that this thesis is dedicated. As such, physical (flume) and mathematically modelling of graded sediment, and associated formula, have been conducted to fulfil the research objectives (Section 1.3).

1.2 General scientific rationale

Sediment entrainment, measurement, prediction and management remain a significant challenge for scientists, engineers and practitioners tasked with river management. Despite over a century of research into these sediment processes (e.g., Buffington and Montgomery, 1997 review), high uncertainties within the empirical equations mean that practitioners invest minimal resources into modelling or managing sediment-related and geomorphological problems in UK catchments. The recent events of sediment-related flooding (e.g., Cockermouth, 2005, 2009; Somerset Levels, 2013-14) have, in particular, brought this issue to light with questions being raised over practitioner capabilities specific to e.g., stable channel design, reservoir sedimentation, design/maintenance of river training works, flow regulating structures; flood risk and defence asset design, ecological balance. Assessment of sediment and morphodynamic related river

risks are noted explicitly within the EU Floods Directive and EU Water Framework Directive drivers of current UK policies (e.g., WEWS, 2003, 2013, 2014; Flood Risk Management (Scotland) Act 2009). In turn, there is a strengthening argument that sediment process research must be urgently improved in a manner appropriate to day-to-day water resource and flood risk assessment modelling tools; this is given 'high priority' research status most recently in the UK's Flood and Coastal Erosion Risk Management (FCERM) (Defra and Environment Agency, 2015). Hence, there is increased appetite and momentum for fundamental research to reduce uncertainty in sediment transport formulae as essential for improved confidence in practitioner-based numerical modelling tools.

Despite a plethora of sediment predicting formulae (e.g., Einstein, 1950; Meyer-Peter-Muller, 1948; Bagnold, 1956; Yang, 1984; Parker, 1990a; Wilcock and Crowe, 2003), the universality in their application has made slow progress. Arguably, uncertainty in the entrainment threshold of sediment is considered the main challenge and 80 years of such research formed the focus of detailed review by Buffington and Montgomery (1997). Whilst this review raised a number of reasons for scatter in entrainment threshold data sets, methodological bias in the definition and measurement of entrainment was a key factor. Even when equivalent data sets were compared (e.g., non-dimensional bedload and shear stress parameter plots) data showed much more sensitivity and complexity at low flows close to the entrainment threshold, indicating additional sensitivity of entrainment to spatio-temporal dynamics in bed structure and turbulent fluctuations. Whilst these processes have received a modicum of attention in the literature (Brown and Willetts, 1997; Papanicolaou et al., 2002; Marion et al., 2003; Zanke, 2003; Aberle and Nikora, 2006; Rollinson, 2006; Cooper and Tait, 2008; Cooper and Frostick, 2009), the specific issue of the time-dependency of process controls has been all but overlooked.

Thus, it is only in the last decade that the temporal controls on sediment entrainment have been researched explicitly. From this small, but growing, body of scientific publications there is emerging evidence of "memory stress" developing in sediment beds subjected to prolonged exposure to sub-threshold flow. Studies infer that it is the time-dependency of processes specific to grain

arrangement and structures which act to control and enhance bed stability so as to alter the threshold of sediment entrainment (e.g., Paphitis and Collins, 2005; Monteith and Pender, 2005; Haynes and Pender, 2007; Ockelford, 2011). To date, there are only these few laboratory data sets specific to "memory stress", performed using planar bed flume systems of uniform or graded sand-gravel beds. These individual research datasets are limited and comparison between them is precluded due to distinction in the methodological approaches applied. In addition, none of these studies has sought mathematical description of memory stress effects on entrainment in a manner appropriate to the correction of sediment entrainment/transport formulae used in practitioner-based models. Thus, the present research has been designed to overcome these deficiencies in a manner advancing memory stress science, reducing uncertainties in sediment transport modelling and providing outputs appropriate to applied river management practices.

1.3 Research objectives

This comprehensive and systematic research is designed to combine flume based analysis with mathematical descriptors as appropriate to quantifying the memory stress of water-worked sand-gravel beds. The research intends to develop a robust methodological framework and dataset, as specific to the correction of sediment entrainment and transport formulae for memory stress. The overall intention of this work is to reduce uncertainty in sediment transport modelling, as urgently required for enhanced practitioner confidence and increased adoption of sediment/morphodynamic simulations in flood risk, infrastructure design and catchment management assessments.

Specific objectives that this research has been designed for include:

- To develop a robust flume-based methodology for memory stress analysis as appropriate to physical and mathematical description and interpretation.

- To undertake flume-based experiments to quantify the effect of memory stress on sediment entrainment threshold. Focus is placed on two

variables: (i) the duration of memory stress applied and; (ii) the grade of sediment used.

- To analyse flume data for the effect of memory stress on bedload, including fractional analysis. This is strategic to both mathematical formulae development and providing insight into bed process controls on entrainment.

- To develop novel mathematical relations (e.g., bedload vs. shear stress) capable of accounting for different temporal scales of memory stress.

- To determine and test a correction factor for memory stress to existing graded sediment formulae.

1.4 Structure of the thesis

Whilst the Table of Contents provides the first impression of the structure of this thesis, a précis of each Chapter is summarised below.

Chapter 1: Introduction of the research
This provides the rationale of the present research, in terms of an overview of scientific context and background. Focus is placed upon the policy and research led drivers of the research, an introduction to the current state of knowledge on graded sediment transport (and associated uncertainties) and the emerging science of memory stress on a grain's entrainment and transport. The objectives of the research are clearly outlined, as strategic to advancing sediment entrainment/transport research and modelling.

Chapter 2: Critical literature review
A detailed critical review of historical research results on incipient motion of graded beds is provided. Given the wealth of material pertaining to this topic, key papers have been selected for inclusion as directly aligned with the aim of the thesis. The general principles, methodologies and equations of the initial motion of graded sediment are comprehensively documented and critiqued throughout. Identified research gaps, uncertainties and the overall importance of addressing these are noted.

Chapter 3: Physical Modelling: experimental set-up and methodology

Details of the flume set-up and applied methodology for unimodal and bimodal experiments are documented. Methods have been designed with due reference to the literature and clearly state how this thesis overcomes the deficiencies/limitations of previous research into memory stress.

Chapter 4: Physical Modelling Results: Unimodal sediment

All experimental results on unimodal sediment mixtures are presented, compared/contrasted and discussed with previous memory stress research. Quantitative evidence on memory effects are provided in terms of: (i) entrainment threshold; ii) fractional and total transport; and iii) novel mathematical relationships.

Chapter 5: Physical Modelling Results: Bimodal sediment

This Chapter adopts an almost identical format to Chapter 4, but with focus upon beds of bimodal grain size distribution. Comparison of data to the unimodal beds of Chapter 4 is implicit.

Chapter 6: Mathematical prediction of bedload transport: a framework for memory stress correction

This Chapter presents development of a correction factor approach to including memory stress effects within existing graded sediment formulae. This novel approach has been validated against nearly 500 data points, including both field and laboratory data sets from previous research. Predicted results have also been compared against uncorrected (i.e., non-memoried) graded sediment transport formulae for the same studies.

Chapter 7: Conclusion and recommendation

A summary of the key results, importance of application and recommendations for future research direction are provided.

Chapter 2: Critical Literature Review

2.1 Introduction

The entrainment threshold of particles from the river bed is the most fundamental parameter in the prediction, measurement and management of sediment transport in rivers. However, it is also a parameter which presents significant difficulty in measurement and is highly sensitive to complex interactions and influences of external controls (fluid, sediment and biological variables). Despite a century of research specific to prediction of entrainment threshold of both uniform and graded beds, there remains a high degree of uncertainty into both the methodological measurement and the mathematical prediction of the onset of motion. Given the vast body of literature pertaining to previous research specific to entrainment determination, the following sections specifically focus on the drivers, rationale and wider considerations of threshold research appropriate to previous and present "memory" research. Whilst this includes demonstration of understanding of the basic force balance underpinning the threshold motion, greater emphasis is placed upon discussion of the strengths and weaknesses of different methodologies to determine entrainment threshold, as essential to defence of the approaches used in the present experimental programme. Similarly, the mathematical approaches (in particular for graded sediment) are considered in detail and the small body of existing "memory" research is critically reviewed. Each aspect provides the rationale for decisions taken later in this thesis for data collection and analysis.

2.2 Threshold motion of sediment

2.2.1 Theory of critical threshold of entrainment

In alluvial rivers, non-cohesive sediment is transported by the forces exerted by water on the particle. The force at the moment of first particle movement is the incipient motion of sediment usually expressed by critical shear stress, denoted by τ_0. Forces acting on a sediment particle are easily identifiable as depicted in Figure 2.1; these include: i) particle weight, ii) fluid force, and iii) frictional force i.e. particle to particle contact force. A particle's weight is straightforward to determine, as the submerged weight per unit volume, acting

vertically downward through the centre of mass. Conversely, fluid forces are much more difficult to measure; these are the resultant of drag and lift forces near the bed, which fluctuate according to the nature of flow (laminar or turbulent). Variables governing the fluid forces acting on a particle are mainly particle diameter, fluid viscosity, fluid density, boundary shear stress, particle's shape, and its surrounding shape. As the packing geometry heterogeneity (shape and surrounding shape) is inherently complex, researchers tend to focus on mathematical description of only the other variables by way of a single dimensionless parameter, which is the boundary Reynolds number (R_{e^*}):

$$R_{e^*} = \rho u_* D / \mu . \qquad \text{Equation 2.1}$$

in which ρ is density of fluid, u_* is shear velocity, D is particle's diameter and μ is dynamic viscosity of fluid.

A particle begins to move when the combined force of lift and drag out balances the counter force of gravity and friction and can be expressed by the following equation:

$$a_1 F_G \sin\alpha = a_2 F_D \cos\alpha \qquad \text{Equation 2.2}$$

Here, the left hand side of the equation represents total moment due to gravity, and the right hand side represents total moment due to fluid drag against the pivot point. In Eq. 2.2, a_1 and a_2 are coefficient of proportionality; a_1 depends on grain shape and packing, while a_2 on fluid flow, pressure and viscous force; and α is the particle's pivot angle. The gravity force: $F_G = c_1 D^3 \gamma_S$ in its expanded definition includes c_1 as a coefficient to account for particle shape and γ_s is the particle's unit weight. Similarly, the drag force $F_D = c_2 D^2 \tau_0$ includes c_2 as a coefficient to account for geometry and packing of the grains. Substituting F_G and F_D in the above equation, and re-writing for the critical condition where $\tau_0 = \tau_c$ (i.e. the applied shear stress is the same as the critical shear stress of entrainment threshold) means that the equation becomes:

$$\tau_C = \frac{a_1 c_1}{a_2 c_2} \gamma_S D \tan\alpha \qquad \text{Equation 2.3}$$

Equation (2.3) signifies the dependence of critical shear stress on particle's geometric properties, such as its absolute size and relative position with neighbouring particles, and on flow dynamics or, in other words, its dependence on boundary Reynolds number. It is worth noting that there is an inherent assumption in Equation (2.1) that the bed slope effect is negligible (however, it is evident from the force balance of sediment that increasing bed slope will decrease critical shear stress). Despite this simplification for slope, Equation (2.3) clearly demonstrates the complexity of measurement of a number of the required variables; for example, the pivot angle of each grain will differ in a naturally packed bed, measurement would require 3D geometry information of the bed without disturbing the packing arrangement, and packing will temporally evolve due to water-working or grain displacement. As such, whilst theoretically robust the logistical use of Equation (2.3) in real river beds is flawed and more general approaches to the calculation of critical shear stress are therefore outlined in further sections below.

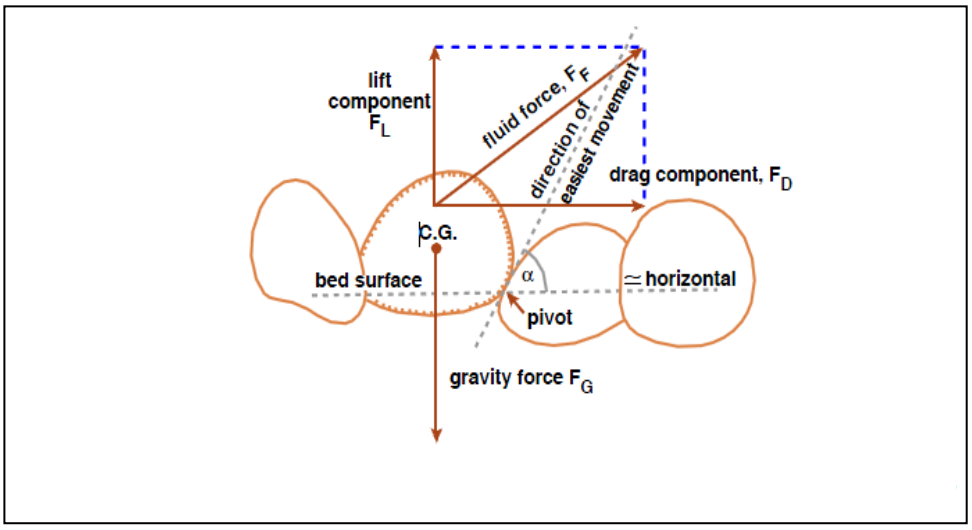

Figure 2.1: Schematic of lift and drag forces on a bed sediment particle (from MIT OpenCourseWare, Chapter 9, Figure 9.4 by G.V. Middleton, web link provided in reference).

2.2.2 Calculation of shear stress

Given the conclusion of Section 2.2.1, practically there are a number of alternative methods of calculating bed shear stress of Eq. 2.3: i) from the depth-slope product (Shields, 1936; White, 1940; Paintal, 1971; Koopaei et al., 2002; Biron et al., 2004; Monteith and Pender, 2005; Ockelford, 2011) , ii) from the logarithmic relation of shear velocity and velocity profile (Ashworth and Ferguson, 1989; Wilcock, 1996; Robert, 1990; Bauer et al., 1992; Biron et al., 1998; Song and Chiew, 2001; Pokrajac et al., 2006; Dey and Raikar, 2007; Piedra, 2010), iii) from the quadratic stress law (Thompson et al., 2003; Biron et al., 2004); iv) from the Reynolds stress using turbulence intensities (Kim et al., 2000; Babaeyan-Koopaei et al., 2002; Pope, 2006); or, v) from the turbulent kinetic energy method (Kim et al., 2000; Williams et al., 2004). The first two methods (depth-slope or log-law) are the most commonly used for determining threshold motion (Buffington and Montgomery, 1997) and a précis of the method, pros and cons of each is provided below.

Firstly, the depth-slope product (Eq. 2.4) is a reach-averaged approach, and thus hydraulic radius (R_0) and slope (S) are used in the equation as representative of a length of channel; these parameters represent total friction, which can arise from grains, bed-forms, bars and planforms.

$$\tau = \rho g R_b S \qquad \text{Equation 2.4}$$

In which, τ is bed shear stress, g is acceleration due to gravity, R_b is hydraulic radius, and S is flume bed slope or water surface slope (these latter two variables are equivalent in case of uniform flow). The advantages of the approach are: easy-to-measure variables; comparability of data to other flume research, where it has been widely adopted; reduced-complexity approach to complex field data analysis. That said, its limitations are well-known in terms of: failure to account for spatial and temporal variation in bed roughness; failure to provide direct measurement of fluid velocities. Where flume-based studies are concerned use of the depth-slope product has, however, been widely defended as reach-averaging can generally be considered appropriate where there is little variation in the bed friction along the flume length. Similarly, the depth-slope

relations are also an accepted simplification of reality where turbulence characteristics are less extreme, e.g., screeded bed flume experiments. Thus, in reviewing previous flume-based entrainment threshold studies (Buffington and Montgomery, 1997), this is the adopted approach providing a plethora of comparative data against which to benchmark further studies.

The second method is the Law of the Wall relation of velocity profile over the depth (Prandtl, 1925). Specifically, this method is based on the assumption that in the lowest 20% of the depth the velocity distribution has a logarithmic profile (Nezu and Nakagawa, 1993; Graf, 1998; Oertel et al., 2004; Wilcock, 1996):

$$\frac{u}{u_*} = \frac{1}{k}\ln\left(\frac{z}{z_0}\right) \qquad \text{Equation 2.5}$$

In which, u_* is shear velocity, k is von Karman's constant, usually 0.3 to 0.4; z is depth above bed, and z_0 is roughness height (height above bed where velocity becomes zero).

$$u_* = \sqrt{\frac{\tau}{\rho}} \qquad \text{Equation 2.6}$$

From the regression of measured velocities over depth, the shear velocity (u_*), shear stress (τ) and roughness height (z_o) can be obtained respectively from the slope and intercept of the equation of the straight line (Eq. 2.5). The advantage of this approach is that it is a measure of local shear stress, and thus can be used to map the spatial patterns of shear stress and roughness height. However, there appears little justification or validation that the velocity profile conforms to logarithmic exactly within and up to the 20% flow depth threshold adopted. Seemingly, the value stems from sand-bed pipe flow work of Nikuradse (1933) rather than open-channel flow *per se*. Indeed, the lack of scrutiny of such a well-cited value receives much debate and extensive literature trawl in Piedra (2010), with his own flow data analysis noting that the logarithmic profile may be valid to notably larger depth ranges, up to 0.5-0.8 z/h (Smart, 1999; Lamarre and Roy, 2005; Piedra et al., 2009). Despite the recognised benefits of use of

direct velocity data in this type of shear stress calculation, Piedra (2010) clearly notes its sensitivity to the velocity data averaging process and the "goodness of fit" of the regression. These issues arise as the flow measurements are contained in the near-bed region where there is: a high degree of velocity fluctuations/turbulence; spatio-temporal development of bed roughness; difficulty in physical sampling of sufficient data points in the lower 20% of shallow flow depths in the flume to provide good regression. Reviewing the datasets on entrainment threshold in Buffington and Montgomery (1997) also indicates that previous studies using the Law of the Wall approach have often erroneously measured and regressed velocity data over the total depth, likely leading to inaccuracy and/or uncertainty in shear stress data.

Recent research by Recking (2009) using several decades of measured flume and field data found that measured critical shear stress variations could not be reproduced with classical Nikuradse logarithmic velocity profile; available flow resistance data when used to fit a velocity profile to fit, it produced increasing critical shear stress due to increasing slope when used in a force balance model. This contradicts with usual consideration where due to gravity force, critical Shields stress should be smaller in increasing slopes. It was explained by the existence of a roughness layer which corresponds to low and uniform velocity profile near the bed. Without appropriate consideration of this roughness layer thickness, which is y/D, where y is flow depth and D is particle diameter, the critical shear stress would be flawed if only Nikuradse logarithmic profile be used.

Thus, such sensitivity of the method and lack of clarity over its application to data presented in the literature mean that application of this methodology should be judicious.

2.2.3 Threshold motion of sediment: Shields parameter

From Section 2.2.1 and 2.2.2 the critical shear stress approach appears the most widely adopted definition for entrainment threshold. In this regard, Shields' (1936) flume-based research is considered one of the earliest studies and it is his development of the non-dimensional approach to the shear stress parameter which has fostered its use as a benchmark data set for comparison of later

studies (e.g., Buffington and Montgomery, 1997 review). This non-dimensional approach continues to be commonly used in today's research and warrants attention herein. In short, Shields' non-dimensional shear stress parameter (τ_C^*) is also known as the Shields number (Eq. 2.7) and describes the ratio of bed shear stress relative to particle's submerged weight.

$$\tau_C^* = \frac{\tau_C}{(\gamma_S - \gamma)D} \qquad \text{Equation 2.7}$$

Here, τ_C is bed shear stress and γ is unit weight of water; the average bed shear stress (τ_C) is related to water depth (or hydraulic radius) and water surface slope (Eq. 2.4); shear stress is a measure of turbulent intensity on the bed and is calculated using Eq. 2.5 or 2.4.

From his experimental results, Shields' legacy develops from his illustration of an envelope (uncertainty band) of entrainment threshold, as established via a non-dimensional plot of Reynolds Number (R_{e^*}) versus Shields number (τ_C^*), see Figure 2.2. The intention of his work was to demonstrate the effect of flow regime on entrainment threshold and is widely recognised for indicating a tendency towards $\tau_C^* \rightarrow$ Constant in hydraulically rough flow regimes (i.e. at high values of R_{e^*}); it is, however, notable that only one data point exists in his original rough regime work and extension of data specific to review of the Constant has been the topic of significant follow-on research (e.g., Neill, 1968; Parker et al., 2003). Crucially, Shields' data include uncertainty via a shaded envelope covering a band width for his dataset (Figure 2.2); this highlights well-known problems with repeatability of

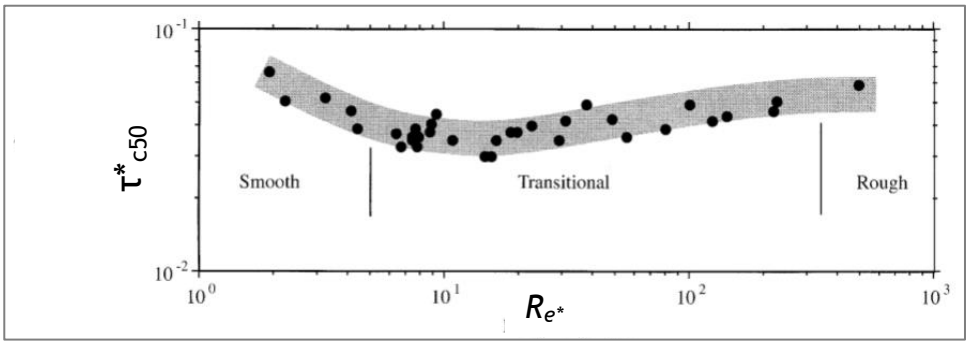

Figure 2.2: Shields' own dataset on incipient motion of uniform sediment (from Buffington and Montgomery, 1997); the abscissa of the diagram represents Reynolds number (R_{e^*}), and the ordinate represents Shields number (τ^*_{c50}) for median size class (D_{50}) as in Eq. 2.7; Shields' dataset covered a wide range of flow regime, from smooth to rough flow region; however, Shields had no data points in rough flows for $R_{e^*} > 589$, or in smooth flows beyond $R_{e^*} < 2$.

experiments stemming from variability in the bed, flow fluctuations and/or user-definition of entrainment. However, later versions of this "Shields Curve" erroneously reproduce the envelope of entrainment as a deterministic single threshold line, as drawn by Rouse (1939). This single line approach was sought to define the Shields number (τ^*_C) at which flow will initiate particle movement (above the line), from that at which the flow is unable to move any particles and the bed remains immobile (below the line). The single-value threshold approach underpins the rationale for the Shields diagram being widely used for engineering practice, particularly based on the assumption that rough regimes ($R_{e^*} > 250$) tend to the constant of τ^*_C =0.06. Such empirical equations are therefore embedded within numerical flow-particle models widely used in flood risk, sediment transport and water quality estimates. Although Shields' work is now considered pivotal in today's practices, this actual methodological approach used to define and measure his own entrainment threshold has received notable review, critique and re-examination (Sections 2.3 and 2.4).

2.3 Determination of entrainment threshold

Given that the actual moment when there exists a balance in the forces promoting and resisting entrainment cannot be observed, the actual determination of critical shear stress still remains a challenge for scientists. Typically, critical shear stress is defined as the condition of flow where some sediment is in motion; this definition of "some sediment" tends to be when loads are practically measurable or visually countable. Clearly, such subjectivity has led to the evolution of both deterministic and statistical approaches for determining critical shear stress and discussion of the most common methods is therefore pertinent to the present thesis; these include: a) reference transport (e.g., Shields, 1936; Parker et al., 1982a; Shvidchenko et al., 2001); b) visual approach (e.g., Gilbert, 1914; Kramer, 1935; Neill and Yalin, 1969); c) stochastic method from probabilistic approach (e.g., Gessler, 1966 and Grass, 1970); d) competence or largest grain method (e.g. Andrews, 1983; Carling, 1983; Komar,1987a); e) theoretical approach (e.g., White, 1940 and Wiberg and Smith, 1987).

2.3.1 Reference transport method

The reference transport approach is, largely, considered the most reliable method for determining critical shear stress for sediment movement (e.g., Fenton and Abbott, 1977; Parker et al., 1982a; Wilcock, 1988). It is based upon direct measurement of sediment transport samples over a range of flows, such that a well-defined relationship between shear stress and bedload transport can be established. Arguably, the most influential entrainment threshold studies have utilised this approach (e.g., Shields, 1936; Paintal, 1971; Taylor, 1972; Ackers and White, 1973; Parker and Klingeman, 1982; Shvidchenko and Pender, 2000; Shvidchenko et al., 2001), even applying it to the individual entrainment thresholds of graded beds.

There are several definitions of reference transport (Shields, 1936; Ackers and White, 1973; Parker et al., 1982a and Shvidchenko and Pender, 2000; Shvidchenko et al., 2001); all definitions have different magnitudes of practically measurable volume of transports, which correspond to initial motion of uniform and graded sediment. Because of these differences, it, therefore,

merits a discussion here about their development, advantage, disadvantage and their applicability.

Shields' research (1936) was the most influential pioneering dataset on threshold motion of uniform sediment. Until the work of Taylor and Vanoni (1972) and Garcia (2000), it was believed that his initial motion dataset corresponded to a zero transport rate. It was largely understood that Shields obtained his threshold condition by back-extrapolating his sediment rating curve to zero transport. Taylor and Vanoni (1972) established the reference transports for his initial motion data; they established a family of contour lines of non-dimensional

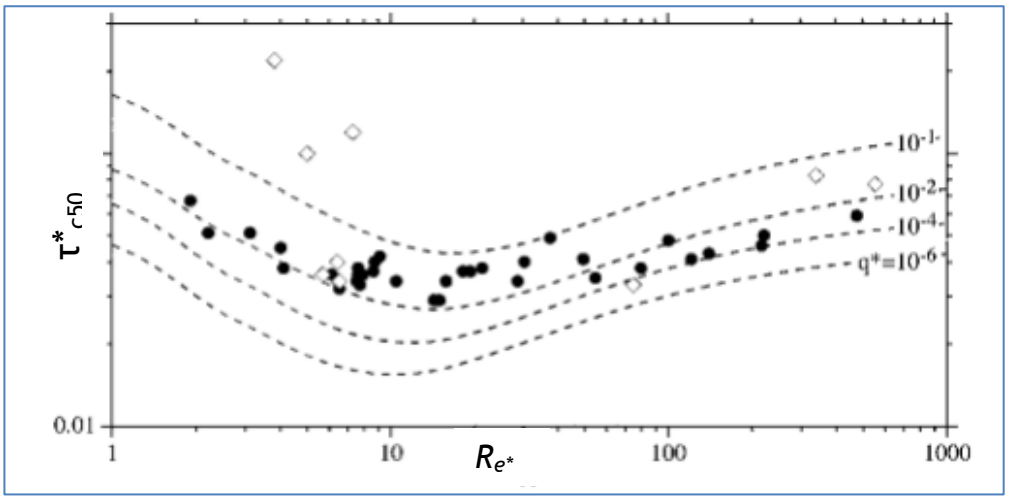

Figure 2.3: Different reference transport (q^*) contours on Shields diagram, as deduced from Shields initial motion data during review and reanalysis as established by Taylor and Vanoni (1972).

transports (q^*); superimposed them on the Shields diagram (Figure 2.3), and demonstrated that all of Shields' threshold motion data envelop a range of reference transports (q^*) between 10^{-4} and 10^{-1}; this study also used data of USWES (1935), Casey (1935a, b) and Taylor (1971). Later, Garcia (2000) demonstrated that Shields had practically measurable transport for his shear stress for incipient motion and there was general agreement in the research community that the Shields band width in his initial motion data poses a

disadvantage to precise definition for a particular transport condition. Thus, Shields' average condition has been represented by many (e.g., Miller et al., 1977; Brownlie, 1981) to correspond to a reference transport of approximately $q^* = 10^{-2}$.

Two deterministic magnitude of reference transports were later proposed by Day (1980) using Ackers and White's (1973) model (herein referred to Ackers and White's reference number), and that of Parker et al. (1982a); both these definitions yielded a different magnitude of transport. Parker's reference transports value was W^*=0.002, and is represented by Eq. 2.8 and 2.9. Parker's reference transports were based on his work with the field data of Oak Creek (Milhous, 1973) of unimodal sediment mixtures. Using Eq. 2.9, Parker's reference transport number W^*=0.002 can be converted to $q^* = 10^{-5}$ for easier comparability with the aforementioned Shields reference transport (q^*). Ackers and White's reference transport, $G_{gr} = 10^4$ (Ackers and White, 1973) is shown in Eq. 2.10 ($G_{gr} = 10^4$ *approximately equates to* $q^* = 5x10^{-3}$*, see Figure 3, top, in Wilcock, 1988)*. Day (1980) validated this reference number to practically measurable transport used in laboratory experimental data for sediment mixtures. The magnitude of reference transport of Parker et al. (1982a) and Ackers and White (1973) were compared by Wilcock (1988) via further experimental data, to find that Ackers and White's (1973) reference transports require about a 20% higher reference shear stress for the entrainment of sediment.

$$W_i^* = \frac{(s-1)gq_{bi}}{f_i(u_*^3)} \qquad \text{Equation 2.8}$$

$$W_i^* = q_i^* / (\tau_i^*)^{3/2} \qquad \text{Equation 2.9}$$

$$q_{bi}^* = \frac{q_{bi}}{\sqrt{(s-1)gD^3}} \qquad \text{Equation 2.10}$$

$$G_{gr} = \frac{q_b}{uD}\left(\frac{u*}{u}\right)^e$$ Equation 2.11

In Eq. 2.8 and 2.10, *s* is submerged specific density of sediment, q_{bi} is volumetric bedload per unit width in i*th* grain size subrange, q_i^* is non-dimenional bedload per unit width (Einstein bedload parameter), τ_i^* is Shields number in i*th* grain size subrange, q_b volumetric bedload per unit width, *u* is mean velocity, f_i is fractional proportion in the i*th* subrange, exponent *e* is a dimensionless parameter which varies according to grain size.

The three reference transport approaches discussed above (Shields, 1936; Ackers and White, 1973 and Parker et al., 1982a) were all deterministic definitions of measurable transport; they therefore lack description of the stochastic nature of fluid turbulence and variability in grain geometry promoting a 'random' element in grain entrainment. As these variables require a more probabilistic approach (Grass 1970), Shvidchenko and Pender (2000), Shvidchenko et al., (2001) used a probabilistic definition of threshold based on intensity of sediment motion for uniform and graded sediment, based on an extensive volume of laboratory data so as to propose a new reference transport value. Shvidchenko and Pender (2000) introduced the probability concept in their sediment mobility number (I), referred to as the intensity of sediment motion in a similar guise to that initially raised by Einstein (1942). Shvidchenko and Pender, (2000) and Shvidchenko et al., (2001) proposed a reference transport of $q^* = 10^{-4}$, which they considered to be the practical lower limit of q^* which can be reliably measured. For grain size ranges between 1.5 and 12mm a relation between intensity of sediment motion (I) with q^* was developed such that at $q^* = 10^{-4}$, the sediment intensity was $I = 10^{-4}$. According to this definition of sediment intensity, 1 in 10,000 particles on the bed surface would be in motion in every second; this was considered the definition for threshold motion of sediment. They compared their sediment intensity curve with Parker et al.'s (1982a) reference transport value ($q^* = 10^{-5}$), for which they found $I = 3x10^{-5}$, i.e. 3 in 100,000 particles are in motion in every second. Shvidchenko et al. (2001) later developed their sediment data set for q^* between 10^{-6} to 10^{-2} such that they proposed an empirical curve (Eq. 2.12), and

derived a relation for predicting incipient motion (Eq. 2.13) at a reference transport of $q^* = 10^{-4}$.

$$q_{bi}^* = \left(\frac{a\tau_i^*}{\varepsilon_i} \right)^{18} S^{-5} \qquad \text{Equation 2.12}$$

$$\tau_i^* = \varepsilon_i \frac{0.6}{a} S^{0.278}, \; at \; q_{bi}^* = 10^{-4} \qquad \text{Equation 2.13}$$

In which *a* is the mobility parameter (Eq. 8 in Shvidchenko at. 2001), ε_i is hiding function ($\varepsilon_i = \tau_{ri}^* / \tau_{50}^*$) and S is flume slope. Shvidchenko et al. (2001) validated Eq. 2.13 to predict the threshold motion for different size classes (including a wide range of data compiled from several other authors), with close observation of their predicted values and measured values. However, this dataset revealed that sediment transport was possible even at lower shear stress than proposed by their reference definition; similar findings are also noted at low flows by others (e.g., Casey, 1935; USWES, 1935; Paintal, 1971, and Taylor and Vanoni, 1972; Parker et al., 1982a). As such, focus on the sensitivity of low flows around the discharge appropriate to entrainment appears warranted as specific to its impact upon a reference transport approach.

2.3.2 Visual method

Although Shields' work was laboratory based, researchers continued to look for alternative measures of entrainment threshold that were non-invasive and less laborious than high resolution bedload sampling. One such method was developed by Neill and Yalin (1969) by way of a visual approach for estimating critical shear stress for unisize sediment movement. Their methodology was based on the assumption that an equal number of grains will be displaced from geometrically equivalent areas (Eq. 2.14) over a kinematically equivalent time period (Eq. 2.15). Thus, they argued that:

$$A_1 / D_1^2 = A_2 / D_2^2 \qquad \text{Equation 2.14}$$

$$t_1 u_{*1} D_1 = t_2 u_{*2} D_2$$ Equation 2.15

In which A_1 is the area of observation for grain size D_1, and A_2 is for grain size D_2, t_1 and t_2 are times of observation in the corresponding areas. Eq. 2.14 provides scaling for determining the area, and Eq. 2.15 provides scaling for selecting time for equal number of grains to be displaced. It is clear from the equations that larger unisize grains will require a larger area and higher sampling time. Therefore, for equal number of grain displacement, the following must satisfy:

$$x_1 A_1 t_1 = x_2 A_2 t_2$$ Equation 2.16

The similarity ratios in Eq. 2.14-16 will lead to:

$$x D^3 / u_* = C$$ Equation 2.17

In which x, x_1 and x_2 are number of particles in motion and C = constant. Neill and Yalin (1969) observed that for any practical and observable sediment movement, the constant in Eq. 2.16 should be 10^{-6}. However, Eq. 2.16 is not directly applicable to mixed size sediments for two reasons: i) the sampling period was scaled with grain size from the unisize bed, which is not applicable for mixed size sediments, and ii) in a mixed bed, grains from each fraction do not cover the entire bed surface. Wilcock (1988) therefore proposed the following scaling relations for corrected application of the visual approach to mixed size sediment:

$$f_{a1} \frac{A_1}{D_1^2} = f_{a2} \frac{A_2}{D_2^2}$$ Equation 2.18

where f_{a1} and f_{a2} are fractional contents from area 1 and 2 such that this satisfied the requirement that an equal number of grains are displaced from the area of same number of grains, in a way that the following must hold equal:

$$x_1 A_1 = x_2 A_2$$ Equation 2.19

where, x_1 *and* x_2 (Eq. 2.19) are number of particles in motion from area 1 and 2 for a particular fraction. Hence, if Eq. 2.18 is inserted into Eq. 219, then to satisfy threshold motion for each fraction will lead to the following relationship:

$$x_i D_i^2 / f_{ai} = C \qquad \text{Equation 2.20}$$

where, C = constant such that Eq. 2.20 is applicable only for a specific sediment mixture, (rather than interchangeable from mixture to mixture) in a manner whereby it is not needed to know the value of the constant in Eq. 2.20 beforehand. Although Wilcock (1988) did derive the logical relations (Eq. 2.18 to 2.20) for sediment mixtures, he noted the severe practical limitations of visual approach for mixed size sediment in terms of the scaling of both area and sampling time. In this regard, an example of the problem is demonstrated as follows: because the particle displacement varies with square of the particle size, for a single displacement of the largest grain size of 16mm in a mixture, 4096 finest particles (1mm) have to be displaced from the same observation area in the same sampling period. Additional limitations of the visual approach in mixtures include the temporal evolution of f_{ai} in the bulk mix due to entrainment during (or between) sampling periods. Thus, Wilcock (1993) noted that visual approach would not truly determine entrainment threshold for each fraction in sediment mixtures where size selective transport is key mode of sediment movement. That said, the visual approach has recently seen a resurgence of laboratory based applications in research that is specific to below-threshold or low transport conditions (e.g., Monteith and Pender, 2005; Paphitis and Collins, 2005; Haynes and Pender, 2007: Ockelford, 2011) and the merits of its ease of use and non-invasive sampling approach should be considered when selecting laboratory based methodology in such studies.

2.3.3 Other approaches

Three alternative approaches are briefly highlighted below, primarily to justify why they are not widely adopted in entrainment studies and secondly to raise

salient points which may aid uncertainty analysis of the more common methods referred to in Sections 2.3.1 and 2.3.2.

Firstly, Buffington and Montgomery (1997) provide comparative threshold data specific to methodological definition comparison, clearly depicting considerable scatter on entrainment threshold values. For example, for the same Reynolds number, the threshold shear stress varies by several folds from smooth to rough flow region. Such scatter is also significantly attributed to the nature of turbulent flow at the granular bed interface; instantaneous fluid forces exerted on a sediment particle can vary widely; as a result, even a weak flow with strong turbulent eddies can cause occasional sediment movement (Paintal, 1971; Zanke, 2003). This is likely a facet of two effects: i) the effective boundary shear stress acting on a particle is higher than the time averaged boundary shear stress, due to instantaneous turbulence, and ii) a particle's projection to flow makes it lighter than predicted, due to instantaneous lift forces. Therefore, at the point of incipient motion, the distribution of flow is much wider than considered by the deterministic approach of Sections 2.3.1 and 2.3.2. Here the hypothesis and findings of Diplas et al. (2008) is worth referring; through laboratory experiments and analytical formulation, they studied the problem of incipient motion; they observes that in addition to the magnitude of the instantaneous turbulent forces applied on a sediment grain, the duration of these turbulent forces is also important in determining threshold motion of sediment; their experimental and theoretical analyses support the hypothesis that impulse rather than force is the relevant parameter for the incipient motion of mobile sediment under the two limiting conditions of pure drag and pure lift. Thus, the stochastic approach to entrainment threshold definition is borne. As this requires high temporal and spatial data resolution to resolve adequately, it has not been readily adopted in sediment entrainment research; however, a précis of the stochastic method based upon the findings of Grass (1970) is important in understanding data uncertainty in other methodological approaches to threshold definition. That is, Grass (1970) proposed the original probabilistic description of shear stress acting on particles to initiate sediment motion in terms of two frequency distributions: i) distribution of instantaneous shear stress (τ_W) on an area over the bed induced by the fluid, and ii) distribution of

instantaneous shear stress required (τ_{WC}) to put the particle in motion (equal to the resisting force). His notion was, correctly, that there must be some overlap between these two frequency distributions for particles to move (Figure 2.4). Such stochastic nature of the incipient motion of sediment in uniform and graded sediment has since been researched by many (e.g., Einstein, 1950; Gessler et al., 1966, 1967; Fredsoe and Deigaard, 1994; Kleinhans and van Rijn, 2002; Dancey et al., 2002; Papanicolaou et al., 2001, 2002; Wu and Chou, 2003), yet these studies not only consider the probabilities of solely the turbulence characteristics specific to Grass' research, but also that the incipient motion of a grain in a mixture depends on its position relative to that of the surrounding particles. Krogstad et al. (1992) and Papanicolaou et al. (2001) provided evidence that bed packing in gravel bed streams affect turbulence characteristics, and thus the entrainment of sediment. Papanicolaou et al. (2001) observed that the ratio of Reynold stress to the standard deviation of downstream velocity is smaller in loosely packed beds than in densely packed beds. Thus, a threshold motion based soley upon time-averaged shear stress under-predicts sediment transport, particularly in loose beds (Papanicolaou et al., 2001). The discussion here on stochastic approach certainly indicates that there is a wider distribution of turbulent flows causing sediment motion, hence sampling in more widely adopted deterministic approaches should be undertaken from as minimum a flow as possible (Paintal, 1971 and Parker et al., 1982a).

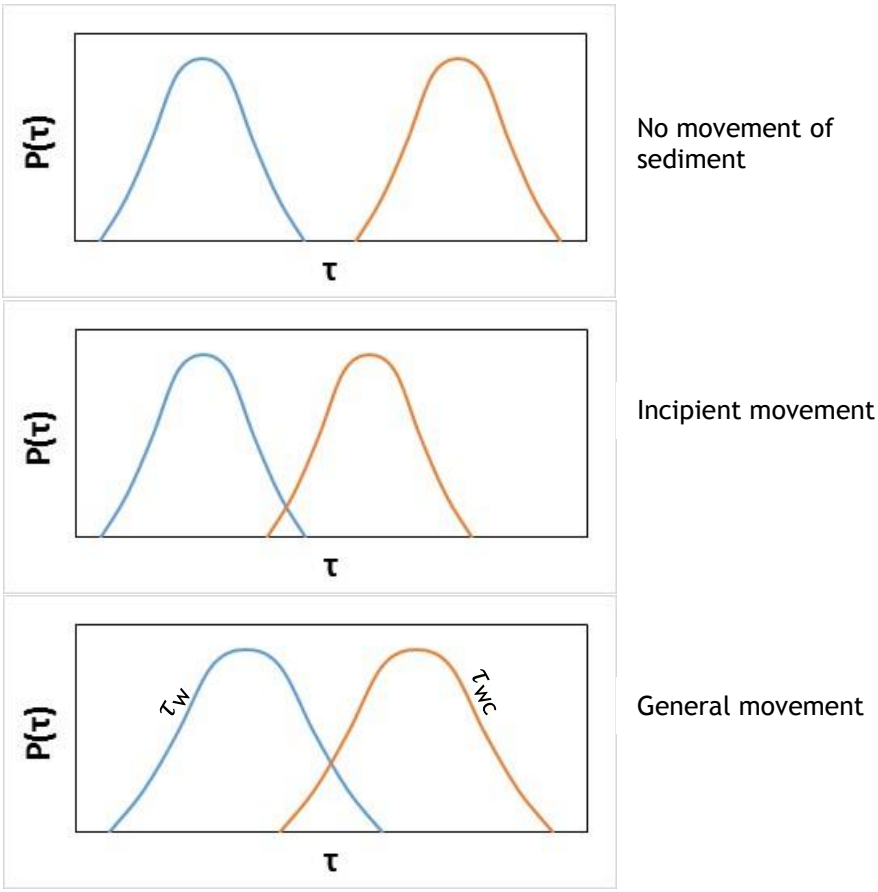

Figure 2.4: Conceptual definition of incipient motion of sediment from frequency distribution of instantaneous fluid forces on bed (τ_W), and frequency distribution of instantaneous fluid forces required (τ_{WC}) for particle to begin movement (schematic: from Grass, 1970); top: no movement of sediment; middle: some overlap of two frequency distribution, and incipient movement; bottom: some degree of overlap, and general movement of sediment.

Secondly, field data sets considering sediment entrainment consider a competence or largest grain method. This approach relates the size of the largest mobile grains to the applied shear stress (Andrews, 1983; Carling, 1983; Komar, 1987a), but suffers from multiple limitations including: i) an assumption of availability of the largest grain class in sampled bedload, ii) sufficiently long sampling period, iii) sufficiently large sampling area, and iv) sufficiently long

period of constant flow. As a result, this approach incurs scaling issues similar to those raised for the visual approach (Section 2.3.2) and is limited to conditions of selective transport where entrainment shear stress is variable with grain size (Wilcock, 1988, 1992a, 1992b). Such restrictions limit the adoption of this technique, with preference more widely afforded to the alternative reference transport approach if bedload transport samples are available.

Theoretical approach: this approach returns to fundamental force balances presented in Section 2.2.1. It assumes the grain's pivot angle to be derived from empirical formula (Miller and Byrne 1966) such that the critical shear stress can be calculated for any grain size and any size class in a mixture. Wiberg and Smith (1987) proposed, arguably, the most cited theoretical model for calculating the entrainment threshold of a non-cohesive sediment as:

$$\tau_C^* = \frac{4}{3}\frac{(\tan\alpha\cos\theta - \sin\theta)}{(C_D + \tan\alpha\, C_L)}\frac{1}{F^2(z/z_0)} \qquad \text{Equation 2.21}$$

where θ is bed slope angle; α is grain's pivot angle; C_D and C_L are drag and lift force coefficients respectively; function $F = u(z)/u_*$, is the logarithmic function, which relates effective fluid velocity acting on a particle to shear velocity; here z is water depth above bed and z_0 is roughness above bed where velocity is zero. Wiberg and Smith's model is based on the key assumption of particle's motion by rolling; similar recent, but more detailed work on this is by Meidema (2010), who considered sliding, rolling and lifting as key mechanism of particle's motion in his mathematical model. Alternative theoretical approaches (and embedded elements) include e.g., White, 1940; Chepil, 1959; Egiazaroff, 1965; Ikeda, 1982; Kirchner et al., 1990; Zanke, 2003. Valyrakis et al. (2013) proposed a new theoretical framework based on energy approach for incipient motion of coarse particles in saltation or rolling mode; energy balance equation was developed; threshold energy curves were provided for both saltation and rolling modes. Their theoretically predicted results perform satisfactorily with their experimental results performed in a series of low-mobility experiments for entrainment of particles. The theoretical approaches as above, however, oversimplifies the issues of bed heterogeneity and shear stress fluctuations in such a manner as to seriously over-predict threshold values. For example, at the

higher Reynolds' numbers (R_{e^*} > 200) common to river beds the predicted initial motion by most of the theoretical approaches cited are higher than Shields $\tau_c^* = 0.06$ threshold by around a factor of two. Such consistent and erroneous over-predictions of threshold values had precluded general adoption.

Discharge based approach: this approach is employed to determine threshold condition (Bathurst et al., 1987, Rickenmann, 1990, Bathurst, 2013) generally in gravel bed stream. Depths are difficult to measure in steep slope channels (Bathurst et al., 1987). They proposed $q_{cr} = 0.15 g^{0.5} D_{50}^{1.5} S^{-1.12}$ to determine critical discharge at the initiation of sediment transport. The advantage of using this relation is that information on flow depth is not needed to determine the critical discharge. Only bed slope, sediment size and density and fluid density are required as input. Rickenmann (1990) modified Bathurst et al. (1987) relation by including density factor (s-1), where is *s* relative density of sediment (ρ_s/ρ). Shields relation for critical shear stress (Eq. 2.7) developed for uniform sediment cannot be applied for steep slope channel without correction. Threshold shear stress at initial motion in steep gravel bed is difficult to determine than finer bed (Wiberg and Smith, 1987), and thus critical discharge method is useful in gravel bed stream. It is worth mentioning here that Lamb et al. (2008) analysing large volume of flume and field data developed an empirical relation explicitly dependent on slope as $\tau_c^* = 0.15 S^{0.25}$; they considered data set only for the rough flow region for Reynolds Number >100, where the Shields Number considered constant value ranging from 0.03 to 0.06 (Buffington and Montgomery, 1997). Many of the data however did not fall within this range; they showed that increasing slope increase the critical shear stress, and established an empirical relation $\tau_c^* = 0.15 S^{0.25}$.

Bathurst (2013) had the most recent work on the entrainment threshold of non-uniform sediment with interesting findings; he used critical discharge approach, and employed large volume of field (24 sites) and flume (37 sets) data. He established a generic relation for predicting entrainment threshold as: $q_{ci} / q_{cr} = (D_i / D_r)^m$ where q_{ci} and q_{cr} are unit critical discharge for size class i and the reference size class r respectively; D_r is the reference sediment class,

which was close to D_{50} in most cases of his data sets. This exponent m is analogous to hiding function exponent proposed by Parker et al. (1982a) and Wu et al. (2000a); however, this exponent is characteristically different than the other authors; for Bathurst, exponent m=0 is a condition of equal mobility transport at entrainment, and m between 1.5 and 2.5 is representation of size selective transport, and in case of Parker et al. (1982a) and Wu et al. (2000a), m=1 represent equal mobility, ad m between 0 and 1 represents size selective transport. In his analysis of the data set, Bathurst, however, did not present any equivalent Shields number corresponding to the critical discharges, and thus makes it difficult to compare his results more directly with widely used Shields number (Buffington and Montgomery, 1997).

Recent research in gravel bed stream (Bunte et al. 2004, 2013) computed critical discharge in gravel bed stream from flow competence curve of bedlaod data collected by bedload traps. Their data also shows high sensitivity of bedload at low flow transport, which varies with exponent upto 16.2 with discharges, similar to Paintal (1971) and Taylor and Vanoni (1972), who however presented the sediment exponent with bed shear stress. Bunte et al. (2004) also calculated the Shields number corresponding to the critical discharges, which are in similar order of magnitude like Shields original data, and thus may seem over-estimate of entrainment threshold (Buffington and Montgomery, 1997 and Parker et al. 2003). Their computation of Shields number that is based on flow competence or critical flow approach requires bed load transport measurements that accurately represent the largest bed load particle size mobile at a specified flow (Wilcock, 2001) and need to sample over a long time to catch the infrequently moving large particles. From flow competence curve, they determined critical discharge and Shields parameter for entrainment of largest grain sampled at respective flows. They also proposed a power relation of predicting entrainment threshold; for stream slope from 0.1 and above. For the 22 mountain rivers, they established critical discharge for the entrainment of largest grain; their relations however predict significantly higher threshold shear stress than proposed by Lamb et al. (2008).

2.4 Modification of Shields parameter

2.4.1 Re-writing the abscissa

In Section 2.2, the fundamental work of Shields (1936) was introduced in terms of his (Shields) Curve tending to a constant of τ_C^* =0.06 for the hydraulically rough regimes (R_{e^*} > 300) typical of natural sand/gravel bed rivers. However, Vanoni (1964) first noted a practical limitation of the curve, in that the incipient motion for any specific grain size could not be explicitly determined because bed shear stress was a variable in both axes (i.e. in the abscissa as τ and in the ordinate as $u_C^* = \sqrt{\tau/\rho}$). Thus, the original Shields curve has been subject to approximation for convenient use (e.g., Bonneville, 1963; Brownlie, 1981; van Rijn, 1984; Soulsby and Whitehouse, 1997). The advance of Brownlie (1981) is of particular note, as he rewrote the abscissa as particle Reynolds number (R_{ep}) such that:

$$\tau_C^* = 0.5\,[0.22\,R_{ep}^{-0.6} + 0.06 \cdot 10^{(-7.7\,R_{ep}^{-0.6})}] \qquad \text{Equation 2.22}$$

$$where \quad R_{ep} = \frac{(\sqrt{(s-1)gD})\;\; D}{\nu}$$

In which, ***s*** is submerged specific gravity of sediment and v is kinematic viscosity of water. Later, van Rijn (1984) took a similar approach in terms of their dimensionless particle number:

$$D^* = D((s-1)g/\nu)^{1/3} \qquad \text{Equation 2.23}$$

Both Brownlie's (1981) R_{ep} and van Rijn (1984) D^* are functional to sediment and water properties and thus helped explicit determination of incipient motion from their curves.

2.4.2 Debating the constant

Figure 2.2 clearly shows this conclusion derived solely from a single datum within the rough regime. Although extrapolation of the Shields curve (e.g., Brownlie, 1981; van Rijn, 1984; Shvidchenko and Pender, 2000) to a constant is appealing for engineering practice, review of additional data and uncertainties in the rough regime require discussion. Thus, Miller et al. (1977) was first to modify and extend Shields curve (Figure 2.5) using only flume data for uniform sediment; this included a wider review and inclusion of similar data from Casey (1935a, 1935b), Grass (1970), Kramer (1935), Paintal (1971), White (1940), Neill (1967), and Vanoni (1964) alongside Shields' own dataset. This yielded notable greater data points in the rough regime such that τ_C^* was revised to a constant of 0.045. Unpicking the raw experimental data used to derive this constant highlights that Miller et al.'s (1977) curve was established via regression of entrainment data merged from two distinct methodologies, the visual and the reference transport approaches (Section 2.3). Thus, whilst the constant of 0.045 is reflective of limited reference transport data, explicit consideration of visual-only data (e.g., data set of Neill, 1967) in the region $R_{e^*} > 100$ reduces τ_C^* to (on average) ~0.025. This clearly indicates methodological sensitivity of the Shields parameter, as recognised specifically in Buffington and Montgomery's (1997) review paper and later review by Shvidchenko and Pender (2000). Figure 2.6 exemplifies such sensitivity, in that τ_C^* from reference transport studies (Figure 2.6a) sits well above visual approach (Figure 2.6b) data. Interestingly, the reference transport approach is also noted to suffer less scatter and uncertainty within and between investigations, possibly providing additional justification for continued, more recent investigator preference in entrainment threshold studies.

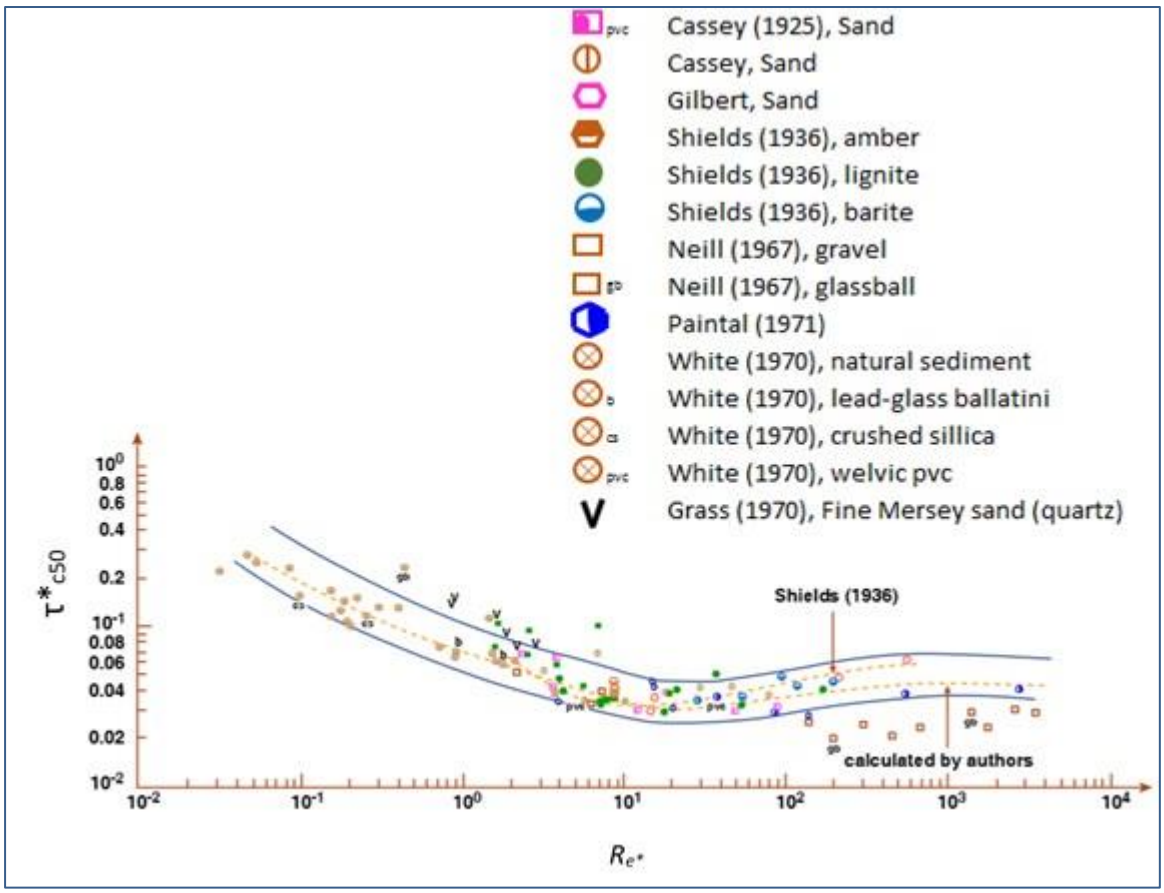

Figure 2.5 Shields numbers compiled by Miller et al. (1977) from different researches on incipient motion studies (adopted from MIT Opencourseware, chapter 9, Figure 9-8; for further detail reference of each dataset shown in this Figure, please see Table 1, Miller et al., 1977, p512). Abscissa of the diagram represents Reynolds number (R_{e^*}), and ordinate represents Shields number by τ^*_{c50} as represented by Eq. 2.7. Miller et al. also showed an upper and lower bound of Shields number bounded by the two blue lines; however, this should be pointed out that this boundary is not same Shields boundary as in Figure 2.2, which Buffington and Montgomery drafted; more-over, Miller et al. although commented the blue boundary lines to cover most dataset, but to be fair, this is not the case for $R_{e^*} > 100$; here many data points remained outside Miller et al. lower bound. Of the two orange-dash lines, one is the Shields single curve drawn by Rouse (1939), and other is Miller et al. curve (1977).

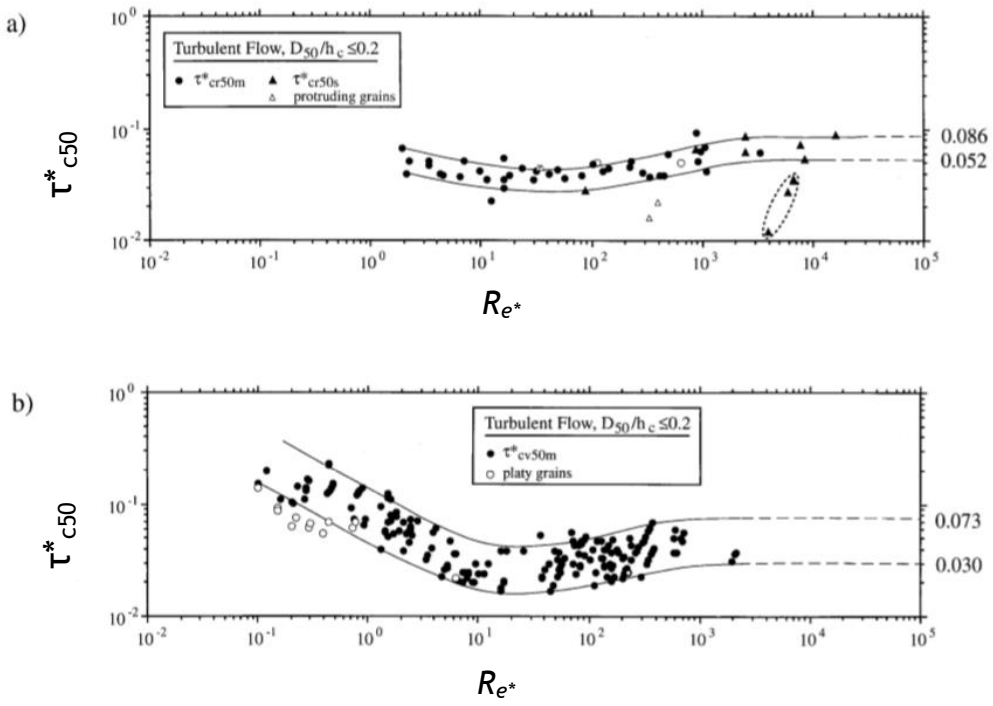

Figure 2.6: Compilation of eight decades of incipient motion data by Buffington and Montgomery (1997); a) Incipient motion data from reference transport approach, b) Incipient motion data from visual transport approach; for more details of the Figure, particularly the legends for data points, please see Buffington and Montgomery (1997); Abscissa is critical boundary Reynolds number and ordinate is Shields number; incipient motion in reference transports lies well above the values from visual approach, particularly in rough flow region for $R_{e^*c} > 400$.

2.4.3 Parker's (2003) update

A further review by Parker et al. (2003) assembled a subset of the eight decades of incipient motion data from Buffington and Montgomery (1997) and data set from three gravel bed rivers (Britain, USA and Canada; after Church and Rood, 1983). Their work was specific to examining the transporting ability and morphology of gravel beds specific to field application of eight mountain gravel bed streams of Idaho. Analysing the Shields number at bankfull discharges they proposed the modification of the Shields curve as they observed that at Shields'

original threshold condition, no sediment moved. In short, Figure 2.7 indicates that the modified regression (based on Neill, 1968) of Parker falls significantly below the Shields curve (Figure 2.5) such that $\tau_c^* \rightarrow$ 0.03. In a manner similar to Brownlie (1981) this revised curve is described mathematically as:

$$\tau_c^* = 0.5\,[0.22\,R_{ep}^{-0.6} + 0.06 \cdot 10^{(-7.7\,R_{ep}^{-0.6})}] \qquad \text{Equation 2.24}$$

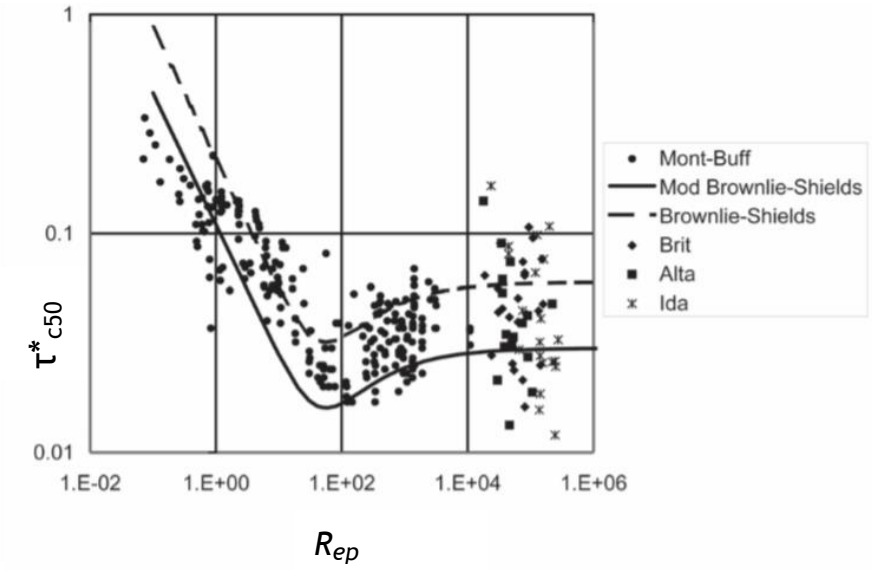

Figure 2.7: Critical shear stress vs. particle Reynolds number (n.b. R_{p50} is the original annotation of R_{ep} taking the median grain size of D_{50} Eq. 2.22 and 2.24); The dashed line is Shields curve approximated by Brownlie (1981) tending to 0.06 in rough regimes; the solid line is Parker's curve (2003) tending to 0.03 in rough regimes. Incipient motion data from Buffington and Montgomery (1997) is given by black filled circles (Mont-Buff), whilst other symbols denote bankfull field data (Britain-Brit; Canada: Alta; USA: Ida). This figure is after ACSE Manual 110 (ASCE, 2007).

Thus, it is clear that recent research continues to apply Shields' approach to entrainment threshold analysis. Whilst the wild variability of data in the rough regime brings a high degree of uncertainty to description via any "constant" in Parker's data, the specific $\tau_c^* \rightarrow$ 0.03 value is increasingly receiving recognition in field studies and laboratory research (e.g., Church and Rood, 1983;

Shvidchenko et al., 2001, Muller et al., 2005; Yang and Wang, 2006; Haynes and Pender, 2007; Lamb et al., 2008; Ockelford, 2011). Lamb et al. (2008) particularly compiles a large volume of field and laboratory data of critical shear stress for $R_{e^*}>100$, mostly around 0.03. This recent paper therefore raises three important issues for continued use of this approach in entrainment threshold studies: (i) possible distinction between the Shields constant appropriate for laboratory-based and field based data; (ii) natural variability in data for the rough regime; (iii) selection of methodology for determination of entrainment threshold, and analysis of only data of equivalent methodologies.

2.5 Transport of sediment mixture

2.5.1 Relative grain size

It is well-known that entrainment thresholds are not a function of the flow properties alone, hence the character of the sediments must be embedded in empirical approaches. The simplest method assumes a bed of uniform grain size which, although viable in laboratory tests, is rather unrepresentative of natural river beds where mixed sizes occur. Thus, a second stage descriptor is used as representative size reflective of the bed. Typically, for sediment transport, this is taken as the median grain size (D_{50}) in the manner already applied in Section 2.4; it is arguable as to whether the intention of this approach is to strictly describe all grain sizes as behaving exactly as that of the D_{50} fraction, or purely that the D_{50} is a ballpark approximation of general bed dynamics. It is for this reason that more detailed equations have developed to specifically consider individual fractions or distributions reflective of the wide range of sorting in sediment mixtures; whilst these dictate detailed measurements (e.g., composition, structure, exposure, pivoting angles) of every individual fraction (which may be an unrealistic expectation, particularly in poorly sorted field settings), the insight on relative grain size effects on sediment entrainment threshold is important.

In basic terms (e.g., Shields diagram, Fig.2.2) the larger the grain size, the heavier the grain and larger the critical shear stress for sediment movement expected. Whilst for a perfectly arranged bed structure of uniform grain size this notion may be true, a natural mixed grain size (graded) bed presents a more

complex structure where individual grain size fractions can be more or less mobile due to the influence of neighbouring grains. Thus, a grain's relative particle size (i.e. that relative to its neighbour) becomes an important influence in predicting individual fractional transport in sediment mixtures. To account for this effect, additional descriptors for mixed size beds include direct sheltering effects of hiding and exposure functions (e.g., Egiazaroff, 1965; Ashida and Michiue, 1972; Parker et al., 1982b; Andrews and Parker, 1987 and Wu et al., 2000b), sorting (Miller and Byrne, 1966; Li and Komar, 1986; Kirchner et al., 1990; Buffington et al., 1992), structures (Nikora et al., 1998; Marion et al., 2003; Rollinson, 2006; Aberle and Nikora, 2006; Cooper and Frostick, 2009; Ockelford, 2011; Mao et al., 2011), particle pivoting (Miller and Byrne, 1966; Fenton and Abbott, 1977; Kirchner et al. 1995) and remote sheltering (Measures et al., 2008; Tait et al., 2008) etc. Although, the time-dependency for the development of these bed structure controls is recognised as crucial to accurate prediction of entrainment and transport from mixed beds (e.g., Haynes and Pender, 2007; Ockelford, 2011) there is, as yet, no mathematical term with which to account for temporal evolution of relative grain size effects (Section 2.6).

2.5.2 Debating the influence of 'hiding effects'

The exact influence of relative grain size over entrainment threshold and sediment transport remains contentious, with scientists providing both field and laboratory-based individual fractional load (q_{bi}) data ranging from no influence to highly significant influence. Descriptors such as equal mobility (Parker et al., 1982a; Wilcock and Southard, 1988), size selective transport (Parker 1990a, Parker et al., 1982a; Kuhnle, 1993; Wilcock and McArdell, 1993; Wathen et al., 1995) and size independent transport (e.g., Shields, 1936; Meyer-Peter and Muller, 1948) have stemmed from this work and warrant introduction, as specific to the mixed bed research of the present thesis.

Einstein (1950) first proposed the effect of hiding function in transport of sediment mixtures. However, his work was considered to be ahead of time and too little data were available to robustly validate his function. Hence, the first accepted hiding function was introduced by Egiazaroff's (1965) simple model with embedded assumption that larger particles, though harder to move because

of their higher submerged weight, are easier to move in mixtures because of their higher protrusion to flow. It is due to this higher protrusion that they experience higher fluid drag from the instantaneous shear stress and the lift component of the fluid flow (Zanke, 2003). On the other hand, smaller particles, though they have lower submerged weight, are harder to move due to being sheltered by the larger particles. Since this work, physical interpretation and mathematical description (e.g., White and Day, 1982; Parker et al., 1982a; Ashworth and Ferguson, 1989; Wathen et al., 1995; Wilcock and Crowe, 2003) can be summarised via two extreme scenarios:

Firstly, it could be assumed that although a river has mixed size sediments, its dynamics operate without any hiding/exposure effects. Each size fraction therefore works independently, irrespective of neighbouring fractions, such that smaller particles require lower entrainment shear stresses and larger particles require higher entrainment shear stresses. This mode of transport is referred as **size independent transport (Figure 2.8)**. In the case of size independence, imagining a bed of sediment mixtures, where every fraction in the mixture were surrounded by the grains of the same fractional size, then τ_{ci} and τ_{c50} would be same, i.e., $\tau_{ci}^{*} / \tau_{c50}^{*} = 1$. If this were true, then in an actual mixture of different size classes, the following holds true:

$$\tau_{ci} = (\rho_s - \rho) g D_i \tau_{ci}^{*} \qquad \text{Equation 2.25}$$

$$\tau_{c50} = (\rho_s - \rho) g D_{50} \tau_{c50}^{*} \qquad \text{Equation 2.26}$$

Rearranging equation 2.25 and 2.26 would provide:

$$\frac{\tau_{ci}}{\tau_{c50}} = \frac{D_i}{D_{50}} \qquad \text{Equation 2.27}$$

$$\tau_{ci} = \frac{\tau_{c50}}{D_{50}} D_i \qquad \text{Equation 2.28}$$

$$\tau_{ci} = const \quad x \quad D_i \qquad \text{Equation 2.29}$$

Equation 2.29 confirms that τ_{Ci} is directly proportional to grain size; the larger the grain size, the higher the critical shear stress for that size fraction and is represented by the diagonal line passing through the origin of Figure 2.8 is thus marked as size independent transport.

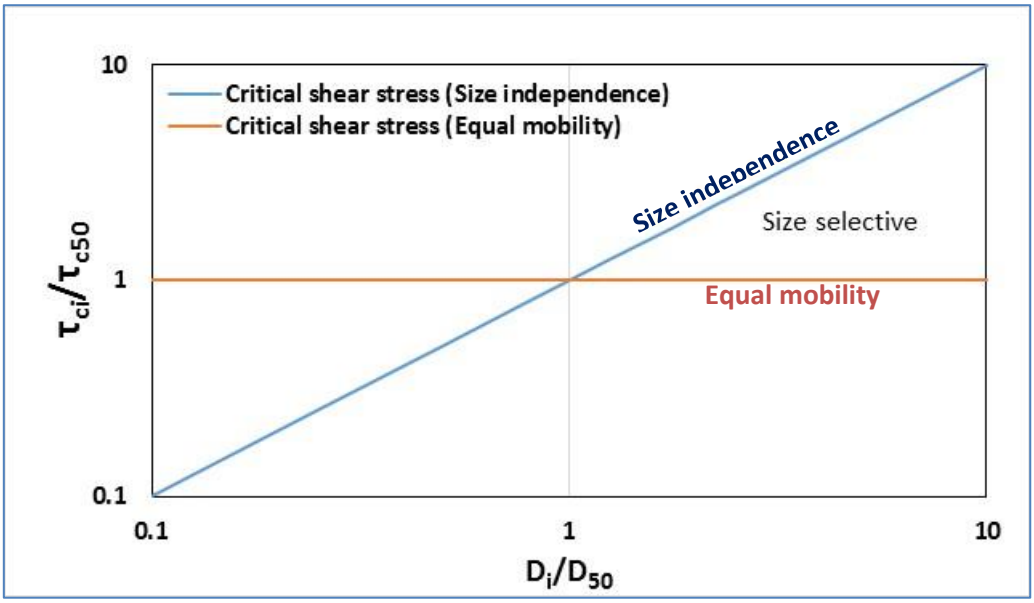

Figure 2.8: Mode of transport mechanisms in sediment mixtures: size independence, size selective and equal mobility.

Alternatively, it can be considered that hiding/exposure effects operate at their maximum. Hence, a larger particle experiences higher exposure to the flow, in that its apex is susceptible to faster flow (and hence higher shear stress) higher in the water column and the grain area exposed to such higher shear stress is larger, termed 'preferential drag' (Einstein, 1950). This makes the larger grains relatively easier to entrain than if they had been in a bed of uniformly sized grain (where their exposure would have been relatively less). Conversely, a smaller particle may experience extreme hiding in the sheltered valley (sometimes termed wake or col) between neighbouring large grains. This would minimise its exposure to flow shear stresses and reduce the likelihood of it being mobilised in a manner where it can move over its larger neighbour. Hence, the

hiding effect dictates that smaller grains require a disproportionately larger shear stress to entrain in a mixed bed than that required from a uniform bed of equal grain sizes. Thus, the hiding and exposure effects counterbalance the mass differences of the larger and smaller particles. As a result, all fractions tend to mobilise at similar critical shear stress. This is commonly referred to as **equal mobility (Figure 2.8)**. Mathematically, such hiding effects and the relation to bed shear stress can be written in its non-dimensional form by reducing Equation 2.25 and 2.26 to:

$$\frac{\tau_{ci}}{\tau_{c50}} = \left(\frac{D_i}{D_{50}} \right)^{1-m} \qquad \text{Equation 2.30}$$

$$\frac{\tau^*_{ci}}{\tau^*_{c50}} = \left(\frac{D_i}{D_{50}} \right)^{-m} \qquad \text{Equation 2.31}$$

Where, *m*=0 provides the case of size independence, with no hiding effect and *m* =1 provides the case of equal mobility.

In reality, transport in rivers is somewhere between these two extreme scenarios and is thus termed **size selective** (Ashworth and Ferguson, 1989; Parker et al., l982) as described by Figure 2.8. Significant experimental research has been undertaken to determine the degree of size selectivity, with experimental data from field and flumes indicate common values of *m* observed between 0.43 and 0.9 (e.g., Andrews, 1983; Komar, 1987; Ashworth and Ferguson, 1989; Parker, 1990a; Kuhnle, 1992; Wathen et al., 1995; a full review of *m* values can be seen in ASCE, 2007 in Table 3-1, p193 ASCE Manual 110). Whilst there is limited in-depth discussion in the literature to conclusively unravel why the *m* values obtained cover such a wide range, two points are agreed upon: (i) true size independence (*m*=0) is not found in mixed sediments, rather the lowest *m* value recorded is ~0.43; (ii) the end fractions of the grain size distribution (i.e. the finest and coarsest) consistently demonstrate stronger size selectivity. Thus, there is general agreement that the threshold shear stress for gravel entrainment depends more on relative than absolute grain size, but does likely retain a degree of dependence on absolute size (Ashworth and Ferguson, 1989) for all fractions. In addition, there is general consensus that the degree of

sorting of a distribution can change this parameter value (White and Day, 1982; Nakagawa et al., 1982; Misri et al., 1983, 1984; Samagae et al., 1986; Gomez, 1989; Kuhnle, 1992, 1993a, 1993b; Wilcock, 1993; Pender and Li, 1995; Wathen et al., 1995; Patel and Ranga Raju, 1999; Shvidchenko et al., 2001). For example, Wathen et al. (1995) observed a shift from size selective transport in a gravel-only mixture (m=0.7) towards equal mobility (m=0.95) with the addition of sand content (i.e. a wider grain size distribution and increasingly poorly sorted mixture); this work was strongly supported by a plethora of studies into enhanced fine mobility in bimodal beds (e.g., Wilcock, 1993; Kuhnle, 1992, 1993a; Shvidchenko et al., 2001; Saadi, 2002; Wilcock et al., 2003), including Wilcock and McArdell's (1993, 1997) well-cited bed-of-many-colours research which specifically tackled individual fraction response to hiding. Similarly, Shvidchenko et al.'s (2001) laboratory-based studies highlighted that an individual fractions' entrainment threshold can lower by 10-20% due to increased skewness towards fines in a distribution relative to skewness towards coarse.

In summary, the majority of these hiding functions have been developed from regression of bedload samples, in particular from the field. The influence of grain size and distribution is of well highlighted importance, in particular the role of sands (modality and skewness) in gravel beds. However, the mathematics requires bed composition analysis for individual fractions and assume that the proportions remain static over time (such that D_{50} is a constant). Given that the very nature of entrainment threshold is the removal of grains from the bed via transport, the temporal evolution of the bed may dictate a non-stationary hiding function. However, no study of hiding functions to date specifically analysed the associated antecedent or evolutionary dynamics. It is also recognised in literature (ASCE, 2007, Chapter 3) that hiding functions cannot generally be expressed in simple power law, because influence of grain size on mobility diminishes as relative grain size decreases; some functions parameterise this in their relations (e.g., Proffitt and Sutherland, 1983; Wilcock and Crowe, 2003), but only in a static manner, without any temporal parameter in the functions. Church et al., (1998) drew the recommendations that threshold motion is a function of the bed surface architecture as well as relative grain size, the former superseding the latter as structure continues to develop. Recent work by Mao et al. (2011) also recognises that grain size characteristics of armour layers are not

enough to infer sediment mobility and bed roughness; rather, they recommended use of detailed elevation models of the bed surface for understanding the availability of sediment for entrainment.

2.5.3 Threshold in sediment mixture and functions for fractional transports

While the preceding Section presents and discusses the generic form of hiding functions, and their possible influences on transport of sediments, this Section presents a discussion on different specific formulae available for predicting fractional transport in sediment mixtures, including the use of thresholds of motion for individual fractions and the determination of these thresholds. Given the wealth of literature available on this topic, the intention of this section is not to précis every existing formulae, rather to highlight their development, discuss those most cited and target specific formulae of particular focus on laboratory data in graded bed research (as specific to this thesis' objectives).

Empirical formulae are used to determine entrainment threshold of individual grain classes from within a mixture. Most of the formulae are dependent on the hiding functions (relative grain size) introduced in the section above and incipient motion of the median (or mean) size class (Eq. 2.32 -36). This approach also includes judicious selection of the Shields value employed (i.e. 0.03 < τ^*_{c50} > 0.06), introducing subjectivity and uncertainty into the approach (Section 2.4). Given that sensitivity in τ^*_{c50} has been attributed to differences in methodological determination of critical shear stress (Section 2.3) and characteristics of the bed material size (Nakagawa et al., 1982; Wilcock, 1993; Kuhnle, 1993b; Pender and Li, 1995; Patel and Ranga Raju, 1999), it is unsurprising that there is variability in documented work specific to fractional entrainment thresholds in different hiding functions (e.g., Egiazaroff, 1965; Ashida and Michiue, 1972; Parker et al., 1982a; Komar, 1987; Ashworth and Ferguson, 1989; Kuhnle, 1992; Wilcock and McArdell, 1997; Wu et al., 2000b). Applying the hiding functions of Egiazaroff (1965), Parker et al., (1982a), Komar (1987a, b), Ashworth and Ferguson (1989), Kuhnle (1992) and Wilcock and McArdell (1997), the work of Shvidchenko et al., (2001) predicted fractional threshold motion for a given Di/D_{50} of a natural bed. Their outcomes noted over

10-fold differences on the predicted incipient motion of the end fractions (in particular for the finer fractions), and suggest that the causes of such differences for the fractional shear stresses have been poorly reported (or misunderstood) in literature.

Taking fractional entrainment threshold determination, Egiazaroff's (1965) relation for incipient motion was one of the earliest pieces of work:

$$\frac{\tau^*_{ci}}{\tau^*_{cm}} = \left[\frac{\log 19}{\log\ (19\frac{D_i}{D_m})} \right]^2 \qquad \text{Equation 2.32}$$

In which τ^*_{cm} is the Shields number for the mean (arithmetic) size class (D_m) and τ^*_{ci} is Shields number for i*th* size class in the mixture; τ^*_{cm} could be considered as Shields' threshold value corresponding to the size (D_m), which Egiazaroff considered as 0.06. Egiazaroff's theoretical relation was developed on simple assumptions that increasing grain weight reduces mobility, and increasing protrusion of larger grains promotes mobility; his relation represents mobility between size independence and equal mobility. Ashida and Michiue (1972) noted a deficiency in Egiazaroff's relation; they observed that finer particles (D_i/D_{50}<0.4) become progressively harder to be entrained, and thus Egiazaroff's relation is particularly not efficient for sediment mixtures of wider distribution. Ashida and Michiue (1972) refined the relation of Egiazaroff (1965); their dataset were exclusively from experiments in sand and gravel beds, and they developed a two stage relation (Eq. 2.33 and 2.34) for the prediction of incipient motion of individual size class:

$$\frac{\tau^*_{sci}}{\tau^*_{scg}} = 0.843\left(\frac{D_i}{D_g}\right)^{-1} \quad for\ D_i / D_g < 0.4 \qquad \text{Equation 2.33}$$

$$\frac{\tau^*_{sci}}{\tau^*_{scg}} = \left[\frac{\log 19}{\log\left(19 \frac{D_i}{D_g}\right)} \right]^2 \quad for\ D_i / D_g > 0.4 \qquad \text{Equation 2.34}$$

In which τ^*_{scg} is surface based Shields number for the mean (geometric) grain size class (D_g) on bed surface, and τ^*_{sci} is surface based Shields number for i*th* grain class.

Parker et al. (1982a) and Parker and Klingeman (1982) introduced the concept of power relations in hiding functions as discussed in Section 2.5.2; similar power relations for hiding functions were subsequently proposed among others by Powell et al. (2001, 2003) and Hunziker and Jaeggi (2002). The hiding function proposed by Parker et al. (1982a) and Parker and Klingeman (1982) is:

$$\frac{\tau^*_{ci}}{\tau^*_{c50}} = \left(\frac{D_i}{D_{50}} \right)^{-m} \qquad \text{Equation 2.35}$$

where *m* is an empirical exponent between 0.5 and 1.0.

Wu et al. (2000a) introduced new hiding function, with improved performance on prediction of fractional entrainment and transports. They overcome the deficiency of D_i/D_{50} and introduced dependence on fractional proportion for fractional classes for their probability of exposure and hiding, and thus on their entrainment and transports. They proposed the following relation:

$$\frac{\tau^*_{ci}}{\tau^*_{c50}} = \left(\frac{p_{ei}}{p_{hi}} \right)^{-m} \qquad \text{Equation 2.36}$$

where P_{ei} and P_{hi} are the exposure and hiding probabilities for the i*th* grain class (Wu et al., 2000a) mainly dependent on their fractional proportion (Wu et al., 2000a); τ^*_{c50} is Shields number for median size class, considered as 0.03, and m=0.6 (calibrated value based on laboratory data).

However, as already discussed in the previous section (2.5.2) that power relation of hiding function is not ideal for predicting entrainment threshold in a bed, which due to water working can lead to development of mobile and static armour, and thus relative size effect in power form is not enough to include the diminishing relative size effect on entrainment threshold. In a bid to improve this, hiding functions were further progressed by Proffitt and Sutherland (1983) and Wilcock and Crowe (2003). The hiding function of Wilcock and Crowe (2003) replaced the constant value of the exponent *m* in the hiding functions by a continuous exponential function, Eq. 2.27:

$$m = \frac{0.69}{1 + \exp\left(1.5 - D_i / D_{50}\right)} \qquad \text{Equation 2.37}$$

Thus, the hiding function of Wilcock and Crowe (2003) is an advancement of the function proposed by Ashida and Michiue (1972), and by others who use constant exponent value to include relative size effect (Parker et al., 1982a, Wu et al., 2000a, Powell et al., 2001, 2003; Hunziker and Jaeggi, 2002).

A recent research by Recking (2010) using a large volume of flume and field data proposed a very simple hiding function as a power law of the D_{84}/D_{50} ratio; from data analysis, they observed that for a given ratio of D_{84}/D_{50}, hiding effect increases with increasing slope, and thus, their hiding function is dependent on slope as $(D_{84}/D_{50})^{-18\sqrt{S}}$ where S is river slope. Using the large bedload dataset and the hiding function, they also proposed a simplistic graded sediment model which predicts total bedload; fractional load computation is not required; discharge, active width, slope, and surface grain diameters D_{50} and D_{84} are the only data requirements; the model can predict 86% of data within the Efficiency Factor (EF) between 0.1 and 10, where EF is the ratio of predicted and observed bedload.

2.5.4 Bed structures, pavement and armouring

Although earlier sections have noted descriptors and controls of selective entrainment in terms of integration into threshold and transport equations, more fundamental, complementary research has been undertaken as specific to wider

structural arrangement of the bed particles. Of particular relevance to the present thesis is the effect of water-working on particle arrangement and structure (e.g., Komar and Li, 1986; Kirchner et al., 1990; Church et al., 1998). In 1990, Kirchner et al.'s research clearly noted that a deterministic value for incipient motion of a grain class in mixture is incorrect, as particle hiding, exposure and friction angles in water-worked bed are more accurately described as probability functions. This drew upon his earlier conclusion that grain friction angles depend not only on grain size but also (possibly more importantly) on local grain topography (Kirchner et al., 1990) which will exhibit spatial heterogeneity across the bed surface. Such small-scale topographic controls have been studied by many (e.g., Church et al., 1998; Nikora et al., 1998; Marion et al., 2003; Rollinson, 2006; Aberle and Nikora, 2006; Cooper and Frostick, 2009; Ockelford, 2011; Mao et al., 2011), and studies such as Church et al. (1998) suggest that entrainment thresholds may double due to the development of grain-scale structures under certain transport conditions for gravel bed rivers.

Armouring is the most well-documented of bed structure controls on entrainment threshold (e.g., Ashida and Michiue, 1971; Hirano, 1971; Proffitt, 1980; Gomez, 1983; Egashira and Ashida, 1990; Tsujimoto and Motohashi, 1990; Tait et al., 1992; Marion et al., 1997; Willetts et al., 1987; Church et al., 1998; Hassan and Church, 2000). It is a natural effect of water-working and partial transport conditions of mixed beds (Parker et al., 1982a: Wilcock, 1997a, 1997b; Lisle et al., 2000; Hassan and Church, 2000), in that low flows (i.e. low shear stresses) preferentially entrain the finer particles in a process called 'winnowing'; this leaves behind coarser particles as the bed surface, considered an 'armour layer'. This dictates that the surface layer is usually coarser than the mean annual load of transported gravel (e.g., Lisle, 1995), hence a number of sediment transport equations (e.g., Parker, 1990a) use the finer composition of the sub-surface as representative of the transport potential of the bed. Yet, it is important to note that by over-representing coarse material on its surface via armour (such that it is more readily available for transport) the river gravel load of an equilibrium river can be transported at the same rate as its finer component (which is less available for transport). The principle of mobile-bed armour is explained in Parker et al. (1982a) and Parker and Toro-Escobar (2002),

and is the most common armour condition in gravel bed rivers. That is, the surface has coarsened to the point necessary to move the grain size distribution of the mean annual gravel load through without bed degradation or aggradation. A mobile-bed armour gives way to a static armour as the sediment supply tends toward zero (Sutherland, 1991; Andrews and Parker, 1987). Of particular note is the study of Dietrich et al. (1989) who quantified the effect of coarsening on entrainment threshold, with armour layers requiring an applied shear stress of entrainment a factor of up to four fold greater than that of the subsurface grain size distribution. Similar work has been widely undertaken in laboratory flumes, with general agreement that water-working under partial transport conditions takes many hours for armour layer development (e.g., Andrews and Parker, 1987; Tait et al., 1992; Tsujimoto, 1999; Pender et al., 2001). Such time-dependency of this process is likely one of the undocumented uncertainties in the multiple entrainment threshold methodologies and studies reviewed by Buffington and Montgomery (1997; Sections 2.2-2.4). Although the mathematical descriptors of armouring are considered outwith the specific requirement of this thesis' research, the reader is referred to e.g., the transport equation of Powell et al. (2001) for detailed explanation.

During the process of armouring studies have also noted specific topographies and distinct patterns within the coarsening surface layer grains. For example, fieldwork undertaken in the Harris Creek, British Columbia by Church et al. (1998) reported identifiable and repetitive patterns such as stone cells and rings within the gravel surface. Their findings noted that such structures specifically increase resistance to sediment motion by up to 60% (Church et al., 1998). This was due to development of reticulate structures by larger grains. That is, they noted from series of runs in a flume of the replicate of Harris Creek that initial bed surface coarsened at low flows with fines winnowed away or sifted into pores of larger particles; larger particles rolled, but in contact with static particle of similar size, and then stopped, resulting cluster development. These then grew into reticulate structures during long hours of water-working of the bed (up to 100 hours), so as to mature with characteristic structure dimensions of length $10D_{84}$ and width $6.5D_{84}$. Similar more recent studies into bed structuring include e.g., Powell (1998), Hassan and Church (2000) and Kleinhans (2010) who draw the general conclusion that such structures increase resistance

to entrainment by an order of up to 4. In a similar regard, the most recent study to consider topographical resistance to entrainment is that of Mao et al. (2011). Their flume-based work clearly notes by analysing armour layers that threshold motion of sediment may increase up to two fold due to surface coarsening and development of surface structures of interlocked grains or clusters; using topographic data, his probability density functions of the bed surface indicated that bed surface are more compact and highly imbricated in static armour layer.

In addition, the effect of "remote" sheltering on initial motion and fractional transports has also received specific attention within the last few years (e.g., Measures and Tait, 2008). This is distinct from the direct sheltering previously considered in terms of hiding factors and neighbour to neighbour relative grain size effects (Section 2.5.2 and 2.5.3); instead, remote sheltering is the effect of a particular grain or structure on downstream flow structures and, thus, the amended shear stresses (and associated entrainment susceptibility) on equivalent particles downstream of the initial perturbation. Measures and Tait (2008) specifically studied the effect of grain scale topography for remote sheltering effects, observing a strong influence on a grain's initial motion and fractional transport. Their data were collected near shear stress of entrainment threshold. However, despite inclusion of remote sheltering as a variable, the model they proposed only predicts entrainment adequately for selective/partial transport conditions and requires very detailed measurements of flow and bed variables so as to have generally, to date, precluded widespread adoption.

Thus, in summary the water-working of the bed is accepted to alter the bed arrangement/structure into one more resistant to entrainment. This process is also accepted to be time-dependent, with full armour-layer development even in laboratory scaled experiment requiring many hours. Despite this, no entrainment threshold studies specific to fractional analysis specifically state, analyse or review the antecedent conditions that the bed has been subject to prior to the measurements taken. As such, it seems increasingly defensible that variability in the water-working of flume or field-based sediment beds can introduce wild uncertainty into entrainment threshold data and may be one reason why the last century of research into sediment transport has struggled to constrain a mathematical descriptor for entrainment threshold.

2.6 Stress history research

Given the conclusions of Section 2.5, the time (and space) dependency of entrainment warrants further review from direct (and indirect) interpretation of the literature. For example, unpicking the detail of Shields' thesis alone notes that he took at least more than 16 hours of experimenting period for one single experiment, one hour for each sediment sample for each discharge in the increasing discharge steps. This provides potential for these bed arrangement processes to be influential over his reference threshold and explanatory of its possible overestimate (compared to that of other studies; Section 2.4). It is for such reason that there is a small, emerging sub-discipline of research particular to examining the role of "memory stress" (alternatively referred to as "stress history") in rivers. This term is specific to describing a time-dependent memory effect, which can change river bed stability significantly enough to influence subsequent entrainment threshold. This typically describes the low flow period between significant sediment-transporting events where sediment transport rates are negligible or of very low partial-transport conditions. Some authors (e.g., Paphitis and Collins, 2005; Haynes and Pender, 2007; Ockelford, 2011) term this as sub-threshold or antecedent stress and, despite discrepancies in the approaches taken towards such incipient research, there is gaining momentum that accounting for the effect of memory stress has the potential to correct prediction of sediment transport and minimise uncertainty in sediment budget assessment.

Arguably, the first real insight of the effects of stress history stem from the field-based bedload data from 11 consecutive flood hydrographs recorded by Reid and Frostick (1986) in Turkey Brook; selected 9 hydrograph records shown in Table 2.1.

Table 2.1: Stress history results on entrainment threshold in Turkey Brook (after Reid and Frostick, 1986)

Flood event dates	Low flow variables between successive floods		Low flow memory duration between consecutive floods (days)	τ^*_{c50}	% higher compared to critical non-dimensional shear stress	
	Water depth (m)	τ^*			Shields (1936): 0.06	Miller et al. ('77): 0.045
10/12/1978	0.55	0.17	125	0.252	320	460
24/12/1978	0.06	-	7	0.029		
25/01/1979	0.17	0.076	25	0.085	42	89
13/02/1979	0.18	0.05	4	0.059	-1	31
13/03/1979	0.27	0.076	24	0.099	65	120
26/05/1979	0.13	0.08	18	0.059	-1	31
09/12/1979	0.28	0.13	189	0.125	109	179
27/12/1979	0.20	0.07	18	0.075	25	67
12/03/1980	0.14	0.09	77	0.120	101	168

Note: depth, shear stress and inter-flood duration were derived by present researcher from Reid and Frostick's raw data and from hydrological (discharge and water level time series) data received from UK Environment Agency

Although stress history relationships were not the intention of their work, later re-evaluation of the data (e.g., Haynes and Pender, 2007) demonstrates that increased memory duration (i.e. extending the inter-flood period from days to months) can increase the initial motion more than 5 fold (Table 2.1), as compared to Shields' initial motion ($\tau_c^* = 0.06$), or more than 9-fold if compared with Parker's empirical curve (Eq. 2.24, $\tau_c^* = 0.03$). These data also suggests that it is not only the duration of the inter-flood period but also the magnitude of 'low' flows during this interval which influence the 'memory' effect; specifically, higher inter-flood discharges (operating within the partial-transport condition) appear to result in more resistant 'memoried' beds. This is demonstrated clearly in the Turkey Brook data; whilst the two longest inter-flood durations (125 days and 189 days, in Table 2.1) induced the highest entrainment thresholds, the 125 day interval yielded the greatest effect due to to higher flow magnitudes during the interval period. In short, it is this data set which prompted wider investigation of the sensitivity of entrainment threshold and subsequent transport to the low flow conditions of the inter-flood periods.

Effect of memory stress on entrainment threshold and bedload transport is shown graphically in the transport of Turkey Brook in Figure 2.9. In the flood event of 10-11 Dec 1978 (top, left graph), initiation of sediment motion and also bedload transport were quite delayed in the rising limb compared to the other three floods. In this event, entrainment delayed considerably upto a higher depth (0.55m), whereas in the other three floods, entrainment and bedload were recorded earlier at considerably lower water depth in the rising limb. The main reason for this that the flood of 10-11 Dec, 1978 had a long dry period gap with the previous flood (125 days, also see Table 2.1) leading to development of a compact and stable bed; whereas in the other three floods, the gaps with the previous flood were very short, 5, 7 and 4 days respectively, and thus, these three flood events entrained sediment well early in the rising limb, which is fairly due to the reason that the bed structures were loosened by the immediate past floods.

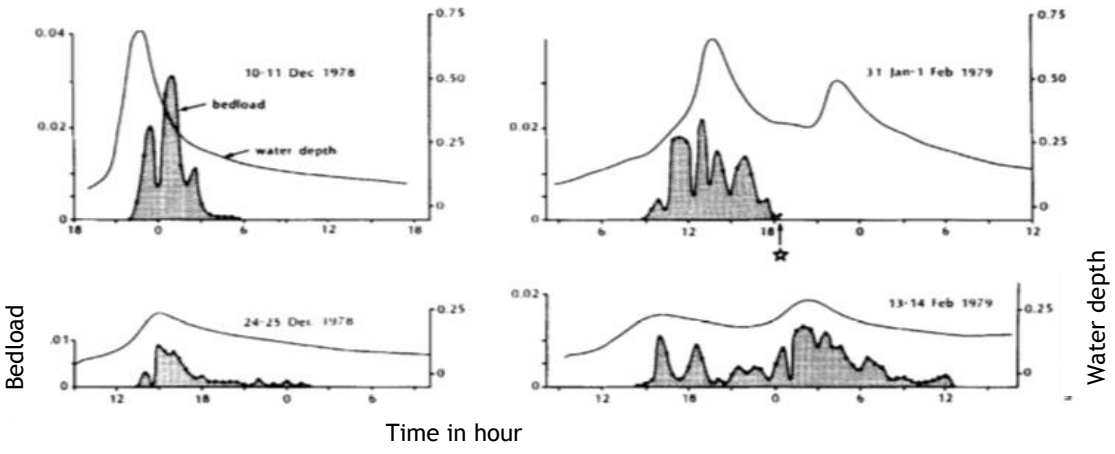

Figure 2.9. Bedload transport from three flood events in Turkey Brook (Reid and Frostick, 1986); in the flood event of 10-11 Dec 1978 (top left), transport is considerably delayed in the rising limb due to memory stress compared with the other three flood events.

The memory effect is further demonstrated in stream power (Figure 2.10) from the flood events recorded in Tureky Brook between 1978 and 1980 (Reid and Frostick, 1986). The transport database demonstrates that stream power needed during initiation of transport was considerably higher than the available stream power at the cessation of transport; in the Figure below, ω_0 is stream power at initiation of motion, and ω_0' is stream power at cessation of transport. This indicates that the prolonged inter-flood durations developed resistance in bed, and delayed transport of sediment at initiation. In the Figure, also shown is Bagnold's 100% efficiency, $i_b = \omega / \tan\alpha$ where α is particle's pivot angle.

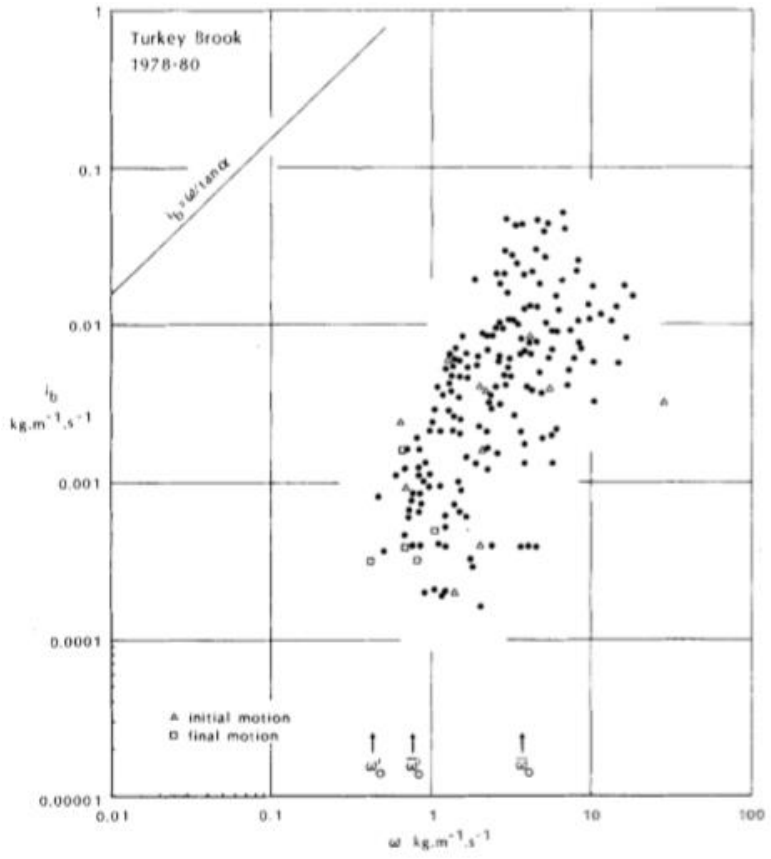

Figure 2.10. Stream power (ω_0) vs. bedload transports (i_b) from Turkey Brook (Reid and Frostick, 1986); eleven flood events between 1978 and 1980 showing requirement of much higher stream power at the initiation of motion than the cessation of transport.

At low flows, one logical complexity of field data (such as Reid's) is the inability to untangle the temporal development of physical sediment dynamics from the bio-chemical dynamics of the river bed (e.g., Gerbersdorf et al., 2005; Vignaga et al., 2011). Thus, recent memory research has deliberately employed flume-based methodology to isolate the physical flow-particle controls and tightly control flow variables during prescribed 'memory' periods. All published flume studies (Saadi, 2002; Paphitis and Collins, 2005; Monteith and Pender, 2005; Haynes and Pender, 2007;, Saadi, 2008; Haynes and Ockelford, 2009; Piedra, 2010 and Ockelford, 2011) are summarised in Table 2.2 and Figure 2.11 and show clear relationship between increased memory duration and increased critical shear stress. For example, the early work of Paphitis and Collins (2005) reported an increase of critical shear stresses (τ_{c50}^{*}) by as much as 60% due to memory stress (up to 120 minutes) effect in uniform sediment of sand size for low grain Reynolds numbers (smooth regime), shown in Figure 2.11 and Table 2.2; (their critical velocities as in Figure 2.12 were converted to critical shear stress by the present author). Whilst the order of magnitude is similar, memory-induced threshold gains are slightly lower for mixed-bed sand-gravel studies of rougher boundaries used in later researches. That is, Haynes and Pender (2007) observed an increase of critical shear stress by up to 48% (R_{e^*} 135-290; R_{ep} 1000-2000) for memory time scale of 5760 minutes in their bimodal mixture; Saadi (2002, 2008) observed a maximum 60% increase for his memory time scale of 540 minutes, and Ockelford (2011) reported gains of up to 12% in similar work (R_{e^*} 220-280) over a 960 minute memory timescale in her bimodal bed. Whilst the order of magnitude of memory related changes to entrainment threshold are in general agreement, differences in methodological set-up and sand content (Section 2.5) account for subtle variability in datasets.

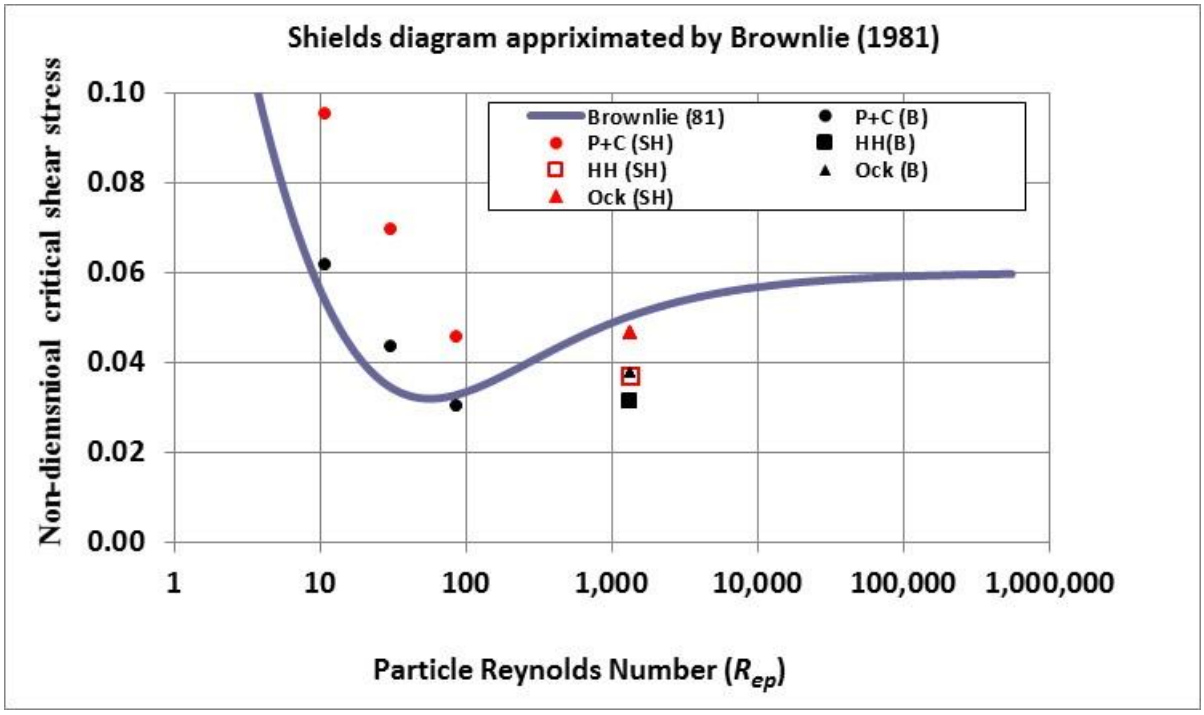

Figure 2.11. Entrainment threshold from stress history research: higher entrainment threshold in stress history (SH) experiment (red markers), relative to baseline (B) of black markers by different researchers plotted on Shields diagram modified by Brownlie (1981); P+C: Paphitis and Collins (2005); HH: Haynes and Pender (2007); Ock: Ockelford (2011).

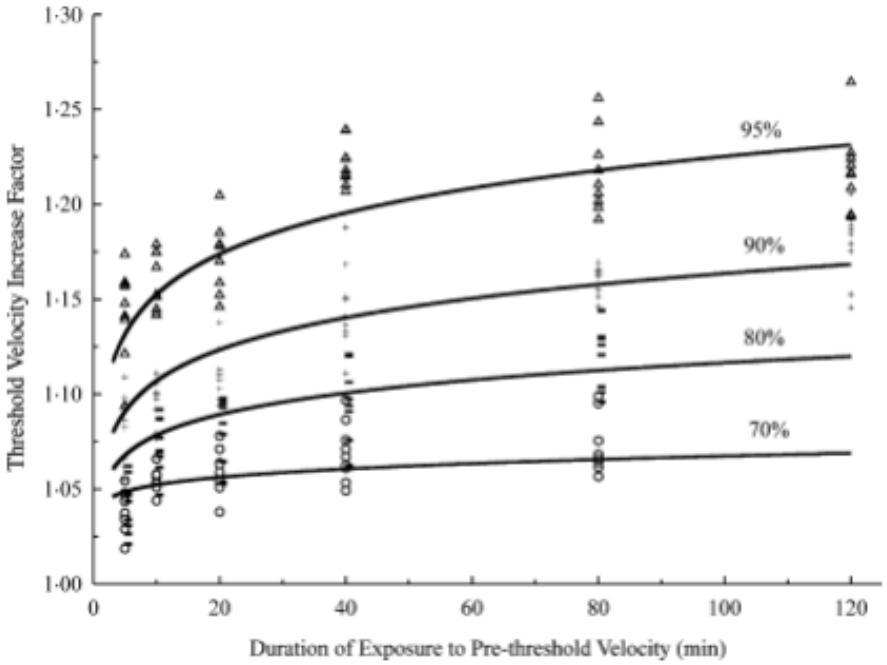

Figure 2.12. Effect of antecedent pre-threshold velocity durations on threshold velocities in uniform sand beds (Paphitis and Collins, 2005); the figure shows higher exposure duration and higher magnitude of pre-threshold velocities (70%, 80%, 90% and 95% of critical velocity) increases threshold shear velocities (e. g., 95% condition increases threshold velocity nearly by a factor of 1.25)

Arguably the largest issue of memory stress studies is inconsistency in methodological framework. Although Paphitis and Collins (2005), Haynes and Pender (2007) and Ockelford (2011) all employed visual approaches for determining their initial motion (Section 2.3), there is some disparity in methodology which precludes direct comparison: Firstly, the magnitude of antecedent sub-threshold flow applied varies between studies, in that all studies employ a flow 50% that of the entrainment threshold of the median grain size, with the notable exception of Paphitis and Collins' (2005) use of 70-95% threshold. Flows closer to threshold are likely to promote isolated dislodgement (in numbers less than the visual reference threshold value), local rearrangement and stronger restricting of surface grains; this may explain why their initial motion thresholds lie well above Shields values in Figure 2.9 (thus, suggesting an over

Table 2.2: Stress history results – comparison of present results with past studies

Researcher	Grain size D_{50} (mm)	Flume gradient	Sub-threshold flow characteristics		Max increase in non-dimensional critical shear stress (%)	Shear Reynolds number (R_{e^*})
			Exposure duration range (min)	Exposure flow magnitude range (%) relative to critical shear velocity/stress, baseline		
Saadi (2002, 2008)	5.19	0.004	180 to 540	-	60	199
Paphitis and Collins (2005)	0.19, 0.39, 0.77	-	5 to 120	70-95	60	3-18
Ockelford (2011)	4.8	0.005	10 to - 960	50	12	221-281
Haynes and Pender (2007)	4.8	0.007	30, to 5760	53 and 77	~48	135-290
Note: maximum increment on critical shear stress noted in this Table are all for longest exposure duration; Piedra (2010) results could not be presented as his comparison was against critical discharge						

estimated threshold). Secondly, notable distinction arises due to differences in investigator selection of sediment grade. Ockelford's (2011) work specifically analyses the influence of grade, suggesting that increased modality decreases the influence of stress history. This is supported by the greater response of Paphitis and Collins' (2005) unisize sand beds, underpinned by general acknowledgement that fines demonstrate higher packing density and stronger angle of repose (Kirchner et al., 1990 and general review of Saadi's memory work which used far higher sand content than other memory researchers). Thirdly, there is subtly in the stepped hydrograph approach used to increase flow towards threshold (step length, discharge increments) and the type of data measured and quantified; for example, the pure visual particle detachment count approach of Paphitis and Collins (2005) was adapted to a hybrid visual-reference transport approach by Haynes and Pender (2007) and Ockelford (2011) whereby it was the change in measured bedload which was analysed to quantify memory effects. This latter point is important, as these hybrid studies indicate that there is a degree of non-linearity between the response of threshold shear stress and bedload to stress history. In short, studies have shown that the bedload is more sensitive a variable. For example, Ockelford's (2011) work in unimodal and bimodal beds, notes a 43 to 96% reduction in bedload (for 10 to 60

minute memory time scales) compared with only ~10% change in the critical shear stress of entrainment threshold. Thus, decisions over methodology, threshold definition and cross-study comparisons must be executed with care and require robust defence as the discipline of memory research evolves. In addition, it is important to note that all studies to date appear to suggest that the influence of memory stress has an asymptotic relationship with antecedent duration, indicating that longer timeframes lead to ever decreasing influence. This appears logical, as the bed will eventually reach its optimum structure, yet as the longest laboratory experiments (Haynes and Pender, 2007) run only to 4 days antecedent flow there is no detailed research or general consensus as to when (or if) the timeframe of memory gains tend to zero.

Such laboratory-based studies have permitted detailed observation of surface based grain processes during this memory period, in terms of subtle changes to composition (e.g., Monteith and Pender, 2005) and specific data on changes to bed topography (Ockelford, 2011). All studies provide compelling evidence of local or in-situ grain-scale restructuring during extended memory durations, in terms of increased hiding effects, greater packing density of the surface and particle re-orientation into more streamlined/stable positions. The likelihood of such processes occurring below or near-threshold have long since been acknowledged, with even the early studies of Bagnold (1941), Chepil (1945) and Bisal and Nielsen (1962) reporting the importance of turbulence for critical shear stress in:

> "that erodible particles 'oscillate or vibrate unsteadily' before leaving the bed. If particles are allowed sufficient time to pass through this stage of vibration, they will essentially be subjected to the repositioning process. Madsen and Grant (1976), in a series of oscillatory flow threshold experiments noted that grains were rocking (in a 'to and fro' motion) about their position on the bed before the threshold criterion was satisfied. Hence, they argued that such movement might cause the bed to become more compact and in effect, more resistant to erosion." (Bisal and Neilsen, 1962)"

In this regard, the laser displacement data of memory-modified surfaces by Ockelford (2011) is the only study to truly quantify these below/near-threshold changes at the grain scale. Specifically, Ockelford reported changes of bed surface topography in response to memory stress; her work observes that particle re-orientation (typically to streamline within 15-30° of the flow direction), vertical settlement and a degree of grain-to-grain structuring (via cluster analysis) contribute to the additional memory stress of graded beds. Of particular merit is her data on roughness length, which develops to a greater amount in bimodal beds than equivalent unimodal or uniform beds. These findings from Ockelford's detailed memory stress work on bed structure in steady uniform flow shows similarity with the unsteady work of Piedra (2010) and Mao et al. (2011). Whilst Mao's work is summarised in Section 2.5.4, the work of Piedra was analysed in terms of critical discharge making direct comparison with shear stress based work difficult.

It needs to be emphasised here the memory stress is a time scale of the duration of sub-threshold stress; this itself should not be considered as a process; however this sub-threshold time scale can induce several processes as discussed herein. Concept of memory stress is an emerging science, and only has been researched in the recent periods. Many past researches, which involved prolonged period of water working (e. g., Shields, 1936, and Church et al., 1998), did not partition their findings, such as how much effect was attributed from sub-threshold memory stress; only future organised research could answer this, which will benefit the practitioners in using the appropriate effect (parameter), rather than lumped parameters. The limited number of memory studies as mentioned in Tables 2.1-2 explicitly quantified the memory effect on the increase of entrainment threshold and subsequent transport. Memory of subthreshold stress alone increases entrainment threshold by upto 60%, and can reduce transport by upto 80%; if this effect not included in bedload transport formula, then they might over-predict the bedload in similar order of magnitude. Their influence on the prediction of transport, particularly the over-estimation effect, is presented in the scope of chapter 6; effects are more categorically quantified due to different memory time scales. Water working of bed by sub-threshold stress leads to development of several key processes such as increasing size selective transport, vertical and horizontal winnowing of the

fines through particle oscillation and preferential entrainment of the smaller particles (Saadi, 2002; Haynes and Pender, 2007; Saadi, 2008; Ockelford, 2011); winnowing of the fines may lead to coarsening of the bed towards mobile armouring; Ockelford and Haynes (2013), due to memory stress, observed changes in local bed structure, particle re-arrangement, and spatial heterogeneity of sediment bed packing characterised by increasing vertical and horizontal roughness. Similar effect, not necessarily and explicitly from water-working by sub-threshold stress, on entrainment threshold and transport was discussed in Section 2.5.4. Key processes developing from such water working include stone cells and ring, armouring (mobile and static), changes in friction angle, changes in hiding and exposure, bio-stabilisation etc. Many of such water working studies (e.g., Komar and Li, 1986; Kirchner et al., 1990; Church et al., 1998) might well have implicitly included the effect of memory of sub-threshold stress; for example, Church et al. (1998) conducted experiments upto 100 hours employing low shear stresses below threshold condition, and then continued upto 2 times of Shields threshold value, and thus clearly embed memory of sub-threshold stress in their experiments, and thus in their overall findings. They noted development of stone cells in parallel to armouring of bed and observed that the joint effect of armouring and stone cells can increase entrainment by 2-fold; Fenton and Abbott (1977) noted an order of magnitude of increase of threshold shear stress due to changes in friction angle from water working. Several such effects were quantified in Section 2.5.4, and thus not repeated here. Vignaga et al. (2011) and Vignaga (2012) studies biostabilisation of sand-gravel bed, and observed 9-150% increase of threshold shear stress relative to abiotic bed.

The above discussion both on laboratory and field data shows that timescale and magnitude of sub-threshold memory shear stress require more attention in future research if their influence upon, and potential reduction in uncertainty for, entrainment threshold and sediment transport modelling of river systems are to be resolved to a much higher degree. To make explicit conclusions and permit direct comparison between memory research, the appropriate methodology and measured variables need to be scrutinised and data normalized. Addressing the mathematical description of memory stress 'correction' for entrainment threshold is also currently omitted from existing

studies, precluding general acceptance or adoption in standard practices (whether laboratory-based on modelling). These therefore form the basis of key objectives of the present thesis.

2.7 Application and drivers of memory stress science

Drivers for memory stress research focus on its impact of changes to sediment transport and the fluvial sediment/morphological system. Thus, all aspects of river management, such as water resource management, fluvial hazard assessment, habitat and fluvial-linked infrastructure design are implicitly dependent on reducing uncertainty in entrainment threshold, bedload and morphological-flow models. This Section therefore seeks to summarise four overarching drivers, as specific to river bed memory: (i) improvement of bedload functions of graded sediment, and sediment transport modelling; (ii) climate change and management of risk on flooding and morphodynamics; (iii) flow regulation, river training and other man-made intervention; (iv) water quality and ecology.

2.7.1 Sediment transport modelling

Despite significant research investment into hydraulic modelling of river systems and connected piped systems (e.g., EPSRC's funded consortia of FRMRC 1, FRMRC 2, FCERM), current river modelling practices generally suffer from minimal consideration of the sediment boundary parameters, variables and dynamics. Whilst in the UK much of this problem arises from a lack of field data on channel morphology, bed grain size distributions and sediment supply, it is exacerbated by the large uncertainty in the underpinning entrainment and transport formulae of sediment transport models, particularly for graded sediments. Sections 2.3 - 2.5 have discussed the causes for uncertainty in detail, documenting that existing bedload functions (e.g., Meyer-Peter-Muller, 1948; Bagnold, 1956; Engelund-Hansen, 1967; Ackers and White, 1973; Yang, 1973; Yalin, 1977; Parker et al., 1982a; Van Rijn, 1984; Parker, 1990a; Wu et al., 2000; Wilcock, 2001; Wilcock and Crowe, 2003) embedded within flow-sediment computational models lead to over estimation of bedload transport. As the effect of memory would appear to counter this error, the overall objective of this thesis (to assess the sensitivity of graded sediment transport models to

memory effects) is driven by the desire to recode sediment models to reduce uncertainty in a manner appropriate to practitioner confidence.

Regarding the specific modelling programmes available to practitioners, it is still most common to employ 1D models for representing the channel. Taking the widely-used examples of ISIS Flood Modeller Pro (ISIS, 2015), HEC-RAS (Version 4.1, 2015), MIKE11 (DHI, 2014) and others, these modelling technologies use a multi-fraction transport approach apparently implying transport of heterogeneous sediment. However, most technologies use uniform sediment formulae for predicting multi-fraction transport, and then use scaling factor for each size class to match fractional load with that observed. In the absence of calibration data, this approach can easily lead to bias towards size independent transport and hence brings more uncertainty to predictions; for example, a mixture of 10 size classes, requires 10 scaling factors. Advances on these commercial 1D models are found in academic level code (e.g., Wu et al., 2000, Parker, 2006; Peng et al., 2014; Qian et al., 2015) which employ graded sediment models, and thus are superior to modelling frameworks based around the scaling of uniform formulae. However, the exponent of the hiding functions in these graded approaches takes the form of a power law (Sections 2.5.1 and 2.5.2) in which the exponent value is constant; whilst it is able to assess the influence of relative size, it is unable to reflect time-dependent changes and structural changes to the bed, which may arise from memory stress. More-over, whilst the software can run in (quasi-) unsteady state, it is typically employed only for a single design flood event. This is problematic, as memory stress is a product of the flow-sediment relationship between multiple events (e.g., Reid and Frostick, 1986; Haynes and Pender, 2007; Ockelford, 2011; Mao, 2012) thus requiring longer-term simulations. Whilst this recent memory research focussed on the combination of two high flow events separated by a variable interval, it is well known that morphodynamic recovery to an initial “norm” may take longer than the interval period, hence there is clearer requirement for multiple event modelling of memory effects. The existing 1D software potential to work over such long time scales is generally inappropriate, as the long simulations compromise the time-step of the model (e.g., Pender et al., 2015) such that the unsteadiness of individual flood hydrographs is lost. As this hydrograph resolution is fundamental to accurate modelling of entrainment threshold and size

selective transport, standard 1D software is difficult to apply robustly to sediment transport modelling.

Two-dimensional sediment morphodynamic modelling for catchment and river scale application has made good progress in the recent decades (Coulthard and Macklin, 2001; Langendoen, 2001); its strength and weakness on working at different spatio-temporal scale are therefore discussed. CAESAR (http://www.coulthard.org.uk/CAESAR.html) is a Catchment or Reach based two-dimensional (2D) cellular modelling technology for predicting morphological changes (Coulthard and Macklin, 2001; Coulthard et al., 2002). It is an extremely powerful tool and can predict in time scale of even thousand years. This technology has been applied to over 100 catchments and reaches around the world including Carlisle catchment in UK, for time scales upto 10,000 years. However, the modelling tool works on steady state conditions, which is a limitation for its application in flood memory driven erosion and flood risk because of the extreme unsteady nature of hydrology and hydraulics in memory driven processes.

2.7.2 Climate change and flood risk management

Widespread research into UK climate change (e.g., UKCP09; Jenkins et al., 2008), concludes that over the last half century more of the winter rain has fallen during intense wet spells and UK seasonality effects in rainfall (less in summer, more in winter) are increasingly pronounced. Future projections suggest that by the year 2080 the wettest day of winter, relative to the baseline period of 1961-1990, will be -10% and +50% (Ekström et al., 2005; Kay et al., 2006; Fowler and Ekström, 2009; Murphy et al., 2009), while summer rainfall will change by -50% to +30%. However, there is notable uncertainty in the effect that these changes will have on river response. Recent ideas are that flood frequency may increase particularly for the smaller floods, while extreme floods may decrease and thus there will be clear changes to the memory timescales and variables of a river system which potentially affect response-recovery cycles of sediment transport and morphodynamics.

The inter-relationship between sediment transport, memory and sediment-related flood risk is recently made explicit via policy and associated research.

For example, the Flood Risk Management (Scotland) Act 2009 was the national transposition of the European Parliament and Council Directive 2007/60/EC (the similar Flood and Water Management Act 2010 exists for England and Wales). Within the document there are numerous references to the role of the Scottish Environment Protection Agency (SEPA) including: (i) to assess change to natural features which *"contribute to the transporting and depositing of sediment, and the shape of rivers"* in terms of exacerbated (or altered) flood risk and; (ii) develop a flood risk map to *"show the potential adverse consequences associated with … areas where floods with a high content of transported sediments or debris floods (or a combination of such floods) can occur"*. This is supported by earlier regulations derived from the Water Framework Directive (EC 2000/60/EC), such as the Water Environment (Controlled Activities) (Scotland) Regulations 2005 which lists engineering/management activities regulated as specific to sediment management in river systems. In short, there is increased awareness that the sediment controls to floodwater conveyance are important for flood risk management.

The underpinning science is that for reaches suffering sediment accumulation, the 'filling' of the channel reduces the cross-sectional area such that, without maintenance (e.g., dredging), the flood risk from bank overtopping is increased (e.g., 2009 autumn flood of Cockermouth; 2014 winter flood of Somerset Levels). As the cross-section of the channel continually adjusts to the imposed flow, the cross-section cannot be assumed a constant. For example, following a major flood the channel will take months/years to 'recover' to the cross-sectional 'norm', during this recovery there may be multiple smaller floods of the same return period, but each will be conveyed in a channel of different cross-section. Yet, this is memory effect, which is not currently accounted for in the design and analysis of fluvial flood defence schemes, which use a single survey of the river channel and floodplains with which to run flood simulations based on a single *X*-year extreme flow event. Adopting such an approach assumes that the capacity of the channel is identical for all *X*-year events simulated, thus failing to account for memory morphodynamics in the system. The recent academic work of Pender et al. (2015) has therefore trialled 1D sediment-flood modelling in HEC-RAS over 50 year timescales for the River Caldew (a tributary of the Eden catchment of the Carlisle floods 2004, 2005,

2009). Although his model underestimates peak flows through use of a daily mean flow (daily time step; see Section 2.7.1), coupling his 1D output changes in channel geometry to a 2D flood inundation model (TUFLOW) demonstrates 'worst-case' scenarios of 160% increase in flood extent for 1 in 2 year RP floods down to a 9% increase in 200 year RP events. This clearly shows the sensitivity of models to sediment memory–recovery cycles and the imperative need for multi-event sediment transport modelling in flood risk assessments. Given the requirement of such models to incorporate entrainment, transport and memory effects this robustly defends the focus of the present thesis' objectives.

Further, wider research into the specific sediment-related flood risks note that climate change impact alone may alter UK catchment sediment yields to increase supply to river channels by up to 35% (Coulthard et al., 2012, CIRIA, 2013). Such elevated risks of greater siltation and reduced floodwater conveyance have led to the Pitt Review update (Evans et al., 2008) highlighting *"…river morphology and sediment supply as top priority for sediment drivers in the 2050s"*. This has been recognised via the "urgent" research priority of sediment management within the national Flood and Coastal Erosion Risk Management (Moores and Rees, LWEC 2011) strategy document. Hence, sediment uncertainty in flood risk is a well-known uncertainty in flood risk research which is rapidly emerging in the UK to attempt to unravel the complexities of temporal dynamics and controls of the river sediment system.

2.7.3 Flow regulation and river training

Natural hydrology is regulated by humans for a variety of purposes, such as flood and erosion control, irrigation, abstraction, flow diversion, hydropower, environmental and ecological balance and amenity. In the UK, 95% of flows (taken at gauge stations) are regulated (Sear et al., 1992) via weirs, sluices, culverts, dams and barriers which act mainly to attenuate flood peaks and increase the interval between high flow events. Such river sections are likely to lack natural channel forming discharge due to flow control, hence can lead to exacerbated sediment deposition which can compromise asset design life. However, the over-prediction of bedload by many bedload functions (Section 2.7.1) may erroneously reduce design life estimates, leading to mismanagement

of the asset in terms of e.g., higher frequency of sediment flushing events than required, which in themselves may reduce the water resource or hydroelectric economic revenue of the reservoir operation.

Another example of thesis drivers is associated with anthropogenic design calculation of river bank protection, particularly that for protecting infrastructure (roads, rails, buildings, and services) from the scour/erosion processes of a morphologically active channel. There are a wide range of "hard" and "soft" engineering techniques that have been successfully applied, including rip rap, gabion baskets, willow spilling, mattresses and vegetation planting. Design guidance on increasingly advocated "soft" bank face protection techniques can be found in the *Good Practice Guide for Bank Protection: Rivers and Lochs* (SEPA, 2008) or *Waterway Bank Protection: A guide to erosion assessment and management* (EA, 1999). One specific driver of the present research thesis is therefore the correct calculation of the entrainment threshold of the bed, as employed in the calculation of basal endpoint controls on toe scour in bank protection measures. Similar issues arise in terms of scour risk of wider river infrastructure, such as bridge piers, abutments, flood defences/embankments and where service pipes are laid within the bed (Cranfield University, 1999; Melville and Coleman 2000; CIRIA C551, 2002; Sear et al., 2003; SEPA, 2010).

2.7.4 Water quality and ecology

The EC Water Framework Directive (2000/60/EC) commits the UK to achieving "good" water quality within our river systems as defined by criteria from biological, chemical, ecological and morphological conditions. Of particular relevance to Scottish rivers is the quality of the benthic habitats which underpin the lucrative sport fishing, of trout species and (most critically) Atlantic Salmon with the inland sport fishing industry worth £126m/year to the Scottish economy each year (Rivers and Fisheries Trusts of Scotland, 2010). Species such as the caddis fly larvae and the midge reside in gravel substrate, feeding the higher trophic levels of the food chain. The benthic habitat is also crucial to the development and protection of the eggs and fry of the Atlantic Salmon. As these benthic species utilise microtopographic features to avoid being entrained by flow (e.g., Death 1996; Effenberger et al., 2006; Rice et al., 2008) and depend

on appropriate bed composition and structure to permit oxygen-nutrient flows within the subsurface, the mobility of sediment at low or moderate flows can damage and dislodge benthic animals (Gibbins et al., 2007). Persistent fine sediment deposits smothering fish eggs are a well-known and widespread cause of reduced fish populations in UK rivers (e.g., Beschta and Jackson, 1979; Carling and Glaister, 1987). Hence, the bed consolidation and delayed entrainment thresholds due to memory effects are likely exacerbating the persistence of fines, as flushing flows may be incorrectly calculated without a memory correction term.

2.7.5 Other drivers

Hiding and size selective transport remains the key mechanism in memory bed; and hiding is stronger in gravel frame-work deposits with heavy minerals depositing in the pore spaces (Reid and Frostick, 1985). Density driven sorting and selective transports are major issues in conglomerates and gravel deposits. Heavy minerals such as placer gold and diamonds are found in gravel deposits of historic or active gravel bed streams (e.g., Hughes et al., 1995). Due to the density difference, these heavy minerals show a downstream decrease in their concentration, and thus their hiding factor becomes higher in the gravel deposits, as does the re-mobilisation threshold of these minerals. Therefore, the sequence (and hence memory stress) of sediment-mobilising flows is important in predicting the location of such deposits.

Similarly, gravel and sand mining can influence sorting and transport of sediment. Large-scale, economic excavation means that mining can often exceed the limit of the supply, and thus influence initial motion and bed degradation/reprofiling (Galay, 1983). Sand and gravel mining is still considered an attractive source of raw material in building industry (Kondolf, 1994; Rinaldi et al., 2005). Such mining can have detrimental effect on channel incision (Rinaldi et al., 2005) and river bank erosion (Kondolf, 1997), leading to scour of bridges, sediment control structures and dams (Kondolf, 1997; Rovira et al., 2005). Mining is common in western United States, and was a popular source of building materials in Europe during the 1950s – 1990s, before UK regulations (e.g., Controlled Activities (Scotland) Regulations) came into practice. Sediment transport models aided with flood memory effects could, theoretically, provide

more robust sediment predicts and thus play an important role in the management of more sustainable mining-recovery cycles.

2.8 Summary research gaps

- Given the detailed, and critical, review of existing sediment entrainment and transport knowledge in previous Sections the identified research gaps are summarised below: Threshold motion data set from research and studies from nearly one century have shown significant scatter and uncertainty; there is emerging evidence (from a handful of recent research studies) that the lack of understanding of memory stress effects may remain a key factor for such uncertainty.

- Methodological differences between investigators of memory stress have precluded detailed analysis of memory stress influence over entrainment and transport. There is need for a methodological framework appropriate for mathematical modelling (i.e. correction) of memory stress.

- The reference transport approach is generally considered the most reliable method for determining threshold motion. Shields (1936), Parker et al. (1982a) and Shvidchenko et al. (2001) have defined practically measurable reference transport rates at initial motion, but do not hold common consensus of the reference value.

- Most existing bedload functions are fitted using the critical shear stress as reference, generally taken from Shields higher value on the curve; because of higher threshold value, it makes their applicability limited in case of memory stress which is dominant in further low flow regime. So, there is scope of research to choose particular formulae which are applicable in low shear stress (e.g., Wu et al., 2000b), and further parameterise them for application in memory stress events.

- Sediment load in gravel bed rivers naturally shows grade dependent response with control lying on transport of each fraction. Ockelford (2011) and Mao (2012) have demonstrated that uniform, unimodal and bimodal beds yield different responses to memory stress. Whilst the present

science and knowledge (Section 2.5 and 2.7.1) do not have explicit parametrisation of predicting such disproportionate response of fractional transports, development of new mathematical functions to incorporate memory effects and their disproportionate grade and fractional responses would be of merit to improved sediment transport modelling.

- The FCERM research priorities (and other UK drivers) suggest focus of the present research would be to identify areas where memory stress can influence sediment regime, sediment related flooding, and ecological balance. Improved sediment modelling and sediment-related risks have become increasingly important to infrastructure resilience, in light of both climate change and extending the design life of river structures.

Chapter 3: Physical modelling: experimental set-up

3.1 Introduction

Based on the outcomes of the literature review, it is evident that the examination of a single variable from river systems with any degree of precision requires tight control in a laboratory setting. Flume-based research has a strong track record of sediment transport analysis and empirical derivation, with all existing memory-specific research being conducted in this environment. Experiments were, therefore, carried out in the Hydraulic Laboratory in the School of Energy, Geoscience, Infrastructure and Society in Heriot-Watt University, Edinburgh, UK using a re-circulating Armfield tilting steel flume of traditional 0.3m width. With this in mind, the present Chapter discusses both the methodology and associated rationale used in the current thesis. Specifically, this addresses: (i) the choice of sediment grain size distribution, in terms of reality and known sensitivities from previous research; (ii) design of the "stability test" assessment of memory effects on entrainment threshold, in terms of overcoming the problems identified in existing studies; (iii) selection of methodology used for entrainment threshold definition, in terms of removing the limitations of earlier works on post-processing for mathematical descriptions.

3.2 Experimental matrix

Overall 84 experiments were conducted, including calibration, test runs and repetitions. Baseline data (i.e. that with *no* memory stress; referred to as non-memoried beds henceforth in this thesis) was repeated several times in determining the entrainment shear stress τ_{c50}^{*} , and in determining the magnitude of memory stress, set to 60% of τ_{c50}^{*} . Each memory experiment was repeated at least three times. Two separate experimental data sets were carried out, specific to using unimodal and bimodal gravel sediment mixtures (Section 3.4). Within each data set, five memory timescales (Table 3.1) were employed, compared with that of additional baseline runs.

Table 3.1: Matrix of experimental runs with unimodal and bimodal sediment mixtures; number of repeat for each run is generally 3 or more; median grain size (D_{50}) for each mixture is 4.8mm; 64 minute stability run is identical in all experiments; over the period of 64 minutes, a 14 step discharge hydrograph is employed at an increment of 1.25 l/s from discharge 2.5 to 18.75 l/s; step of 6 minute duration are employed at sediment sampling steps between 7.5 to 18.75 l/s; magnitude of memory stress is 60% of entrainment threshold; each memory experiment is run for respective memory duration prior to stability period of 64 minutes

Experiment type	Experimental code	Memory stress time scale (min)	Total experimenting period: run time in memory stress + time in stability test (min)
Unimodal mixture: Baseline	UM_B_0	0	0+64
Unimodal mixture: Memory experiment	UM_SH_10	10	10+64
	UM_SH_30	30	30+64
	UM_SH_60	60	60+64
	UM_SH_120	120	120+64
	UM_SH_240	240	240+64
Bimodal mixture: Baseline	BM_B_0	0	0+64
Bimodal mixture: Memory experiment	BM_SH_10	10	10+64
	BM_SH_30	30	30+64
	BM_SH_60	60	60+64
	BM_SH_120	120	120+64
	BM_SH_240	240	240+64

Repetition of experiments helped in assessing confidence limits, uncertainties and outliers of dataset in the experiments (Wilcock and McArdell, 1993; Shvidchenko et al., 2001; Saadi, 2002). Generally, repetitions were within ± 0.5% (based on threshold shear stress) and less than ± 10% (based on bedload); where outliers to these trends have been observed these have been justified in the relevant results sections. The variation is higher in bimodal bed than in unimodal bed as bimodal was more responsive to memory than other beds; this is discussed in detail in the results section (Chapter 5). Considering the memory response on bed shear stress in previous research (Section 2.6), this degree of variation of shear stress is expected to have little (or no) impact on the

assessment of memory effect on entrainment threshold (as shown in the result section in Chapter 4 and 5). Whilst the variation in bedload from repeatability may seem higher, it is comfortably in line with other studies specific to low flows, where bedload is extremely sensitive to minor changes in bed shear stress (for example, Paintal, 1971; Parker, 1989; Shvidchenko et al., 2001, Bunte et al., 2004). The sensitivity in terms of mathematical function of bedload vs. shear stress developed in this study are sensible and discussed in more detail in the results sections of Chapters 4 and 5.

3.3 Flume - 0.3m wide facility

Experiments were carried out in an Armfield recirculating rectangular flume (a 3D schematic shown in Figure 3.1. The steel bed, and glass walled flume has 7.0 m of working length, 0.3m width, and 0.5m height; this is considered a traditional flume dimension, equivalent to flumes employed in all other stress history studies (Paphitis and Collins, 2005; Monteith and Pender, 2005; Haynes and Pender, 2007; and Ockelford, 2011). Whilst a few studies note the possible influence of side-wall effects in the narrow channel (e.g., Shvidchenko, 2000), these effects are typically constrained to < 0.02 cm affected near-wall width in low flow experiments (such as those considered herein) and will be akin to those of earlier memory research (hence permitting direct comparison). The flume can be tilted to a prescribed slope via a mechanical jack located towards the upstream end of the flume. Whilst the Armfield equipment proffers a Vernier scale, the accuracy of manual mechanical jack is well-known to be limited and the present project iteratively fine-tuned the slope using surveying techniques (level-staff gauge survey; Figure 3.3) of the flume bed and flume rails. Given that the screed board used to level the initial bed and the instrument carriage ran on the rails, it was essential that both flume bed and flume rail were parallel. The instrument carriage set on the flume rails held the pointer gauge (for bed and water surface profiling; Section 3.5.4).

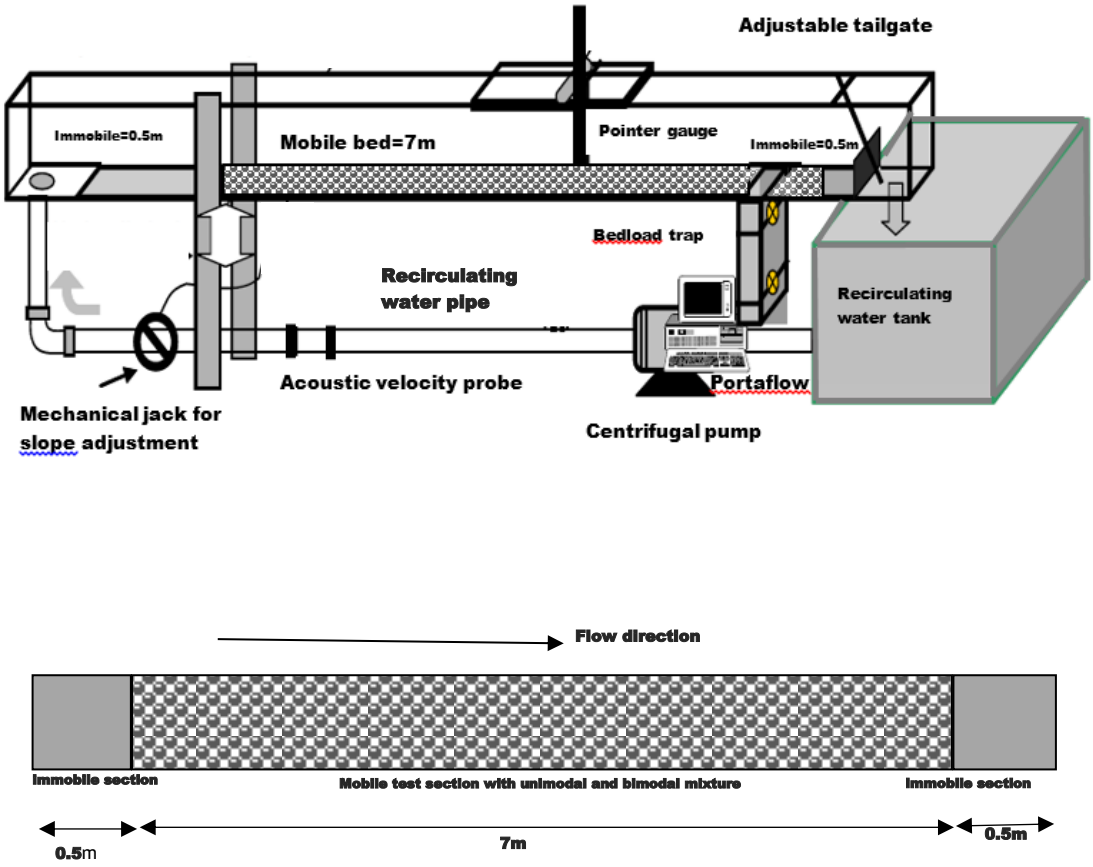

Figure 3.1: Top figure: 3D schematic of re-circulating Armfield flume showing 7m long working section with experimental sediment bed, and two immobile reaches prepared with much larger sediment size (25 mm) at flume inlet and flume outlet; immobile bed at inlet is aimed to prevent any scour due to sudden entry of flow, and help to generate turbulent boundary layer; the immobile bed at outlet is aimed to trap mobile test sediment and prevent it from being washed into the water tank; Bottom figure: plan view of flume bed showing 7m long mobile bed with test sediment, and immobile bed at each end.

The flume re-circulated water from a tank placed at the outlet of the flume by an impeller pump and pipe network back to the inlet of the flume. The discharge of the pump through the pipe is displayed on a PortaFlow velocity and discharge measurement system. Two acoustic sensors are attached to the flow pipe, which transmits acoustic signals to the PortaFlow; velocity is calculated from these acoustic signals and discharge is calculated using the pipe's flow area. The

minimum signal strength value of the PortaFlow recommended by the manufacturer is 40%, while the strengths recorded during all experiments were above 80%. Given the accuracy and precision of the Portaflow in velocity measurement, which is ±0.01m/s, the discharge hydrograph for the present set of experiments has confidently been automated and controlled using an input file for the pump's frequency (Hz) vs. discharge, giving an advantage over manual pump flow settings used in previous stress history research. These discharge-frequency rating curves were developed through several pilot experiments (run prior to the main experimental programme Section 3.5.3). In all runs, the oscillation of the pump generated discharge was within ±2% of the target discharge values (Section 3.5.3). Shear stress was calculated for each target discharge; discharge steps were varied in incremental steps of 1.25 l/s between 2.5 and 18.75 l/s (Section 3.5.3). The ±2% variation over the target discharge translates as shear stress uncertainty of less than ±0.3%; thus, there was negligible impact on the derivation of shear stress and thus assessing the impact of memory can be assumed.

Water was recirculated from the open water tank situated at the tailgate end of the flume; thus, generally the same water being maintained at ambient room temperature was recirculated in each experiment (except occasional minor refilling of the tank, probably due to evaporation or loss); thus the water temperature was estimated in the room temperature range between 18 and 23 degree centigrade for the majority of the experiments. Water temperature in the Portaflow set-up was maintained in the above temperature range for discharge calculation. Significant changes in water temperature can result in different shear stress from same the discharge. Viscosity is a measure of resistance (Wikipedia) of a fluid, which is water in the present thesis; viscosity tends to fall as temperature rises, and thus exerts less resistance to flow. Therefore, same discharge, in case the water temperature is higher, will generate higher velocity and bed shear stress due to less resistance, and thus will generate higher bedload transport. Taylor demonstrated this effect by carrying out experiments in 21^0C and 36^0C (Taylor, 1971). Thus, the results section specifically includes discussion of outlier data specific to water temperatures in the laboratory.

3.4 Sediment: unimodal and bimodal mixtures

Past work has clearly evidenced memory effects being present in both sands (Paphitis and Collins, 2005) and sand-gravel mixtures (Reid and Frostick, 1986; Monteith and Pender, 2005; Haynes and Pender, 2007; Ockelford, 2011). Given that most UK river beds are gravel based mixtures and Ockelford's recent study indicates that modality and, possibly, the finer fraction of mixtures exhibit relationships with memory, the present experimental programme judiciously selected two grain size distributions specific to assessing these issues. Thus, two grades of sand-gravel mixture of unimodal and bimodal distribution, were used in the experiments in the present thesis. Both the mixtures comprised eight classes of sediment ranging from coarse sand (1 mm) to medium gravel (16 mm); see Figure 3.2. Two classes are medium to coarse sand (1.0 to 1.4 mm and 1.4 to 2.0 mm); the other six classes are gravels from 2.0 to 16 mm. The geometric standard deviations, σ_g, of the unimodal and bimodal mixtures are 1.65 and 1.93 respectively, and thus, both mixtures comprised "poorly sorted" sediment (i.e. $\sigma_g \geq 1.6$) as calculated from $\sigma_g = (D_{84}/D_{16})^{0.5}$. This selection of sorting is in line with many other flume studies (e.g., Shvidchenko 2000; Monteith and Pender, 2005; Haynes and Pender, 2007; Ockelford, 2011) and approximates to natural river beds in the UK (Ashworth and Ferguson, 1989 for Allt Dubhaig in Scotland; Reid and Frostick, 1986 for Turkey Brook, in England; Piedra, 2010 for Endrick Water in Scotland). The fractional contents of the unimodal mixture are similar to those used by Ockelford (2011) and Shvidchenko et al. (2001); the composition of bimodal mixtures is similar to Monteith and Pender (2005), Haynes and Pender (2007) and Ockelford (2011), except that the bimodality index has been made more pronounced in the present mixture for the finer class of gravels (2 to 2.8mm), see Figure 3.2. Bimodality index is defined by the relation $D_c/D_f * \Sigma p_m$, (Eq. 4 of Wilcock, 1993), where D_c and D_f are particle size of the coarse and fine modes respectively, and p_m is the fractional proportion of the two modes. Accordingly, bimodality index of the present mixture is 1.22. Overall, the results from the present experiments will allow direct comparison with existing stress history research and wider flume-based research data sets. The subtle increase in the bimodality index as mentioned above has been made in the present set of experiments, compared to that of Ockelford's research, so

as to better test her conclusion that modality strongly influences memory effects upon bedload transport and entrainment threshold.

The distribution of the size classes in both of the mixtures is approximately normal for the unimodal mixture, with very minor skewness (towards larger fractions) noted in the bimodal distribution (see Figure 3.2). Importantly, the choice of the minimum size class in the sand range prohibits development of bedform, around the flow condition of entrainment threshold of the median size class particularly in gravel bed rivers (Young and Warburton, 1996).

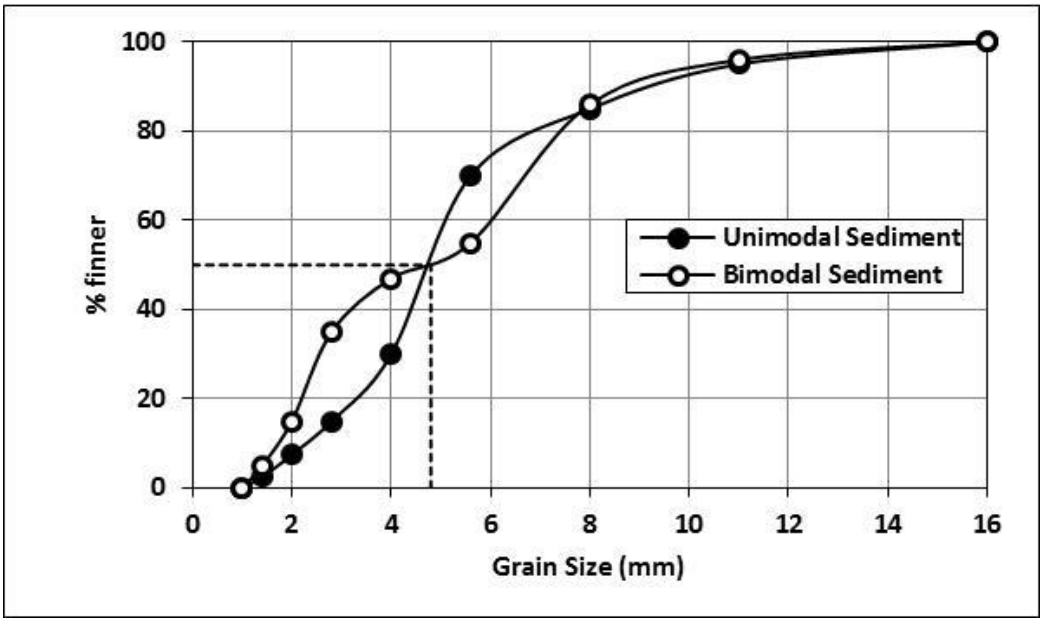

Size range (mm)	Fractional contents of size classes in the mixtures	
	Unimodal	Bimodal
1 - 1.4	0.025	0.0.05
1.4 - 2	0.05	0.1
2- 2.8	0.075	0.20
2.8 - 4	0.15	0.12
4 - 5.6	0.4	0.08
5.6 - 8	0.15	0.31
8 - 11.2	0.1	0.1
11.2 - 16	0.05	0.04
D_{50} (mm)	4.8	4.8
D_{16} (mm)	2.9	2.1
D_{84} (mm)	7.9	7.85
σ_g	1.65	1.93
Skewness	-0.05	-0.25
Note: Density of sediment is considered as 2600-2650 kg/m^3 (Shvidchenko et al. 2001)		

Figure 3.2: Grain size distribution curves: unimodal and bimodal sediment mixtures; dotted line showing point of intersection for 50 percent finer at median grain size of D_{50}=4.8mm, which is same for both distributions.

3.5 Flume Set-up

3.5.1 Flume slope

Preparation of the flume slope was started from horizontal bed (zero slope) of the flume; this was established via a mechanical screw-type jack, and slope reading manually from

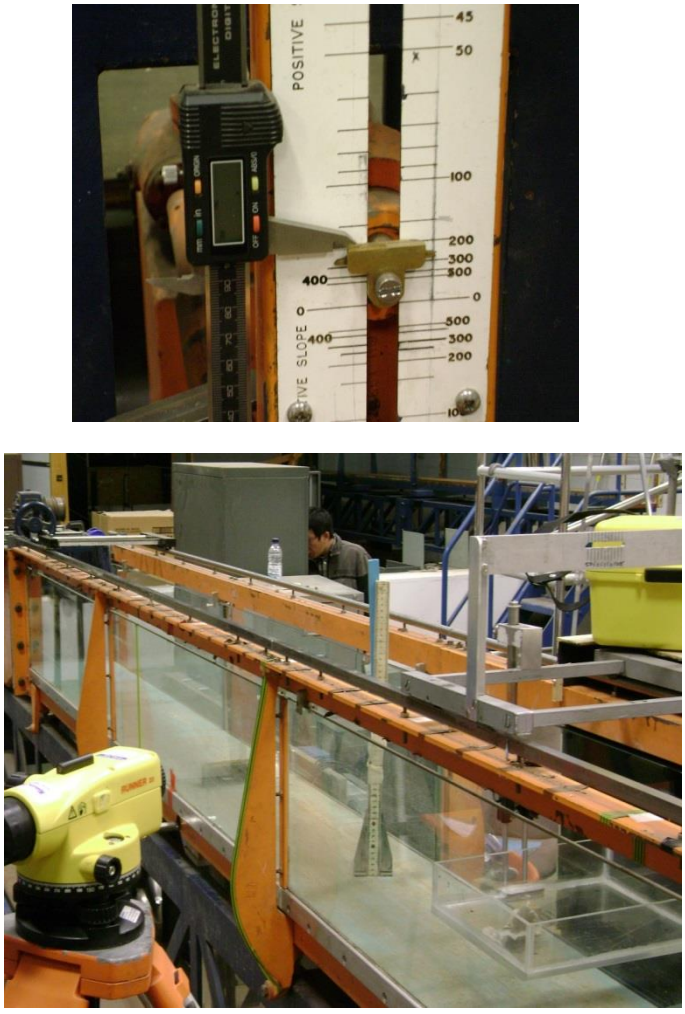

Figure 3.3: Flume slope preparation: Level-staff gauge survey of flume bed and flume rails (bottom); Vernier scale for fine tuning of slope (top)

the Main and Vernier Scale (Figure 3.3, top), accurate to approximately ±0.05mm. The zero slope along entire flume length and across flume width was fine-tuned through a level-staff gauge survey of both the flume bed and instrument rails (Figure 3.3, bottom); readings were taken at every 0.5m along the flume length. A flume slope of 1 in 200 was established and cross-checked for all runs using this technique (Figure 3.4).

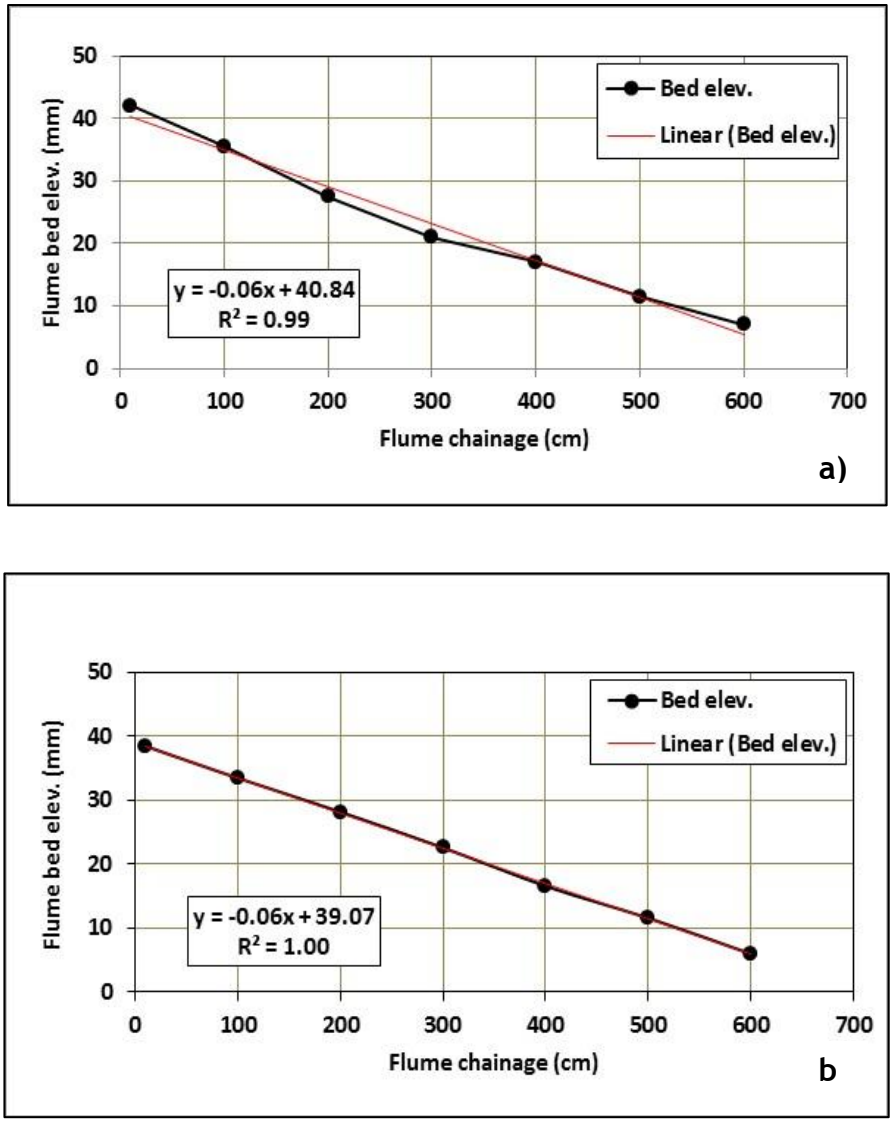

Figure 3.4: Flume slope of 1 in 200: a): after initial setting of slope by mechanical jack-screw, b); fine-tuned slope after iterative level-staff gauge survey.

3.5.2 Flume bed

A 60 mm thick flume bed was prepared for each experiment with the unimodal and bimodal sediment mixtures; based on the D_{50} fraction this approximates to > 10 layers of sediment and is deemed appropriate to preclude scour to the flume bed during low-flow, low-transport experiments such as those employed here (e.g., Shvidchenko and Pender, 2000; Monteith and Pender, 2005; Ockelford, 2011). The underpinning methodology had four stages:

Firstly, sediment stocks of each mixture were prepared. The mixtures were prepared in batches and the principle was simple; the lower is the volume/weight of each batch, the better the mixing. As such only 5% of the total weight (173 kg) was taken in each batch to prepare the mixture, and finally with full volume of mixed sediment, the bed was screeded by a screedboad. Screeding of bed may have effect on the statistical distribution of bed relative to the bulk mix (Cooper and Tait, 2008). Thus, during screeding one operator was employed (researcher himself) to prepare all experimental beds to keep consistency of the distribution in the screeded bed; further the consistency of the screeded bed was checked by taking photographs after preparation of the bed, and by counting the coloured D_{50} and D_{84} grains in an area of 150mm by 150mm. To aid photographing and counting of sediments on the screeded beds, three classes of sediments were coloured by ultra violet colour: D_{16}: red, D_{50}: yellow and D_{84}: orange. The theoretical ratio of the fractional proportion of D_{50} and D_{84} in the bulk mix for unimodal and bimodal bed ratio is 3.2, and 0.39 respectively; photographic counts of the screeded bed from test runs and from selected experiments provided the ratio of the proportions of D_{50} and D_{84} were found slightly higher, less than 0.5% to the theoretical ratios. Thus, the screeding seems to give a similar representation of the bulk mix, and would not lead to any notable bias on distribution from the theoretical mix.

Secondly, the two immobile reaches of coarser gravels (D ~25mm) as described in the caption of Figure 3.1, were screeded to a depth of 60mm for a 0.5m length near the inlet and outlet of the flume; the functionality of these two immobile reaches was already described in the caption of Figure 3.1.

Thirdly, the remaining 7m "test section" of the flume length was screeded to the prescribed 60mm thickness of either unimodal or bimodal sediment using a steel screedboard, which slides along the two rails of the flume pre-set to the 1 in 200 slope condition. This is routine practice for sediment bed preparation (e.g., Haynes and Pender, 2007; Piedra, 2010 and Ockelford, 2011).

Fourthly, for each experiment, full mixing of the bed/sediment was carried out for the entire 7m test length of the flume, with near-outlet material re-sieved to remove trapped particles and recycled them back into the test bed. An equivalent weight of material as that "lost" to the bedload trap was also added back into the test bed. All experiments had an equivalent draining period, to ensure that beds were of equal antecedent moisture content, as earlier studies (e.g., Monteith and Pender, 2005) had hypothesised that drier beds exhibited weaker packing arrangement, higher mobility and greater uncertainty with regard to stress history; the draining periods were maintained digitally in a run log file from the Portaflow, which helped to maintain identical draining periods between consecutive experiments.

The above procedure was specifically designed to overcome well-known problems relating to screed-induced bias in the statistical distribution of the surface sediment sizes as discussed in earlier paragraph.

3.5.3 Flow Settings and stepped discharge hydrograph

The theoretical stepped discharge hydrograph was designed in the present thesis based on the research results from previous stress history experiments (Haynes and Pender, 2007 and Ockelford, 2011) and other past research on incipient motion of unimodal and bimodal sediment mixtures (Paintal, 1971; Taylor and Vanoni, 1972; Wilcock, 1993; Wilcock, 2001). Crucial to this was an initial estimate of entrainment threshold of the bed and an estimate of general transport conditions. This review yielded a peak discharge of 18.75 l/s, considered to be sufficient for mobility of the highest grain class (11.5 -16 mm) in both of the unimodal and bimodal mixtures in the present thesis. The lowest discharge of 2.5 l/s is considered sub-threshold for the beds used (confirmation is provided in Section 4.5.3). And, the incremental step of 1.25 l/s induces approximately 2% increase in bed shear stress; given that previous stress history

research has recorded a minimum memory effect of a 4% change to bed shear stress, a 2% step is considered appropriate resolution so as to determine memory-induced alteration to entrainment threshold.

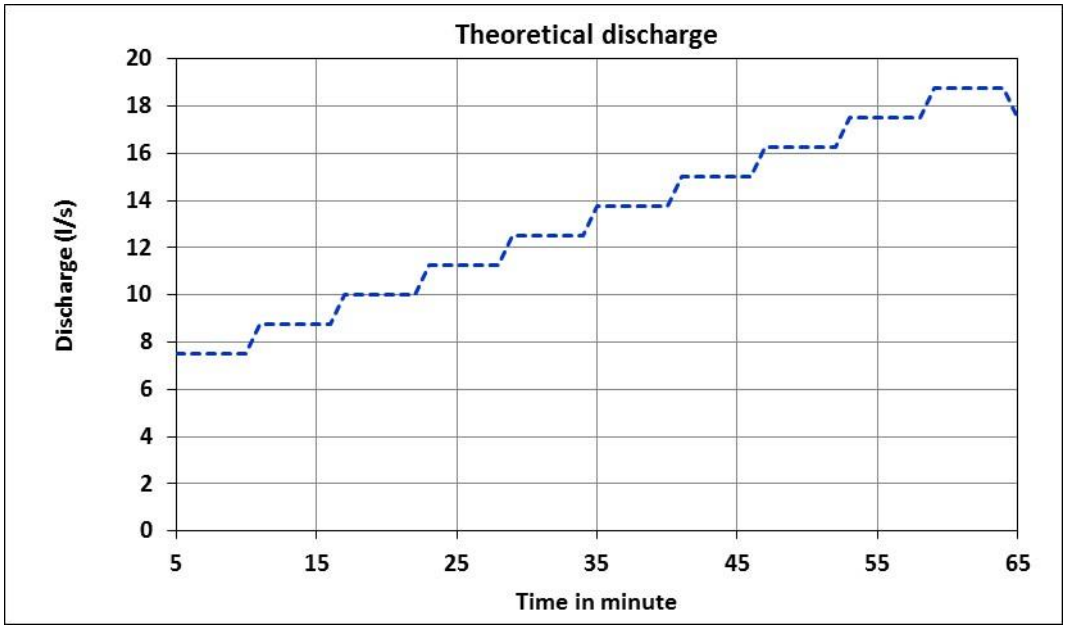

Figure 3.5: Theoretical discharge hydrograph used in the stability test (shown for bedload sampling steps starting at 7.5 l/s).

Inflow discharges to the flume were operated automatically by being programmed through an input file (electronic/digital file) of the frequency (Hz) of the pump. The frequency (Hz) data of the pump is a pre-processed excel file, and was read from a computer to the flow control system (inverter and Portaflow) to run the pump; see Section 3.3. Thus, the pump's frequency (Hz) needed to be calibrated to generate the discharges according to the target values. Pilot experiments were carried out to generate a dataset of discharge vs. Hz, and a rating curve was established (Figure 3.6). This rating curve was used to predict Hz values for the set of target discharges to the flume for all experiments. Respective rating curve was established for each sediment grade as it was observed that the rating curve developed for unimodal mixture was not applicable for the bimodal bed. Because experimental set-up (and instruments) were same in all experiments except the sediment mixtures, it is fair to assume that bimodal bed was likely to offer different friction to flow due to grain size

distribution (Ven T., Chow, 1959) with unimodal bed and thus affects discharge through the flume, and so affects pump's efficiency (Hz) and necessitated a different rating curve for discharge vs. Hz.

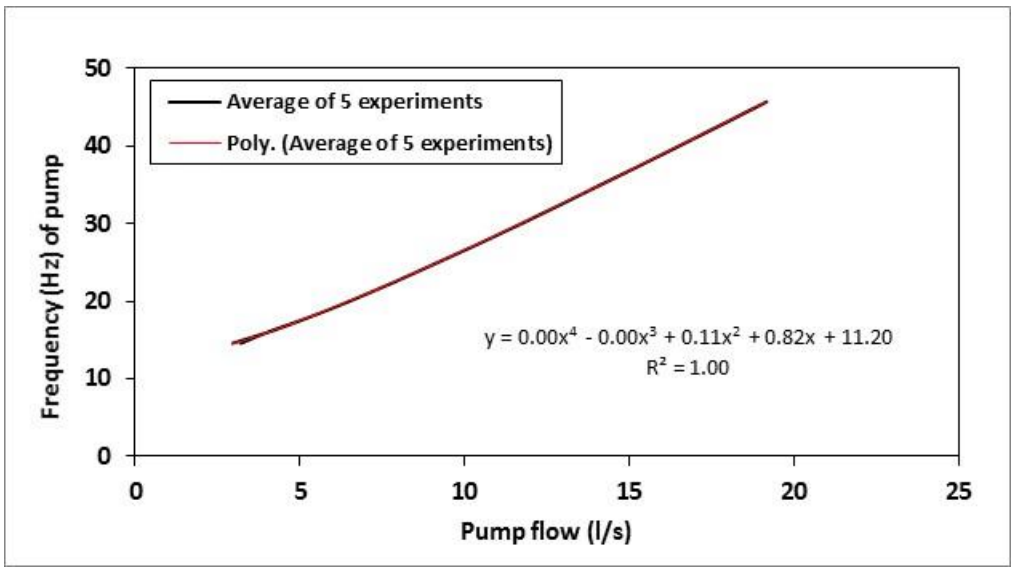

Figure 3.6: Calibration of pump discharge against pump frequency for generating target discharge (theoretical discharge).

In comparison with earlier memory experiments, the advantages of the automated system used herein include: high precision of timing of flow changes; perfect equivalence of rate of flow transitions; provision of extra user capability for wider manual measurements e.g., bedload sampling, depth measurement and photographing; overall, minimisation of uncertainties and errors in data collection. Thus, this methodological control capability is considered a significant advance over earlier memory studies and the pump's fluctuations in Figure 3.7 are quantified in Section 3.3 in line with defending a robust set-up.

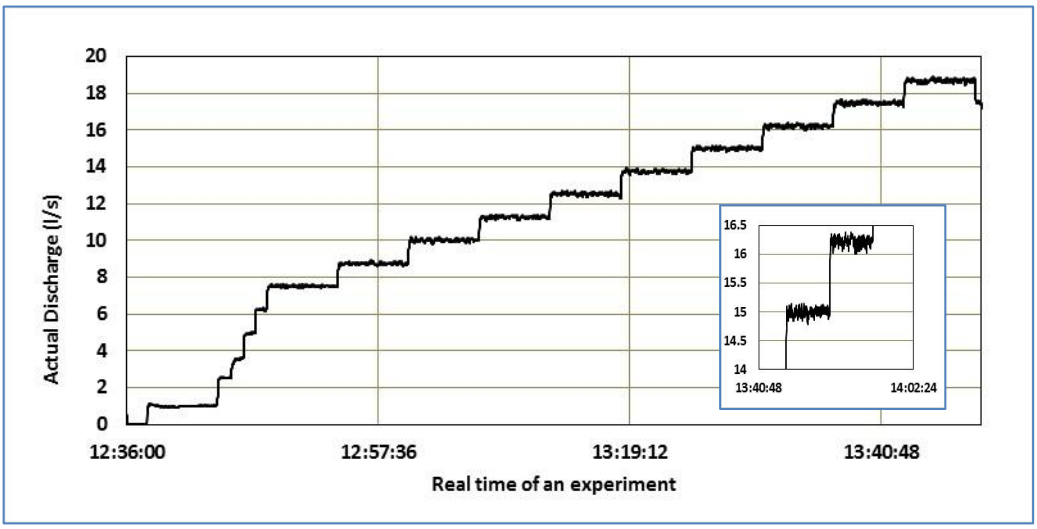

Figure 3.7: Actual hydrograph used in an experiment generated by the pump from pre-defined Hz (derived from pump rating curves, Figure 3.6) (actual hydrographs for each experiment are recorded in digital log file); there is oscillation in pump generated discharges; range of such oscillation is more clearly shown in the inset of the Figure (variation of discharge is less than ±2% of target discharge, and the variation in shear stress is maximum upto ±0.5%).

3.5.4 Uniform flow set-up

Establishing uniform flow in a laboratory flume is vital. In uniform flow, gravity forces are in equilibrium with the frictional forces. Thus, if uniform flow can be established, the experimental results are free from other external disturbances (e.g., precluding back water effects from tailgate (downstream boundary), or perturbations in bed formation in the upstream reach of the flume). Thus, uniform flow was assessed and controlled via adjustment of the tailgate during pilot runs where, simultaneously, water surface elevation and bed level were recorded at 0.50m interval by a Mitutoyo Pointer gauge (model SD-12" A; accuracy of ±0.01mm) mounted on the instrument rails. Uniform flow depth from two reference chainages (3m and 6m) are compared for uniform flow performance and presented in Table 3.2. From these data, differences in depth between the two chainages at all discharge steps were found to be typically less than ± 0.5% along the test section. One setting of tailgate position for each

mixture (unimodal and bimodal) was determined which provided the best uniform flow depth.

Table 3.2: Example data set on the uniform flow depth along the length of the flume

Discharge (l/s)	Flow Depth (mm) at different chainage along length of flume		Difference with average (in %)	
	Depth (mm) at ch. 3m	Depth (mm) at ch. 6m	ch. 3m	ch. 6m
2.50	80	82	-1.23	1.23
3.75	89	88	0.56	-0.56
5.00	92	93	-0.54	0.54
6.25	99	100	-0.50	0.50
7.50	104	105	-0.48	0.48
8.75	110	110	-0.23	0.23
10.00	113	114	-0.44	0.44
11.25	117	119	-0.85	0.85
12.50	121	121	0.00	0.00
13.75	122	123	-0.41	0.41
15.00	127	127	0.00	0.00
16.25	130	130	0.00	0.00
17.50	133	134	-0.37	0.37
18.75	139	139	0.00	0.00

3.5.5 Bedload transport

Bedload transport was sampled for each step of the rising flow hydrograph, starting at a discharge of 7.5 l/s for unimodal experiments, and 8.75 l/s for bimodal experiments. The first (lowest) step for sample collection was decided from pilot experiments and visual observation of sediment movement; these deduced that sediment deposition into the sediment trap at discharge smaller than the above values was negligible and impractical to collect at lower discharges.

The sediment trap (0.15m width x 0.03m downstream length) is located at chainage 5.25 m from the upstream end of the test bed (Figure 3.8). Each sample was collected for a duration of 6 minutes during each period of constant discharge on the hydrograph; this duration was decided upon with consideration of the time required for flow and sediment movement to stabilise within each

step (Shvidchenko et al., 2001) and bedload samples are collected under steady state uniform condition in each step. The free fall of sediment through the rectangular sediment slot/trap to the rectangular perspex box is controlled by a rotating cylindrical/axial type brass shaft (Figure 3.8) which has two holes. This shaft, when open, allows free fall of sediment entering the sediment trap into the sediment collecting box. The shaft when closed is fully blind. Axis rotation (open-closed/empty/replace-open) takes approx. 30 seconds. The replacement Perspex box was filled with water prior to re-opening and remaining air released via a horizontal side-valve; this precluded escaping bubbles artificially dislodging bed sediment local to the trap, as noted in previous stress history experiments as a major cause of uncertainty in collected bedload data (e.g., Monteith and Pender 2005).

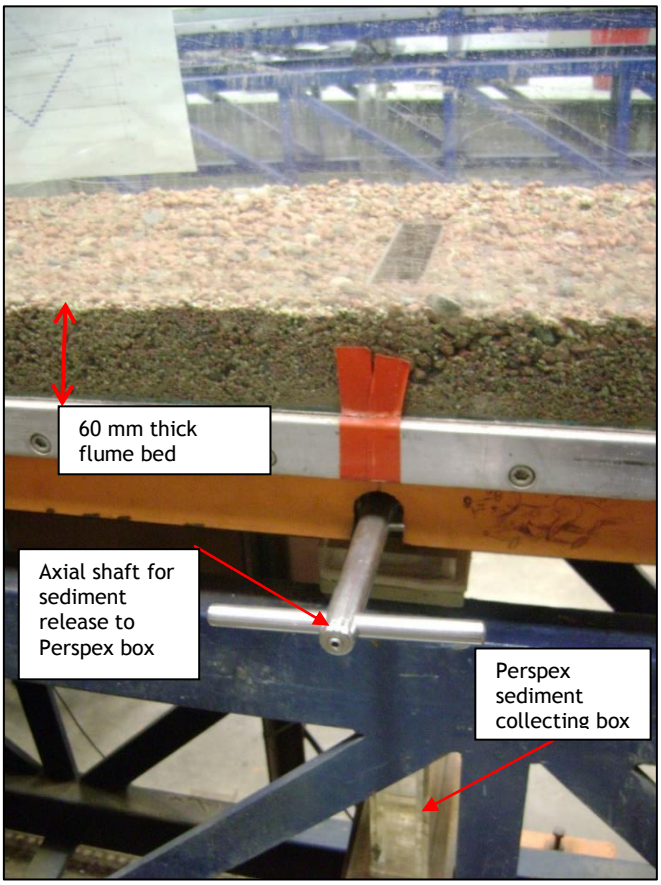

Figure 3.8: Bedload sediment slot/trap on the flume bed at chainage 5.25 m from the inlet of the flume.

Each sediment sample collected in the trap was oven dried, weighed and sieved for their analysis. Sediment mass of the dried sediment (in grams) was recorded to ±0.001g accuracy. Sieving at ½ phi interval provided equivalence to the initial grading of sediment generating the mixtures. This analysis was consistently controlled by use of a digital sieve shaker, using identical prescribed sieve settings and durations for all samples. Results from the analysis are presented in the Chapters 4 and 5. In all analysis (Chapters 4-5) and also in chapter 6 while compared with model predicted results, observed and predicted sediment load were converted from mass transport to volumetric transport; for conversion, density of natural sediment was used as 2650 kg/m^3 (Shvidchenko et al. 2001; Recking, 2010). The present research uses sediment of the same source as Shvidchenko et al. (2001), who derived the density as 2600-2650 kg/m^3.

In previous memory stress research, the memory effect has been assessed on entrainment threshold and on bedload transport using a constant offset value of memory gains over a non-memory benchmark condition. In all studies to date, this analysis has employed a visual approach for determining entrainment threshold. However, the literature review (Chapter 2) clearly notes that the entrainment threshold can significantly differ if a reference transport approach is adopted, rather than a visual technique. Further, there is a recognised disagreement of the definition (value) of reference transport employed by different authors (Shields, 1936; Parker et al., 1982a; and Shvidchenko et al., 2001). Moreover, past studies have shown that bedload transport may be generated in gravel bed streams at flow condition which are well below the reference transport value of Shields (1936), which is traditionally the most common reference value used in engineering practice. With these factors in mind, the present thesis rationalises and justifies a change in memory-based methodology, away from the deterministic visual definitions of Paphitis and Collins (2005), Monteith and Pender (2005), Haynes and Pender (2007) and Ockelford (2011), towards a reference transport based approach using a stepped hydrograph for the following reasons: (i) low flow steps permit analysis of first motion, progressive entrainment-transport, and general transport conditions; (ii) this permits examination of a range of existing reference transport thresholds, against the present data set; (iii) such references can be scrutinised for applicability and sensitivity to memory effects; (iv) references provide a directly

measurable, more robust and more strongly empirical approach to entrainment definition; (v) the holistic data set, with detail at near-entrainment values, allows quantification of the non-linearity of memory effect. The advantages of this methodology are returned in the Results sections discussions (Sections 4.7 and 5.6).

3.5.6 Selection of memory stress characteristics

The aim was to choose memory time scales for which memory effect is known to be more sensitive, and a higher resolution of memory scales than previous studies, so as to allow better representation of non-linearity in the mathematical descriptor of memory stress, which is a key objective of the present thesis (Chapter 1).

In previous memory research, shorter memory durations were observed to allow greater reaction to bed stability, entrainment threshold and transporting ability (Haynes and Pender, 2007, Ockelford, 2011). In 10 to 60 minutes memory time scales, the rate of increase in entrainment threshold and rate of decrease in bedload were observed to be significantly higher than at longer memory time scales, such as 5760 minutes employed by Haynes and Pender (2007), and 960 minutes employed by Ockelford (2011); in the longer memory time scales, the rate of increase (or decrease) was attenuated, and the trend line of the variables tends to be asymptotic with time axis as described in Chapter 2 (Section 2.6). The present thesis, therefore, employed short memory time scales with a high resolution (10, 30, 60, 120, and 240 minutes) appropriate to the intention to develop a robust mathematical function for bedload, and to capture better description of memory effect on non-linearity on bedload.

The present thesis employed a memory stress magnitude, which is 60% of the threshold condition of the non-memoried bed. This is in line with previous memory stress research, including lying central to the range employed by Haynes and Pender (2007) (53% of τ_{c50}^{*} to 77% of τ_{c50}^{*}). Due to the range of the pump, lower discharges suffer higher oscillations of flow and thus data would be subject to greater uncertainty. Similarly, the graded work of Haynes and Pender (2007) suggests that far higher memory discharges may lead to erasing of

memory effects, although this is controversial and counters the data of Paphitis and Collins (2005) in uniform beds.

3.5.7 Sequential steps in running an experiment

In baseline and memory experiments, the sequence of running an experiment was as follows:

i) Bedding-in period: common in all experiments; prior to each experimental run (baseline and memory experiment), the flume is run with trickling flow to remove bed screeding effect and air bubbles/pockets from the bed; this period is referred as bedding-in time, and was maintained digitally for 3 minutes duration in each run

ii) Baseline experiment run: following the bedding-in period, flow steps start from 2.5 l/s, and increase to 18.75 l/s. In 14 steps of discharge the total run time is 64 minutes. The first four steps of discharge from 2.5 to 6.75 l/s are of 1 minute duration each, and next 10 steps from 7.5 to 18.75 l/s are of 6 minutes duration each (so as to facilitate bedload collection). The 64 minutes run time during this stepped sequence is consistent for baseline and memory experiments (see next bullet); this period will be referred as the "stability test period" in this thesis (in line with similar terminology used in other memory experiments).

iii) Memory experiment run: this comprises an equivalent bedding in-period, as in baseline experiment. This is followed by a memory stress period where the flume is run at memory flow of (Q=2.5 l/s, $\tau^* = 0.018$) which is 60% of τ^*_{c50}; the duration of this memory period varies (10, 30, 60, 120 and 240 minutes). There is then the same "stability test" period run, as described for that of the baseline experiment.

iv) Sediment transport sampling in baseline and memory run: in unimodal bed, bedload was collected at each discharge step starting from 7.5

l/s upto 18.75 l/s; in bimodal bed, bedload was also collected at each discharge step, but starting from 8.75 l/s upto 18.75 l/s

These experiments are summarised as shown in Table 3.1.

3.6 Summary of flume Set-up and experimental methodology

In a standard flume facility, the experimental methodology has been objectively designed and executed to fulfil the research objectives set out in Chapter 1. In summary:

- Flume set-up has been successfully prepared with very satisfactory setting of flume slope (1 in 200) and satisfactory achievement of uniform flow condition within ±0.5% variation on flow depth along the flume length.

- Appropriate automation of flow control has been proven, with less than ±2% variation against target discharges and minimal (or no) influence on shear stress analysis.

- Sediment preparation of the flume bed has accounted for the effect of antecedent moisture, by standardising the draining timeframe. This overcomes well documented problems in memory runs of previous researchers.

- The grades of unimodal and bimodal sediment mixtures have been justifiably chosen, which are primarily representative of natural sand-gravel sediment beds in UK rivers. Specific selection of the proportion of fractions in the mixtures are comparable to other memory stress research, as appropriate to quantifying grade dependent response, particularly the known influence of fines in the bimodal bed.

- Selection of five memory time scales of 10, 30, 60, 120 and 240 minutes are optimised appropriate to fulfilling the gaps identified in earlier research. The chosen time scales will help quantify the most reactive

response period on bed's stability, entrainment threshold and on transporting ability as envisaged from earlier memory research.

- Bedload sampling in the stepped discharge hydrograph enabled achieving the key objectives of this research in quantifying maximum memory effect, non-linear variation of memory effect in low flow regime and development of mathematical functions for bedload, which are able to represent memory effect.

Chapter 4: Physical Modelling Results: Unimodal Sediment

4.1 Introduction

The literature review in Chapter 2 has indicated that there is significant scatter found in the entrainment threshold of sediment movement (i.e. the Shields parameter). Review of the Shields parameter from the last eight decades of research by Buffington and Montgomery (1997) clearly highlights methodological biases as one of the key reasons for scatter in threshold data over many orders of magnitude. As this parameter is fundamental in determining the timing of the onset of sediment movement, and thus the volume transported during a high flow event, there continues to be significant merit and scope to look for definitive reasons to explain such scatter in a manner appropriate to removing this uncertainty from sediment transport modelling. Whilst Buffington and Montgomery's paper considers a range of methodological uncertainties, it fails to consider the timescales of experimental set-up, water-working or measurement period. However, there is strong emerging evidence that memory stress is important in dictating bed structure and subsequent resistance to entrainment (e.g., Reid and Frostick, 1984; Reid and Frostick, 1986; Paphitis and Collins, 2005; Haynes and Pender, 2007; Ockelford, 2011) which, coupled to wider interest in the time sequencing of flood clusters from recent winters' severe weather in the UK (e.g., 2013/4), provides strong motivation for providing a detailed data set on memory effects within sediment beds subjected to flow.

Two specific research questions within memory stress science are addressed within the present Chapter. Firstly, as UK Rivers are predominantly sand-gravel systems of mobile bed, it is appropriate that the present Chapter focusses upon memory effects within the transport of heterogeneous sediment (Ashida and Michiue, 1972; Parker, 1980; Parker et al., 1982a; Parker and Klingeman, 1982; Diplas, 1987; Wu et al., 2000a; Hunziker and Jaeggi, 2002; Powell et al., 2001, 2003; Wilcock and Crowe, 2003). Implicitly, this requires analysis of fractional bedload such that indications of any preferential size-specific fractional response to memory stress can be deduced. Secondly, as memory stress science is still in its infancy, its effect on graded bed entrainment threshold is yet to be quantified in any mathematical or empirical relationship. By overcoming this

known deficiency, the present Chapter seeks to improve the predictive performances of existing graded transport functions, which are well noted to be still unsatisfactory for practical purpose (Gomez and Church, 1989).

The present Chapter provides both definitive and quantitative evidence in a gravel bed mixture that: (i) the entrainment threshold of sediment movement in unimodal beds is responsive to memory effects; (ii) the relationship between memory period and subsequent sediment threshold can be mathematically described; (iii) the scale of such effect can be translated into the graded sediment transport functions leading to improvement of predictive ability.

4.2 Matrix of unimodal experiments

This Chapter presents results from the experiments of unimodal sediment beds subjected to various flow memory (sub-threshold) durations. Whilst specific details and the rationale underpinning experiment design is provided in Chapter 3, the key variables and set-up specific to the unimodal runs are highlighted below. The unimodal sediment mixture used has median grain size (D_{50}) = 4.8 mm, standard deviation σ_g is 1.65 calculated from the relation $(D_{84}/D_{16})^{1/2}$ and the mixture is composed of eight classes of sediment from coarse sand (1mm) to medium gravel (16mm). Bedload transport was sampled throughout the rising stepped flow sequence of the stability test; this data were analysed in both dimensional (mass in grams) and non-dimensional forms, and were utlilised for comparison among memoried and non-memoried (baseline) bed, and with historical data (Shields, 1936; Meyer-Peter and Muller, 1948; Einstein, 1950; Vanoni, 1964; Paintal, 1971; Taylor and Vanoni, 1972; Luque and van Beek, 1976, Parker et al., 1982a, Shvidchenko et al., 2001). These data form the basis for later development of mathematical entrainment threshold descriptors and correction factors for response to memory stress.

The experiments have been given logical identification code/numbers for their easy referencing according to sediment grade and memory duration. The coded experimental matrix for the unimodal (UM) sediment bed is presented in (Table 4.1). The code name UM_B_0 represents the non- memoried runs; this is the benchmark experiment with which to compare other experiments. UM_SH_ represents the application of a memory stress period; this prefix is followed by

the numeric value representing the duration of memory applied in minutes. For example, the code name UM_SH_10 represents an experiment with 10 minute memory of sub-threshold stress. Similar identification codes have been used for 30, 60, 120 and 240 minutes of memory stress history experiments.

Table 4.1: Matrix of experiments in baseline and memory stress condition in unimodal sediment mixtures

Experiment Identification Code	Median grain size (D_{50}) (mm)	Experimental condition	Memory stress		Run duration of experiment (min)
			Magnitude: % of baseline τ^*_{c50}	Exposure duration (min)	
UM_B_0	4.8	Baseline	-	0	0+64
UM_SH_10	4.8	Memory experiment	60	10	10+64
UM_SH_30	4.8	Memory experiment	60	30	30+64
UM_SH_60	4.8	Memory experiment	60	60	60+64
UM_SH_120	4.8	Memory experiment	60	120	120+64
UM_SH_240	4.8	Memory experiment	60	240	240+64

4.3 Hydraulic regime of unimodal sediment experiments

The 64 minute stability test used in all experiments employed 14 constant-discharge steps (2.5 l/s up to 18.75 l/s). Table 4.2 notes the measurements and calculations made from all runs. It is clear that the condition of flow was hydrodynamically fully rough, based on particle Reynolds number calculations, as used in Shields' diagram (Brownlie, 1981). The particle Reynolds number (Parker et al., 2003, ASCE, 2007, Figure 2.29) $R_{p50}=(\sqrt{[(s-1)gD_{50}}\,]\,D_{50})/\nu$ for this mixture of unimodal sediment is 1338; R_{p50} can be determined when properties of sediment and water are known; g is acceleration due to gravity, s is specific density of sediment (used 2.65 in the calculation), D_{50} is surface median grain size, ν is kinematic viscosity of water ($1x10^{-6}$ m^2/s used in the calculation). Similarly, the shear Reynolds number $R_{e*}=u*D_{50}/\nu$ was also required to be hydrodynamically rough for this series of experiments, i.e. R_{e*} was larger than 100 (Rouse, 1937; Taylor, 1971). For this calculation, shear

velocity $u*$ was derived from each experiment using the relation $u_* = \sqrt{\tau / \rho}$, where τ is boundary shear stress, and ρ is density of water. Data are shown in Table 4.2; this justifies the hydrodynamic set-up as fully rough and sub-critical[1] (Fr < 1) as commensurate with the majority of UK and other natural river reaches at the onset of sediment entrainment.

Table 4.2: Unimodal sediment experiments: hydraulic regime of baseline and memory experiment

Experiment Identification Code	Flow depth range (mm)	Flow velocity range (m/sec)	Froude Number (*Fr*)	Shear Reynolds Number: R_{e*}
UM_B_0	33 - 95	0.23 – 0.66	0.40 – 0.68	175 - 297
UM_SH_10	33 - 94	0.23 – 0.64	0.40 – 0.69	175 - 284
UM_SH_30	33 - 95	0.23 – 0.66	0.40 – 0.69	175 - 285
UM_SH_60	33 – 95	0.23 – 0.66	0.40 – 0.68	175 - 286
UM_SH_120	33 - 94	0.23 – 0.66	0.40 – 0.69	175 - 284
UM_SH_240	33 - 94	0.23 – 0.67	0.40 – 0.70	175 - 284
Flow range: same ranges of flow used for all experiments: 2.5 l/s to 18.75 l/s at an incremental step of 1.25 l/s				

4.4 Sediment entrainment and bedload transport analysis of unimodal experiments: parameters and variables

Diagrams, rating curves, empirical relationships of water discharge, sediment discharge and bed shear stress analysis can all help interpret changes to graded bed rivers (Parker, 1990a), and therefore are able to quantify the effect of memory stress on those parameters. Thus, the present Section focusses upon absolute measured data of bedload, shear stress and discharge. These data are then non-dimensionalised for two key variables, i.e. shear stress and bedload transport, as commensurate with the original idea of Shields (1936) and well-used since for study-to-study comparison purposes. Shear stress has been non-dimensionalised using Eq. 2.7, and bedload transport using Eq. 2.8-9. Of particular note here is that the non-dimensionlisation of measured total bedload transport required selection of representative grain size from bed surface; this

[1] $Fr = u / \sqrt{gh}$ where *u* is velocity, *h* is water depth

selection has been a considerable source of debate in sediment transport studies of the past. Whilst some researchers have used D_{35} (Meyer-Peter et al., 1934; Haywood, 1940; Einstein, 1950; Ackers and White, 1973), others (e.g., Meyer-Peter and Muller, 1948) have used a diameter varying between D_{50} to D_{60}. However, the median size D_{50} is by far the most commonly used grain size to represent a sediment mixture and, herein, is also a suitable choice given the logarithmic grain size characterising grain size distributions. As this approach is commonly accepted in natural rivers of unimodal grain size and, in the present thesis, this median size also coincides with geometric mean and mode of the distribution, D_{50} has therefore been used to non-dimensionalise total bedload transport henceforth. The non-dimensional transport presented and discussed below is, thus, representative of the median size of the graded mixtures.

Further, as this study analyses several definitions and relationships (i.e. equations) of dimensionless reference transport for entrainment, it follows that the magnitude of shear stress (non-dimensionalised to the Shields parameter) will also be different, as specifically relative to each reference transport approach. Therefore, significant analysis in the present thesis focusses upon appropriate presentation of the above variables, both in dimensional and non-dimensional forms, as rating curves as a function of the independent variables (such as discharge, time, shear stress). This appears to be the first time that such rating relations both from absolute data and from non-dimensional parameters have been employed to assess quantitatively and mathematically how memory stress in river beds can affect the entrainment and transport of sediment.

To summarise: as quantitative data specific for flow-sediment analysis were required, measured data have been used directly in analysis and for derivation of the above variables and parameters. The key hydraulic parameters which have been quantified in this Chapter include:

i) Time averaged mass bedload transport (q_b, averaged over a period of 360 seconds within each step of the incremental flow sequence) as a function of discharge and bed shear stress. This parameter is useful in snap-shot analysis for simple quantitative assessment of the

transporting capability for sediment under specific shear stresses applied and is in line with previous researchers (e.g., Ockelford, 2011). This analysis forms the basis of the results presented in Section 4.5 and provides quantitative values with which to compare baseline and memory experiments.

ii) Integrated volumetric bedload transport (Σq_b), which was obtained by integrating bedload over 10 time steps (Σq_b) precisely over the duration of 60 minutes. Use of the 10 steps (rather than full 14 steps of the stability test) is specifically selected so as to commence sampling from a low value of τ^* = 0.02 (Chapter 3). This analysis is useful to assess how memory effect develops over time as it provides a growth curve showing when the effect triggers, how the effect grows over time in increasing discharges/shear stress, and when the effect diminishes. Data are discussed in Section 4.5.2

iii) Non-dimensional parameters for bedload q^*, and boundary shear stress τ^*; only non-dimensional parameters enable comparison of results from this study with those of previous researchers. Section 4.5.4 considers this in detail.

The distinction between datasets is important. The first two outputs specifically use directly measured data from the flume experiments, yet are case study specific to the flume employed; these will provide an immediate comparison among the dimensional numbers about the effect of memory stress within this research. The latter output uses non-dimensional variables more generically comparable to other paired data sets of shear stress and sediment transport from the literature and, although data are derived from standard empirical equations, it is underpinned by measured data. Particularly the non-dimensional transport data will be crucial to draw comparison with: i) reference transport values of Shields (1936), Parker et al. (1982a) and Shvidchenko et al. (2001) which are widely used as entrainment conditions (Chapter 2), ii) transport from other memory stress research (Saadi, 2000; Haynes and Pender, 2007; Saadi, 2008; Ockelford, 2011), and iii) transport from other field and laboratory

research at low flow transport around incipient motion (Paintal, 1971; Meyer-Peter and Muller, 1948; Taylor and Vanoni, 1972; Reid et al., 1995).

4.5 Bedload sediment transport

The first objective of these results is to ascertain if bedload transport rate is sensitive to sub-threshold flow duration (i.e. memory stress). Thus, the following analysis focusses on changes to the volume of bedload transport as a function of discharge, shear stress and time subsequent to different flow memory durations:

The degree of non-linearity of bedload transport with discharge is significantly different from that of shear stress; discharge is more of a volumetric parameter representative of the entire width and depth of the flume, whereas shear stress is a more localised parameter (i.e. the force from the flowing fluid inserted on sediment bed over a unit area). It is well established in research that bedload transport in low flows is highly non-linear in response to shear stress; such non-linearity is significantly less with discharge (Ryan, 1988; Ryan and Emmett, 2002; Bunte et al., 2004). Most previous research has related the entrainment threshold and transport of sediment to shear stress with their dimensional and non-dimensional forms; however, some other schools of research relate it to discharge and thus critical discharge for entrainment of sediment (Bathurst, 1985; Bathurst et al., 1987; Rickenmann, 1990). Both approaches are considered herein.

Time averaged sediment load (q_b) has been analysed for mean and minimum values as commensurate with deciphering entrainment threshold response (Table 4.2 and Table 4.3). Firstly, the overall idea was to identify any variability in the minimum discharge which triggers sediment entrainment, in response to memory effects; this was demonstrated using minimum load data from respective experiments. Secondly, analysis was intended to demonstrate that this memory effect not only affects transport (and entrainment) at a discrete point, but prevails over a range of discharges; graphical trendline analysis and mean transport data are therefore provided.

Sediment load sampling started at the smallest practical water discharge of 7.5 l/s (corresponding $\tau^* = 0.02$) aligned with knowledge from previous researchers (Haynes and Pender, 2007; Ockelford, 2011). For the same grade of sediment mixtures, Haynes and Pender's (2007) critical discharge was 8.75 l/s in a steeper flume slope (0.0067) than the present research (0.005). Therefore, a discharge of 7.5 l/s as the start point for sediment sampling was a fair and conservative choice. Moreover, the non- dimensional shear stresses (τ^*) of the reference transports of Parker et al. (1982a), Shvidchenko et al. (2001) and Shields (1936) sit at higher values than the first sediment sampling point ($\tau^* = 0.02$) and thus, the transport data from the present study are appropriate for direct comparison with the reference transport of entrainment of others.

4.5.1 Bedload v. discharge relationship

The response of bedload transport to memory duration, as a function of discharge, is shown in Figure 4.1. Bedload transport (q_b) is within the range from $1x10^{-9}$ to $1\ x10^{-5}$ m^2/s. Baseline (non- memoried) runs indicate higher bedload rates at each discharge point within the same range of sediment load ($1x10^{-9}$ to $1\ x10^{-5}$ m^2/s) implying that for the same discharge the effect of memory yields a lower capacity (ability) of the system to transport sediment; this implicitly indicates that the baseline bed has become more resistant to entrainment due to the application of memory (Table 4.2).

All runs with flow memory imparted (10-240 minutes) indicate negative offset in the trendlines of Figure 4.1. Two specific points of interest are noted from these Figure:

Firstly, the memory effect on bedload rate appears larger at lower discharges; this is particularly notable for SH-30, 120 and 240. The difference in bedload transport between these baseline and memory data at the lowest discharge point is approximately an order of magnitude. Further review of Figure 4.1 shows that at higher discharges this effect gradually weakens, until nearing convergence with baseline data towards the largest flow (18.75 l/s) in the present experiments.

Secondly, the duration of memory applied appears influential in the magnitude and persistence of reduced bedload rates, compared with baseline. The most pronounced difference is noticed for the longest memory duration of 240 minutes (Figure 4.1) where bedload is reduced by more than an order of magnitude at the lowest discharges and continues to record values well below those of baseline even at the highest discharges tested. Analysis of the sediment rating curves from other memory experiments suggests that there is a general relationship between memory duration and the magnitude of change in bedload observed. Detailed review of Figure 4.1 generally shows sensitivity to memory response of 10, 30, 120 and 240 minutes; however, the relationship is weakened by the seemingly over-response of the SH_30 at low discharges (which may be a facet of bed screeding). Thus, to examine these trends further, statistical analysis is provided in Table 4.3 below.

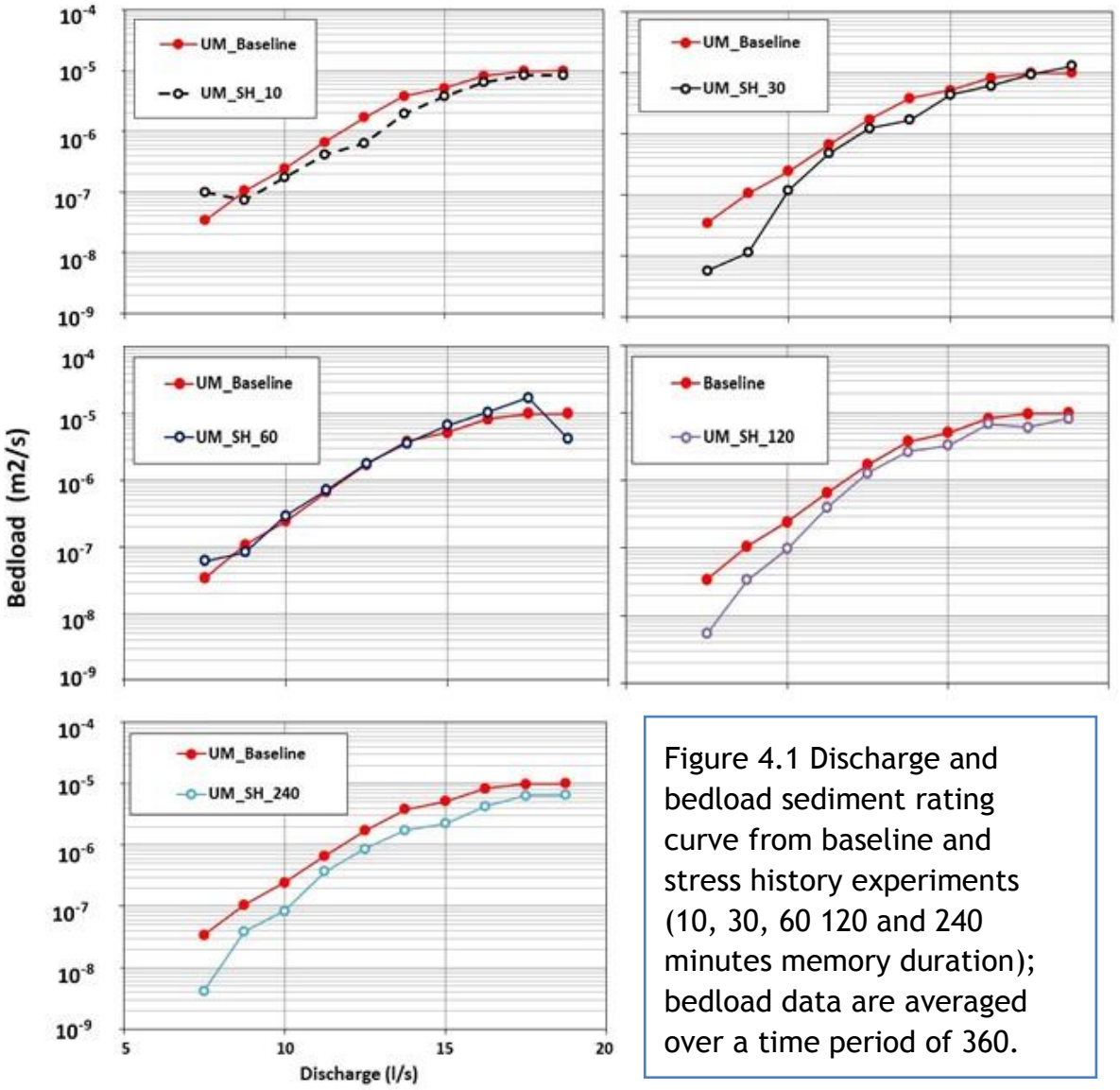

Figure 4.1 Discharge and bedload sediment rating curve from baseline and stress history experiments (10, 30, 60 120 and 240 minutes memory duration); bedload data are averaged over a time period of 360.

Table 4.3 specifically and quantitatively analyses further the significant reduction in the transport of bedload in memory experiments, particularly at low flow ranges. Data show the range of reduction in bedload transport from 31 to 89% (Table 4.3) at the minimum discharge. The aforementioned response of bedload reduction to memory duration is evident and quantified by Table 4.3, with the exception of the SH_60 data set as outlier. Even when data are reprocessed to calculate the arithmetic mean of all data (between discharge 8.75 and 18.75 l/s) in the incremental stepped flow test, data clearly show this memory effect to be significant; Table 4.3 shows a 34 to 52% reduction in

transport due to memory. The lower statistical values of the mean data (compared with minima data) are reflective of the progressive reduction in the memory effect at higher discharges. Further, as the mean bedload (arithmetic mean) is calculated over the whole range of data points, this reduction in mean bedload transport is also an indicator for in which experiment the memory effect sustains for a longer period. The percent reduction on the mean value from Table 4.3 then clearly indicates that in higher duration memory experiments (240 minutes), the memory effect sustains for longer period.

Table 4.3: Unimodal sediment experiments: volumetric sediment transport in baseline and memory experiments

Experiment Identification Code	Bedload transport: q_b ($m^3/s/m$)		Bedload transport: q_b ($m^3/s/m$)	
	minimum	% reduction of q_b relative to baseline(1)	Mean(2)	% reduction of q_b relative to baseline
UM_B_0	1.06E-07	-	2.86E-06	-
UM_SH_10	7.32E-08	31	1.93E-06	33
UM_SH_30	1.12E-08	89	2.01E-06	30
UM_SH_60	8.25E-08	22	3.38E-06	-18
UM_SH_120	3.34E-08	68	2.12E-06	26
UM_SH_240	3.89E-08	63	1.37E-06	52

Note:
1) Bedload collection starts from 7.5 l/s (very first data point in the graph in Figure 4.3 was not used in analysis as collection of the very first data point induces some manual effects, and sample mass was also too little in most experiments)
2) mean bedload is the arithmetic mean of all bedload at discharge points between 8.75 and 18.75 l/s (Figure 4.1)

Whilst statistical analysis of Table 4.3 is useful in quantifying snapshot data, a more appropriate analysis is to consider all bedload data within each experiment so as to permit direct comparison between experiments, as shown in

Figure 4.2. This regression analysis (logarithmic functions with satisfactory R^2 value) uses a 'discrepancy ratio' factor to quantify memory effect, compared with baseline data. The 'discrepancy ratio' is defined as the ratio of bedload transport in baseline (q_{b_B}) with that in the memory experiment (q_{b_SH}), i.e., discrepancy ratio = q_{b_B}/q_{b_SH}. In short, a discrepancy ratio (y-axis) of 1 means that the transport in baseline and memory stress experiments is exactly the

same, whilst a value >1 represents the order of magnitude that bedload transport has reduced by as a consequence of the memory stress effect. This approach is sometimes used in engineering practice to compare a mathematical prediction of bedload with a directly measured field data set (e.g., White et al., 1975; Yang, 1976; Alonso, 1980; ASCE, 1982; Yang, 2001). Previous research-based evaluation of evidence from the literature often yields a discrepancy value ≥ 2 , indicating that mathematical entrainment/bedload equations are a poor fit to the measured field data and, hence, that the derived equations fail to consider one or more processes influential of sediment transport. Thus, using discrepancy analysis for comparison of memory and baseline experiments will provide a measure of discrepancy, comparable to literature studies, and help demonstrate if memory may be a possible reason for the inability of existing bedload transport formulae to correctly fit measured field data.

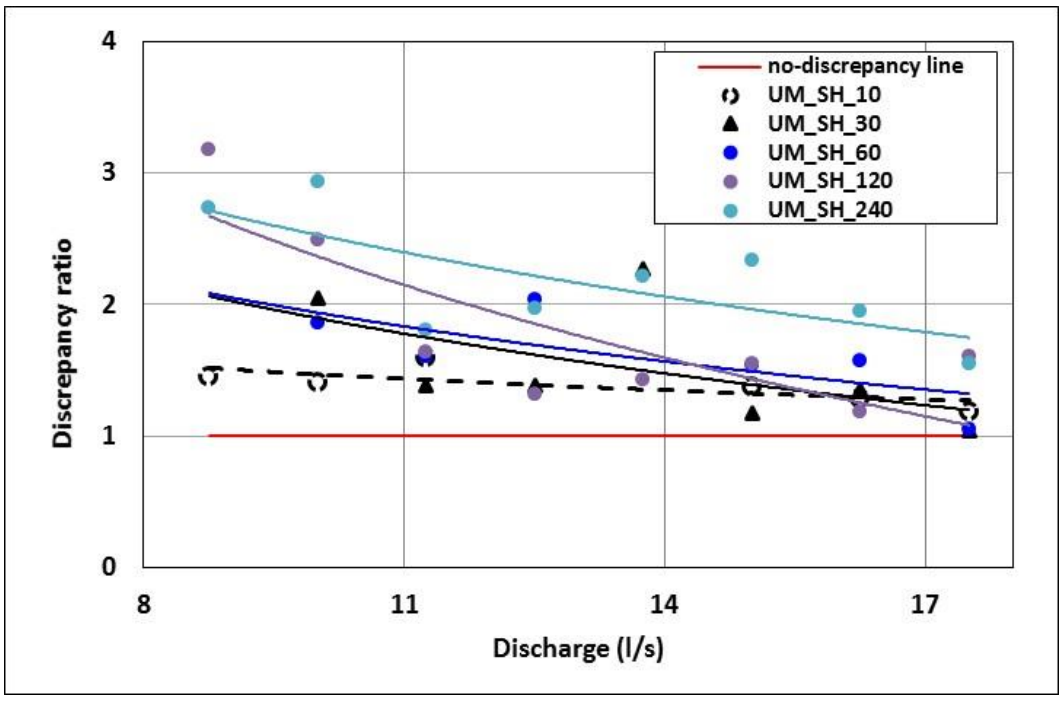

Figure 4.2: Discrepancy ratio in bedload transports as a function of discharge (Q) between baseline and memory experiments of 10, 30, 60, 120 and 240 minutes duration.

All of the trend lines are expressed in logarithmic functions; the functions define the vertical translation of the discrepancy ratio, mainly within the domain of memory influence; thus the vertical translation generally remains above the x-axis (due to the two constants (intercepts) 5.73 and 7.64). All trend lines show significant discrepancy ratios at low discharges; particularly the trend lines from SH_120 and SH_240 indicate a 2-3 fold discrepancy ratio in volume of transport at low discharges. This is in line with previous literature comparing bedload transport functions with field data, hence suggesting that memory may have some control over bedload processes. Given that the discrepancy ratio are evident in

Figure 4.2, and the natural logarithmic functions are similar in all memory experiments, the functions for the distinct cases (SH_120 and SH_240) from

Figure 4.2, are shown in Eq. 4.1-2:

$$\frac{q_{b,baseline}}{q_{b,\,SH\_240}} = -1.39\ln(Q) + 5.73, where\ R^2 = 0.52$$ Equation 4.1

$$\frac{q_{b,baseline}}{q_{b,\,SH\_120}} = -2.29\ln(Q) + 7.64, where\ R^2 = 0.66$$ Equation 4.2

It is interesting to note from the two functions that the discrepancy ratio gradually diminishes as the discharge increases (→ 1, i.e. minimum (or no) discrepancy); this trend occurs earlier for SH_10, 30, 60 and 120 than in the SH_240 experiments; this indicates that the memory effect is sustained for longer subsequent to more extended periods of applied memory. The function in Eq. 4.1 for SH_240 is greater (i.e., higher magnitude of discrepancy ratio due to smaller sediment load in this experiment) than the function in Eq. 4.2 of SH_120 and therefore the decay (memory effect) is much higher for all discharges > 0. For example, for a discharge of 11 l/s, the discrepancy ratio in SH_240 is 2.3, while the discrepancy ratio for the same discharge in SH_120 is 2.0. Such decay (or growth effect of the memory condition, also see Figure 4.2) will continue for discharges > 0, the domain for which the logarithmic functions are defined. Because logarithmic function indicates slow change, the functions gradually

converges around the no-discrepancy line (discrepancy =1); hence, the functions mathematically will likely become equal at large discharges (however, this cannot be easily proven as such high discharges are impractical to attain within the flume used in this study). As such, a preferable statistic for use would be where the discrepancy ratio $\rightarrow 1$, i.e. the effect of memory has been removed from the system. Figure 4.3 clearly shows that this over-writing of memory is viable at higher discharges where full mobility of the sediment bed is found.

Thus, the overall summary of findings from bedload versus discharge relationships are in line with those of Ockelford (2011) in that: (i) memory effects indicate up to an 80% reduction in bedload; (ii) there is, generally, a hierarchical reduction in bedload with increasing memory duration;(iii) a discrepancy ratio of 2-3 fold is found in the present data set, particularly in higher duration memory experiments. These findings suggest that memory is significant in determining entrainment/bedload. That said, all the findings are dependent on the use of discharge relationships which are case study specific to the flume used in the experiments, hence refinement of analysis to a more generally applicable variable is required (Section 4.5.3). Whilst the functions in Eq. 4.1-4.2 can be useful tools for quick assessment of whether a sediment load has memory, Section 4.5.4 undertakes similar analysis of these parameters in their non-dimensionalised form to develop generic functions appropriate to wider use.

4.5.2 Integrated bedload transport

Given that Table 4.3 provides only a snapshot quantitative analysis for a given discharge step and that the discrepancy ratio (

Figure 4.2) requires a best-fit line estimate, the data were reprocessed for integrated sediment volumes ($\sum q_b$) that quantify the effect of memory as an overall effect over the volumetric transport q_b. As such, cumulative sediment volume around incipient motion has been derived by summing up the sediment volume collected over all the steps of discharge (Figure 4.3). Further to this, a derivate variable, which is rate of change in sediment load between two steps (Figure 4.4), has been calculated from the cumulative load. Baseline and memory data have been compared, as in Section 4.5.1. Thus, Figure 4.3

quantifies the difference in absolute magnitude of cumulative sediment volume between baseline and memory experiments, whereas, Figure 4.4 interprets the rate of change data in a manner appropriate to understanding if memory effects are gradually lost during rising bedload transport rate or catastrophically 'washed out' at certain trigger points associated with a particular discharge step. Thus, importantly, the data are looking at the maximum and minimum rates of change for memory experiments.

From Figure 4.3, it is evident that SH_240 transports the least volume of sediment; over the stability test the cumulative sediment volume for the baseline run is $1.44x10^{-2}$ m^2 yet reduces to only $8.08x10^{-3}$ m^2 following SH_240. This leads to ~40% reduction in sediment volume due to memory effects. Similar comparison of the cumulative sediment from SH_120 indicates a 24% reduction in sediment volume, compared with the baseline experiment. Yet, these percentage reductions are much smaller for the shorter memory experiments (SH_10, 30, 60), primarily due the filtering effect of summing of both positive and negative effects over time from a discrete point. Nevertheless, the cumulative graphs (Figure 4.3) can demonstrate the memory effect attractively.

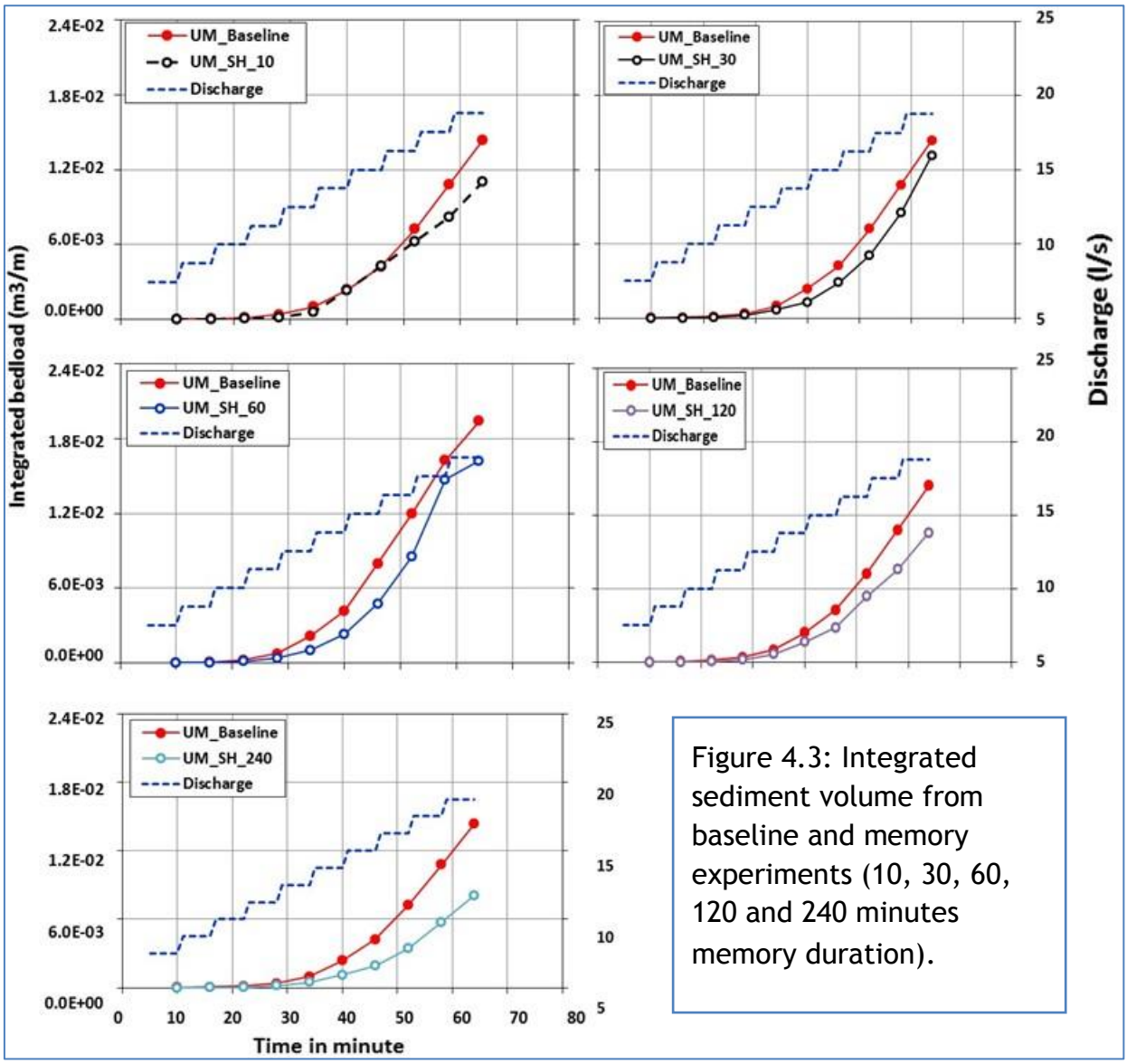

Figure 4.3: Integrated sediment volume from baseline and memory experiments (10, 30, 60, 120 and 240 minutes memory duration).

Whilst Figure 4.3 appears to indicate that bedload response to memory is gradual, progressive and non-linear, it is difficult to discern whether the response is more pronounced at specific flow steps so as to infer any trigger point of memory being erased. Thus, Figure 4.4 is meritable for more detailed analysis. From Figure 4.4 it is clear that within the first 30 minutes of rising flow stage, sediment transport is low for all experiments and memory effects, whilst present, do not appear to strongly influence the absolute rate of change of bedload. Yet, between 30-60minutes of all experiments, memory experiments show a far smaller rate of change than baseline runs, i.e., larger memory effect. For SH_10, SH_120, SH_240 runs the magnitude of the reduced rate of change increases until it most differs from baseline at 40 minutes (flow step Q=17.50l/s); this indicates a strengthening of memory effect on the bedload measured up until this point in the flow test. Following the subsequent flow step, the rate of change slowly recovers to equal that of the baseline at the highest

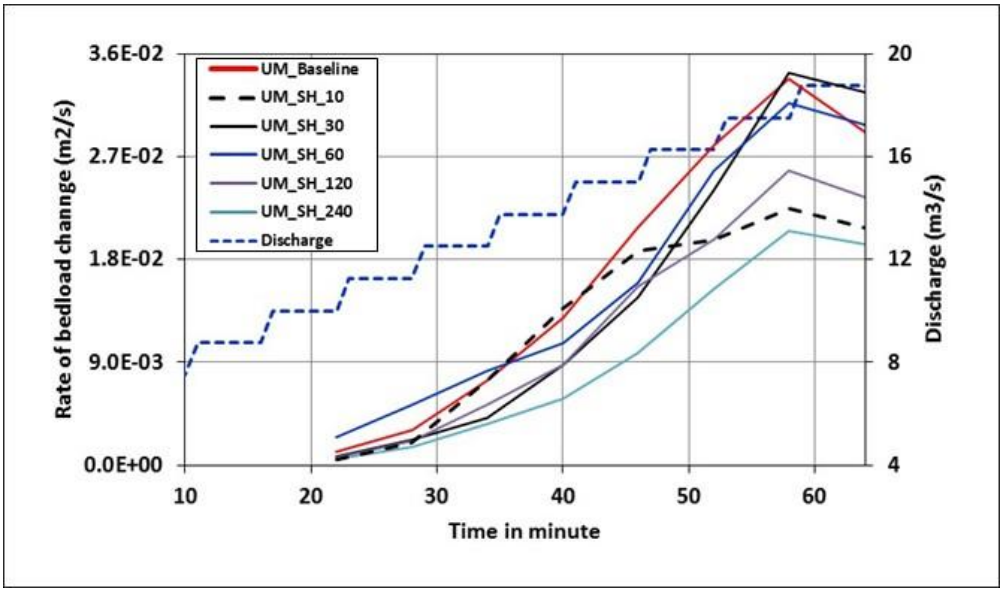

Figure 4.4: Progressive development of memory in flume bed in baseline and memory stress experiment shown in incremental change in bedload transport rate; smaller incremental rate means less transport of volume between successive time step.

discharges at the end of the flow test. Thus, there is some implication here that Q=17.75 l/s at 56 minutes acts as a trigger point in starting to over-write memory effects, thus recovering the bed to baseline equivalence. In explanation, this may correlate to a specific coarser fraction of the bed now being mobilised under the elevated discharges. If it is therefore likely that the stability of a particular fraction may be responsible for memory effects, fractional bedload analysis (Section 4.6) is required.

Also, it is worth noting that whilst SH_10 exhibits an equivalent trigger point at 56 minutes, it tends more to the baseline rate of change throughout 0-40 minutes; this may signify that very short memory durations (10 minutes) lead to an incomplete process of memory-related stabilisation. Whether this is particular fractions of the bed, or spatial regions of the bed is unclear. One thought is that the data in Figure 4.4 indicates behaviour similar to the baseline experiment occurring early in the flow test when low flows were applied, thus it is possible that it is the finer fractions which have failed to gain memory effects and are therefore lost at the same rate as baseline; this is something that will be further examined by fractional bedload analysis (Section 4.6).

In summary of the findings of the cumulative bedload analysis section it is highlighted that: (i) memory effects indicate up to a 40% reduction in cumulative bedload volume; this indicates that memory effect is a progressive non-linear process varying over time with variation of discharge; (ii) memory effects persist and strengthen up to a discharge of Q=17.5 l/s (56 minutes); (iii) for all runs, a discharge of Q=17.5 l/s (56 minutes) appears to act as a 'trigger point' for the progressive erasing of memory, suggesting that this discharge may be responsible for a particular critical fraction of the bed mobilising; (iv) data suggest that the generation of memory effects is incomplete after 10 minutes of sub-threshold flow. Thus, there appears scope for fractional bedload analysis (Section 4.6) to further investigate the reasons for memory effect generation and erosion.

4.5.3 Bedload vs. boundary shear stress relationships

A more generically applicable approach to memory data sets is to present bedload transport as a function of bed shear stress instead of discharge (Section 4.5.1). Bed shear stress has been calculated from depth-slope product (Eq. 4.3)

and the applicability, advantage and limitation of this method were discussed in Chapter 2.

$$\tau = \rho g R_b S \qquad \text{Equation 4.3}$$

τ = boundary shear stress, R_b = hydraulic radius (has been corrected for wall effect while used in calculation); S= flume bed/water surface slope (for uniform flow). The correction of the hydraulic radius has been done for glass walls in this relatively less narrower flume being significantly smoother than a gravel bed; such differential friction to flow requires correction using Manning's-Strickler's roughness formula (Strickler, 1923) in the same manner as Shvidchenko (2000) and Ockelford (2011). Sidewall correction procedure is based on the Manning's roughness coefficients of the bed (n_b) and walls (n_w). The principal assumption is that the cross-sectional water area can be divided into bed area and wall area having the same energy gradient (equal to the bed slope) and mean flow velocity U of the total section. Applying the Manning's formula $U = R_b^{2/3} S^{1/2} / n$ to each part of the water area, we obtain $R_b = R(n_b / n)^{2/3}$ (also see Wu, 2007 for this derivation, and also chapter 6 in this thesis), and $n = (P_b n_b^{1.5} + P_w n_w^{1.5})^{2/3} / P^{2/3}$. Here R is the hydraulic radius of the total area, n is the equivalent Manning's roughness coefficient, P is the wetted perimeter of the complete section, P_b, and P_w are the wetted perimeters associated with the bed and walls, respectively. The roughness of the bed is expressed by the Strickler formula $n_b = 0.048D^{1/6}$ (Carson and Griffiths 1987) and roughness of glass wall, $n_w = 0.010$ (Chow, 1959). The above wall corrected R_b then have been used in Eq. 4.3 to calculate the shear stress.

Using this approach, data for all experiments are presented in Figure 4.5. Predictably, the relationship of shear stress estimates from flow depth culminates in similarity of important trends equivalent to those of Section 4.5.1, due to discharge also having relationship to flow depth. For the sake of brevity, these overall trends are not restated here; instead, focus is placed on the magnitude of change to shear stress relationships with bedload. The memory effect both delays transport and requires a higher shear stress to transport the same load as in the baseline condition; this delay is generally up to the shear

stress 3.58N/m^2, at which memory gradually weakens (Figure 4.5). Detailed analysis of individual data points on Figure 4.5 shows that transporting the same load in memory experiments will require up to 20% more shear stress than baseline. Given that such large effects are found predominantly at the lower discharges applied in the flow test, a more representative comparison of shear stress from baseline and memory experiments is presented in Table 4.4. Here mean sediment load has been calculated up to the discharge steps at which memory effect starts to diminish, i.e, up to Q=17.5 l/s. Then, corresponding to that reference transport line (mean load, q_b = *3.74x10^{-6}* m^2/s), shear stress has been derived from the x-axis for each condition of the memory experiment and for baseline. The derived shear stress then shows "the increment of shear stress", following the memory condition, which is required to transport the same volume of load. This comparison also shows that up to 11 % more shear stress (Table 4.4) will be required in SH_240 to transport the same load (*3.74x10^{-6}* m^2/s) as transported in the baseline; this increment in shear stress may be considered similar to the results obtained by Ockelford (2011), who found 8% increment in her unimodal sediment bed for her 60 minute memory time scale.

Table 4.4: Unimodal sediment experiments – different magnitude of shear stress for transporting same sediment load in baseline and memory experiment

Experiment Identification Code	Mean sediment load (m^2/s): *3.74x10^{-6}*, see note below	
	Shear stress (N/m^2)	% increase in shear stress
UM_B_0	3.23	-
UM_SH_10	3.40	5
UM_SH_30	3.45	7
UM_SH_60	3.32	3
UM_SH_120	3.48	8
UM_SH_240	3.6	11

Note:

i) In column 2, these are the different magnitudes of shear stress both from baseline and memory experiments, but transporting the same magnitude of sediment, and thus showing that higher shear stress is needed to transport same magnitude of sediment relative to the baseline

ii) the sediment load consider here is the mean load over the steps of discharges from baseline experiment; then corresponding to that magnitude line, the shear stress has been calculated from the x-axis of the above graph

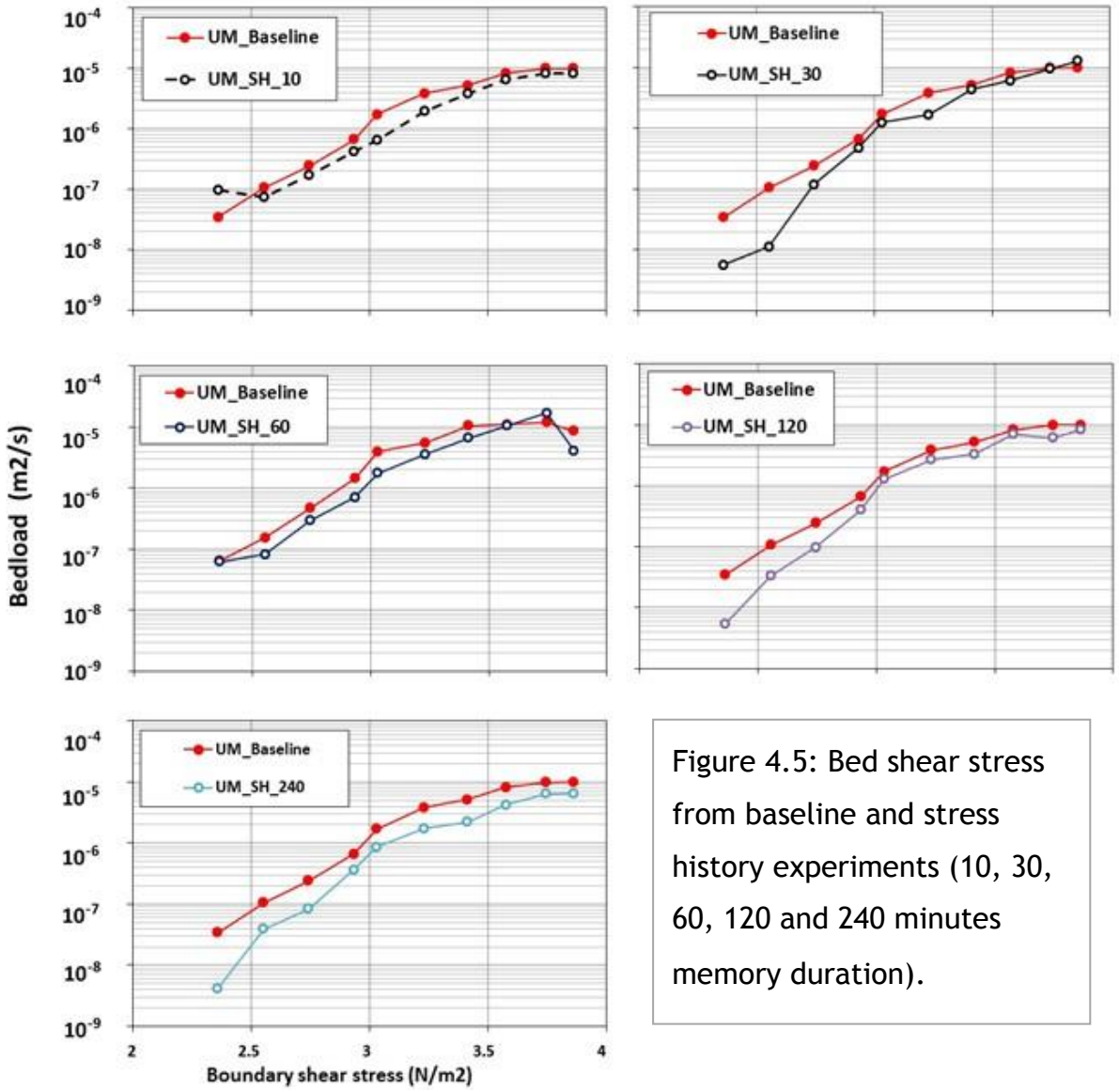

Figure 4.5: Bed shear stress from baseline and stress history experiments (10, 30, 60, 120 and 240 minutes memory duration).

It should be emphasised here the significance of such enhancement in shear stress on bedload transport, which is extremely non-linear (sensitive) at low shear stress. For the range of shear stress between 2.3 N/m^2 and 3.8 N/m^2 (which is an increase of 1.6 fold), the bedload transport varied in the order of 10^{-3} (from $1x10^{-8}$ m^2/s to $1x10^{-5}$ m^2/s, see Figure 4.5). A similar degree of non-linearity of bedload transport was also demonstrated by other researchers; e.g., Taylor and Vanoni (1972) showed that a 10% increase in shear stress at low transport/shear stress can increase bedload by 100%. As shear stress data are seemingly in line with at least the order of magnitude of change from research

by Ockelford (2011), it appears a more applicable and transferrable variable (than bedload vs. discharge rating curves as in Section 4.5.1) to employ for generic memory correction factor development (Section 4.5.4).

Thus, in summary of this section: (i) bedload vs. shear stress relationships with memory demonstrate trend equivalence to those of bedload vs. discharge relationships; (ii) data indicate up to an 11% increase in shear stress due to memory; (iii) there is clear non-linearity in response of shear stress to memory, in that the effect is most pronounced at lower shear stresses applied; (iv) the order of magnitude of memory effect on shear stress is similar to that noted in similar studies by Haynes and Pender (2007) and Ockelford (2011); v) sediment transport response was extremely non-linear at low transport rates, and thus memory effects producing an 11% increment in shear stress show significantly greater sensitivity in bedload data, with about 80% decrease in transport (i.e., nearly about two order of magnitude).

4.5.4 Non-dimensional analysis of sediment transport relationships

The following section further analyses raw data from Sections 4.5.1-4.5.3 using the non-dimensional approaches of Shields parameter and reference transport rate, as accepted and widely employed by sediment transport researchers, modellers and practitioners. Non-dimensionalisation of the parameters makes the data set generic, to compare and contrast them with the same parameters from previous research. Whilst the general theory is provided in Chapter 2, the specific calculations and derived data are provided below. The intention of this Section is to calculate non-dimensional sediment rating equations as appropriate to determining a parameter or variable responsive to and/or inclusive of recognising a memory function. This is entirely novel, as no previous study has attempted any mathematical description of memory effects on sediment entrainment or transport.

The shear stress approach (Chapter 2) is adopted herein to determine the incipient motion using Eq. 2.4. As recognised by Buffington and Montgomery (1997), the most reliable approach of parameter calculation is via the collection of sediment load under different fluid stresses, and then to determine the non-

dimensional shear stress τ_c^* (Eq. 2.7) corresponding to a certain reference transport, (i.e., a non-dimensional parameter represented by q^*). There are several definitions of reference transport (Chapter 2), of which three common equations have been used to calculate the corresponding τ_{c50}^* in the present thesis; these are: Parker et al. (1982a), Shvidchenko et al. (2001), and Shields (1936, from Taylor and Vanoni 1972). The rationale for selection of these specific definitions is as follows:

- Parker et al. (1982a) stems from a large field data set, encompassing bedload vs. shear stress relationships at low shear stresses close to incipient motion. His work is specific to graded beds by use of unimodal gravel bed data from Oak Creek (Milhous, 1973). This is, arguably the most commonly referred to reference transport approach, implicit in most widely used sediment transport models.

- Shvidchenko et al. (2001) stems from a large data set developed from only flume-based data. The flume dimensions and unimodal grade are equivalent to those used in the present thesis. Both general and incipient motion relationships are developed and there is analysis of data fit to wider field data. Whilst likely of most similarity to the present data set, these equations have received less attention by practitioners.

- Shields' (1936, from Taylor and Vanoni, 1972) reference transport to entrainment threshold was first developed as the Shields curve using scattered experimentally-derived data points. This large flume data set was of assumed near-uniform sediments of grain size ranging from fine sand to gravel. The trendlines of non-dimensional transport on the Shields curve are the most well-known of all reference transport curves and typically used to benchmark and discuss more recent alternative approaches.

By use of the above methods, the non-dimensional transport (q^*) has been derived according to Eq. 2.8-9 for baseline and memory stress experiments

(Figure 4.6 and Figure 4.7 and Table 4.5). The values of the reference transports (q^*) for the above scientists are:

- Parker et al. (1982a) reference transport, q^* =*1x10*$^{-5}$ (for *W** = 0.002, where $W^* = q^*/(\tau^*)^{3./2}$). This is the lowest reference transport value of all compared and contrasted values.

- Shvidchenko et al. (2001) reference value, q^* =*1x10*$^{-4}$; which was developed specific to minimum measurable sediment transport associated with entrainment threshold.

- Shields' reference transport (from Taylor and Vanoni, 1972), q^* = *1x10*$^{-2}$ (average value), although Shields' transport generally spans between *1x10*$^{-1}$ and *1x10*$^{-4}$ to cover the scatter of τ^*_{c50} of Shields data points.

Given that the reference transport relationships described above represent transport at different levels of sediment motion, the derived Shields parameters (τ^*_{c50}) are accordingly different at 0.026, 0.033 and 0.051 respectively in order of the above three reference transport conditions. Taking baseline data (which by ignoring memory effects would assume equivalence of data to previous studies) a comparison of the derived τ^*_{c50} from the present thesis dataset (Table 4.5) with the theoretical values of previous studies is possible. At Reynolds numbers between 200 and 300 (approximately representative of flow stage of 7.5 l/s of the present study), baseline compares well with that of Parker et al. (0.029); the result also compares well with Shvidchenko (0.034) at a representative flow stage of approximately 11 l/s. Thus, the ratio of the τ^*_{c50} from the present baseline with that of Parker et al. is 1.11, and that with Shvidchenko et al. is 1.03. Given that Parker et al. value is based on their empirical relation (Eq. 2.24), and Shvidchenko et al. formed a relation of their reference shear stress with that of the Parker et al. (Eq. 10 in Shvidchenko et al., 2001), it is neither expected nor practical that results from present research will be identical to them. Given the degree of non-linearity of sediment load at low flow, the amplification ratio of 1.11 (with Parker et al.) and 1.03 (with

Shvidchenko et al.) should be considered very satisfactory from the present study. Further, Table 4.5 shows that the expectedly higher values of the Shields reference transport indicate that, for the same Reynolds number, the Shields value is 0.045, whereas in the present baseline this value is 0.051. As the finer methodological detail of Shields' experiments is vague, the discrepancy with the data of the present thesis seems reasonable. Thus, overall from Table 4.5, it is concluded that the baseline experiment is generally acceptable as a satisfactory dataset when compared with others.

Table 4.5: Unimodal sediment mixtures: entrainment threshold of median grain size of baseline and memory experiment

Experiment Identification Code	Shields parameter according to reference transports criteria of:		
	Parker et al. (1982a): $q^* = 1x10^{-5}$	Shvidchenko et al. (2001): $q^* = 1x10^{-4}$	Shields (1936): $q^* = 1x10^{-2}$
	τ^*_{c50} (-)	τ^*_{c50} (-)	τ^*_{c50} (-)
UM_B_0	0.026	0.033	0.051
UM_SH_10	0.03	0.034	0.056
UM_SH_30	0.03	0.035	0.055
UM_SH_60	0.031	0.033	0.055
UM_SH_120	0.031	0.035	0.055
UM_SH_240	0.031	0.036	0.059
Note: Minor extrapolation of rating curve needed in case of Shields and Parker et al. reference number; Parker et al. reference transport value of comparison is 0.029; Shvidchenko et al. is 0.034 and Shields' is 0.045.			

Although in the above tabular data, the memory effect stress effects are obvious in the entrainment threshold in each of the reference transport criteria, the intention here is not to quantify the increment of entrainment threshold for a discrete data point. Rather, memory effect appears more appropriately described and assessed by an overall mean value, and cumulative value over the low flow ranges, and can better be described by trendlines (Figure 4.2 to Figure 4.4) and empirical relations (Eq 4.5-10); these are able to describe the growth and decay of memory effects. Further validation of the baseline dataset by non-dimensional transport has, therefore, been carried out by forming mathematical relations as power functions (Eq. 4.5 and Figure 4.6) and by comparing them

with some widely used bedload relations, including Meyer-Peter and Muller (MPM, 1948), Einstein (1950), Paintal (1971), Luque and van Beek (1976) and data set of Casey (1935a, b) and USWES (1935). In justification, the relations of MPM, Einstein, Casey and USWES were formed for higher transport rates and are mainly representative of gravel beds, although for representative size; as these are commonly used in hydraulic-sediment models, they are presented in Figure 4.6 to debate their (in)appropriateness for use at low transport (as in present study). On the other hand, Paintal (gravel bed) and Luque's (sand and gravel) relationships were developed at similar low transports to the present study; these are therefore directly comparable with the present study dataset. Further rationale is discussed in Section 4.7.

It is clear from Figure 4.6 that the baseline data of the present study plot at slightly lower τ^* values than previous studies; this is likely due to meticulous set-up, fine control and pedantic removal of memory effects from the experiments from water working prior to entrainment of sediment (compared with the previous more general laboratory and field tests). Specifically, baseline data plot close to Casey (1935), Paintal (1971) and Luque and van Beek (1976); this is expected for the low shear stress data of Luque ($2.5 < \tau^* / \tau^*_{c50}$) and Paintal ($0.007 < \tau^* < 0.06$), but similarity to Casey is surprising. Casey used the same flume as Shields (1936), i.e. a non-re-circulating 0.3m wide flume, with sediment fed by hand and indication that his water working was much less than Shields and many later standard research set-ups; as such, Casey's Shields number was low (Buffington, 1999) and he recorded transport at these much lower shear stresses, which hold equivalence to the present thesis.

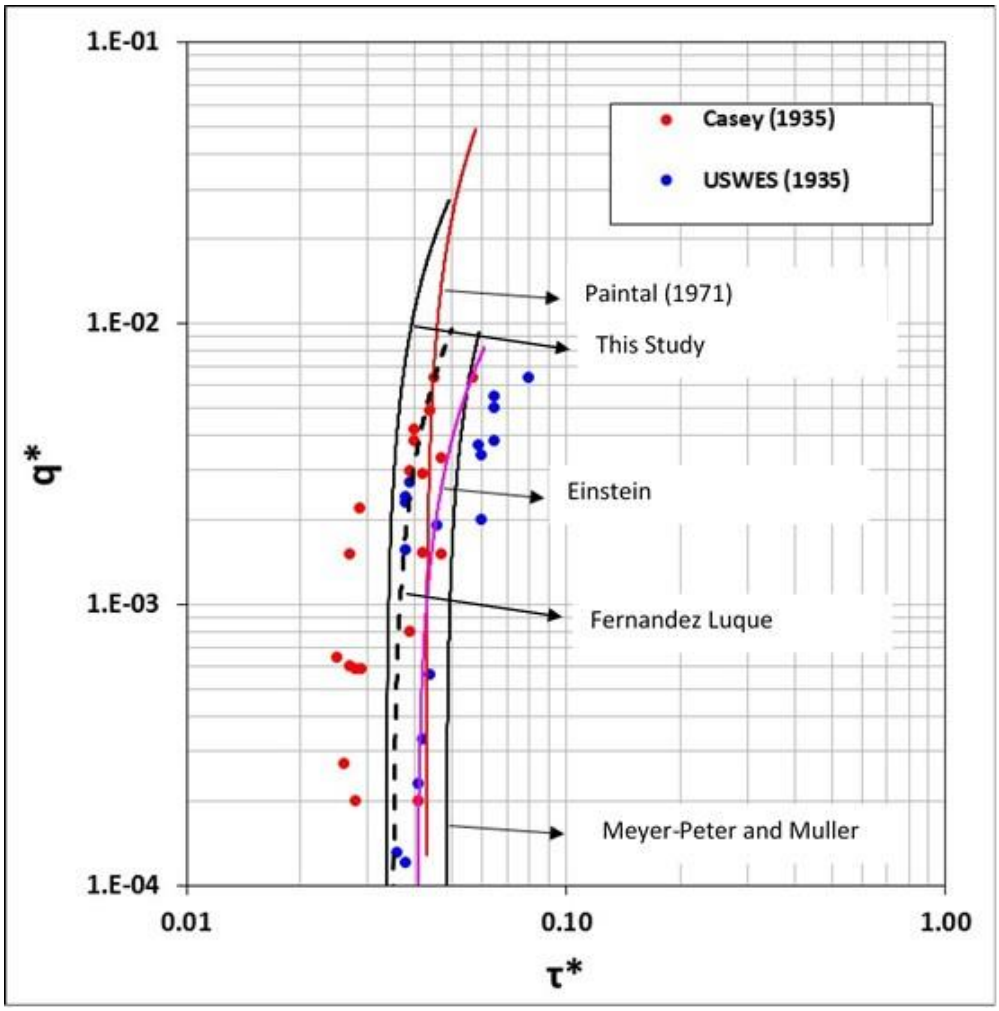

Figure 4.6: Baseline experiments: non-dimensional transport versus non-dimensional bed shear stress from this research, and from wider literature.

Of the three studies of similarity to baseline data, it is elected to compare the data with Paintal (1971). This is because Paintal's relation is an extensive data set, widely recognised in sediment research/modelling and developed with data from gravel beds of size range similar to the present thesis, both uniform and graded (D= 2.5 to 22.2 mm, σ_g=1.7 to 2.7). Importantly, Paintal had most of his data at very low transport rates as of interest to the present study on entrainment threshold deviations due to memory. His sediment relation is valid for $0.007 > \tau^* < 0.060$; this range contains all values of the present study as derived in Table 4.5 and appears an appropriate comparison data set. Paintal's (1971) function at low transport is shown in Eq. 4.4 and the equivalent power

relation of the baseline dataset from the present research is shown in Eq. 4.5; there is clear similarity in the exponent (16.2 in the present research) which provides confidence in the use of Paintal's relationship form to describe the present data set.

$$q^* = 6.5x10^{18}(\tau^*)^{16.0} \qquad \text{Equation 4.4}$$

Given that the above relationships for baseline data appear comparable to external studies, confidence is provided in this approach. Thus, its application and potential for adaptation to memory experiments is explored in the section below. Using the form of Paintal's power relation, a family of bedload functions in the form of $q^* \sim C(\tau^*)^b$ (as per the derived baseline relationship, Eq. 4.5) have been developed accounting for the effect of memory. These transport relations are shown in Table 4.6; the magnitude of both the exponent *n* and coefficient *A* show very systematic and hierarchical trends clearly associated with memory effects.

Table 4.6: Sediment transport functions proposed for low transports around incipient motion in memory stress condition

Experimental condition	Memory stress duration (min)	Sediment rating Equation: $q^* \sim C(\tau^*)^b$	
UM_B_0	0	$q^* = 6.5x10^{18}(\tau^*)^{16.2}$	Equation 4.5
UM_SH_10	10	$q^* = 1x10^{24}(\tau^*)^{17.3}$	Equation 4.6
UM_SH_30	30	$q^* = 1x10^{25}(\tau^*)^{17.9}$	Equation 4.7
UM_SH_60	60	$q^* = 6x10^{26}(\tau^*)^{16.9}$	Equation 4.8
UM_SH_120	120	$q^* = 2x10^{26}(\tau^*)^{19.0}$	Equation 4.9
UM_SH_240	240	$q^* = 2x10^{30}(\tau^*)^{21.5}$	Equation 4.10

From the above Table 4.6, there is indication that longer memory durations of the sub-threshold applied memory stress leads to both the exponent and coefficient increasing systematically. From a baseline exponent of 16.2 increasing the memory duration to SH_240 causes the exponent to rise to a value of 21.5. Thus, there will be less transport (q^*) following applied memory than for the same value of non-dimensional shear stress (Figure 4.7) in a baseline run. The only exception to the hierarchical rise is SH_60 minute, which though shows

the effect of memory (i.e. the exponent of 16.9 > baseline (16.2)) appears to suffer from a significantly different coefficient value. To elucidate further, the growth curves are graphically shown in Figure 4.7; this clearly permits comparison of strengthening memory effects as memory duration increases through SH_10, 30 and 120. Whilst these 3 runs indicate similarity of the entrainment condition (i.e. the lowest q^* and τ^* values have equivalence), SH_240 illustrates significant negative offset from the other plotted data, showing far lower bedload transport being recorded at the lowest τ^* value of incipient motion than in other experiments. Thus, it appears that for this particular run, memory effects are stronger both at incipient motion and during low sediment transporting conditions.

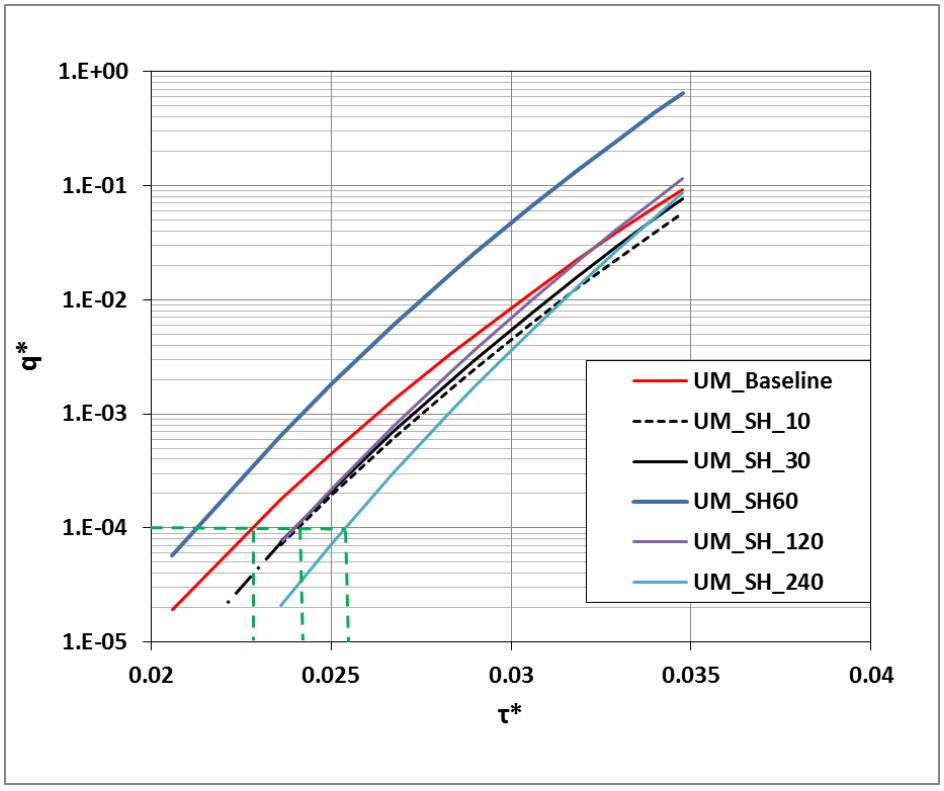

Figure 4.7: Family of rating curves of non-dimensional bed shear stress versus non-dimensional transports from baseline experiment and memory conditions. For a non-dimensional transport of q^*=1x10^{-4}, the requirement of increased non-dimensional shear stress due to memory is shown by drawing perpendicular lines (dashed lines) on the abscissa corresponding to same q^*. Note: SH_60 is the outlier in the trend as seen in the exponent and coefficient from Table 4.6 lying

outwith the hierarchical development of mathematical memory effects; however given the sensitivity of bedload in low flows in natural rivers (Recking 2010), this trend difference is not surprising.

Overall, the findings of non-dimensional analysis are that: i) the dimensionless parameter for transport and shear stress at low transport from the present study align only with similar studies specific to near entrainment conditions (e.g., Paintal); (ii) it is inappropriate to use alternative widely used bedload functions developed at higher transport conditions (e.g., Meyer-Peter and Muller) for describing near entrainment or memory relations; iii) it is unrepresentative to quantify the progressive, non-linear development of memory effects against a single datum point, fixed constant or specific reference transport value (e.g., Parker, Shvidchenko or Shields), iv) memory effects are best expressed by a reference transport relation specific to low transport conditions where the rising exponent and coefficient reflect the role of memory; v) use of Paintal's relation for the present data set provides the first ever mathematical descriptor for memory effects in a manner highly appropriate for future development aimed at generic inclusion into widely used sediment transport models.

4.6 Fractional transport

Previous researches (Haynes and Pender, 2007; Saadi, 2008 and Ockelford 2011) have proposed that memory effects are dependent on the disproportionate response of finer material to local or in-situ rearrangement into more stable configurations (Haynes and Pender, 2007; Saadi, 2008 and Ockelford 2011). Finer grain classes smaller than the median size is thought to fill the surface pores, increasing the hiding effects so as to generate a better angle of repose for those size classes. Specific to memory, only two previous papers focus on graded beds in a manner appropriate to determining such fractional bed response: Haynes and Pender (2007) analyse fractional bedload composition over their 'stability test', yet as their flow stage is of constant discharge above entrainment threshold, it was noted that selective entrainment and first fractional response was masked by the methodological set-up. Ockelford (2011) later overcame this issue via use of an incremental flow step test (similar to the present study) to indicate selectivity of transports; however, the ability of her dataset to clearly distinguish the size selectivity for finer fractions was limited by the fact that her

experiment finished at the entrainment threshold of the median size D_{50}, rather than consider the full flow range of size-entrainment relationships. The present data set was therefore designed with appropriate advantages such that the incremental increase in the flow steps was continued up to the ratio of $\tau^* / \tau^*_{c50} = 2$, as specific to examining size selectivity more fully, including its response to memory. From the results of fractional transport and size selective transport, the following key question has been addressed: *Given size-selectivity of entrainment, can it be confirmed that the finer fractions show a disproportionate response to memory?*

Firstly, it is important to acknowledge the particle mechanics of hiding effects, in line with brief examples of trends towards entrainment via equal mobility (e.g., Parker et al., 1982a) versus those via selective entrainment (e.g., Wilcock and Southard, 1989). In short, there are two limiting scenarios which can explain the significance of hiding in sediment transport: (i) the absence of hiding, known as size independence; (ii) equal mobility of all sizes within a mixture. Taking the former process of independence each grain class will have its own absolute shear stress such that smaller particle requires smaller absolute shear stress to move, and thus there will be more fractional load of the smaller classes (q_i) than the median (and larger) classes in the measured fractional load than in original bulk mix, assuming the system is not supply-limited. Alternatively, taking the latter case of equal mobility for initiation of motion, every particle will move at a single absolute shear stress implying that q_i in the measured load for each class will be the same as in the original mix.

The most common way to examine the balance of processes is via the normalisation of fractional bedload transport data. Transport for each grain class has been normalised by dividing the transport for the class by its fraction in the original mix; i.e., $q_{bi} = (p_i / F_i) q_b$, where q_{bi} = fractional transports for ith grain class, p_i is fraction of the ith grain class, F_i is the fraction in the bulk mix, and q_b is total transport. Thus, in the first limiting case of independence, the ratio of p_i/F_i will be > 1 for the grain classes $D_i/D_{50} < 1$, and $p_i/F_i < 1$ for grain classes greater than $D_i/D_{50} > 1$. In the second limiting case of equal mobility, the ratio of p_i/F_i will be = 1 irrespective of size class, and the condition of equal mobility for

$p_i/F_i=1$ may hold true at and around entrainment threshold as long the extreme hiding effect of the finer particle is counterbalanced by the higher mass effect of the larger particle, such that both move at same shear stress, and this condition may hold true for several steps of shear stress instead of one specific shear stress. Relative size effect counteract the absolute size effect by decreasing the mobility of finer fractions and increasing the mobility of coarse fractions (Wilcock and Southard, 1988). Thus, if hiding functions exist, then finer fractions are sheltered from the larger fractions so as to require a higher shear stress to move and p_i/F_i are expected to be less than <1 for the finer fractions (D_i/D_{50} <1); the opposite is true for the larger fractions which are more exposed to flow to be entrained, i.e. normalised transport will increase (p_i/F_i>1) for larger fraction (D_i/D_{50} > 1) (Wilcock and Southard, 1988; also see Fig. 14-9B, MIT OpenCourseWare, chapter 14). Thus, the plotted curve will tend to an "n-shape" straddling the p_i/F_i = 1 axis. This approach is commensurate with that of Haynes and Pender (2007). It should, however, be mentioned here that in case of size independence bias, normalised transport may decrease as size increases (see Fig. 14-9A, MIT OpenCourseWare, chapter 14).

Whilst there is notable controversy about the practicality of equal mobility condition since it was introduced by Parker et al. (1982a), it is now widely accepted that hiding effects are generally present in graded beds, and data will lie somewhere between size independence and equal mobility. Typically the conclusion of Wilcock and Southard's (1989) flume experiment in unimodal sediment is accepted, in that there is more bias towards the latter scenario (Parker et al., 1982a, ASCE, 2007) and it is this bias which helps underpin the common argument of considering D_{50} as a representative size class (as already have been discussed in previous sections) for transport relationships to be examined. Thus, the present Section uses this approach to examine the transport processes and bedload fractions affected by memory and to whether D_{50} can be considered representative for use in the power relations presented in previous section.

Fractional transports from the present data set have been derived from the integrated mass transport (later converted to volumetric transport in all analysis); in short, this requires dry sieving of the total mass of load transported

over the stability test flow steps. The shape of the p_i/F_i vs. D_i/D_{50} plots is then examined to determine any influence of hiding and exposure effects and comparison is then made between baseline and memory experiments. For analysis, focus is placed upon the transport of the fractions finer than the median size (D_{50} = 4.8mm) of the mixture in line with previous memory experiments which hypothesised that these fractions dictated memory response. This data is therefore provided in Figure 4.8. This clearly shows an 'n-shaped' profile suggestive of hiding effects being present; end fractions are relatively immobile, and middle fractions are relatively mobile, as per the typical characteristic feature of transport in gravel bed mixtures (Wilcock and Southard, 1989). The transport of the three finer grain classes (1.2mm, 1.7mm and 2.4mm) is significantly influenced, with p_i/F_i ratios ranging from <0.01 to 0.5. Whilst the coarsest fraction (D_i = 13.6mm) also indicates less mobility than expected, this outcome should be treated with caution as it may be a facet of the truncation of the flow steps at a discharge approximating to its independent entrainment threshold. The mid-size fractions (five grain classes) show bias towards equal mobility with a horizontal line nearer to 1, which is also characteristic feature of transport in graded sediment mixtures (Parker et al., 1982a; Wilcock and Southard, 1989).

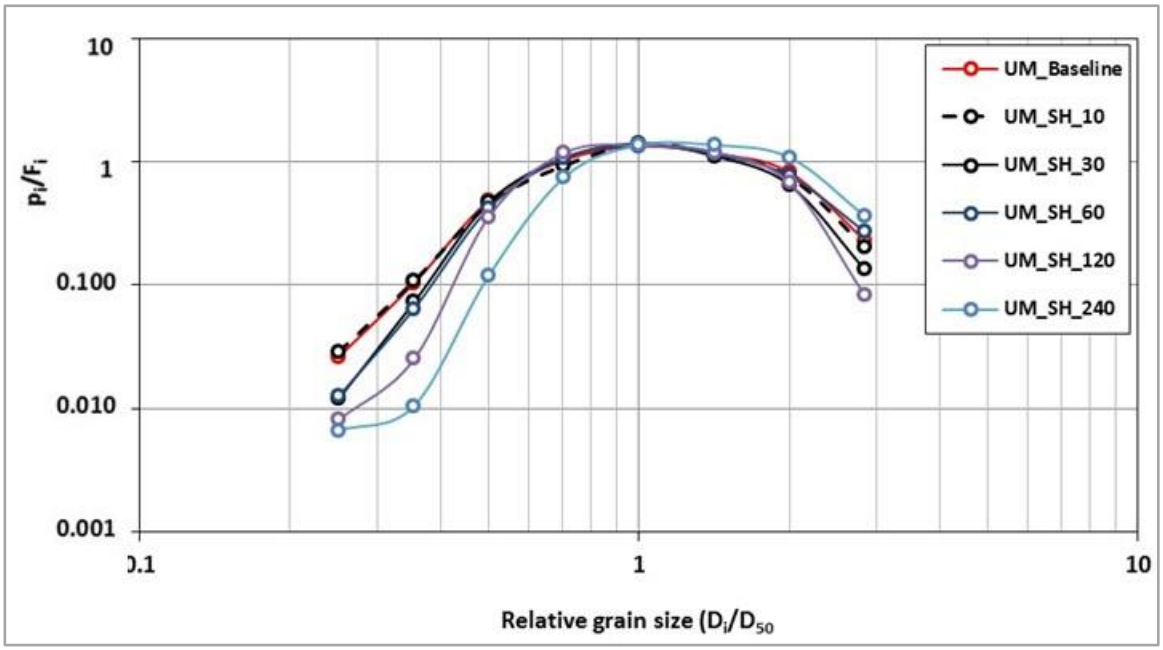

Figure 4.8: Normalised fractional transport rates p_i/F_i vs. relative grain size D_i/D_{50} showing size selective transport for finer grain classes, equal mobility transport bias for middle part of the classes (in literature, equal mobility transport are also referred for some size classes in the mixture, see Wilcock and Southard, 1988, and MIT OpenCourseWare, Chapter 14).

Also from Figure 4.8, it is clear that memory effect leads to more pronounced hiding effects and there is a clear hierarchical effect of memory on the transport of the finer classes. The SH_240 condition induces the greatest hiding effect on the finer fractions. Given the earlier analysis of total bedload transport (Sections 4.5.1 and 4.5.2), it follows that the more pronounced hiding effects of the fines are likely responsible for the increased overall stability of the bed and reduced sediment transport.

The logarithmic style of the commonly drawn Figure 4.8 masks easy interpretation and comparison of the memory induced changes on absolute magnitude and the percentage reduction of transport for each fraction relative to that of baseline data. Thus, Figure 4.9 (absolute magnitude for each fraction)

and Figure 4.10 (percentage reduction for each fraction) have been provided to aid quantitative comparison from baseline; threshold motion for each fraction is also presented in Table 4.7. Data in Figure 4.9 and Figure 4.10 show that SH_240 shows the highest reduction in the transport of finer fractions, with the two finest fractions being most responsive with up to a 94% reduction. For SH_120, 60 and 30, these percentage reductions are maximum of 70, 63 and 57 respectively. Data also show that it is the finest or 2nd finest fractions, which are typically the most responsive, 30-94%; the only exception to this is results found in the SH_10 experiment where fines are not responsive to memory effect (as also been noted in previous sections (4.5.1 and 4.5.2).

Table 4.7: Threshold shear stress for different size classes in baseline and memory experiment; however, as baseline and memory threshold are very similar, then the Figure does not show any sensitivity, thus not added

Di(mm)	Di/D50	UM_Base	UM_SH10	UM_SH30	UM_SH60	UM_SH120	UM_SH240
		τ_{ci}^{*}	τ_{ci}^{*}	τ_{ci}^{*}	τ_{ci}^{*}	τ_{ci}^{*}	τ_{ci}^{*}
1.2	0.25	0.088	0.115	0.118	0.111	0.118	0.118
1.7	0.35	0.062	0.081	0.083	0.079	0.083	0.083
2.4	0.50	0.044	0.058	0.060	0.056	0.060	0.059
3.4	0.71	0.033	0.044	0.045	0.042	0.045	0.042
4.8	1.00	0.026	0.034	0.035	0.033	0.035	0.030
6.8	1.42	0.021	0.027	0.028	0.026	0.028	0.021
9.6	2.00	0.017	0.022	0.023	0.022	0.023	0.015
13.6	2.83	0.014	0.019	0.019	0.018	0.019	0.010

Figure 4.10 indicates that the percentage reduction approximates to a constant (10-40%) for fractions equal to or larger than the median size i.e. $D_i/D_{50} \geq 1$; as no hierarchical response to memory stress is found, this may support larger fraction bias towards equal mobility transport (Figure 4.8) and/or bias of manual screeding towards some degree of artificial hiding for the largest particles (removal or burial due to planar screeding process).

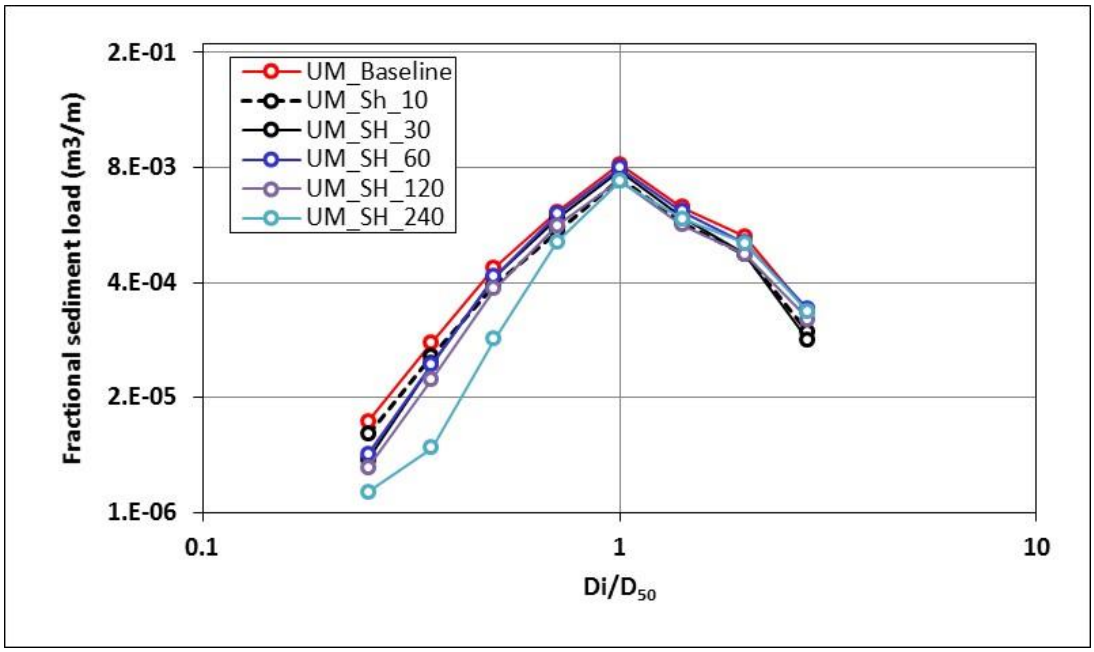

Figure 4.9: Fractional transports vs. relative particle size D_i/D_{50} showing strong size selectivity in transporting sediment for finer grain classes.

The trend in Figure 4.8 and 4.9 is further discussed here, which apparently may look surprising due to higher p_i/F_i values for larger size classes in memory experiments than baseline. In Figure 4.9, absolute magnitude of fractional load for larger size classes (for $D_i/D_{50}>1$) is higher in baseline than in memory experiments; while p_i/F_i values for those size classes in Figure 4.8 tend to show opposite trend for the memory results. This has been explained with examples; let us consider the largest size class (D_i=13.6 mm; D_i/D_{50}=2.83 mm).

i) p_i (for 13.6mm class): ratio of q_b (13.6mm) with the total bedload (q_T).
ii) Fractional load for 13.6mm is referred as $q_{b\_}13.6$; according to Figure 4.9, $q_{b\_13.6\_baseline} > q_{b13.6\_memory}$
iii) In all memory experiments, total bedload (q_T) is smaller than the baseline condition (see Table 4.3)
iv) p_i (for 13.6mm class) in memory= $q_{b\_13.6\_memory} / q_{T\_memory}$
v) p_i (for 13.6mm class) in baseline= $q_{b\_13.6\_baseline} / q_{T\_baseline}$

Here, $q_{b\_13.6\_memory} < q_{b\_13.6\_baseline}$ and $q_{T\_memory} < q_{T\_baseline}$. Thus, the p_i value (s) for the larger size classes in memory experiments are the ratio of two smaller numbers (bedload) as in (iv), while p_i value (s) for the baseline is the ratio of two larger numbers as in (v); thus in the p_i/F_i plot in Figure 4.8, the p_i for

memory can still lead to a larger value (opposite trend than in Figure 4.9) due to the reduced total load (q_{T_memory}) in memory condition by the disproportionate response (due to memory) of other size classes; thus the opposite trend in p_i/F_i plot for larger size classes in memory experiments (Figure 4.8) may not necessarily be an anomaly. More-over, as the vertical settlement of finer grains seems to make a stable bed for coarser particles as well by creating a better angle of repose (Fenton and Abbott, 1977), the reduced mobility of the larger grain classes in memory experiments are not surprising.

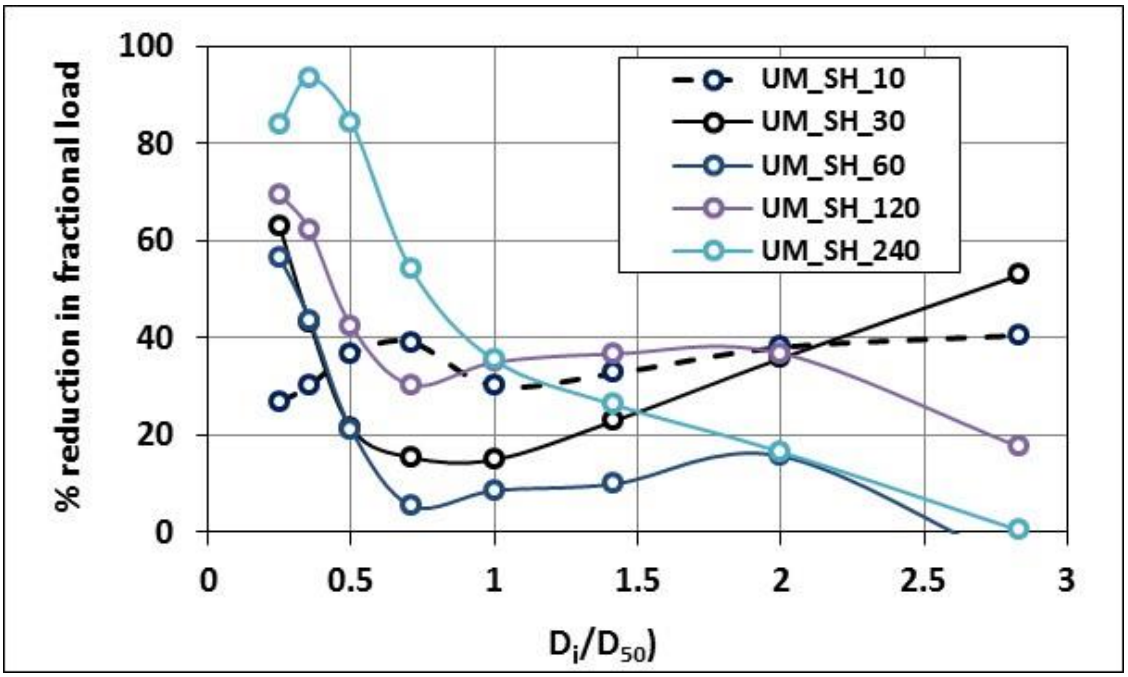

Figure 4.10: Percent reduction in fractional transports vs. relative particle size D_i/D_{50} (compared to baseline runs), showing strong size selectivity in transporting sediment for finer grain classes.

In summary of this Section on fractional data: (i) hiding effects of fine fractions of the bed appear strongly influential upon the transport process of the unimodal bed; (ii) the finer fractions of the bed do illustrate a disproportionate response to memory effects, compared with other fractions (particularly the middle fractions and the median size class); (iii) there is clear hierarchical response of hiding effects, of the fines, to memory duration. Thus, by extending

the applied flow sequence to higher discharges, compared with previous studies, clearer evidence has been provided that corroborates earlier hypotheses that the fine fractions' hiding effects appear the responsible process for memory effects to develop in a time-dependent manner.

4.7 Discussion of results

4.7.1 Influence of memory on bed shear stress and entrainment

Shear stress is the more generic parameter used in sediment transport and for entrainment of sediment. The parameter from the present research, both in its dimensional and non-dimensional form has been compared and contrasted with the similar research on memory stress. Haynes and Pender (2007) and Ockelford (2011) carried out stress history experiments with unimodal mixtures of gravel with equivalent median size (D_{50}=4.8mm), although Haynes had a higher bias towards the finest classes. Whilst subtle methodological differences in 'stability test' set-up have been alluded to earlier in this Chapter, it is also worth highlighting that both previous studies used a visual entrainment threshold assessment, based upon Yalin's approach (Yalin, 1972). As this is distinctly different (see e.g., Buffington and Montgomery, 1997 for discussion) from the reference transport definition of threshold used in the present study, this further limits direct comparison of data. That said, the equivalence of their objectives, sediment, memory and flume equipment (0.3 m width) mean that discussion is warranted, in terms of confidence in the present data set and general explanation of processes responsible for memory effects. With regard to absolute critical shear stresses (baseline data), the present study notes values of 2.00 N/m^2, 2.55 N/m^2 or 4.00N/m^2 (calculated via Parker, Shvidchenko or Shields' approaches respectively); the first two of these values approximate to the equivalent unimodal data of Ockelford (2.82 N/m^2) and Haynes (2.91 N/m^2) with subtle differences likely reflective of the different threshold definition applied (Haynes and Pender, 2007; Ockelford, 2011). Discrepancy with the Shields value is a facet of a higher reference transport value, more akin to general transport than incipient motion (Shvidchenko et al., 2001). To investigate this further, the dimensional value of the shear stress from Haynes

and Pender (2007) and Ockelford (2011) studies were post-processed and normalised to non-dimensional values (τ^*_{c50}). The non-dimensional critical shear stress values of Ockelford (0.039) and Haynes and Pender (0.038) sit well below the Shields reference transport of the present study (0.051), Table 4.8; this outcome is expected, as Buffington and Montgomery (1997) noted that reference transport approach entrainment value from historical researchers was biased towards Shields' work and threshold values sit well above those calculated from visual approaches. Thus, overall baseline data from this thesis appears generally consistent with previous flume studies simulating near-threshold flows over unimodal sediments.

Table 4.8: Shields number from indirectly comparable memory studies by previous researchers

Researcher	Median Grain size D50 (mm)	Flume width (m)	Flume gradient	Baseline: τ^*_{c50}	R_{e*}	Approach of calculating threshold shear stress
Ockelford (2011)	4.8	1.8	0.005	0.027	250	Yalin's visual approach
Ockelford (2011)	4.8	0.3	0.005	0.039	260	Yalin's visual approach
Haynes and Pender (2007)	4.8	0.3	0.007	0.038	259	Yalin's visual approach
This study	4.8	0.3	0.005	0.026	175-297	Parker ref. transport
				0.033	175-297	Shvidchenko ref. transport
				0.051	175-297	Shields ref. transport

Although a range of uncertainties exist within and between existing memory data sets, it is fair to consider that when results from a single investigator are presented in relative terms, the influence of uncertainties diminishes. Therefore comparison of relative results is more worthy than review of absolute values. As the incremental stability test of Ockelford is of closest equivalence to the present thesis methodology, it is notable that her memory experiment noted ~ 8% increase in shear stress (absolute magnitude) at SH_60. For identical memory duration, the present study found this increase to be only 3%; however, the SH_60 datum is clearly noted as an outlier to the overall trend of Table 4.4 in that SH_30 and 120 minute data indicate a 7% and 8% memory effect respectively. Thus, it appears that both studies do show similarity in the order of magnitude of memory response (Figure 4.11) and confidence is afforded to the more advanced analysis into non-dimensional and mathematical model development undertaken within the present thesis.

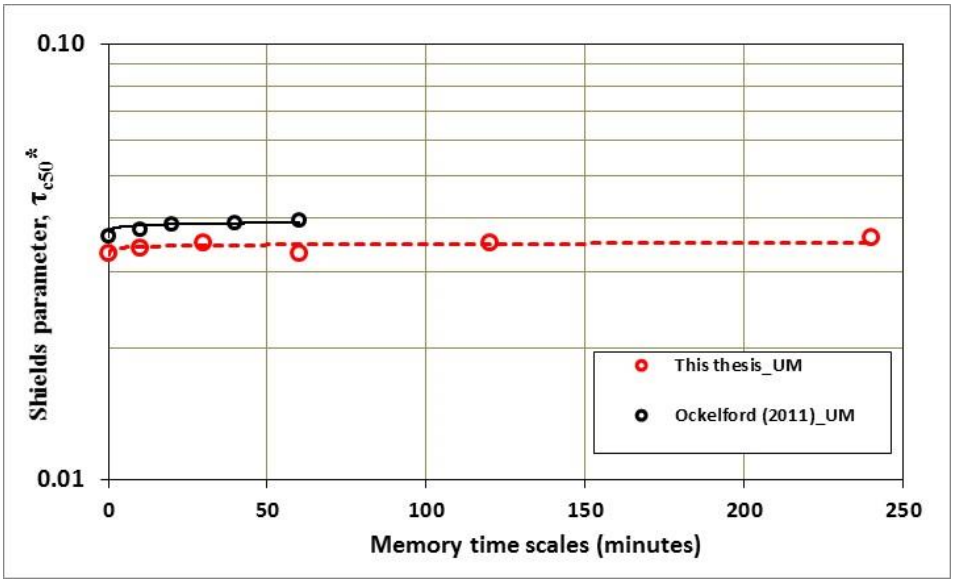

Figure 4.11: Response of memory stress of varying time scales on sediment's threshold motion in unimodal sediment mixture.

Results presented above are from limited number of memory studies, yet showing general similarity on the trend (Table 4.8 and Figure 4.11). Memory stress is a time scale of sub-threshold stress which leads to development of several key processes such as increasing size selective transport, vertical and

horizontal winnowing of the fines through particle oscillation and preferential entrainment of the smaller particles (Saadi, 2002; Haynes and Pender, 2007; Saadi, 2008; Ockelford, 2011, and the present thesis); winnowing of the fines may lead to surface coarsening of the bed towards development of mobile armouring. Ockelford and Haynes (2013), due to memory stress, observed changes in local bed structure, particle re-arrangement, and spatial heterogeneity of sediment bed packing characterised by increasing vertical and horizontal roughness. Similar effect due to water working, not necessarily and explicitly from water-working by sub-threshold stress, also changes entrainment threshold due to development of stone cells and ring, armouring (mobile and static), changes in friction angle, changes in hiding and exposure, bio-stabilisation etc. Many past researches involved prolonged period of water working (e. g., Shields, 1936, and Church et al., 1998), but did not partition their findings, such as how much effect was attributed from sub-threshold memory stress alone. Many of such water working studies (e.g., Komar and Li, 1986; Kirchner et al., 1990; Church et al., 1998) might well have implicitly included the effect of memory of sub-threshold stress; for example, Church et al. (1998) conducted long hours (upto 100 hours) of flume experiment in cobble – gravel bed (Reynolds number range 100 to 1600, i.e., mainly gravel bed rivers); they noted development of stone cells in parallel to armouring of bed and observed that the joint effect of armouring and stone cells can increase entrainment by 2-fold, and sediment load decreased by the order of 10^3. This impact of this water working not only happened at τ^* / τ^*_{c50} <1; this also happened for the condition τ^* / τ^*_{c50} > 1. Fenton and Abbott (1977) noted an order of magnitude of increase of threshold shear stress due to changes in friction angle from water working. Several such effects were quantified in Section 2.5.4, and thus not repeated here. Vignaga et al. (2011) and Vignaga (2012) studies biostabilisation of sand-gravel bed, and observed 9-150% increase of threshold shear stress relative to abiotic bed. The effect of water working on entrainment threshold is the key parameter in sediment transport management, and thus partitioning the effect of memory stress from other water working, due to individual or collective processes development, will benefit the practitioners in using the appropriate parameter, rather than lumped parameters in prediction and management of sediment transport. This implication is discussed

in the follow-up sections in relation to bedload transport formulae, river flow regime, and areas of application, particularly in gravel bed streams.

4.7.2 Role of memory on bedload transport and river bed stability

In a similar manner, comparison of previous memory studies can be made in terms of bedload data. Bedload transport is directly measurable and exhibits a disproportionately high response to memory effects (compared with shear stress). In short, Ockelford (2011), Haynes and Pender (2007) and the present study have demonstrated that memory reduces the transporting ability of the flow. The present thesis notes a reduction of bedload transport by 40, 63, 44, 70 and 80% for memory time scales 10, 30, 60, 120 and 240 minutes by applying a sub-threshold stress, 60% of τ^*_{c50} (Table 4.3, Figure 4.12); Ockelford observed 90% reduction in her unimodal mixtures by applying a sub-threshold stress, 50% of τ^*_{c50} for memory time scale of 60 minutes. Subtle differences between the two studies are likely due to the longer pre-experiment 'bedding-in' time (30 minutes) applied by Ockelford, compared with the 3 minute period employed herein; in explanation, whilst bedding in flow is of extremely low discharge and applied shear stress, it does constitute a small component of memory and is likely able to contribute to enhanced bed stability in its own right. Similarly, comparison with Haynes and Pender (2007) shows their data to have a 47.9% reduction in sediment load, but in a much longer memory time scale of 5760 minutes using a sub-threshold stress, 53% of τ^*_{c50}. This is distinctly less than the 240 minutes scale of the present thesis. In justification, this is reasonably attributed to Haynes and Pender's use of a constant high discharge stability test which likely led to a more 'catastrophic' failure of the bed tending to equal mobility transport bias, hence loss of subtle memory signals more notable at lower shear stresses with selective entrainment bias. Once again, when taken overall, it does appear that memory effects on subsequent bedload are significant and data from the present thesis is in line with those published by others, given the degree of extreme non-linearity of a bed's response at low flows (See Eq. 4.5 to 4.10; and Paintal, 1971; Parker et al., 1982a, and Shvidchenko et al., 2001) and strong fluctuation of turbulent eddies at low flows (Zanke, 2003).

Importantly, in considering memory effects it has been found that bedloads at low transport rates were extremely non-linear in their response to applied shear stresses. Whilst the implications for generic, non-dimensional mathematical modelling of memory effects are discussed later (Section 4.7.5), it is worth noting that similar non-linearity has been found by other researchers (Paintal, 1971; Taylor and Vanoni, 1972, and Parker, 1990a). Non-dimensional transport in non-memoried bed varies with a 16.2 power of the bed shear stress in the present thesis (Eq. 4.5); this degree of non-linearity is similar to Paintal's exponent of 16, Taylor and Vanoni's of 17.5, and Parker's of 15.7. Specific to memory hierarchy, comparison of such non-linearity to previous memory studies (Haynes or Ockelford) is not possible due to limitations in their bedload sampling. However, relevance to other studies is worth discussing in terms of the non-linearity of the memory effect itself. Previous studies have assumed that memory effects tend to a constant after long memory durations. Haynes and Pender (2007) intimate a logarithmic relationship between memory duration and bedload transport tending towards a constant at memory timeframes > 24 hours; this stems directly from long-memory experiments (up to 4 days). Ockelford (2011) rejects the logarithmic relationship of Haynes and Pender, noting that their relationship implicitly precludes tendency towards a constant, instead favouring a bounded power law relationship; however, her data set memory periods are too short to examine the value of the proposed constant with any certainty. Thus, the present thesis data have been re-evaluated to ascertain the validity of the 'memory → constant' notion and presented in Figure 4.11 (response on entrainment threshold) and Figure 4.12 (response on bedload transport).

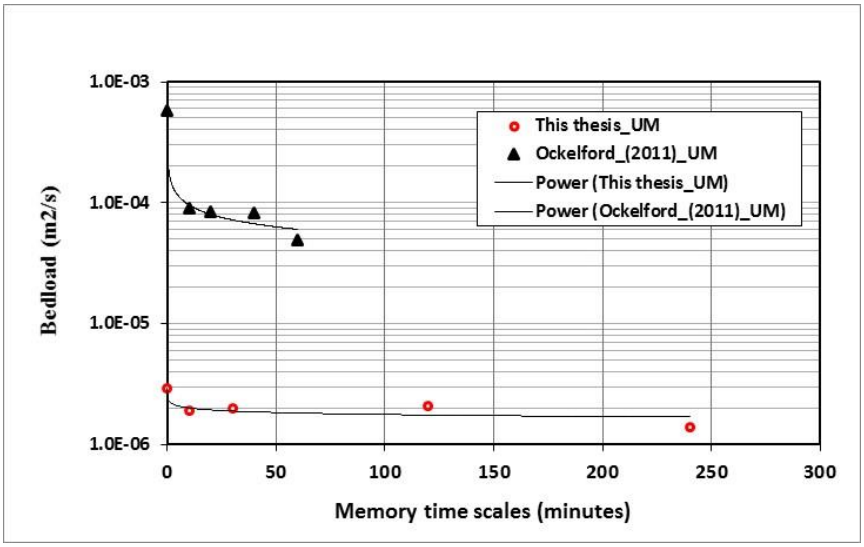

Figure 4.12: Response of memory stress of varying time scales on bedload transport in this thesis and in Ockelford (2011).

The effect on both threshold motion presented in preceding section (Figure 4.11) and bedload (Figure 4.12) clearly indicates that effect of memory stress at longer memory time scales tends towards an asymptotic value if not towards a constant value. Short duration memory stresses are far more responsive (i.e. a faster rate of change in the Figures above) up to SH_60 minutes, and then for longer memory time scales the decay (for bedload) and growth (for entrainment threshold) shows very slow process tending towards a constant. As such, this holds general agreement with the previous notion of Ockelford (2011).

A further important point that stems from the hierarchical bedload to memory relationship, is the two-phase response. Section 4.5.2 has shown that memory effects persist and strengthen with rising discharge (Phase 1), before a discharge of Q=17.5 l/s (56 minutes) appearing to act as a 'trigger point' for the progressive erasing of memory (Phase 2). Review of the literature for traditional non-memory graded entrainment/transport data sets indicates that multi-phase temporal development of beds/bedload is common (e.g., Proffitt and Sutherland, 1983; Tait et al., 1992 and Pender et al., 2001). For example,

research into degrading flume systems with armouring processes by Pender et al. (2001) suggests distinct 'trigger points' in the flow-sediment system; Phase 1 of his beds' development exhibited loose packing and sediment easily entrained, before Phase 2 commenced an armouring process where the degradation 'memory' starts to consolidate and stabilise the bed, leading to reduction in bedload transports. Essentially, the present thesis exhibits a reversal of Pender's phases, due to the sub-threshold memory period applied herein. The memory period has been found to undergo a process 'akin to armouring' (Ockelford, 2011); i.e. without active transport, alternative stabilisation processes of in-situ hiding and particle reorientation (Ockelford and Haynes 2013) serve to restructure the bed locally (Mao et al., 2011). This memory effect requires >10 minutes (at least) to develop, as only beds SH_30-240 minutes exhibit memory response in the present thesis. In the present study, Phase 1 of the incremental flow-step period reflects this enhanced structural resistance to entrainment of the bed, which delays bedload until higher discharges. Phase 2 then represents the trigger threshold for the reversion to 'normal' bedload transport, when the applied shear stress is now sufficient to entrain the stronger structure of the memoried bed and begins to erase the memory effect by tending to more general bedload transport. Interestingly, the trigger threshold for Phase 2 occurs at similar shear stress, independent of memory duration; this may be: i) due to the mobility of the larger fractions, which were least affected by memory stress (Figure 4.8) hence initiate their mobility at a similar shear stress, ii) that this is the shear stress at which the exposure of larger particles and the hiding of the fines balance each other, triggering a general (equal) mobility.

4.7.3 Fractional transports in response to memory in bed

Based on the above speculation for trigger point mechanics, it is important that we consider briefly the fraction-specific processes responsible for memory effects. In short, the present data agrees with the long-standing principle of size selective transport for graded beds (e.g., Egiazaroff, 1965; Ashida and Michiue, 1972; Parker et al., 1982a; Parker and Klingeman, 1982; Komar, 1987a, b; Ashworth and Ferguson, 1989; Kuhnle, 1992). Similar to Ockelford's (2011) unimodal data, this study finds relative mobility of the middle fractions, relative immobility of end fractions and, crucially, a strong memory effect enhancing size selectivity. As speculated by Haynes and Pender (2007), the memory effect

is strongest in relation to increased hiding of the finer proportion of the bed. Previous literature cites vertical winnowing (Hoey et al., 1997; Ockelford, 2011) of these fines through the pore spaces of the larger fractions to be the hiding mechanism (Reid and Frostick, 1986; Marion et al., 2003; Haynes and Pender, 2007). Under the sub-threshold flow applied herein, this process is likely induced via gravity, local bed vibrations, local boundary fluid inrushes and/or neighbouring grain rotations rearrangement.

Data herein notes hierarchical memory effects particularly prominent in the finer fractions where fractional bedload reduced by 57-94% for SH_30-240 minutes of applied memory. Ockelford (2011) also notes size selective entrainment in the finer fractions (1.4 to 5.6 mm) of her unimodal bed, although she did not quantify this specifically. Thus, given that the memory response of the larger fractions is typically far less (typically <20%) than that of fines, Haynes and Pender's (2007) original hypothesis that increased size selectivity of the finer grain classes is likely the key factor for increasing stability of memoried bed therefore appears valid.

More widely, this finding is supported by e.g., Frostick et al. (1984); Reid and Frostick (1986); Church et al. (1998); Wilcock and Crowe (2003), whose works also demonstrated that sand content can reduce the entrainment threshold of the median grain size. Ockelford's (2011) laser data goes further, to provide conclusive evidence of local reorientation of surface particles, likely triggering "sieving" of the fines to deeper pores which would leave larger surface pores and freedom for coarse particles to rotate into a more stable structures (Saadi, 2002, 2008).

4.7.4 Normalised stress and transport: this thesis and others

Section 4.4 has strongly detailed the derivation and comparison of non-dimensional parameters of bedload and bed shear stress, indicating that the memory condition and its timescale has a significant and hierarchical effect on river bed stability, transporting ability, and entrainment threshold of sediment. Three aspects are the focus of this Section: (i) satisfactory performance of baseline data, compared with similar studies using non-dimensional approaches; (ii) detailed examination and critique of the Shields number, in light of re-

review of his original data for memory; (iii) development of non-dimensional approaches for inclusion of memory effects. As much of the rationale underpinning the mathematical development is already discussed in Section 4.4, only a short discussion is noted here, as specific to demonstrating the wider issues surrounding the selected mathematical approach.

4.7.4.1 Non-dimensional reference shear stress (τ_{c50}^{*})

The threshold shear stress (τ_{c50}^{*}) in this thesis was based on the reference transport approach of Shields (1936), Parker et al. (1982a) and Shvidchenko et al. (2001). From Section 4.5.4 it was found that the Shields reference determined was too high for use in the current data set, hence the baseline τ_{c50}^{*} values in this thesis were concluded to be 0.026 and 0.033 respectively based on the reference of Parker et al. (1982a) and Shvidchenko et al. (2001). As such, discussion is warranted as to why the "pivotal" work of Shields falls short of capturing the entrainment threshold of the present thesis.

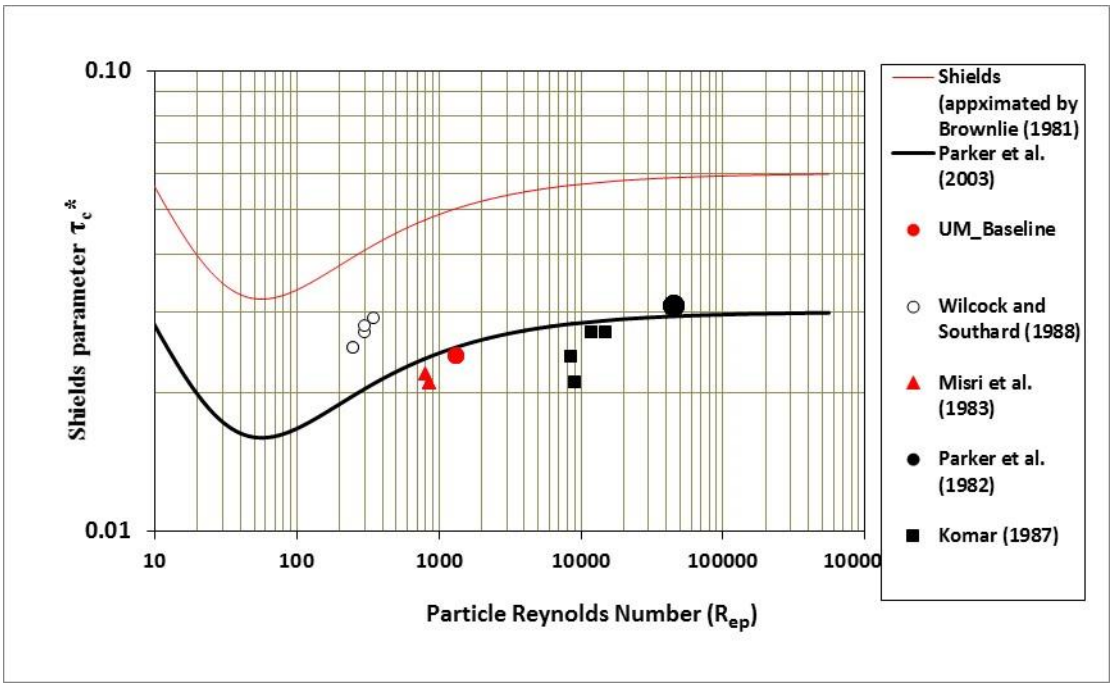

Figure 4.13: Non-dimensional shear stress from baseline experiment and from other researches in gravel beds.

For illustration purposes, Figure 4.13 shows the baseline τ_{c50}^{*} data (calculated using Parker's method) compared with the original Shields curve (Eq. 2.22) and the modified Shields curve of Parker (Parker et al., 2003; Eq. 2.24).

Also shown are comparative entrainment threshold values (non-memoried) from similar laboratory based studies observed in wider literature (Parker et at. 1982; Misri et al., 1983; Komar, 1987; Wilcock and Southard, 1988;). All these data show reasonable similarity with Parker's curve for natural gravel bed rivers (Section 2.5, Figure 2.7), yet fail to be predicted by Shields. Thus, three notable problems with the Shields reference curve use in graded and memoried beds are raised:

Firstly, Shields' data arise from a near-uniform bed. When this method is applied to a graded bed the τ_{c50}^{*} should theoretically be lower, due to exposure effect of larger particles (Section 2.5.1 and 2.5.2; Eq. 2.25-2.36); because relative size effect counteracts the absolute size effect, and decreases mobility of finer fractions, and increases mobility of larger fractions (Wilcock and Southard, 1988), and hence larger fractions have lower threshold compared with their uniform size threshold. Also, in order to obtain a τ_{c50}^{*} similar to Shields curve would imply that the transport of this thesis' unimodal mixture demonstrates size independence; this is not the case, as fractional transport (Section 4.6) showed strong size selectivity. There is hardly any evidence of mixed sediment showing size independence where the hiding function exponent *m* in Eq. 2.30 to 2.31 approaches zero. Rather, existing literature supports the exponent value typically ranging between 0.4 and 1.0 indicating partial, size selective, and equal mobility of transport (Komar, 1987, Parker, 1990a, Carling, 1991 and Ashworth et al., 1992) in graded sediment as found here in the present study. Thus, Shields curve fails for graded sediments and Section 6.3.1 is specifically dedicated to detailed analysis of the size selective exponent value for memory effects.

Secondly, Shields' curve is likely over-estimated due to undocumented (hence ignored) water working effects (i.e. memory) in his original data; this factor got hardly any attention in the literature. Although in their review of Shields and

threshold data, Buffington and Montgomery (1997) noted that τ^*_{c50} could vary by an order of magnitude due to water-working changes in particle projection and angle of repose (Fenton and Abbott, 1977), they do not conclude that Shields' own experiment suffered this. Thus, the present thesis has re-reviewed the original Shields publication (translated to English) specific to the water-working period(s) of his employed methodology. This clearly states that Shields (page 33, Shields 1936) obtained "16 different water depths by gradual increase of discharge; each time a state of equilibrium was awaited over an hour". Therefore, to attain his perceived equilibrium state, it can be deduced that he took over 16 hours to complete each experiment; most likely, each experiment was completed over two days of time (i.e. a drained bed, stagnant body or flowing body was therefore left during the overnight period). This set-up holds equivalence to memory stress, hence Shields' threshold motion is likely delayed to higher shear stresses (thus explaining his higher reference threshold curve). Very crude extrapolation of the present thesis' memory stress data would therefore pro-rata as 44% increase in threshold due to 16 hours of memory in Shields experiments; however, if his runs were performed over two days with flowing water overnight then the increase in threshold shear stress would be approximately 100%. This would account for approximately an order of magnitude difference between the present thesis and Shields' data. Although the work of Parker et al. (1982) cannot be directly unpicked for memory, the similar reference threshold value of Shvidchenko (2000) is certainly derived from non-memoried data, as all his experiments were completed within 12-15 minutes.

Thirdly, photos from Shields' work (Figure 4.14) clearly show that bedforms developed in his flume bed. As the bed of Shields' flume was near uniform sediment, its susceptibility to bedform development during the memory (water working) period appears valid, likely in response to burst-sweep turbulence length scales, rather than local rearrangements due to bed roughness, as found in graded bed research (Reid and Frostick, 1986; Church et al., 1998; Haynes and Pender, 2007; Ockelford, 2011). However, mechanics aside, the effect of bedforms on threshold (e.g., Wiberg and Smith,1989) show that τ^*_{c50} values can decrease more than two fold (from 0.10 to 0.04-0.05) after adding corrections

for bedform friction. Thus, it is logical that bedform development during memoried experiments is important in explaining why Shields' values are higher than alternative reference transport values and those of the present thesis.

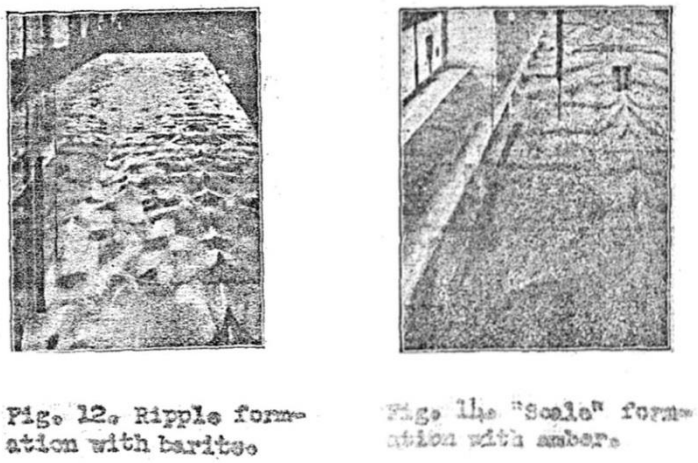

Figure 4.14: Shields flume: initial flat bed turning into significant bedforms (probably from long hours (over several days) of experiment in same bed (Source: photograph taken from Shields original publication, Shields, 1936).

In summary, the baseline τ^*_{c50} from present thesis showed consistency and similarity with threshold motion of sediment mixtures in well cited literature, tending to Parker et al. (1982a) and Shvidchenko et al.'s (2001) reference values. Strong rationale for the differences to Shields' over-estimated reference value have been provided, including evidence that Shields' data suffered from bedform development and memory stress.

4.7.4.2 **Bedload transport relations**

In Section 4.4, non-dimensional transport of baseline experiments has been compared and contrasted with a number of bedload transport relations (Casey, 1935a, b; USWES, 1935; Meyer-Peter and Muller, 1948; Einstein, 1950; Paintal, 1971; Luque and van Beek, 1976). The outcome of the comparison was that relationships developed for data sets specifically including results near entrainment threshold were most appropriate for use, when grain size similarity was also present. Paintal's power law (Eq. 4.4) matched well with the relation

of baseline transport from the present study, due to generation of initial data at similar low transport regimes, use of gravel bed mixtures and data collection from flume experiments. Thus, there is logical motivation of developing power law functions similar to Paintal for both baseline and memory stress conditions (Eq.4.5 to 4.10) which are able to quantify memory effects over a range of low flow transport conditions. Chapter 6 is dedicated to this development, as specific to bedload formulae aligned to low threshold shear stress (e.g., Wu et al., 2000b).

4.7.5 Significance of memory and relevance to reference transports in low flow

Memory stress effects exist over a good range of low flow reference transport (q^*) values between 10^{-1} to 10^{-5} (Figure 4.15). Inserted into this Figure were the reference transport based determination of entrainment threshold from Shields (1936, q^*=10^{-2}), Parker et al. (1982a, q^*=10^{-5}), and Shvidchenko et al. (2001, q^* =10^{-4}) (Section 4.4) and the conclusions drawn from these data support the discussion raised in Section 4.7.4.1. In short, Shvidchenko's reference value of 10^{-4} approximates to baseline data, thus appearing a reasonable (or slight over-estimate) reference threshold for non-memory runs. However, it is too high a reference for memoried runs where a more reasonable reference value would be towards Parker (q^*=10^{-5}). That said, it has been shown that memory duration leads to hierarchical and nonlinear response in reference threshold value, and thus the reference threshold must also be a sliding scale which, in the present thesis, appears to range between 10^{-4} and 10^{-5} for memories up to 240 minutes. This is further complicated due to the recognised 'trigger point' (~3.7 N/m^2 (Q=17.5 l/s) in the present study) where memory effects erase such as to 'revert' to non-memoried, baseline transport rates; this 'trigger point' threshold falls around a reference value of $q^* = 10^{-2}$, which can be used to indicate a shift to full mobility and more general transport conditions as described by Shvidchenko (2000).

It is clear from the above data that threshold reference of transport sits on a sliding scale depending on memory duration, hence its (in)correct selection will

affect the accuracy of sediment transport model predictions. For example, use of Parker et al. (1982) reference transport approach means that critical shear stress will increase from 15 and 19% due to memory effects from 10 and 240 minutes memory time scales; while for Shvidchenko et al. (2001) reference transport, the increase is between 3 and 9%. These percentage data were derived from Table 4.5, while Figure 4.15 is shown only to demonstrate qualitatively that selection of a particular reference transport will yield different memory effect, which is clearly visible in this Figure as the memory effect gradually diminishes with the increase of shear stress. They key reason of Shividchenko et al. (2001) reference transport as entrainment threshold will lead to smaller memory effect is that this reference transport occurs at a higher shear stress than Parker et al. (1982), where the memory effect starts to weaken. Although this increase in threshold value may seem relatively small, the nonlinear response of bedload to shear stress means that the present study finds it to cause sediment load to reduce by up to 80%.

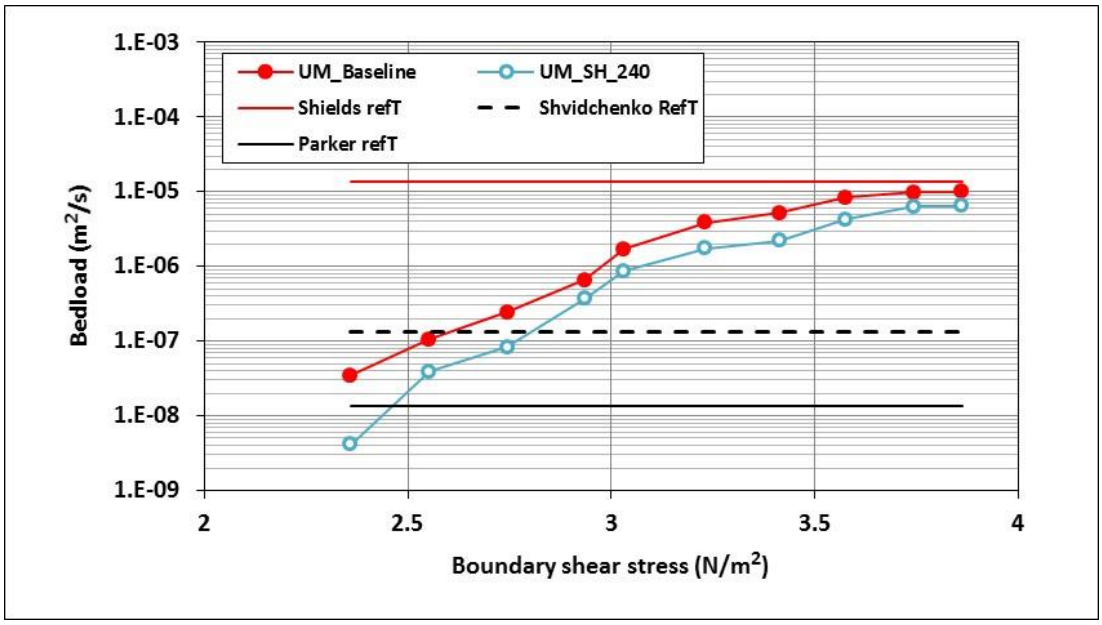

Figure 4.15: Sediment rating from present research for baseline and 240 minute memory stress condition; also shown Shields reference transports (1936, q^*=10^{-2}), Parker et al. (1982a, q^*=10^{-5}), and Shvidchenko et al. (2001, q^*=10^{-4}).

This non-linearity is well-known (e.g., Taylor and Vanoni, 1972; Paintal, 1971) and can be appropriately considered using reanalysis of Turkey Brook data (Reid and Frostick, 1986) as a typical UK gravel bed river known to exhibit memory stress. For this river, Figure 4.16 clearly shows that near-entrainment bedload data typically fall lower than the Shields reference threshold, rather tending to that of Parker and Shvidchenko's reference values. This lends support to the laboratory-based findings of the present thesis. Thus, given that the typical transport of Turkey Brook calculates around 2-3 tonnes of sediment a day (derived by present researcher from Reid and Frostick, 1986); it follows that (i) if memory effects are implicit in this measurement, current modelling practice would lead to a 20-fold of over-prediction of bedload transport in this river; or (ii) if this measurement masks memory effects due to event-scale or averaging measurements, then the under-prediction will be of a similar order of magnitude. This issue is expanded upon further in analysis of bedload prediction in Chapter 6, as its importance to predictions of scour, erosion or deposition are crucial to accurate pre-emptive river management and intervention strategy design.

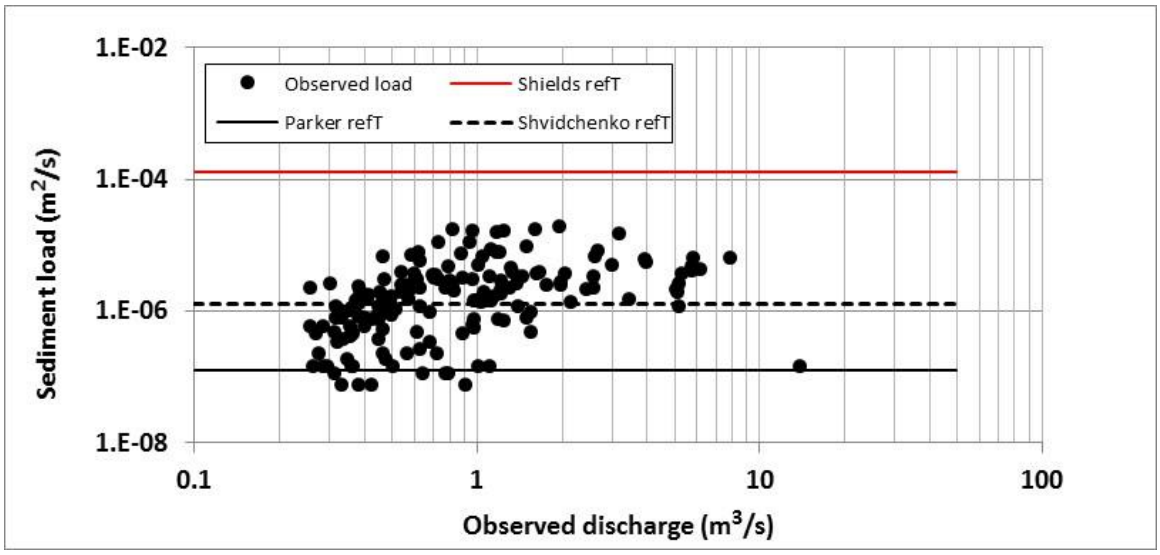

Figure 4.16: Gravel bedload transports in Turkey Brook (observed load) in low flow shear stress within the threshold limit of Shields (1936), Parker et al. (1982a) and Shvidchenko et al. (2001).

4.7.6 Memory in bed: need for a correction factor to bedload functions

Thus, when taken as a whole, the earlier discussions of Section 4.7 generally conclude that memory effects are well-demonstrated with a degree of certainty and significance appropriate to including a memory "correction" into existing entrainment and bedload transport formulae.

Almost all bedload transport formulae whether for uniform or graded sediment include non-dimensional critical shear stress in their functions. Hence, a generic form of a bedload transport formula (Chapter 3 by Parker, ASCE, 2007) can be given by:

$$q^* = T_b(\tau^*, D_i / D_{50}, R_{e*}) \qquad \text{Equation 4.11}$$

In which T_b is the dimensionless bedload transport function. It is obvious from the above formula that to address effect of memory stress in predicting bedload, several parameter adjustments are possible to account for the varying degree of memory response on a bed's stability, threshold motion and disproportionate fractional response. Thus, at this stage of the research, it appears possible to parameterise memory effect within one or more of the following terms: i) the reference shear stress, τ^*, ii) the hiding function via the relative size term D_i/D_{50}, and/or iii) the shear Reynolds number, R_{e*}, which in effect corresponds to the non-dimensional roughness height (Zanke, 2003) as able to account for structural changes on bed. This conclusion underpins the approach discussed and executed in the detailed framework for memory stress correction of bedload transport provided in Chapter 6.

4.8 Key outcomes

The memory stress of unimodal mixture of sediment subjected to unidirectional sub-threshold flow has been modelled; the mixture comprised two sand classes and six gravel classes with median grain size (D_{50}) of 4.8mm and sorting coefficient (σ_g) of 1.65. Flume experiments have been conducted in beds without memory (baseline experiments) and with memory so as to quantify the effect on

entrainment threshold, on the transporting ability of the flow and size selective transport. Memory condition experiments included 10, 30, 60, 120 and 240 minute memory stress durations.

Key outcomes from the above experiments are presented below:

- Memory stress duration increased the stability of the bed, delayed the entrainment threshold of sediment movement, and thus reduced the subsequently transported sediment volume.

- Entrainment threshold has increased an average up to 19% for the median grain size (D_{50}) using Parker et al. (1982a) reference based transport ($q^* = 10^{-5}$); using the alternative Shvidchenko et al. (2001) reference based approach ($q^* = 10^{-4}$), the increase is 11%. This distinction is expected as Shvidchenko et al. reference transport corresponds to a higher shear stress than that of Parker et al., and memory effect was observed to weaken with rising shear stress at higher transport rates (see Figure 4.5).

- Due to rise in entrainment threshold, subsequent transport decreased by up to 80%; the longer the memory time scale the higher the reduction.

- Size selective transport was observed as the key transporting mechanism. All end fractions suffered relatively less mobility than the middle fractions. The finest fractions reduced availability for transport by up to 95% due to memory; this was most pronounced for the longest memory experiments (240 minutes). The larger fractions were found biased towards equal mobility of transport; their transport reduced between 10 - 40% due to memory. This supports the notion of fines being most responsive to memory effects.

- Effect of memory stress on the transporting ability of flow was found to prevail mainly in low transport condition of q^* between $1x10^{-6}$ *to* $1x10^{-1}$ for a Shields parameter range between 0.02 and 0.06. It therefore indicates that use of the Shields threshold condition (of 0.06) is

inappropriate to assess memory effect as it is too high relative to the domain where memory effect dominates.

- Memory effects were found to vary non-linearly over the low flow transport range; this has been embedded in a family of mathematical descriptors using rising “exponents” of the function to quantify degree of non-linearity of transport to shear stress, whilst changes in the structure of the bed due to memory are described within in a lumped “coefficient”. Response on the coefficient due to memory stress was observed more reactive than on the exponents. For memory time scale SH_10 to 240, the exponents vary approximately between 17 and 21, which is about a 1.3x rise relative to baseline; while the coefficients show a rise of eleven orders of magnitude relative to baseline. This clearly shows that memory effects strongly relate to bed structure; this is certain for two reasons: i) analogous to this many bedload formulae include effect of form roughness and granular scale roughness in the coefficient term in the bedlaod vs. shear stress power law (Meyer-Peter and Muller, 1948; Smart, 1984 and Wu et al. 2000a); ii) because applied bed shear stress is same in all experiments, and bedload is a measured variable, while this coefficient is the major unknown parameter; thus even if we would have considered same exponent as in baseline (baseline and memory exponent differ maximum only by a factor 1.3), the coefficients must have to adjust in the bedload vs. shear stress power law to match the measured bedload in different memory experiments. And worth mentioning that similar magnitude of coefficient was noted by Paintal (1971).

Chapter 5: Physical Modelling Results: Bimodal sediment

5.1 Introduction

Given that in graded sediments of gravel the river bed consists of either unimodal (Chapter 4) sediment or bimodal sediment (Kondolf, 1988), Chapter 5 presents results from bimodal sediment experiments with memory in the bed. The presence of two modes of particle size complicates the mechanics underpinning sediment stability/instability and the prediction of transport of sediment; this is predominantly due to the hiding and exposure of the finer and coarser particles respectively (Klingeman and Emmett, 1982; Ferguson and Ashworth, 1989; Kuhnle, 1993a; Wilcock, 1993; Powell, 1998; Wilcock, 2001). Thus, it is uncertain as to whether the memory effects observed in unimodal beds (Chapter 4) will be found to be equivalent in bimodal sediment systems.

Two objectives are researched within the present Chapter. Firstly, do 'memory' effects exist within the transport of heterogeneous sediment, and comparing bedload transport data specifically for bimodal sediment with that of others (Kuhnle, 1994; Wilcock et al., 2001; Almedeiji et al., 2006; Ockelford, 2011). Secondly, to improve the predictive performances of bimodal sediment entrainment/transport formulae (Ashida and Michiue, 1972; Bagnold, 1980; Parker, 1990a; Kuhnle, 1992; Wilcock, 1998; Wu et al., 2000a; Hunziker et al., 2002; Wilcock et al., 2003; Powell et al., 2001, 2003), the data are used to mathematically describe any effects of memory.

The present Chapter adopts a near-identical format to Chapter 4, providing novel laboratory data for bimodal bed to determine: (i) if the entrainment threshold of bimodal beds can be quantitatively measured as responsive to 'memory' effects; (ii) if a straightforward mathematical descriptor can be developed to describe the relationship between memory period and adjusted threshold; (iii) if memory effects can be included in general graded sediment transport functions; (iv) if the memory response is distinct from that observed in the unimodal bed.

5.2 Matrix of bimodal experiment

Following the methods and procedures outlines in Chapters 3-4, distinction in the methodology of the present Chapter is specifically in terms of the sediment mixture used and some minor, well-justified, adaptations in data collection. These distinctions are provided below:

Firstly, the bimodal sediment mixture deliberately employed the same median grain size (D_{50} = 4.8 mm) as of the unimodal mixture (Chapter 4). However, the mixture contains a greater proportion of sand fractions (15%, D_i<2mm) than in the unimodal mixture (7.5%) and higher proportion of materials for grain classes smaller than the median class (47%, D_i/D_{50} <1) than in the unimodal mixture (30%). Due to the above differences in the sediment distribution, geometric standard deviation became larger to 1.93 compared with that of unimodal mixture (1.65), leading to relatively weaker sorting in the bimodal than in the unimodal mixture.

Secondly, the initial bedload sample was taken at a discharge step one increment higher on the rising stepped flow sequence ($\tau^* = 0.025$ and discharge = 8.75 l/s) compared with that used in Chapter 4 (Q=7.5 l/s) for unimodal mixture. This reflects visual observations that sediments were harder to be moved in the bimodal mixture than in the unimodal. Although the number of flow steps differs from unimodal data, direct comparison of sediment transport is still straightforward as the 'missing step' can correctly be ascribed a zero transport value for the bimodal bed. Volumetric and non-dimensional forms of bedload transport data are analysed in line with the procedure outlined in Chapter 4 and specific to comparing both baseline (non-memoried) and memory adjusted entrainment thresholds with the work of an identical set of previous researchers (Shields, 1936; Paintal, 1971; Meyer-Peter and Muller, 1948; Einstein, 1950; Vanoni, 1964; Taylor and Vanoni, 1972; Luque et al., 1976; Haynes and Pender 2007; Ockelford, 2011).

With the exception of bimodal (BM-) prefixes to experiment coding, all nomenclature and other experimental variables used (Table 5.1) have been kept consistent with those of Chapter 4.

Table 5.1 Matrix of experiments in baseline and memory stress condition in bimodal sediment mixtures

Experiment Identification Code	Median grain size (D_{50}) (mm)	Experimental condition	Memory stress		Run duration of experiment (min)
			Magnitude: % of baseline τ^*_{c50}	Exposure duration (min)	
BM_B_0	4.8	Baseline	-	0	0+64
BM_SH_10	4.8	Memory experiment	60	10	10+64
BM_SH_30	4.8	Memory experiment	60	30	30+64
BM_SH_60	4.8	Memory experiment	60	60	60+64
BM_SH_120	4.8	Memory experiment	60	120	120+64
BM_SH_240	4.8	Memory experiment	60	240	240+64

5.3 Sediment and bedload transport analysis of bimodal experiments: parameters and variables

Similar to Chapter 4, an identical set of measured and derived variables are presented, analysed and discussed with the help of graphs, rating curves and tabular data. Discharge and bedload are directly measured variables; shear stress is a derived variable (Chapters 2). Both bedload and shear stress have been non-dimensionalised (see Chapters 2 and 4) to transform the dataset to a more generic type, so that they can be compared and contrasted with similar datasets from other researchers.

5.4 Bedload sediment transport

As the degree of dependence and non-linearity of bedload is different for discharge and bed shear stress (Chapter 4), presentation of both correlations has merit, and helps to underpin and quantify the true extent of memory effect on bedload transport and bed stability.

5.4.1 Bedload vs. discharge relationship

The response of bedload transport to memory duration, as a function of discharge, is shown in Figure 5.1. Bedload transport (q_b) is within the range from $1x10^{-8}$ to $1\ x10^{-5}$ m^2/s. Baseline runs show higher bedload rates at each discharge point, compared with memory runs which systematically show lower transport rates at discharges upto 17.5 l/s; only 10 minutes memory run shows earlier convergence with baseline at lower discharge around 15 l/s. This implies that for the same discharge the effect of memory yields a lower capacity (ability) of the system to transport sediment; this implicitly indicates that the memory bed has become more resistant to entrain sediment due to the application of memory (Table 5.2).

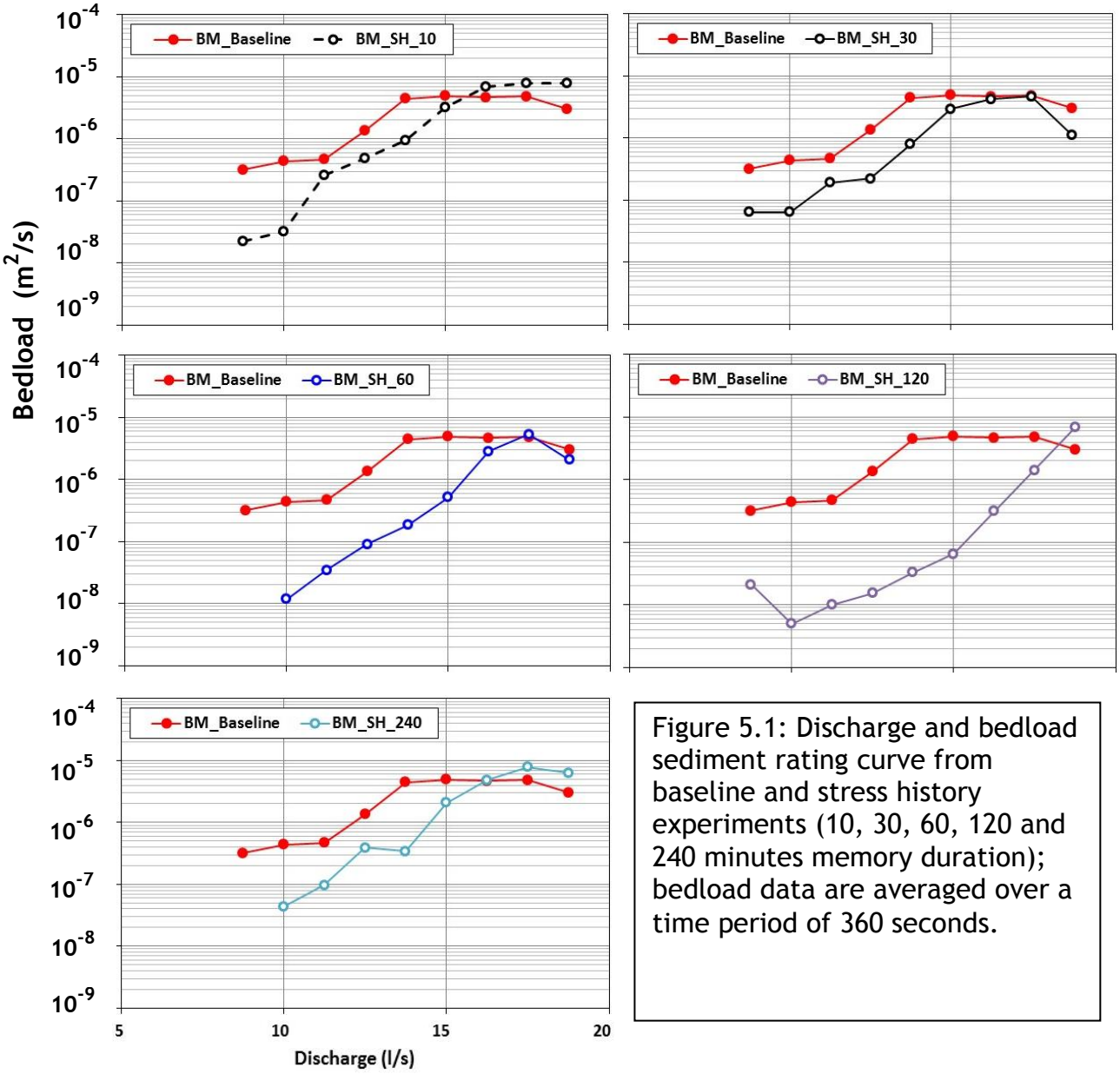

Figure 5.1: Discharge and bedload sediment rating curve from baseline and stress history experiments (10, 30, 60, 120 and 240 minutes memory duration); bedload data are averaged over a time period of 360 seconds.

From Figure 5.1, two important points of interest are noted:

Firstly, the memory effect is most pronounced at lower discharges; for discharges ≤ 10 l/s bedload is approximately an order of magnitude less in runs with memory applied. However, at increasing discharges, the effect of memory gradually weakens until bedload tends to equivalence with baseline data at the highest discharges from 16 to 18.75 l/s. This suggests that memory effects are significant only at near-entrainment flows, possibly at partial transport conditions. Once flows have increased significantly so as to promote general transport and full mobility conditions, the bed has overcome memory effects to revert to 'normal' transport rates.

Secondly, the duration of memory applied appears influential in the magnitude and persistence of reduced bedload rates, compared to baseline. From Figure 5.1 it is clearly evident that the offset between baseline trendline and SH_10 and SH_30 data is relatively small and progressively converges to baseline ~15l/s. Yet, for SH_60 and SH_120, the offset remains over a wider range of discharges (up to 17.5l/s), more than an order of a magnitude different in bedload to baseline data. Thus, it can be concluded that the duration of memory is influential over the degree of reduction and general persistence of bedload transport response.

It is worth noting that the BM_SH_240 experiment does show memory response, but the data fall outwith the general hierarchy of bed stability increasing with rising memory time scales. For purpose of completeness, the result from this experiment has been presented in relevant figures. However, clarified here are possible reasons and uncertainties involved in this experiment. Specifically, inconsistencies in temperature control during this particular experiment warrant attention. The flume room is subject to air temperature fluctuations, which, during the summer of 2013 (July and September), varied diurnally by up 20^{o}C in extreme cases, and 10^{o}C in general (UK Met office, http://www.metoffice.gov.uk/climate/uk/es/print.html). This extreme was recorded for a four day period when the 240 minute experiment was conducted. This is considered likely responsible for excessive drying of the bed material between runs, such that the initial screed is unlikely to be well replicated

compared to other runs. And, for such a long run (for an experiment started at 9am, sample collection started at about 2pm, when summer day temperature rises to the peak), rising water temperatures may affect turbulence variation and viscosity. Whilst water temperature changes would moderate those of the surrounding air, it is notable that Taylor (1971) researched that increases in temperature do increase sediment transport significantly, by up to a five-fold increase in sediment load for 15°C rise. This makes sense, as in low flow, turbulent bursts are the main driver for dislodging sediment from bed and any increase in turbulent intensity per unit area on the bed would increase sediment load. This is particularly critical in low Reynolds numbers, such as the shear Reynolds number in present experiment between 150-300 (Blinco and Partheniades, 1971). Thus, it is concluded that the extreme air temperature changes erroneously inflated the BM_SH_240 minute bedload data; hence it is omitted from further analysis in this Chapter.

Quantitative comparison becomes more meaningful where comparison was made against a representative transport rate (minimum and mean transport rate).In comparing *minimum* transport data, the memory effect seems very similar; i.e. comparison of the shortest (SH_10) and longest (SH_120) memory experiment indicates similar response, respectively 93% and 99% reduction in bedload transport due to these memory scenarios. This strongly indicates memory

Table 5.2 Bimodal sediment experiments: volumetric sediment transport from baseline and memory experiments

Experiment Identification Code	Bedload transport: q_b (m^2/s)		Bedload transport: q_b (m^2/s)	
	minimum	% reduction of q_b relative to baseline(1)	Mean(2)	% reduction of q_b relative to baseline
BM_B_0	4.35E-07	-	2.71E-06	-
BM_SH_10	3.23E-08	93	1.98E-06	27
BM_SH_30	6.37E-08	85	1.42E-06	48
BM_SH_60	1.18E-08	97	6.18E-07	77
BM_SH_120	4.98E-09	99	7.42E-08	97

Note:
1) corresponding discharge to minimum bedload is 10 l/s (very first data point at discharge 8.75 l/s was ignored from each memory time scale
2) mean bedload is the arithmetic mean of all bedload between discharge 10 and 16.25 l/s

influence at near-threshold flow, but such effects make little distinction among the memory time scales. Thus, a logical alternative statistic is also provided in quantification of the memory effect against the *mean* transport over a range of low discharges. This shows a very distinct and hierarchical effect of memory time scales, progressively reducing bedload by 27-97% with increasing memory of SH_10-120. In short, these latter statistics appear more representative, as they minimise noise captured at individual data points (such as for the minimum) and indicate memory to be highly significant in stabilising a bimodal bed against entrainment.

In line with Chapter 4, an alternative, but simpler presentation of memory effect is provided via the discrepancy ratio plot (Figure 5.2). The approach is simply the ratio of baseline load to each memory experiment load (i.e., $q_{b,baseline}/q_{b,\,memory}$), and is expected to be more than unity due to memory, and approaches unity when the baseline and memory experiments converge towards similar loads. Thus, this more readily indicates memory hierarchy of response with increased memory timescales, with clear distinction at timeframes >SH_30. Whilst the discrepancy factor of SH_60 and SH_120 runs may seem excessively high (>50), this is a function of a non-linear relationship; for example, a 50% reduction in bedload would give a discrepancy ratio of 2, a 70% reduction would yield a value of 3.3, a 90% reduction would give a value of 10 and, a 99% reduction would yield 100. In support, data in the present study are similar to those recorded in other bimodal stress history research (Church et al., 1998; Ockelford, 2011; Section 5.6.2).

Figure 5.2 also shows a possible tendency in all runs for memory effects to be erased at high discharges (i.e. between 15 and 18.75 l/s) with bedload rates reverting to baseline equivalence at these discharges. The regression relations of the two pronounced memory time scales of SH_60 and SH_120 are shown in Eq. 5.1 and 5.2; such relations (of satisfactory R^2 value) are applicable for simpler analysis for predicting transport in memory condition or in baseline, and assessing when the memory effect starts to disappear.

$$\frac{q_{b,baseline}}{q_{b,SH\_60}} = -73.55\ln(Q) + 214.26, where\ R^2 = 0.65 \qquad \text{Equation 5.1}$$

$$\frac{q_{b,baseline}}{q_{b,SH\_120}} = -131.5\ln(Q) + 393.25, where\ R^2 = 0.639 \qquad \text{Equation 5.2}$$

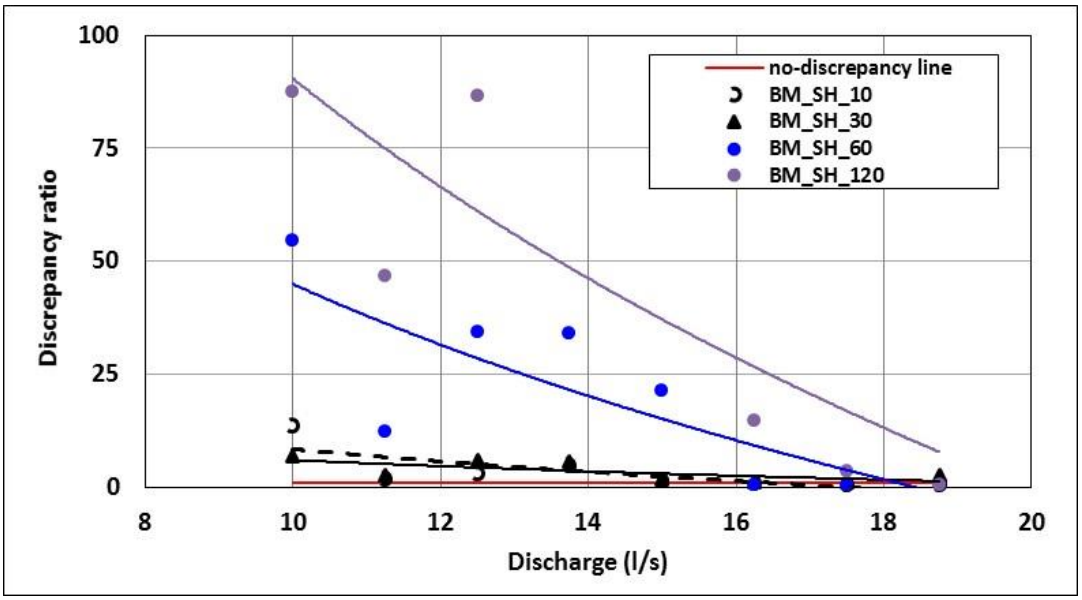

Figure 5.2: Discrepancy ratio in bedload transport as a function of discharge (Q) between baseline and memory experiments of BM_SH_10, 30, 60 and 120.

5.4.2 Integrated bedload transport

Cumulative sediment volume over the steps of rising discharges (Figure 5.3) and the derivative variable of this parameter (Figure 5.4) are analysed in line with the rationale presented in Section 4.5.2. In particular, focus is placed on the derivative variable in Figure 5.4, which more explicitly quantifies the growth and decay of the memory effect.

The overall effect of memory over the rising flow steps is distinctly hierarchical in the cumulative load of transport (Figure 5.3). Relative to baseline, the reduction in bedload transports is 5, 42, 54 and 65% for memory durations of SH_10, 30, 60 and 120; a note of caution is added here in that Figure 5.3 statistics reflect the cumulative (total) reduction over all discharge steps, while the percentage reduction is against the mean transport over the range of low steps between 10 and 16.25 l/s (also see texts in note 2 of Table 5.2). This cumulative effect due to the varying slope of the curves (Figure 5.3 and Figure

5.4) is an effective way of quantifying that memory effect is neither a constant nor is it a linear variation over low flow discharges; it persists dynamically and non-linearly over the range of low flow discharges before gradually diminishing at higher discharges.

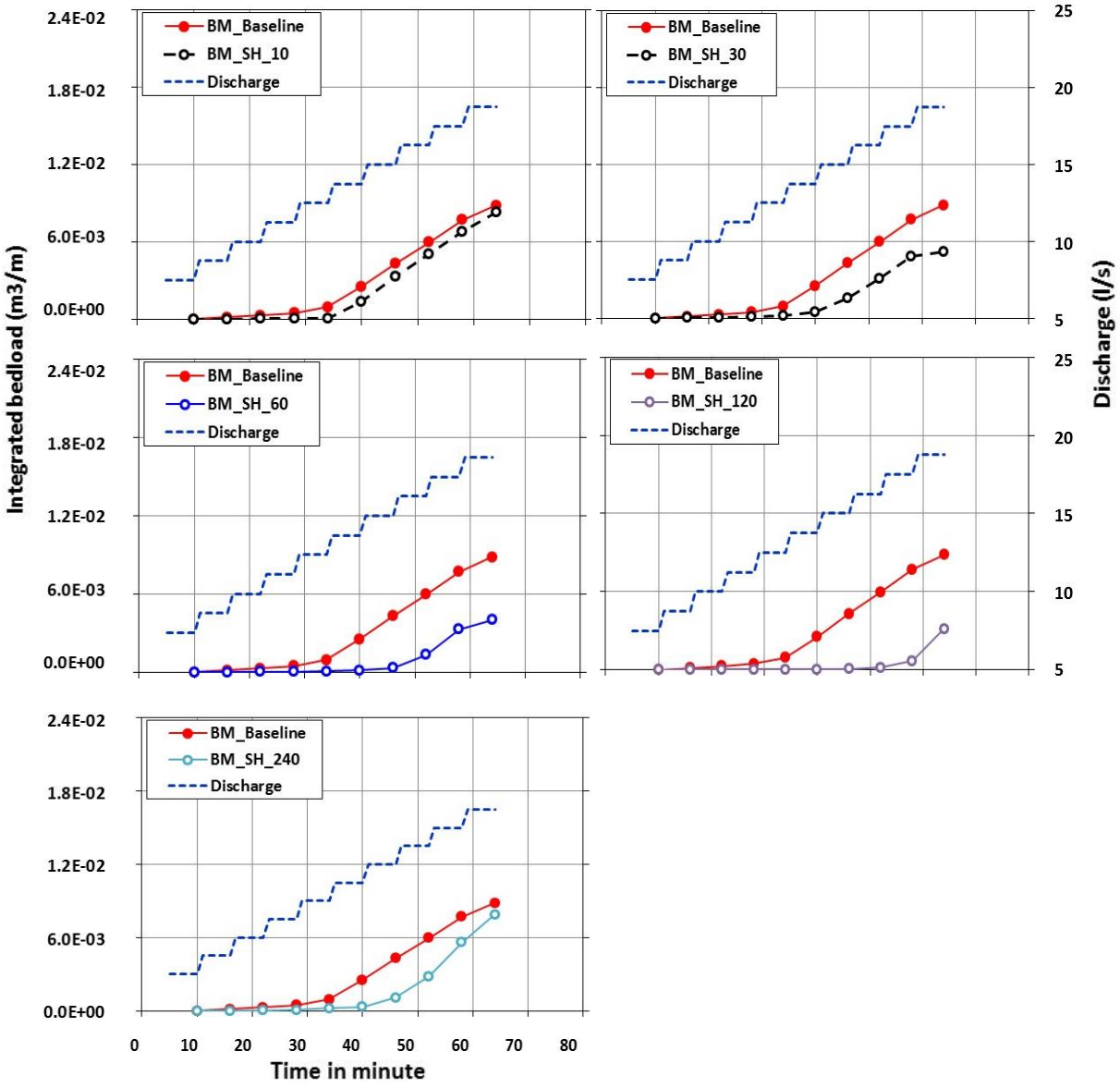

Time (min)	5	10	11	16	17	22	23	28	29	34	35	40	41	46	47	52	53	58	59	64
Q (l/s)	7.50	7.50	8.75	8.75	10.00	10.00	11.25	11.25	12.50	12.50	13.75	13.75	15.00	15.00	16.25	16.25	17.50	17.50	18.75	18.75

Figure 5.3: Integrated sediment volume from baseline and memory experiments in bimodal mixture from baseline, 10, 30, 60,120 and 240 minutes memory duration.

As noted in Chapter 4, the non-linear response of integrated bedload is relatively difficult to examine as depicted in Figure 5.3. However, SH_30, 60 and 120 all indicate a change in gradient ~50minutes into the rising limb. This is more explicitly demonstrated in the derivative parameter (rate of change of sediment load) in Figure 5.4, which is a trendline plot of 4-point moving average of the actual rate of change. In Chapter 4 the maxima of these data were described as a "trigger point", possibly representative of the discharge at which the bed's memory effects start to lose their significance and be over-written towards the baseline / normal transport conditions. In the present bimodal data set, a similar maxima is observed (Figure 5.4). The longer the duration of memory, the longer the lower incremental rate of transports persist; thus, maxima are delayed. Specifically, in SH_10 minute duration memory experiment, the effect diminishes earlier around at the 40th minute of the experimenting time; while for SH_30, SH_60 and SH_120 minute memory experiments, the effect diminishes later around 45th, 50th and ~60th minute of the experimenting time respectively. This suggests that the trigger point is indistinct (Figure 5.4), rather covering a small range of discharges Q= 16 to 18.75 l/s commensurate with 50-60 minutes of rising limb flows.

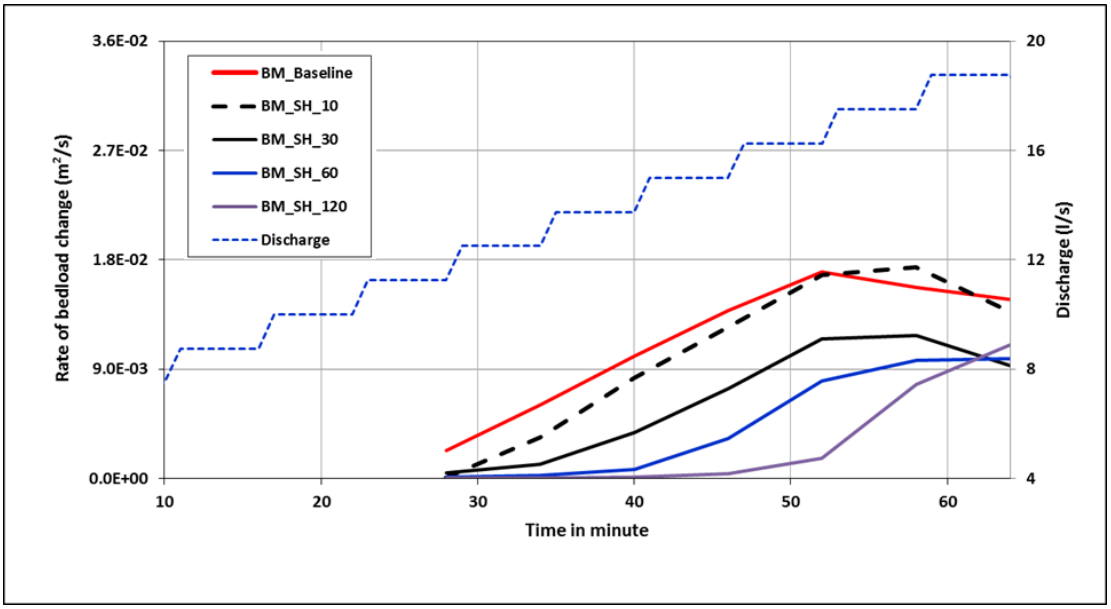

Figure 5.4: Progressive development of memory in flume bed in baseline and memory stress experiment in bimodal mixtures shown in incremental change in

bedload transport rate; smaller incremental rate means less transport of volume between successive time steps.

In summary of the findings of the bedload vs. discharge relationship it is highlighted that: i) bed stabilisation was found to be a function of applied flow memory time scales, with bedload reducing hierarchically from 27 to 97% with SH_10 to 120 minutes of applied memory; ii) cumulative bedload analysis section indicated up to a 65% reduction in cumulative bedload volume; iii) for SH_10 and SH_30, the discharge 16 l/s seems to act as trigger point when memory starts to disappear; while for SH_60 and SH_120 experiments, the effect seems to sustain longer until higher discharges up to Q=18.75 l/s; iv) the difference in percentage reduction of bedload between mean (or minimum in) and cumulative transport underlines the fact/mechanism that memory induces a non-linear effect on the stability of bed and its subsequent transport of sediment at low discharges.

5.4.3 Bedload vs. boundary shear stress relationship

In the same way as in Section 4.5.3, a more generic parameter in sediment transport and entrainment threshold is the bed shear stress, rather than project-specific discharges. Thus, the objective of this section is to demonstrate the effect of memory on the shear stress to bedload relationship. However, the comparison methodology presented in Chapter 4 cannot be employed in the current Chapter. This is because the reduction in bedload due to memory is far more significant in bimodal beds (Figure 5.5) than unimodal beds (Figure 4.5); thus, using the mean baseline bedload transport 'reference' approach of Chapter 4, leads to comparison of data at 'high' bedload values where the memory effects are being erased and baseline-memory data beginning to converge. Therefore, comparing the effect of memory on bed shear stress at the mean transport level of baseline data in the bimodal bed will not provide a fair judgement about the effect of memory. This led to the comparison/evaluation method being revised in the present Chapter to quantify the memory effect as more representative of values overall. In short, this now calculates the mean and median transport for each *memory* experiment as the reference, then used for comparison with the baseline data (i.e. rather than the other way around, Chapter 4). Using Figure 5.3, Table 5.3 is generated for direct comparison of

the percentage difference in shear stress for a given reference sediment transport (mean and median of the memory data) due to memory. Following the same approach, a revised calculation for unimodal load has been carried out, which will allow direct comparison between the two sediment grades; this has been presented and discussed in Section 5.6.2.

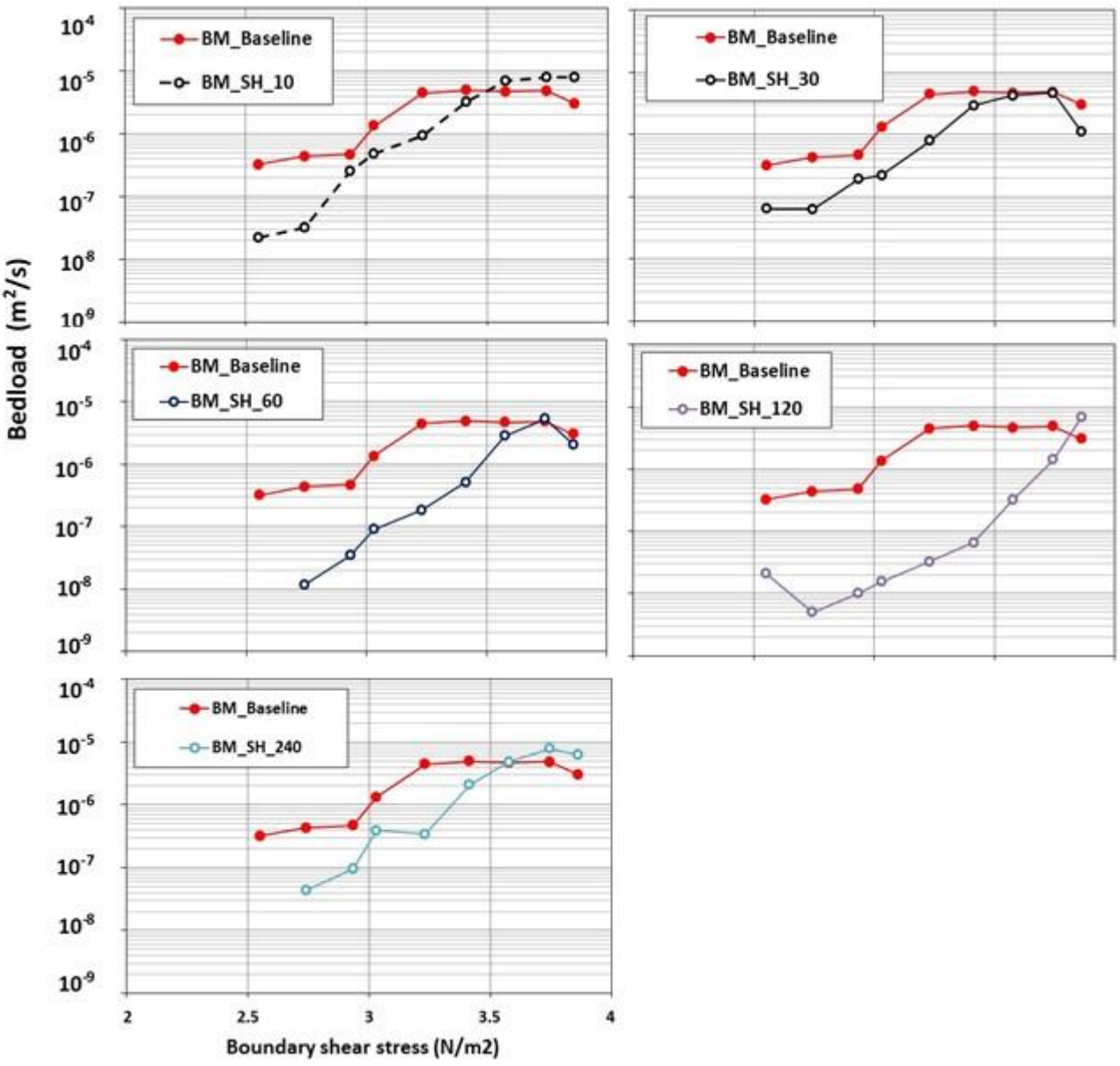

Figure 5.5: Bed shear stress in bimodal mixture from baseline and stress history experiments (10, 30, 60, 120and 240 minute memory duration.

Using an example for discussion, the shear stresses corresponding to the mean and median transport from the memory condition of 120 minute are respectively 3.7 N/m^2 and 3.25 N/m^2. For the reason outlined above, the mean is slightly skewed towards the higher values of shear stress, and thus higher value than median. The corresponding shear stresses in the baseline experiment at the same transport levels (mean and median transports of memory experiment) are 3.0 N/m^2 and 2.3 N/m^2. This leads to respectively a 23% and 46% increase of shear stress in memory experiment relative to the baseline condition for transporting the same volume of sediment. This clearly demonstrates the degree of dependency and sensitivity on the choice of methods of determining the relative effect with baseline. Based on *mean* transport, the effect of memory is hierarchical, ranging between 7 and 23% increase in bed shear stress for transporting same volume of transport as in baseline. Whereas based on *median* transport, the memory effect is also

Table 5.3: Bimodal sediment experiments – different magnitudes of shear stress for transporting the same sediment load in baseline and memory experiments; mean and median bedload in each memory experiment has been used as reference transports, and for that transport, the difference in shear stresses has been used to quantify memory effect

Experiment Identification Code	Shear stress corresponding to Mean sediment load from memory experiment		Shear stress corresponding to Median sediment load from memory experiment	
	Shear stress: Memory* (baseline), (N/m^2)	% increase in shear stress	Shear stress: Memory (baseline), (N/m^2)	% increase in shear stress
BM_B_0	-	-	-	-
BM_SH_10	3.4 (3.17)	7	3.21 (3.0)	7
BM_SH_30	3.3 (3.1)	6	3.22 (2.95)	9
BM_SH_60	3.5 (3.1)	13	3.38 (2.7)	25
BM_SH_120	3.7 (3.0)	23	3.35 (2.3)	46
Note: *i) the numbers outside brackets are from memory experiments, and those inside brackets are from baseline experiments				

hierarchical, but significantly higher; now from 7 to 46%. The mean transport is generated at a higher shear stress, while the median transport represents a

lower flow stage. Therefore, the comparison above confirms and provides a quantified measure that the effect of memory is much stronger at low flow stages, and thus indicates that determining entrainment threshold around low flow transport according to the definition of reference transport does not quantify the true extent of memory effect on river bed stability. This supports the earlier finding that the memory effect is a non-linear function, and should not be addressed with a constant value on the entrainment threshold. Rather it should either be included in standard bedload transport functions which are generally represented by a power law in most of the existing bedload transport formulae (MPM, 1948; Paintal, 1971; Engelund-Hansen, 1967; Ashida and Michiue, 1972; Ackers and White, 1973; Hunziker and Jaeggi, 2002; Parker, 1990a; Powell et al., 2001, 2003) or included in a correction factor with a non-linear function.

A summary of this section yields: (i) memory effect on river bed stability and bedload transport is a non-linear process i.e. the memory effect is higher at low flow stages, and gradually diminishes at higher flow stages, ii) due to greater memory effects in bimodal sediment, the analysis methodology required adjustment towards a more generic approach to reference values based on memory data, rather than baseline data; iii) based upon mean and median transport references, bed shear stress may increase up to 23% or 46%, respectively; iv) because of the non-linear variation of memory effect on river bed stability, the determination of the memory effect on entrainment threshold by any reference transport approach will not quantify the true extent of memory effect on bedload transport at low flow stages.

5.4.4 Non-dimensional analysis of sediment transport relationship

Bed shear stress and bedload transport have been non-dimensionalised using the same approach as in Chapter 4, by using Eq. 2.7 – 2.9 in Chapter 2. Entrainment threshold in baseline and memory experiments have been determined via the reference transport approach using reference values of Parker et al. (1982a) and Shvidchenko et al. (2001), see Figure 5.6, More elaboration on their derivation and application/use in quantifying memory effect can be found in Chapter 2 and 4; output data for the non-dimensionalised parameters are provided in Table

5.4. It is important to note that the Shields' (1936) reference value (tested in Chapter 4) cannot be applied to the bimodal data set, as the measured transport rates are significantly lower than the Shields' reference value; this is to be expected, given that Shields' data were designed for more general transport in non-memoried near-uniform beds and even the unimodal data of Chapter 4 concluded that Shields' reference was too high to be of merit in memory experiments.

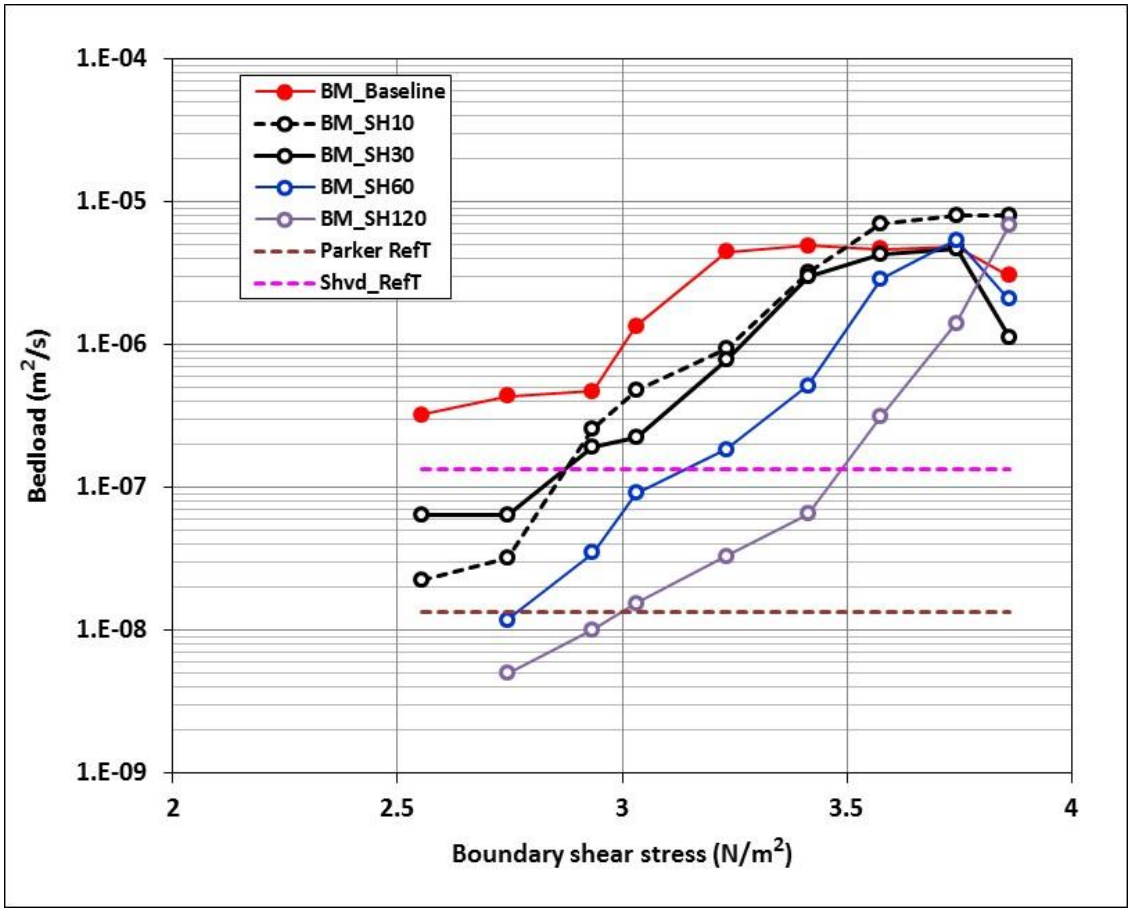

Figure 5.6: Reference transport of Parker et al. (1982a) and Shvidchenko et al. (2001) superimposed on the volumetric transport vs. shear stress rating curves of bimodal experiments (dimensional shears stress obtained from x-axis for each experiment corresponding to reference transports of each author non-dimensionalised using Eq. 2.8-9*). Note: The rise of the first two transport data points in 30 minute memory time scale relative to the 10 minute may indicate whether it is due to temperature variation; within such short time, significant temperature variation was not expected, and thus the rise on those two data points only due to temperature is probably unlikely. More-over, memory time scale can lead to*

development of several processes as described in Section 2.5 and 2.6. Thus, it is challenging to pinpoint specific causes of sampling inconsistency at a particular and/or discrete data points; keeping this in mind, the majority of the analysis in this thesis has been done against representative values, such as "mean" and "cumulative" load.

From Table 5.4, the entrainment threshold from the baseline of the bimodal mixtures compares well with the entrainment threshold of the original values of Parker et al. (1982a) (0.029) and Shvidchenko et al. (2001) (0.034). The similarity in the entrainment threshold of D_{50} between the two mixtures (unimodal and bimodal, for unimodal, see Chapter 4) is consistent and re-assuring with the assumption made in literature that median grain size (D_{50}) is a good choice of the representative size for a sediment mixture in gravel beds (Parker et al., 1982a; Wilcock and Southard, 1989; ASCE, 2007). The similarity of the entrainment threshold of the two mixtures also enhances confidence in the baseline data, and enhances the credibility of quantification of memory effect, which has been determined relative to the baseline condition.

Table 5.4: Bimodal sediment mixtures: entrainment threshold of median grain size (D_{50}) from baseline and memory experiments

Experiment Identification Code	Shields parameter τ^*_{c50} according to reference transports criteria of:			
	Parker et al. (1982a): $q^* = 1x10^{-5}$		Shvidchenko et al. (2001): $q^* = 1x10^{-4}$	
	τ^*_{c50}	% increase relative to baseline	τ^*_{c50}	% increase relative to baseline
BM_B_0	0.026	-	0.030	-
BM_SH_10	0.031	19	0.037	23
BM_SH_30	0.029	11.5	0.037	23
BM_SH_60	0.035	35	0.040	34
BM_SH_120	0.038	46	0.045	49

Note:
1) Minor extrapolation of rating curve needed in case of Parker reference number based on eye-ball estimation using three nearest data points;
2) Parker et al.'s reference transport value of comparison is 0.029; Shvidchenko et al.'s is 0.034
3) Entrainment threshold using Shields' reference transport has not been derived as his reference transport is too high and outside the data range in the present set of experiments

Specific review of Table 5.4 in light of memory effects indicates that, according to Parker's reference transport, the increase of entrainment threshold due to different memory time scales (SH_10, 30, 60 and 120) ranges between 21 to 49%. These magnitudes are generally hierarchical according to the duration of memory time scales; i.e. the longest duration memory time scale (SH_120) induced the highest increment in entrainment threshold. However, SH_30 is anomalous to the memory hierarchy; this is not due to fact that the experiment itself is wrong, rather a reflection of the relatively higher transport rates of this particular memory bed (Figure 5.6) showing the risk and limitation of determining entrainment threshold using a reference transport approach based on transecting a trendline at a discrete location. In Table 5.3, where dimensional shear stress values using more representative transport condition (mean and median) have been compared with memory, the SH_30 experiment there showed good hierarchical effect, and is not an anomaly at all against comparison with median values in hierarchical merit. Further, this approach of analysis using sediment rating curves (e.g., Figures 5.5 and 5.6) is enough to draw notable inconsistency in sediment transport, where 10% deviation in shear stress can cause 100% change in transport. Chapter 4 has already discussed this limitation and sensitivity, lending weight to examining the memory effect via quantification against mean transport and shear stress (Table 5.2 and 5.3).

Interestingly, according to Shvidchenko et al.'s reference transport, almost similar (to Parker et al.) range of memory effects have been calculated, between 23 and 49% increase in entrainment threshold. Using this approach, magnitudes are perfectly hierarchical according to the memory duration. It is worth a comment that the similarity of this approach outputs to those of Parker et al.'s is a little surprising. Shvidchenko et al.'s reference transport (10^{-4}) represents a relatively higher transport on the sediment vs. shear stress rating curve than Parker et al.'s (10^{-5}); the above reference transports of Parker et al. and Shvidchenko et al. are superimposed on the volumetric transports vs. shear stress curve shown above in Figure 5.6; thus, Parker et al.'s approach would be expected to reflect greater memory effects near entrainment than Shvidchenko et al.'s approach which lies closer to the mean/median transport and data convergence with baseline (Figure 5.6). This raises two issues: (i) which approach is advisable, and; (ii) whether the bedload sampling resolution is too

coarse to account for small variations in the bedload transport to capturing differences between the two approaches.

In addressing these points, firstly, analysis of the flow steps indicates that Parker et al.'s and Shvidchenko et al.'s reference transport levels lie in discrete discharge steps in the present experiment; this validates the use of the present methodology for appropriate resolution of data capture. Secondly, in debating which method is advisable the following discussion is important. Given the observations in previous sections that memory has a non-linear effect on river bed stability over low flow transport, Shvidchenko's reference transport lies closer to mean or median transport of the memory experiments and is both more representative of the 'overall' memory response of the bed and less sensitive to the near-threshold fluctuations in first motion of sediment. Although Parker et al.'s reference value represents the maximum sensitivity of the bed to memory, such very low transport may be impractical to sample hence extrapolation of research dataset would be required (introducing wider uncertainty into memory corrections/analysis). Further, to employ Parker et al.'s reference value, capturing the data at the lowest flow is highly sensitive to the operation of the sediment trap, as the first operation of the trap in each run tends to generate external disturbances (water/air bubble, sudden drop of sediment etc.), less evident in subsequent operations. Thus, at this juncture in the thesis, there is increasing support for use of Shvidchenko's reference transport rate in memory experiments.

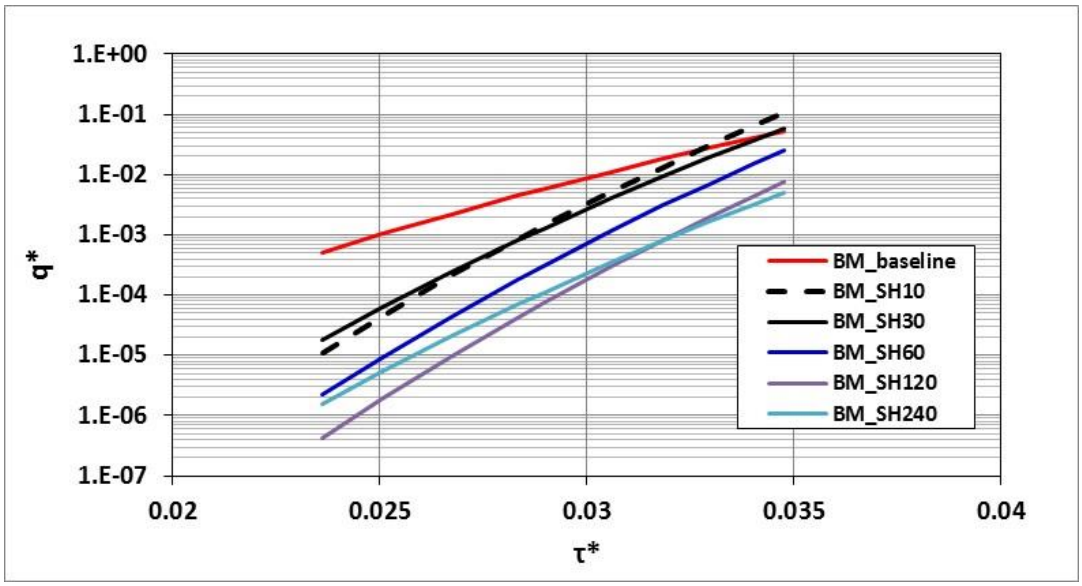

Figure 5.7: Family of mathematical functions (see equations in Table 5.5) of non-dimensional bed shear stress versus non-dimensional transports from baseline experiment and memory conditions in bimodal mixtures.

The non-dimensionalised parameters of the sediment load and bed shear stress in Figure 5.7 were subsequently used to form mathematical functions (power functions) to represent the effect of memory time scales. These proposed functions are similar to the bedload power functions of Paintal (1971) and Parker (1990a), which work without reference to a single entrainment threshold value in their functions. The power functions for the baseline and the memory experiments are presented in Table 5.5 and the trendlines in Figure 5.7. The co-efficient matrix, and the exponents in further recursive relations show excellent correlation (R^2 >0.9) and distinct hierarchy according to memory time scales (see Figure 5.8 and Figure 5.9 and Eq. 5.9 and 5.10); i.e. the exponents range from 12 (baseline) to 25 (SH_120). That said, the exponent range with memory (SH_10 to SH_120) is restricted to 21-25. Disruption to the hierarchy by SH_30 appears reflective of the higher transport values associated with the lower applied shear stresses of the SH_30 specific experiments (See Figure 5.6); this may relate to high temperature sensitivity due to the time of year that these experiments were undertaken (see Section 5.4.1); rise in the ambient water temperature would lower viscosity resulting into higher velocity (shear stress) at the same

discharge, and thus SH_30 generated higher (or similar) sediment load as of SH_10. Worth mentioning here that the family of power laws (Table 5.5) are valid for low shear stresses around entrainment threshold (Paintal, 1971), and thus higher the exponents, lower would be the sediment load. As a results, the fall out of SH_30 in the hierarchy, ambient temperature could be one key reason.

Table 5.5: Mathematical functions for sediment transport proposed for low transports around incipient motion in bimodal sediment mixtures in baseline and memory stress condition

Experimental condition	Memory stress duration (min)	Sediment rating Equation: $q^* \sim c(\tau^*)^b$
BM_B_0	0	$q^* = 1.77x10^{16}(\tau^*)^{12}$ Equation 5.3
BM_SH_10	10	$q^* = 5.66x10^{33}(\tau^*)^{23.8}$ Equation 5.4
BM_SH_30	30	$q^* = 2.17x10^{29}(\tau^*)^{20.9}$ Equation 5.5
BM_SH_60	60	$q^* = 5.84x10^{33}(\tau^*)^{24.2}$ Equation 5.6
BM_SH_120	120	$q^* = 1.06x10^{35}(\tau^*)^{25.5}$ Equation 5.7
BM_SH_240	240	$q^* = 1.86x10^{28}(\tau^*)^{20.95}$ Equation 5.8

The mathematical functions (Eq. 5.3 to 5.7) clearly indicate that a longer memory time scale has higher exponent, with minor exceptions of BM_SH_30. Similarly, the coefficients are also larger in the longer memory time scales, again with the same BM_SH_30 exception. Therefore, following the pattern in the coefficient and the exponent matrix, recursive mathematical functions are possible to form which can replace the set of equations in 5.3-7. The recursive form of the regressions are presented in Eq. 5.9 and 5.10 for the coefficient and the exponent respectively, and help eliminate noise from the SH_30 outlier so as to be used in an improved generic form of transport equation (Eq. 5.11). Depending on the memory time scale, the coefficient *"C"* and exponent *"b"* can be worked out using Eq. 5.9 and 5.10, and bedload transport can be predicted using Eq. 5.11. As both the coefficient and the exponent both lead to good

regression relations, it is useful to analyse which parameter is more responsive to memory; this is of particular merit given that the range of increase due to memory in the bimodal exponent is very similar to that of the unimodal (Section 4.5.4). It is also critical to our process-based understanding of memory effects as the coefficient mainly represents the effect of bed friction and bed structure, whilst the exponent is dependent on the applied shear stress. Although the appropriate analysis is presented herein, a wider discussion is presented in Section 5.6.4. Thus, mathematically, the following is relevant:

The equation for the coefficient matrix is:

$$C = 5x10^{25}(T)^{4.50} \qquad \text{Equation 5.9}$$

where *C* represents the coefficient in the power form of the equations 5.3-5.7, and T is memory time scale in minute.

The equation for the exponent matrix is:

$$b = 17.59\ (T)^{0.0789} \qquad \text{Equation 5.10}$$

where *b* represents the exponent in the power form of the equations 5.3-5.7. Thus, the general form of the transport equation (replacing Equations 5.3 to 5.7) is:

$$q^* = C\ (\tau^*)^b \qquad \text{Equation 5.11}$$

When plotted graphically, the following Figures are generated for the coefficient (Figure 5.8) and exponent (Figure 5.9):

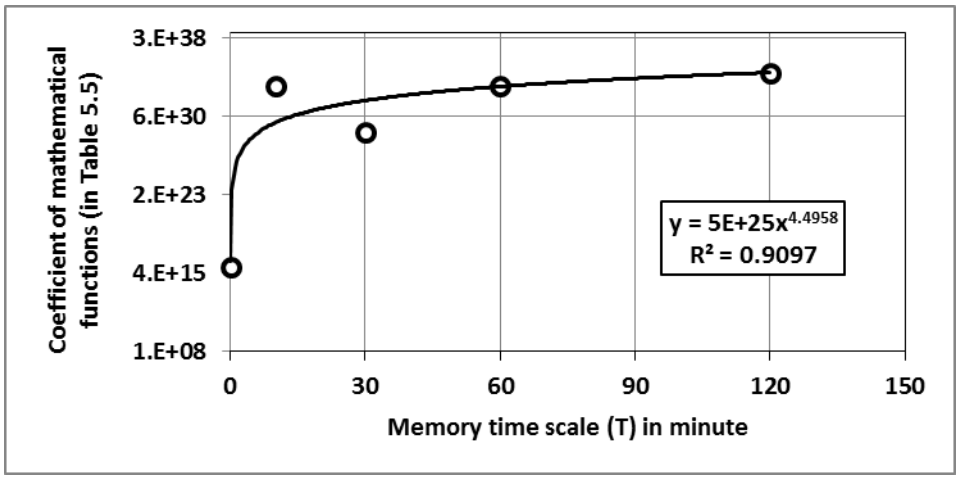

Figure 5.8: Correlation of the coefficient matrix with memory time scales of the mathematical functions (Eq. 5.3 to 5.7) for bimodal sediment transport.

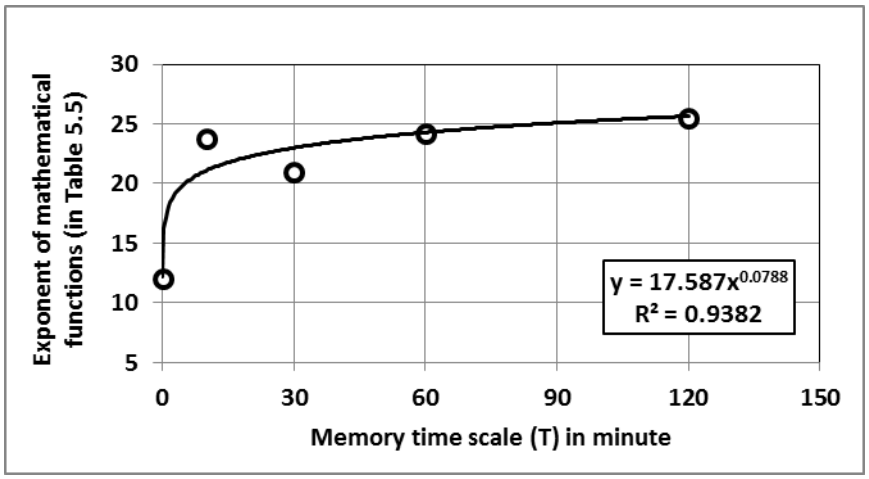

Figure 5.9: Correlation of the exponents with memory time scales of the mathematical functions (Eq. 5.3 to 5.7) for bimodal sediment transport.

Figure 5.8 and Figure 5.9 provide an important solution as to how to develop a generic correction factor for memory effects. In short, the curves can be read in two different ways to estimate the exponent and coefficient of a sediment rating equation: (i) if the timescale of memory in a river system is constant, or known for the specific event to be modelled, then a single value can be read from the curve; if the timescale is in excess of the dataset then extrapolation of the curve may be required; (ii) if the timescale of memory in the system is

variable, then the curve can read within the upper and lower bounds of the memory timescales to get a range of exponent/coefficient values which can be used as uncertainty bounds for a modelling domain. The importance of this outcome should not be understated, as it is the first mathematical solution for correcting sediment transport models for memory effects.

Thus, from the section above, these key findings are noted: i) entrainment threshold of the median grain size in the baseline experiment matched well with the reference transport values of Parker and Shvidchenko; this provides confidence in the methodology applied herein; ii) memory time scales have significant and hierarchical influence on the non-dimensional shear stress (τ^*) in low flow transport conditions with τ^* increasing by 21 to 49%; this delays transport and lowers values of τ^*; iii) rising exponents of the family of mathematical functions have taken the form of power law (similar to Paintal, 1971 and Parker, 1990a) to adequately account for the different memory effects in a manner which can significantly improve bedload prediction in gravel bed mixture; iv) plotting separately the exponent and coefficients against memory timescale, suggests that the granular scale structures (embedded in the coefficient term) are of greater importance/sensitivity to memory than the non-linearity represented by the exponent; v) the trendlines fitted to the exponent and coefficient plots against memory timescale are highly appropriate to estimating and including memory in generic sediment transport modelling. Overall, this section of the thesis has brought novel and important knowledge gains to sediment transport research and are the focus of the discussion section of Chapter 5.

5.5 Fractional transport

Size selective, equal mobility and size independence transport have often been referred in this section; thus, definition of these terminologies are worth presenting (they have previously mathematically expressed with pi/Fi term in Section 4.6). Size selective transport: due to relative sizes, when effect of hiding and exposure are present, the transport is referred as size selective; here a finer particle suffering hiding effect will require higher shear stress its mobility than its uniform size, and a coarser particle if suffering exposure effect will

require a lower shear stress for its mobility than its uniform size. Equal mobility transport: have been referred as transport at extreme hiding condition; thus, the hiding and exposure effects counterbalance the mass differences of the larger and smaller particles, and both (or all) size classes tends to mobilise at same shear stress (Parker et al., 1982a later referred his Oak Creek equal mobility as an approximation of *"near equal mobility"*). Size independence transport: this is referred as transport in a mixture if different size classes behave as if they are independent of their neighbouring sizes, and thus in the mixture a smaller grain requires a lower shear stress like their uniform size, and similarly a larger grain requires a larger shear stress than their uniform size for their mobility. Thus, transport of a mixture can become bias towards size independence. (For detail reference, please see Chapter14, MIT OpenCourseWare).

In a similar manner to Chapter 4, the fractional transport is assessed using p_i/F_i ratios (See Figure 5.10). Both baseline and memory experiments indicate approximate equal mobility of transport (p_i/F_i ~1) for all fractions, except the two end fractions (i.e. the finest and the largest). These end fraction responses do indicate the presence of hiding and exposure effects (hiding for finer fractions and size independence of larger fractions) in the bimodal bed, which curtail the entrainment potential of the finer and the larger fractions.. Interestingly, the over-representation (p_i/F_i > 1) of two modes of the distribution correlates with a dominance of these grain sizes in the mixture; this relative "instability" of the fraction may relate to reduced hiding potential of these fractions given that neighbouring grains are more likely of equivalent or similar dimension to the grain in question. Also, the D_{50} fraction shows near equal mobility of transport; according to existing hiding functions (Ashida and Michiue, 1972 and Parker, 1982a), equal and size independence mobility of median size class is the same point (see Figure 2.8), which although very rare in natural condition (ASCE, 2007), however seems to have realised here, which may be due to stronger hiding effect by the finer classes.

The selectivity in transport for all fractions finer than the median class (D_{50}) clearly demonstrates strong hierarchical hiding effects due to memory in bed. Specifically, the strongest effect is seen for the smallest grain size after the longest duration of memory was applied (Figure 5.10). This seems to strongly affirm that memory-induced stability is largely a function of a disproportional response by finer grains. This is likely due to hiding of the finer fractions due to vertical winnowing (for finer fractions with p_i/F_i <1) which will

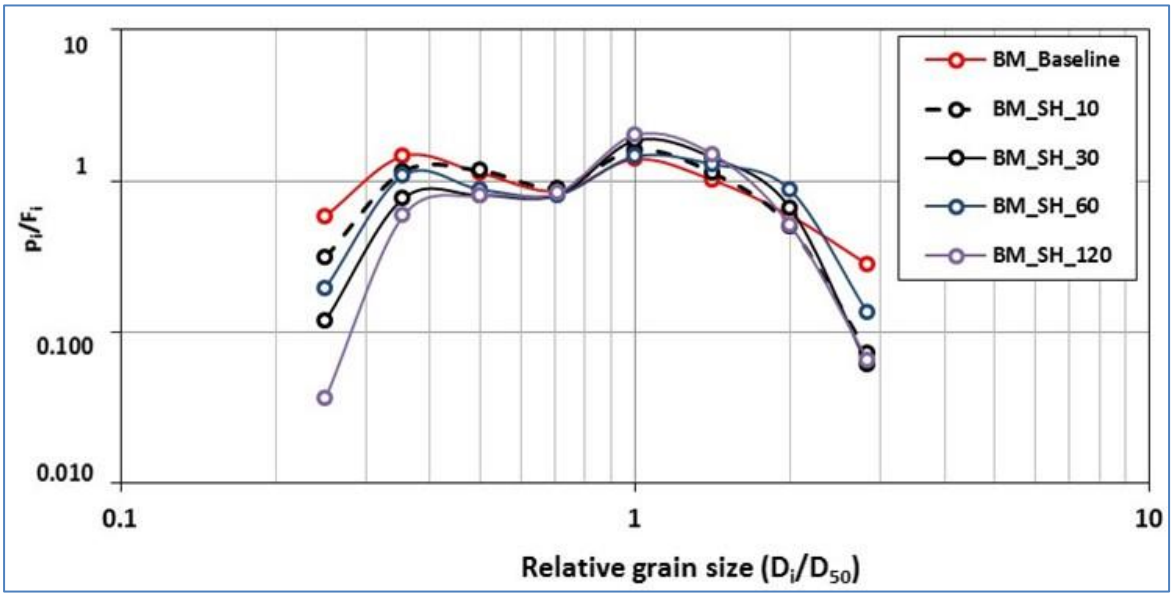

Figure 5.10: Normalised fractional transport rates p_i/F_i vs. relative grain size D_i/D_{50} in bimodal mixtures showing size selectivity in transport for finer grain classes, equal mobility transport bias for middle part of the classes.

have increased their entrainment threshold (a similarity towards extreme hiding and a bias of the fines towards equal mobility transport, which is fairly true for all finer fractions except the smallest fraction), and thus, reduced their volumetric transport (Figure 5.11). On the other hand, the larger fractions in the mixture (D_i/D_{50} > 1) tend towards equal mobility transport with weaker memory response (Figure 5.10). The logarithmic scale of Figure 5.10 does to some extent mask the degree of memory hierarchy; however, it is still present and shows that increases in memory duration do lead to a preference of selective entrainment of coarser particles. It is unclear whether this is a result of increased exposure of coarser grains in response to the hiding of fines, or whether only coarser

fractions are available for transport if fines are effectively "lost" to the surface due to vertical winnowing, sieving etc. to the subsurface.

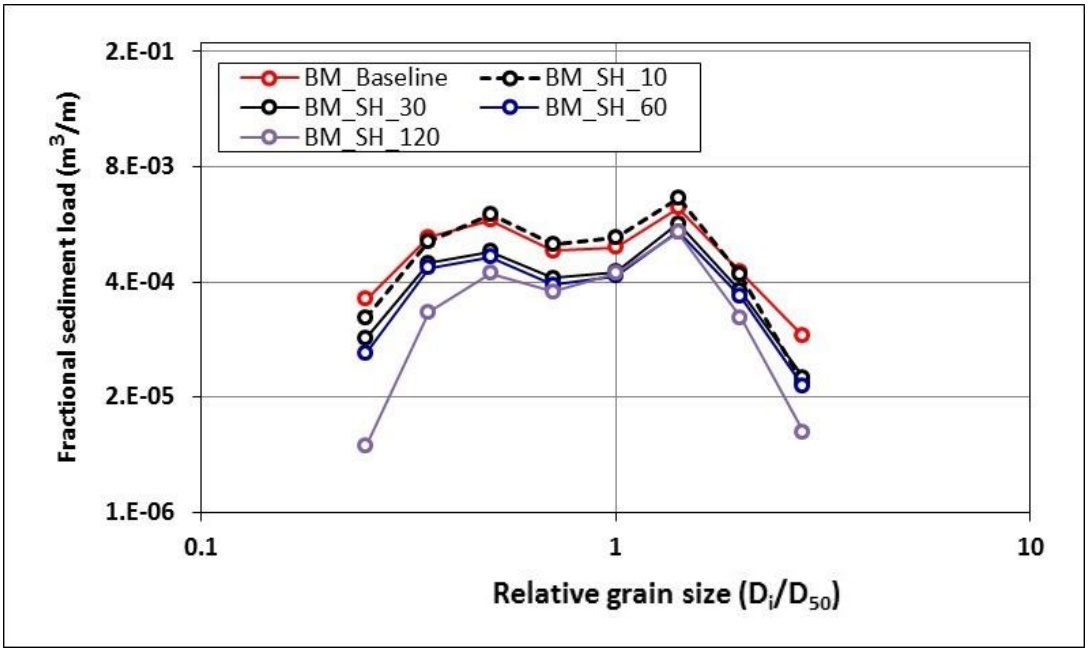

Figure 5.11: Fractional transport vs. relative particle size D_i/D_{50} in bimodal mixture showing strong size selectivity in transporting sediment for finer grain classes.

Although the p_i/F_i analysis is preferable in fractional analysis, as it indicates availability-corrected entrainment, Figure 5.11 and Figure 5.12 provide raw fractional data analysis. This explicitly shows two findings. Firstly, Figure 5.11 shows that only the finest fraction (D_i =1-1.4mm) shows a response to SH_10 minutes of applied memory; hence supporting the notion that fines are most memory-responsive. Secondly, Figure 5.12 provides a quantified percent reduction of transport for each fraction; this shows that for long memory runs (SH_120) all fractions indicate transport reductions between 50 and 95%. The SH_30 and SH_60 experiments also show hierarchical reduction of fractional transport on either side of the median grain class showing reductions of 34-66% and 47-75% respectively.

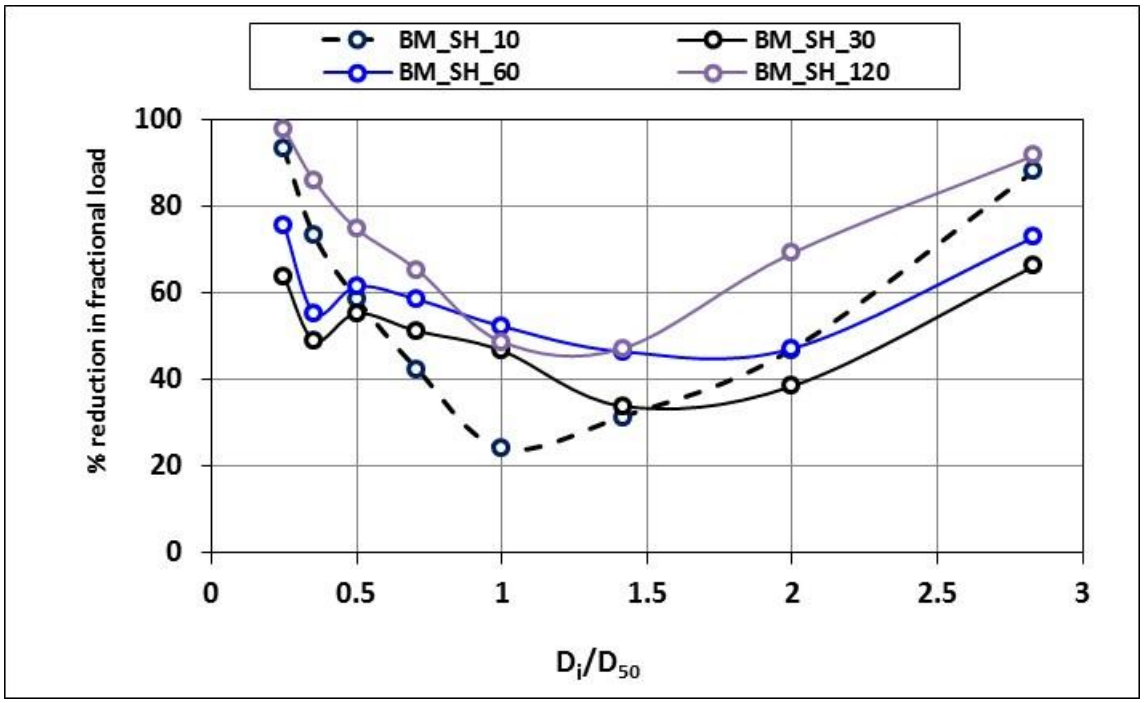

Figure 5.12: Percent reduction relative to baseline in fractional transport vs. relative particle size Di/D_{50} showing strong size selectivity in transporting sediment for finer grain classes.

In summary, the key findings are: i) bimodal mixtures demonstrated size selectivity in the fractional transport of grain classes finer than the median size, likely due to hiding and vertical winnowing; ii) median and larger fractions showed bias towards near equal mobility transport (p_i/F_i between 0.7 to 2) being the effect of extreme exposure with weaker memory effects in these fractions; while the largest fraction showed size independence bias as if a uniform sediment of largest size requiring highest shear stress, and thus showing reduced transport; this is like less exposure for a larger (largest) grain class, may be an effect of tighter packing due to screeding; iii) the longest memory time scale induced the highest reduction in the fractional transport, up to 95% in the finest fractions, and 75% in the largest fractions.

5.6 Discussion of results

Bimodal sediment mixtures are common in graded bed rivers. The entrainment threshold of individual fractions (as well the median) is of particular importance

to entrainment and transport due to the grade modality; other parameters in a sediment distribution such as standard deviation and skewness in distribution have been observed to have little influence on the entrainment threshold of the grain classes (Rakoczi, 1975; Wilcock and Southard, 1988). Hence, the focus and distinction of grain mixtures in this thesis has been placed solely on comparison of bimodal (Chapter 5) to unimodal (Chapter 4) distributions of equivalent grain size, in light of their response to memoried conditions.

The objectives of this discussion are as follows: i) to discuss the magnitude and process controls of memory on bimodal bed stability, entrainment and bedload transport with respect to previous relevant research; ii) to compare and contrast the memory response of bimodal to unimodal beds, including process-based explanation; iii) review the non-dimensional analysis presented to make recommendation towards methodology appropriate to memory effect inclusion in sediment transport prediction and modelling.

5.6.1 Influence of memory on entrainment threshold and bed shear stress

5.6.1.1 Review of baseline τ^*_{c50} data:

The non-memoried bed τ^*_{c50} in present thesis is found to be considerably lower than that of the uniform size sediment in the Shields curve (Figure 5.13); this is in line with previous memory stress research by Haynes and Pender (2007) and Ockelford (2011). Specific data show Shields values to be 1.66 times higher than data of the present thesis; 1.61 times that relative to Ockelford (2011); and, 1.35 times that of Haynes and Pender (2007). Wider literature is also agreeable with the present thesis, with Shields' τ^*_{c50} up to 1.8 times higher than that of other bimodal beds researched (Figure 5.13). This is as expected from review of the hiding function theories of Section 2.5 (Einstein, 1950; Egiazaroff, 1965; Ashida and Michiue, 1972; Parker et al., 1982a, Parker and Klingeman, 1982; Komar, 1987; Ashworth and Ferguson, 1989; Kuhnle, 1992; Wilcock, 1993), and Section 4.7 has presented in detail the underpinning processes of relative grain size, hiding, exposure and protrusion which lead to these effects.

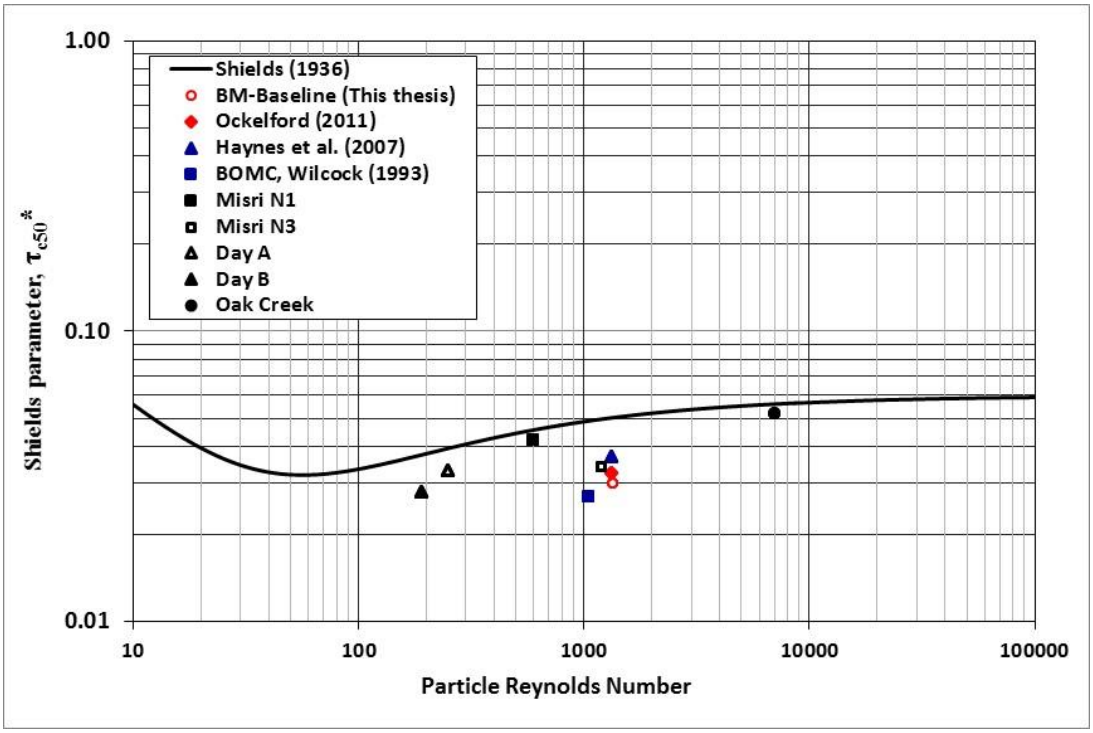

Figure 5.13: Non-dimensional critical shear stress τ_{c50}^* for median size class from baseline experiment and from other researches in bimodal gravel sediment mixture (BOMC τ_{c50}^* calculated by present author taking bed shear stress for D_{50} from Wilcock 1993, median size obtained from Wilcock 2001; τ_{c50}^* for Haynes and Pender 2007, and Ockelford 2011 also calculated by present author by using their original data; other τ_{c50}^* in the graph was adopted from MIT OpenCourseWare, chapter 14).

5.6.1.2 Review of memory stress effect on shear stress

Results from the present bimodal mixtures show a stronger response of entrainment threshold compared with the previous research on stress history by Ockelford (2011) and presented in Figure 5.14 and Figure 5.15. For example, whilst the present thesis observed an increase of entrainment threshold of 34% for SH_60, Ockelford notes only a 9% increase for the same memory period. This may be reasonably attributed to one or more of the following reasons:

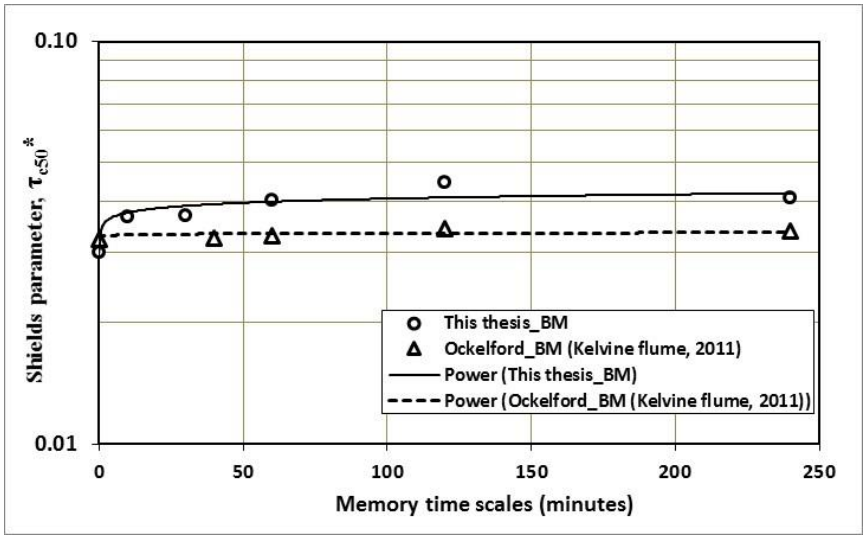

Figure 5.14: Bimodal bed entrainment threshold from for median grain class: this thesis and Ockelford (2011, higher width-depth ratio dataset from a 1.8m wide flume, referred as Kelvine Flume relative to the Shields flume of 0.3 mi width, see Figure 5.15).

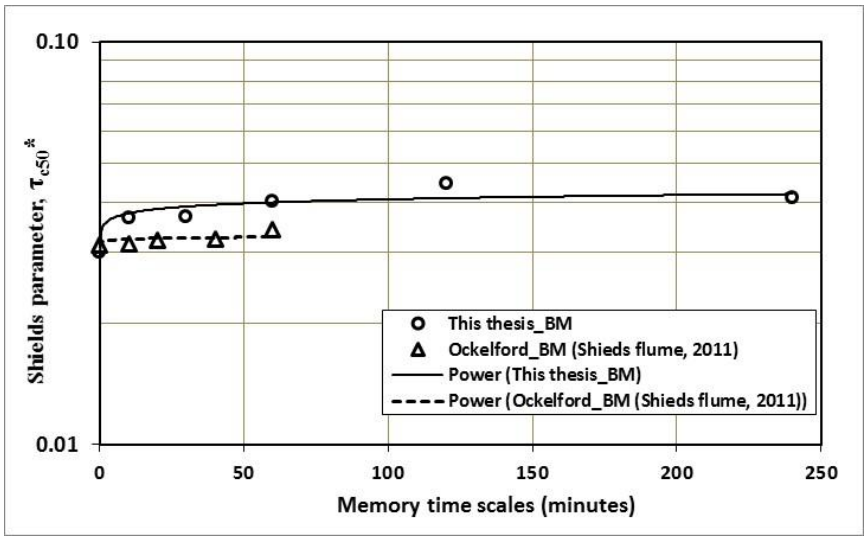

Figure 5.15: Bimodal bed entrainment threshold for median grain class: this thesis and Ockelford (2011, lower width-depth ratio dataset from a 0.3m wide flume, referred as Shields Flume, relative to the 1.8m wide Kelvine flume, see Figure 5.14).

Firstly, the present research adopted the most practical way of assessing entrainment threshold by collecting bedload samples (Fenton and Abbott, 1977), and then applying the reference transport approach by assessing several definitions of reference transport values (Shields, 1936; Parker et al., 1982a; Shvidchenko et al., 2001). This approach has certain advantages, in that use of a stepped discharge hydrograph provides data gained from rating curves to assess the maximum memory stress effect on the rating curve. The alternative visual approach (Yalin, 1972) was used by Ockelford (2011) which restricted her analysis of entrainment threshold to a certain (single) discharge step of the hydrograph. Given that the Yalin count invariably requires multiple particles to be in motion to define threshold, it is likely that this approach calculates entrainment at a relatively higher discharge step than Parker et al. (1982a) reference transport where the present thesis has shown memory gains less significant.

Secondly, it therefore follows that Ockelford's baseline and memory data points (τ^*_{c50}) are relatively closely spaced (0.032 to 0.036 in Kelvine Flume in Figure 5.14 and 0.031 to 0.034 in Shields Flume in Figure 5.15), compared with those in the present thesis in the respective two Figures. Whilst specific discharge data of her flow steps are unavailable, the closely spaced τ^*_{c50} values (of baseline and memory in both of the higher and lower width-depth ratio flumes) may be indicative of coarser resolution in Ockelford's discharge step, thus contributing to a less notable memory response. To exemplify, if the baseline and memory visual entrainment thresholds both fell inside one discharge step, then subtle distinctions in threshold may be masked; this has knock-on effects to data accuracy in particular where averages of repeat runs are employed, as in Ockelford's study. Such data resolution is important in low flow steps, because the shear stress to sediment mobility relationship is well-known to be highly sensitive and non-linear at low shear stresses (Bunte et al., 2004; Recking, 2010).

Thirdly, when compared to Ockelford's sediments, the present thesis has a greater proportion of fines in the first mode (20%, rather than 15% by Ockelford). Given that both studies propose a positive relationship between finer grain response and memory timescales, it is therefore logical that the greater

proportion of fines in the present mixture results in stronger hiding effects and associate stability gains for the bed as a whole. Assessing such sensitivity in the proportional contents of the fines was a deliberate incorporation within experimental design of the present thesis.

Finally, Ockelford (2011) used a longer bedding in time (30 minutes) compared with present thesis (3 minutes). Although bedding in flow is very low, it can also contribute to memory stress development. Thus, Ockelford's memory response on entrainment threshold might have been masked by longer bedding in time leading to dissipated memory response compared with the present thesis for the bimodal bed (as in Figures 5.14 and 5.15).

5.6.1.3 Memory response on the threshold of individual grain classes

Threshold values for individual size classes, (using Ashida and Michiue, 1972, Eq. 2.33-34) indicate important issues related to hiding and exposure (Figure 5.16). In the non-memoried bed, three finer grain classes suffered a varying degree of hiding effect as their threshold values rose higher than Shields uniform size values; the remaining five coarser fractions suffered a varying degree of exposure effect as their threshold values fell to lower than their unisize values, implicitly indicating that the coarser fractions might have formed more tighter packing with better angle of repose (hence more resistant to entrainment). The underpinning processes seem to be tightly placed sediments of non-uniform sizes, and having lower Manning's n (lower resistance to flow) meaning a smoother/cemented bed (Wu, 2007). And thus, in memory experiments, the particles are harder to be entrained and the threshold shear stresses (τ_{Ci}^{*}) for all size classes are higher than those in the baseline experiment.

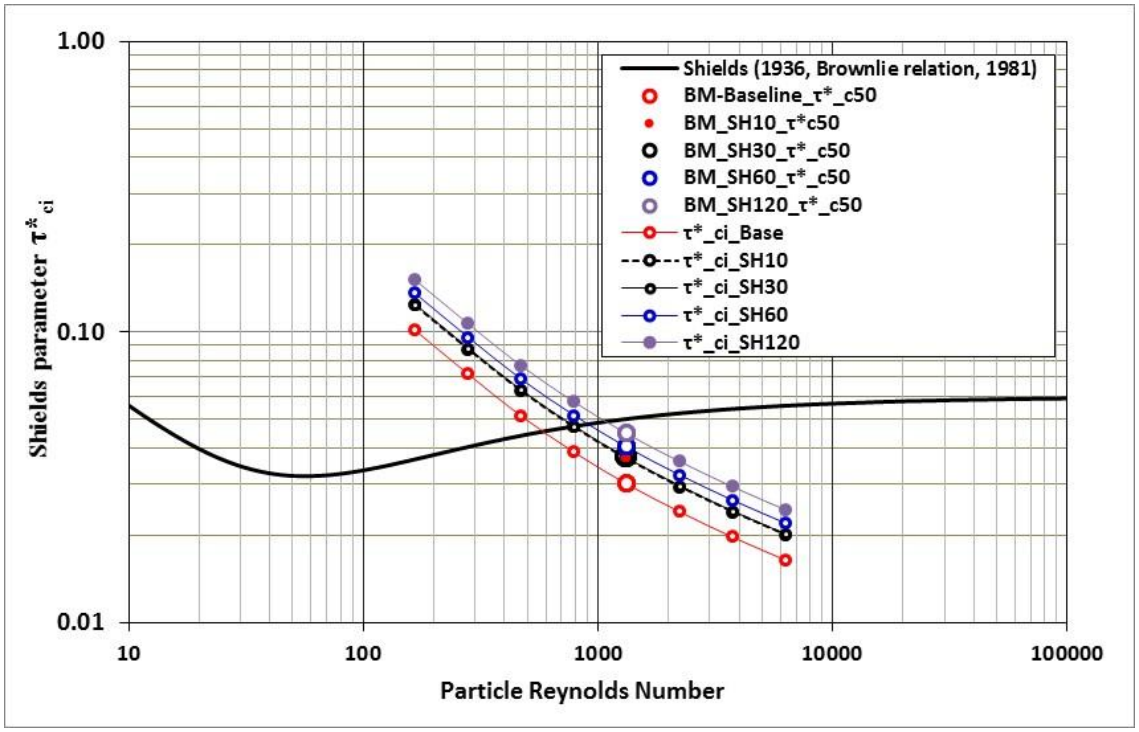

Figure 5.16: Bimodal bed entrainment threshold of median and other grain classes from baseline and memory experiments (Reynolds number used in the abscissa is referred as Particle Reynolds (R_{ep}) number defined by Brownlie (1981); $R_{ep} = (\sqrt{[(s-1)gD_{50}]}\, D_{50})/\nu$), where *s* is specific sediment density used as 2.65.

However, when memory is applied to the bed, the τ^*_{c50} value progressively increases towards that of Shields' value (Figure 5.16) with increasing memory timescales. This reflects the increased stability of the bimodal bed and time-dependent resistance to entrainment for the median size class (Section 5.5). Further review of Figure 5.16 shows that as the memory effect becomes stronger, this exposure and hiding mechanism changes such that a greater number of fractions are affected by hiding (absolute and relative entrainment for each size class is shown in Table 5.6 and Figure 5.17). Similarly, the coarser fractions, settling to a smoother and tighter bed, loses their preferential exposure to flow to be entrained easily due to memory (Section 5.5). The strengthening of these processes due to memory are unsurprising, given earlier data in this thesis.

Table 5.6: Bimodal sediment mixture: threshold shear stress for individual size classes:

D_i (mm)	D_i/D_{50}	BM_Base	BM_SH10	BM_SH30	BM_SH60	BM_SH120
		τ_{ci}^*	τ_{ci}^*	τ_{ci}^*	τ_{ci}^*	τ_{ci}^*
1.2	0.25	0.101	0.123	0.124	0.136	0.151
1.7	0.35	0.071	0.087	0.088	0.096	0.106
2.4	0.50	0.051	0.063	0.063	0.069	0.076
3.4	0.71	0.038	0.047	0.047	0.052	0.057
4.8	1.00	0.030	0.037	0.037	0.040	0.045
6.8	1.42	0.024	0.029	0.030	0.032	0.036
9.6	2.00	0.020	0.024	0.024	0.026	0.029
13.6	2.83	0.016	0.020	0.020	0.022	0.024

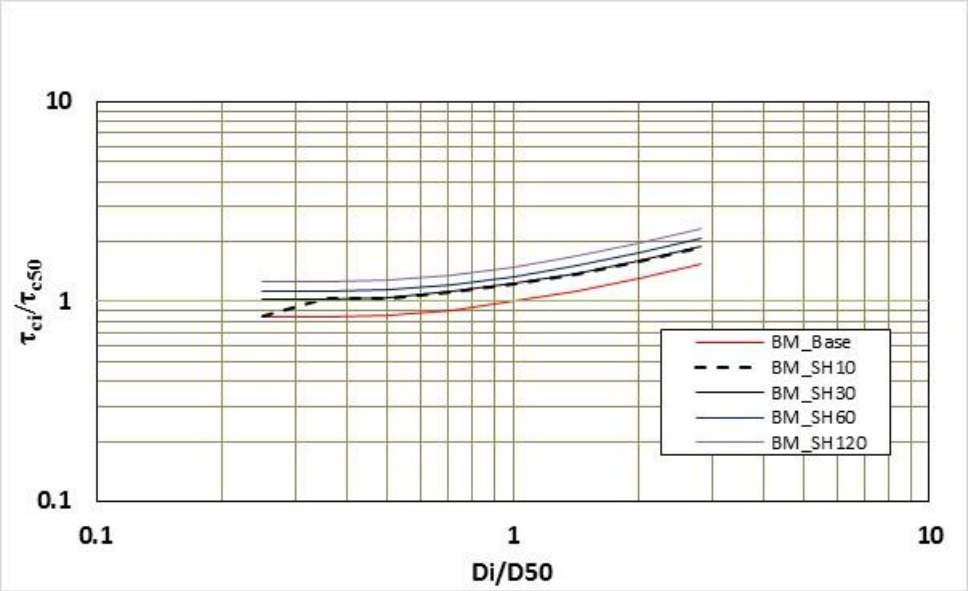

Figure 5.17: Relative entrainment threshold of all size classes vs relative size ($D_i/D5_0$)

5.6.1.4 Effect of modality on memory-based processes

From the basic data presented in Chapters 4 and 5 (Tables 4.5 and 5.4), it transpires that the memory response at entrainment threshold of the bimodal bed is higher than that of the unimodal bed (Figure 5.18). Specifically, entrainment threshold (determined using Shvidchenko's (2001) reference) in bimodal beds (Table 5.4) increases from 23 to 49% over time scales SH_10 to SH_120, while for the same memory time scales the increase is 3 to 8.5% in the unimodal bed (Table 4.5). However, due to the sensitivity and uncertainty of exact threshold and other reasons noted in Section 5.4.3, the scope of analysis was widened to assess data against both the mean and median transport. To make the comparison consistent between unimodal and bimodal datasets, the unimodal data has been revised adopting the approach described in Section 5.4.3 and presented in Table 5.7 and Table 5.8. It is evident that both beds exhibit similar orders of magnitude of response after short memory timeframes of ~10 minutes; this is likely reflective of the equivalent availability of fines on the surface for sorting and restructuring. For longer memory timeframes, the unimodal bed illustrates only weak hierarchical memory effects, yet the bimodal bed clearly shows time-dependent strengthening of memory-related stability. This is likely reflective of the larger proportion of available fines for progressive development of hiding and associated surface restructuring processes discussed in detail Section 4.7. Thus, distinction between grades is very strongly evidenced in both the entrainment threshold and the statistical analysis of the subsequent transporting conditions (median and mean data).

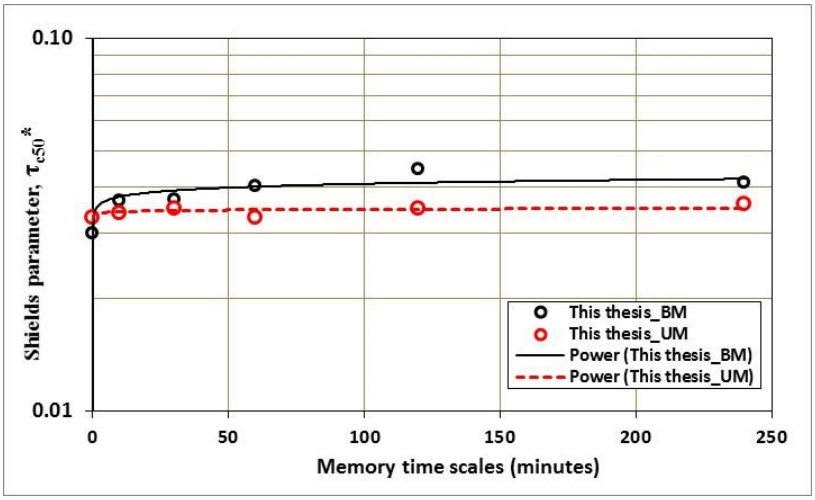

Figure 5.18: Bimodal and unimodal bed: comparison of entrainment threshold for median grain class in different memory time scales.

Table 5.7: Bimodal and unimodal experiments – different magnitudes of shear stress with reference to "Median" transport in respective memory experiment

Experiment Identification Code	Bimodal bed: Reference: "Median" sediment load from memory experiment		Unimodal bed: Reference: "Median" sediment load from memory experiment	
	Shear stress: SH (baseline), (N/m^2)	% increase in shear stress	Bed shear stress	% increase in shear stress
Baseline	-	-	-	-
SH_10	3.21 (3.0)	7	3.15 (3.0)	5
SH_30	3.22 (2.95)	9	3.16 (3.01)	5
SH_60	3.38 (2.7)	25	3.17 (3.0)	6
SH_120	3.35 (2.3)	46	3.18 (3.02)	5

Table 5.8: Bimodal and unimodal experiments – different magnitudes of shear stress with reference to "Mean" transport in respective memory experiment

Experiment Identification Code	Bimodal bed: Reference: "Mean" sediment load from memory experiment		Unimodal bed: Reference: "Mean" sediment load from memory experiment	
	Shear stress: SH (baseline), (N/m^2)	% increase in shear stress	Bed shear stress	% increase in shear stress
Baseline	-	-	-	-
SH_10	3.4 (3.17)	7	3.34 (3.16)	6
SH_30	3.3 (3.1)	6	3.34 (3.17)	5
SH_60	3.5 (3.1)	13	3.33 (3.2)	4
SH_120	3.7 (3.0)	23	3.24 (3.13)	3.5

5.6.2 Role of memory on bedload transport and river bed stability

Section 5.4.4 presented data on the variability of bedload collected over several steps of increasing discharges around the incipient motion (this is not the same as the deterministic threshold analysis of Section 5.6.1.4) via analysis of "mean", "minimum" and "total/cumulative" load indicators. Comparison using "mean" and "minimum" data indicates that the memory effect varies non-linearly with increasing applied discharge. Effects are at a maximum at the lowest discharge of the longest memory run (93-99% reduction in bedload), but progressively reduces as flow steps increase in discharge (hence the mean data indicate only a 27 to 97% reduction in load due to memory).

The alternative analysis using "total" load (referred to as cumulative load over the stability test period) showed much weaker memory effects (5 to 65% reduction in load), due to dilution by higher discharges where memory effects are low or erased. However, previous memory stress research by Monteith and Pender (2005) and Haynes and Pender (2007) adopted hybrid visual-transport methodology yielding analysis most similar to the "total" load approach of the present research. Whilst Ockelford (2011) used a similar method, her stability test period was truncated earlier (i.e., at entrainment of the median size fraction) than in the present thesis; thus, the author's stability test results are likely to include memory effect from a flow stage while memory effect still strongly persists, and thus the author's data set are better compared (fairly)

with the "mean" bedload data measured in the present thesis. Figure 5.19 therefore compares mean data.

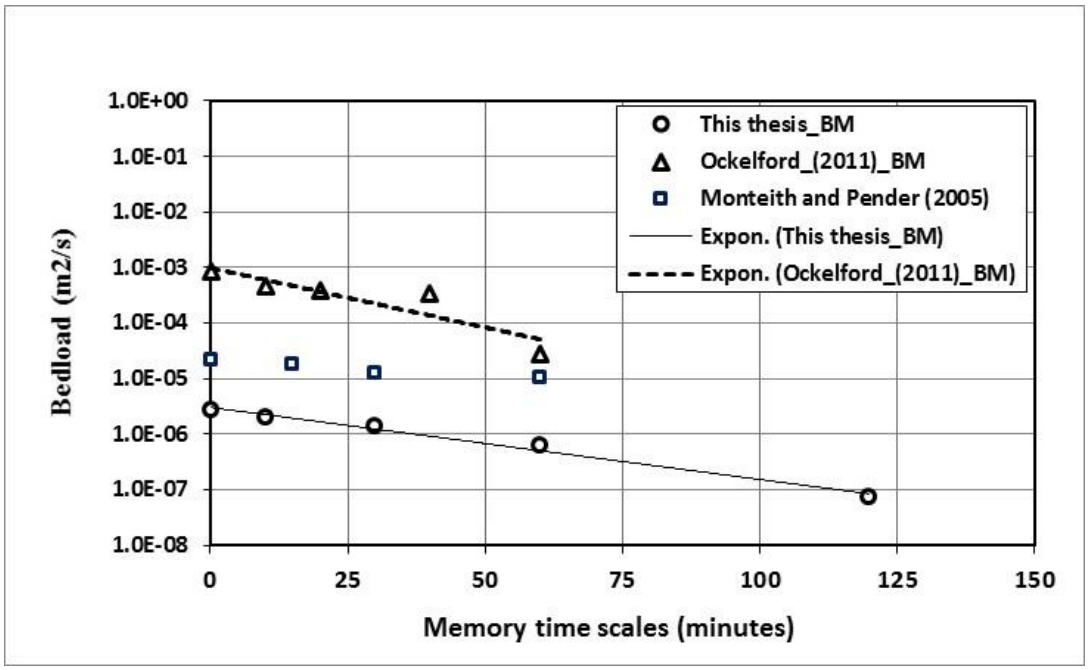

Figure 5.19: Bimodal bed bedload transport from baseline and memory stress experiments: this thesis, Monteith and Pender (2005) and Ockelford (2011); Ockelford's data taken from Figure 4-5 of her thesis, and Monteith and Pender (2005) data taken from Table 3.

Using Figure 5.19 it is clear that the general trend and slope of the line of Ockelford (2011) is equivalent to that of the data collected in the present thesis. The notable offset of Ockelford's data to higher bedload is a facet of her use of the visual approach (discussed in Chapter 2) for the median grain size.

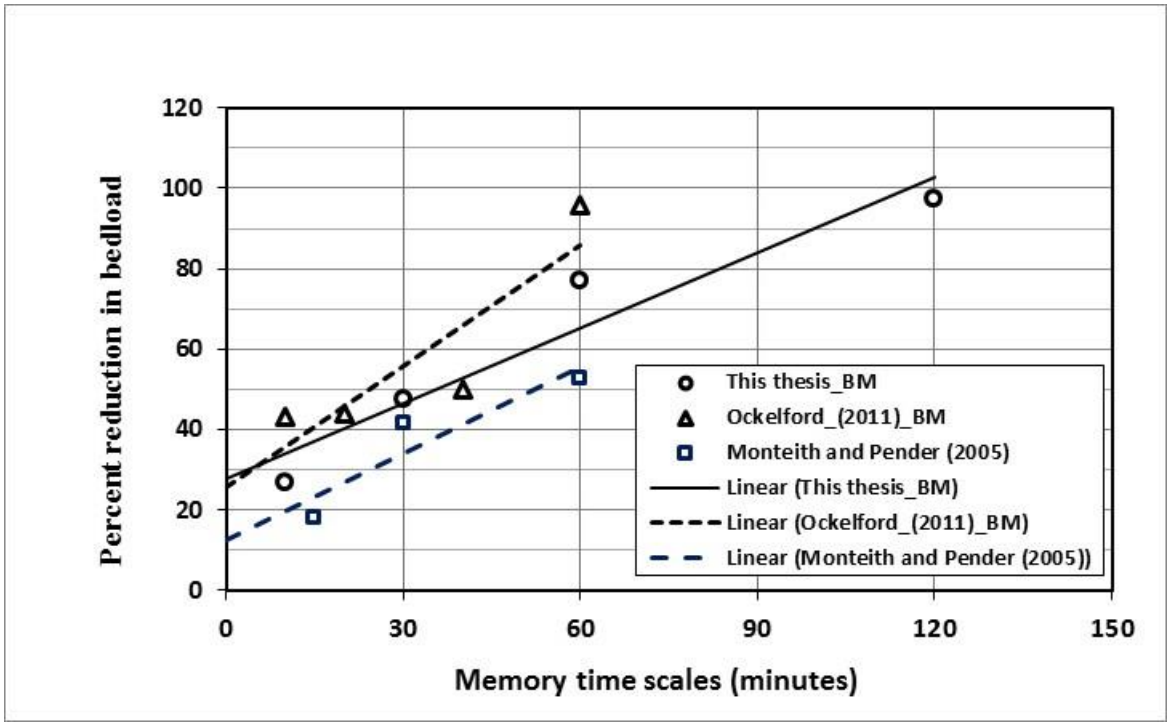

Figure 5.20: Bimodal bed reduction of bedload transport in memory experiments: this thesis, Monteith and Pender (2005) and Ockelford (2011).

As Monteith and Pender (2005) assessed "residual" memory effect from their dataset at $\tau^*/\tau^*_{c50} = 1.19$, their reduction is expected to be lower but approximately parallel to trends of both the present research and those of Ockelford. This is clear in Figure 5.20. Thus, the importance of a benchmarked methodological framework for memory studies is highlighted, with Sections 5.6.1 and 5.6.2 clearly demonstrating that the set-up of Chapter 3 appears most appropriate to detailed analysis of both entrainment and transport statistics.

5.6.3 Grade dependent memory response on bedload and bed stability

From data presented in Section 5.4 and 5.5, the bimodal bed showed more memory response (bedload reduction of 27-97%) than the unimodal bed (14-30%). This is supported by Ockelford's (2011) data, and was justified due to the higher proportions of fines in her bimodal bed (47% $<D_{50}$) than in the unimodal (30%) creating stronger hiding effects and stronger bed structuring.

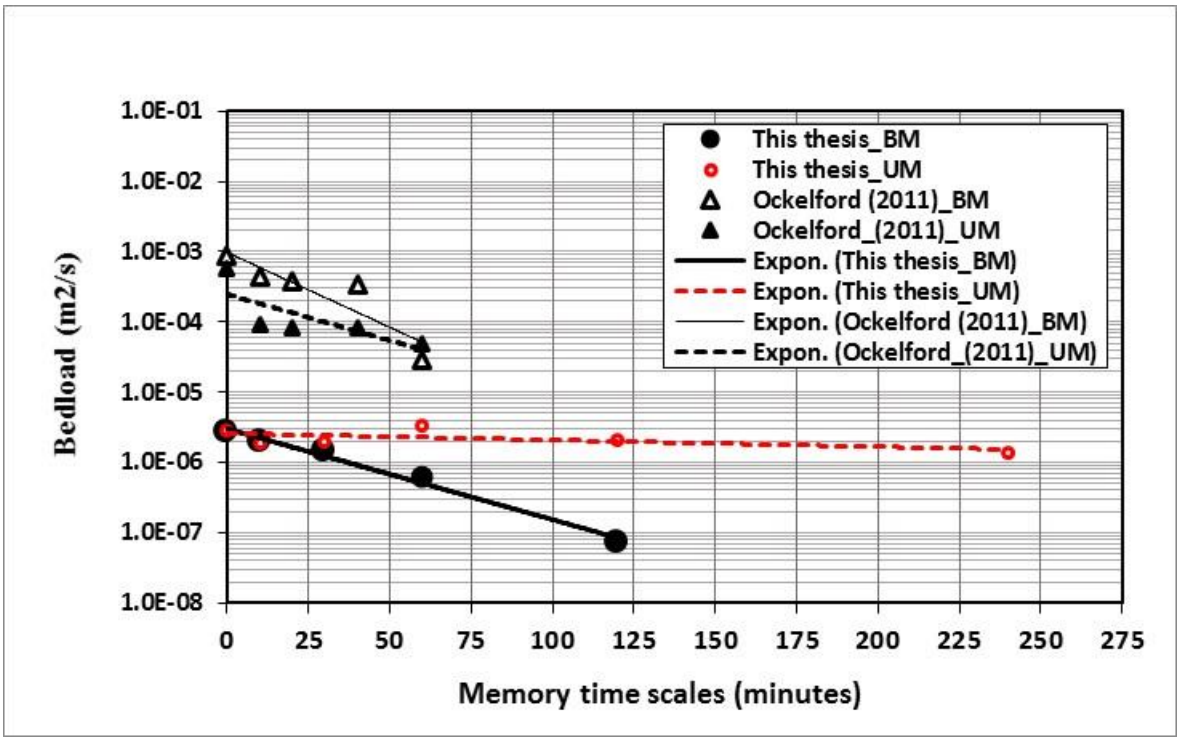

Figure 5.21: Bimodal and unimodal bed: bedload transport in baseline and memory experiments: this thesis and Ockelford (2011).

The simplistic approach in the discrepancy ratio plot in Figure 4.2 and Figure 5.2 clearly shows that reduction rates of the "mean" transport from the present thesis' bimodal bed (Figure 5.2) are closely comparable with those of Ockelford (derived from Fig. 4-5 in her thesis). In Figure 5.2, discrepancy ratios around mean transport rates (which is between discharge 12 and 14 l/s) is approximately 3-15 for the memory time scales 10-60 minutes, while the discrepancy ratios of Ockelford for her bimodal bed in the same memory time scales are approximately 2-12; given the high sensitivity of bedload at low flow transport, the comparison of these reduction rates (i.e., discrepancy ratios) between the two studies are fairly similar, which is also clearly seen in the slope of the lines for bimodal beds (Figure 5.21). Although Ockelford captures higher bedload both in her baseline and memory experiments, probably due to methodological difference (she applied Yalin's (1972) visual approach to determine entrainment threshold and memory effect); this outcome on the similarity of discrepancy ratios, and rate of decrease of sediment load in memory experiments is found to enhance the confidence of the regression laws

applied later in this thesis to develop memory correction approaches in Chapter 6, and used to develop Eq. 6.1 and 6.2.

5.6.4 Normalised transport and shear stress: influence on mathematical functions of bedload

The implication of memory response encapsulated in the power functions (Eq. 5.3 to 5.7) of the non-dimensional parameters of shear stress and bed load is worth discussing. This is primarily important due to the fact that the variation of the exponent due to memory obtained in bimodal bed is not much different to that of the unimodal bed; i.e. 20.9-25.5 and 17.3-21.5 respectively. Particular note is given to the finding that the variation of this exponent across memory time scales seems to be similar in range (+4) for both beds. Yet, as it has already been established that the bimodal bed has a significantly higher response both on bed shear stress and bedload transport, the similarity in "exponent" variation between the two beds must have been compensated in the coefficient terms, and thus the coefficient terms must be better understood.

Whilst the exponent term represents the dependency of transport on the applied force, the coefficient term accounts for the effect of many factors such as grain friction, bedform friction, bed compaction, sediment shapes, sediment and water density and many other terms (Chapter 2 and ASCE, 2007). Whilst it is certain that both the exponent and coefficient contribute to memory response, the insensitivity to grade of the memory-induced variation of the exponent raises the question as to which parameter is more dominant in contributing to memory response. Via two matrices of datasets for the two sediment mixtures (Figure 5.22 and Figure 5.23), both parameters illustrate non-linear relationships, yet it is the coefficient which seems more sensitive.

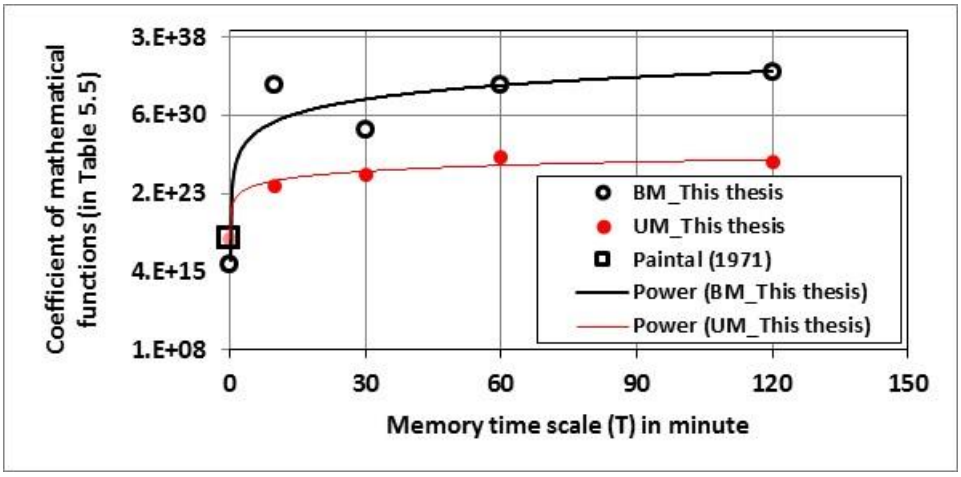

Figure 5.22: Dependence (regression law) of the coefficient of bedload formulae (Eq. 5.3 to 5.7) on memory time scales.

From Figures 5.22-23, the exponent increases by a maximum factor of 2.13, while similar comparison between the coefficient reveals extremely high increase of the coefficient, by an order of 10^{19}. Therefore, memory effects appear to be largely controlled by changes in structure of the bed due to the factors associated with the coefficient term. This is re-examined in the mathematical formulae developed in Chapter 6 for the prediction of bedload with memory stress correction.

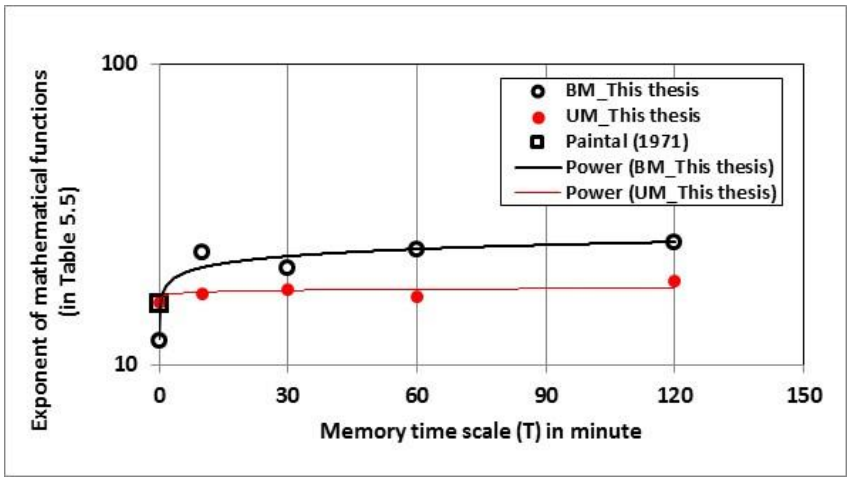

Figure 5.23: Dependence (regression law) of the exponent of bedload formulae (Eq. 5.3 to 5.7) on memory time scales.

5.6.5 Fractional transport in response to memory in bed

Reviewing the general literature suggests that higher fractions of sand content in gravel mixtures will enhance the mobility of the sediment (Jackson and Beschta, 1984; Ikeda and Iseya, 1988; Wilcock, 1988). This is in contrary to the observations of fractional and total load in the bimodal mixtures of the present thesis, in particular, for memoried beds where the total transport reduced by 95%, yet, whereas sand (or finer fractions) contents were increased in the bimodal mixtures (35% fractions are finer in bimodal than the first mode; in unimodal it is 17% of the mixture), and mobility of the mixtures, particularly for the larger fractions reduced significantly than the unimodal (see previous section, and also Figure 5.10 to Figure 5.12). This is also in contrary to the observation of Ockelford (2011), who noted that it was the sand fraction (in bimodal bed), which determines the overall stability of the bed. In case of bimodal in the present thesis, it seems that these are the coarse fractions and their size independent transports, which would determine the overall mobility of bimodal bed.

5.7 Key outcomes

The memory of sub-threshold shear stress in beds with bimodal mixtures has been physically modelled. The same median size (D_{50}=4.8mm) and same number of fractions have been used as in the unimodal mixture of Chapter 4; however, a higher fine proportion (47%) is present (compared with unimodal mixture 30%) such that a higher sorting coefficient (σ_g) of 1.93 is employed; this is specific to assessing the sensitivity of fines to memory stress. For the five memory time scales (SH_10, 30, 60, 120 and 240 minutes) experimented upon, the key outcomes from the above experiments are:

- Bimodal beds are more sensitive to memory stress than unimodal mixtures; threshold motion rises upto 49% in bimodal bed, while the rise is 9% in unimodal bed.

- Bimodal bed memory stress increases entrainment threshold up to 49% for the median grain size (D_{50}) both in Parker's reference based transport (q^*

$=10^{-5}$) and in Shvidchenko's reference based approach ($q^* = 10^{-4}$); there is a direct relationship between memory duration and higher entrainment threshold.

- Due to rise in entrainment threshold, "mean" transports over the low flow range decreased up to 97%; longer memory time scales yield greater reductions in transported sediment volume.

- Size selective transport was observed as key transporting mechanism; both finer and coarser end fractions suffered a similar degree of memory effect, particularly with longer memory time scales; i.e. the mobility of finer fractions reduced by up to +98%, while that for the coarser fractions reduced by up to +90% in SH_120.

- The effect of memory stress on transport was found to be sensitive at q^* values between $1x10^{-7}$ *to* $1x10^{-1}$ and for a Shields parameter range between 0.02 to 0.06. Therefore, use of the traditional Shields threshold condition (0.06) is inappropriate to assess memory effect as it is too high relative to the domain where memory effect operates.

- The memory effect can be adequately embedded in a family of mathematical descriptors using rising "exponents" for non-linearity of transport to shear stress, and changes in the structure by a lumped "coefficient" (in a manner akin to that used in Chapter 4). The response of both the exponent and the coefficient is more sensitive in bimodal beds than in unimodal beds. For SH_10 to SH_120, the exponents rise from 21 to 25.5; while the coefficients rise by an order of $6x10^{18}$ relative to baseline. This supports data in Chapter 4 suggesting that memory is a structural process response.

Chapter 6: Mathematical prediction of bedload transport: a framework for memory stress correction

6.1 Introduction

The scope of improving mathematical formulae for bedload transport prediction to account for memory stress is investigated in this Chapter. Section 2.5 has presented unambiguous evidence regarding the unsatisfactory performance of a plethora of existing bedload transport formulae in the literature, and Chapters 4 and 5 have clearly proven the significance of memory effect control over the entrainment and transport of sediment. Thus, incorporation of the additional stability effect of memory duration into existing graded sediment transport formulae is a logical consideration and can be reasonably performed via modification of coefficients, terms and/or parameters in existing formulae. As this thesis' focus is experimental analysis of memory effects (with the wealth of data collected and analysed), the present Chapter's aim is to provide only a first-stage analysis of memory-modified formulae approaches, as appropriate to ascertaining the future merit of this research direction.

6.2 Introducing frame work for memory stress correction

Whilst a wide range of existing sediment transport formulae have been reviewed in the present thesis to unravel the predictability of the formulae, the evidence of memory data from the laboratory has been simultaneously analysed from Chapters 4 and 5 and previous memory experiments (Haynes and Pender, 2007; Ockelford, 2011). From this, two intuitive and evidence-based approaches to inclusion of memory effects in transport formulae have been deduced.

Firstly, **modification of the hiding function exponent** (*m*): this exponent controls the size selectivity of transports in graded sediment transport formulae (Ashida and Michiue, 1972; Wu et al. 2000a; Powell et al. 2003; ASCE 2007-chapter 3); therefore modification of *m* in graded sediment transport formulae would account for the increase in size selectivity of entrainment due to memory effects (Chapter 4 and 5; Haynes and Pender, 2007; Ockelford, 2009; Ockelford and Haynes, 2013). In summary, higher values of *m* induces size selectivity of

transport with the extreme value *m*=1 providing perfect equal mobility transport and m=0 providing size independence transport; thus, memory will likely adjust the value of *m* upwards from the original non-memoried value (Parker et al., 1982a, Parker and Klingeman, 1982; Wu et al., 2000a). However, it is important to note caution in how this adjustment is made. Most formulae focus upon the threshold motion of median grain size (τ^*_{c50}, D_{50}); hence, if memory is directly implemented it assumes a constant scaling of the transport of each fraction. Using existing data sets, including the present thesis', calibration of these memory-adjusted hiding functions can be undertaken.

Secondly, **scaling of the roughness term in bedload functions** can be justified. Direct evidence from measured data sets of memoried beds by Ockelford and Haynes (2013) clearly shows spatial heterogeneity of sediment bed packing, typically characterised by regions of increasing vertical roughness, and horizontal roughness at granular scale characterised by Hurst scaling components in both streamwise and lateral direction (Ockelford, 2011); Ockelford (2011) found Hurst scaling components to decrease over all memory durations in unimodal and bimodal bed indicating increasing bed complexity and confirming re-structuring of bed under sub-threshold memory stress. More recently, Mao et al. (2011) also clearly found particle rearrangement under different hydrograph shapes (equivalent to unsteady memory effects). Thus, this scaling function in graded sediment transport formulae can account for granular scale roughness (typically defined by A_n) to account for memory effects, in a manner whereby memory would increase A_n as the roughness scale develops over time. This parameter (A_n), expressed in Eq. 6.4, has been historically used by well cited researchers representing granular scale roughness to parameterise loose or tighter packing of planar bed (Strickler, 1923; Meyer-Peter and Mueller, 1948; Li and Liu, 1963; Zhang and Xie, 1993; Patel and Ranga Raju, 1996; Wu and Wang, 1999).

The next step is to decide upon a graded formula to use as a framework for revision and development appropriate to these initial memory incorporation tests. Chapter 2 provides the range of literature (Ashida and Michiue, 1972; Parker et al., 1982a; Wu et al., 2000a, Powell et al., 2001, 2003; Hunziker and Jaeggi, 2002; Wilcock and Crowe, 2003) which has been reviewed in the present

thesis. From this Wu et al. (2000a) has been selected for the following reasons: (i) it is a generally accepted, widely used and recently developed formula for graded beds developed by making use of the plethora of earlier research available in the literature; (ii) the hiding function is clearly defined by the exponent *m*; (iii) despite use of τ^*_{c50}, individual grain class information is explicitly recognised via the fractional *i* term; (iv) the roughness term A_n is straightforward to embed; (v) his formula uses τ^*_{c50} = 0.03, which is similar to values obtained in the present thesis and wider memory experiments from Haynes and Pender (2007), Ockelford (2011) and other field studies (Parker et al. 1982a, Parker et al., 2003) such as to hold good applicability to studies with focus upon low flow conditions; (vi) direct collaboration with the author of the formula was possible. Whilst the full derivations of Wu et al.'s formula can be found in the citation Wu (2007), a précis appropriate herein is provided below of the key elements modified in the present memory approach. Specifically, determination of the threshold motion of an individual grain class is given through the hiding function of Wu (2007) as in following equation:

$$\frac{\tau_{ci}}{(\gamma_s-\gamma)D_i}=\tau^*_{c50}\left(\frac{p_{ei}}{p_{hi}}\right)^{-m} \qquad \text{Equation 6.1}$$

In which τ_{ci} is critical shear stress for grain class i; D_i is grain diameter of size class *i*; τ^*_{c50} is critical shear stress (non-dimensional) for median size class, P_{ei} and P_{hi} are respectively the exposure and hiding probabilities for grain class *i*. In a non-uniform mixture, $P_{ei} \geq P_{hi}$ for coarse fractions, and $P_{ei} \leq P_{hi}$ for finer fractions. In uniform sediment, $P_{ei} = P_{hi} = 0.5$. Detail derivation of P_{ei} and P_{hi} can be found in Wu (2007), and briefly presented in Section 6.3.2. The strength and weakness of the hiding and exposure parameter is further discussed in Section 6.3.2. However, it is noted above that use of τ^*_{c50} must be specifically manipulated as specific to incorporating memory time scales, hence Eq. 6.2 is derived as:

$$\tau^*_{c50\_memory} = C(T)^b \qquad \text{Equation 6.2}$$

In which, *T* is memory timescale, and *C* is coefficient and *b* is exponent in the power relation; both *C* and *b* are functional to memory stress timescale. Non-dimensional bedload (q_i^*) for fractional class (*i*) is then calculated from Eq. 6.3 and 6.5:

$$q_i^* = 0.00053\left[(n'/n)^{3/2}\frac{\tau_b}{\tau_{ci}} - 1\right]^{2.2} \qquad \text{Equation 6.3}$$

In which, τ_{Ci} is bed shear stress for grain class *i* and, specifically, n' and n'' are Manning's roughness coefficients for skin (grain) and bedform respectively; $\tau_b = \tau_b' + \tau_b''$ where $\tau_b = \gamma R_b S$ is bed shear stress divided into skin (grain) shear stress (τ_b') and bedform shear stress (τ_b''). Einstein (1942) suggested division of hydraulic radius R_b into two parts: R_b' for skin friction and R_b'' for form friction. Thus, $\tau_b' = \gamma R_b' S$ and $\tau_b'' = \gamma R_b'' S$. These relations through assumption of equal velocity provide: $U = R_b^{2/3} S^{1/2}/n$, $U = R_b'^{2/3} S^{1/2}/n'$, $U = R_b''^{2/3} S^{1/2}/n''$. This leads to: $R_b' = R_b(n'/n)^{3/2}$ and $R_b'' = R_b(n''/n)^{3/2}$. From the above relations, now total Manning's roughness can be transformed into $(n)^{3/2} = (n')^{3/2} + (n'')^{3/2}$, also see Wu (2007) for detail derivation. Hence, Manning's roughness coefficient at the grain scale is related to bed material size by the relation:

$$n' = (D_{50})^{1/6}/A_n \qquad \text{Equation 6.4}$$

These equations provide the avenue for use of A_n as a memory adjustment factor in the present thesis. A_n affects the grain roughness, and thus mobility of transport.

As different values of A_n have been observed by scientists in developing bedload formula, using this term as a variable appears appropriate in accounting for time-dependent memory effect development. For example, A_n values between 17 and 20 are commonplace for loosely packed beds (e.g., Strickler, 1923; Li and Liu, 1963; Zhang and Xie, 1993; Wu and Wang, 1999); yet in more tightly packed beds higher values of A_n between 24 and 26 are documented (e.g., Meyer-Peter and Muller, 1948; Patel and Ranga Raju, 1996). Thus, Wu's function in Eq. 6.3 can be re-arranged to the form in Eq. 6.5 below. The correction factor representing packing arrangement (i.e. the compactness of bed) for additional stability due to memory stress is to be accounted in the co-efficient term as in Eq. 6.5 so as to scale the threshold motion for individual grain classes; this, in turn, scales the ability of the available shear stress for sediment mobility through the term τ_b / τ_{ci}. Hence,

$$q_{bi}^{*} = 0.00053 \left[\{(D_{50})^{1/6} / nA_n\}^{3/2} \frac{\tau_b}{\tau_{ci}} - 1 \right]^{2.2} \qquad \text{Equation 6.5}$$

Detailed data and parameter input for model run in each approach are presented and discussed further in Section 6.3, yet the above equations provide the overall framework within which the research of this Chapter is undertaken.

6.3 Prediction of transport with memory stress

6.3.1 Memory incorporation via hiding function scaling (m)

Key data inputs for the Wu et al. (2000a) model, using both of the approaches mentioned in the preceding Section, include: τ_{c50}^{*}, median grain size, size of each grain class, fractional proportions for each grain class, Manning's roughness coefficient, and total available shear stress; while the variables remain the same, their values vary according to whether the unimodal or bimodal size distribution is being analysed. The output process is two stage: firstly, the model calculates the threshold motion for each grain class; secondly, the model predicts the non-dimensional bedload transports for each grain class, whose summation provides the total bedload transport for grain classes. The prediction

was made over the full hydrograph; however, the comparison of predicted load with observed load was carried out against the integrated load over the hydrograph as the memory effects in Chapter 4 and 5 were quantified and discussed against this parameter.

Using the hiding function framework to account for memory (Section 6.2), the key inputs for each memory scale model run are presented in Table 6.1 (for both unimodal and bimodal bed); it is important to note that in this approach, two dependent variables, τ_{c50}^{*} and exponent "*m*", are updated in each memory scale run to include the memory effect (shown in blue shaded data values), while all the other variables (inputs) remain constant in all model runs. The detailed calculation sheet for model run is presented in Appendix C (Table C.11; same excel sheet is used for calculating bedlaod by varying A_n).

Table 6.1: Key inputs in the runs of Wu's (2007) model for the unimodal and bimodal beds of this thesis, as appropriate to implementing memory stress through a hiding function framework. Blue shaded inputs are the only varying variables in each memory time scale run (detailed calculation sheet is presented in Appendix C). Grain sizes are shown in mm, but must be converted to metres for model runs. No data are provided or analysed for bimodal SH240 due to outlier status ascertained in Chapter 5. The Manning's n value is the same for all memory timescales, as calculated from velocity under uniform flow assumptions. Shear stress is the same for all memory timeframes, as described in Table 4.2. The A_n value of 20 (similar to non-memoried bed) is used for all memory time scale in this approach because memory stress bed stability is incorporated through increasing τ_{c50}^{*} and varying the exponent *"m" (*therefore A_n=20 eliminates implementing double effect of memory); or in other words, the effect of memory on roughness (or A_n) increasing entrainment threshold values have directly been used from the observed values in this thesis (values in row 3-uniodal; row 4-bimodal)

Variables	Memory time scale in minutes					Comment
	10	30	60	120	240	
τ^*_{c50} *for* D_{50}	0.034	0.035	0.036	0.035	0.036	Unimodal: Table 4.5 Chapter 4)
	0.036	0.037	0.040	0.045	-	Bimodal: Table 5.4 Chapter 5)
D_{50} (mm)	4.8					-
Fractional size class (D_i) (mm)	1.2	1.7 9.5	2.4 13.4	3.3	4.7	6.7	Same in both grades of bed
Fractional contents (F_i) (-) for eight size classes	0.025	0.05 0.1	0.075 0.05	0.15	0.4	0.15	Unimodal: Table 3.2, Chapter 3
	0.05	0.1 0.1	0.2 0.04	0.12	0.08	0.31	Bimodal: Table 3.2, Chapter 3
Manning's n ($m^{-1/3}$.s)	0.02						-
Shear stress (N/m^2)	See Figure 4.5 and 5.5 (same for all runs) and Appendix D						-
Hiding function exponent *"m"* (-)	Variable 0.4 to 1.0						-
Grain scale roughness (A_n) ($m^{1/2}$. s^{-1})	20						-

The two approaches employed for calibration of predicting load are referred as scaling process; one is scaling by varying the hiding function exponent (Eq. 6.1), and the other is varying the A_n in Eq. 6.5. Use of scaling in prediction of bedload is a common practice in sediment transport (van Rijn, 1984) due to the empirical nature of bedload formulae. The use of n, n' and *An* should all be considered as scaling the predicted value. Now as in Table 6.1, n=0.017, and n'= $(D_{50}/20)^{1/6}$, which is 0.02 may apparently look inconsistent. However, there was a basis for choosing them as a start point of the calibration process. n=0.017 was initially obtained by using Manning's uniform flow formula (see Table C.11, in last row), while it is expected that the roughness (n) should also adjust due to memory (Ockelford, 2011). Similarly, n'= 0.02 (with An=20) is applied in literature for non-memoried bed (Wu, 2007). So, in the calibration processes, these two values n=0.017 and n'=0.02 were used as starting point in both approaches of calibration. Use of An between 18 to 25 in Tables 6.5 and 6.6 with n=0.017 may look contradicting for the An values of 18. 19, and 20; same is true for the case of Turkey Brook for all An values smaller than 20. However, in all cases, n=0.017 has been consistently used, whether An is greater than 20 or smaller than 20. Therefore, use of n=0.017, and varying use of n' by varying the An values should be considered as a numerical art of scaling rather than an inconsistency. Further to note about n = n' in case of planar bed (when n"= 0 as there is no bedform). Apparently in a planar bed, we often refer n=n'; however, practically

in a river bed (planar), the total roughness may not be equivalent to individual grain roughness (n'); Professor Weiming Wu (The Clarkson University) expressed this view during a meeting with him that no matter whether a river bed is planar; due to particle interaction, total roughness is always different than grain scale roughness. Therefore if n value is changed from 0.017 to 0.02, then it will need to be done for all An values smaller than 20; this will rather make the scaling process more inconsistent, and then prediction will not be comparable with like for like. While use of n=0.017 in all cases rather made the prediction method more consistent.

Predicted load has been evaluated against an "Efficiency Factor - EF", which is the ratio of predicted and observed bedload. In several organised researches, the EF for different sediment transport formulae were evaluated (White et al., 1975; Yang, 1976; Alonso, 1980; ASCE, 1982, and Yang and Huang, 2001); they considered the EF values between 0.5 and 2.0 as satisfactory standard for the sediment transport formulae they considered in their evaluation. In the present thesis, the above EF range was considered as reference for satisfactory prediction for the Wu et al. (2000a) model. Given the extreme sensitivity of bedload transport in low flows (Bunte et al., 2004), some authors further relaxed this EF range between 0.1 and 10 (e.g., Recking, 2010).

Predicted bedload with memory effects for both unimodal and bimodal data is presented in the Table 6.2 and Table 6.3. The EF values in Tables 6.2 and 6.3 clearly show that memory effects can be predicted satisfactorily by adjusting the hiding function exponent "*m*"; with evidence supporting use of *"m"* values within the range of 0.2 to 0.6 and a weak suggestion of higher *m* values for longer memory durations. This shift towards equal mobility transport after longer memory timeframes appears appropriately reflective of improved packing arrangements and hiding within the bed fractions.

Table 6.2: Unimodal bed: Efficiency Factor (EF) of predicted load (hiding function framework, *m*). Blue shaded cells are within the acceptable range of prediction

Experiment Identification Code	Efficiency (EF) range for predicted load: q_b_Predicted /q_b_Observed load				
	m=0.2	m=0.4	m=0.6	m=0.8	m=1
UM_SH_10	0.78	0.54	0.42	0.39	0.60
UM_SH_30	0.65	0.50	0.33	0.30	0.44
UM_SH_60	-	0.25	0.17	0.14	0.21
UM_SH_120	0.55	0.36	0.26	0.21	0.31
UM_SH_240	0.39	0.56	0.39	0.31	0.41

Table 6.3: Bimodal bed: Efficiency Factor (EF) of predicted load (hiding function framework, *m*). Blue shaded cells are within the acceptable range of prediction

Experiment Identification Code	Efficiency (EF) range for predicted load: q_b_Predicted /q_b_Observed load				
	m=0.2	m=0.4	m=0.6	m=0.8	m=1
BM_SH_10	0.9	0.6	0.3	0.2	0.2
BM_SH_30	1.3	0.7	0.4	0.2	0.2
BM_SH_60	2.0	1.1	0.6	0.3	0.1
BM_SH_120	2.4	1.30	0.61	0.19	0.002

In the unimodal bed, *m*=0.2 predicts bedload above the 50% EF limit (Table 6.2) for memory time scales 10 to 120 minutes; the 240 minute memory time scale seems to require a higher *m* value (0.4). In the bimodal bed, only the shortest memory time scale of 10 minutes appears successful at the smaller *m* value of 0.2; although 30 and 60 minutes memory time scales are also within the efficiency range (EF values below 2), these two long memory times scales together with 120 minutes memory require higher *m* values (0.4 to 0.6) to achieve a better EF values, and extrapolation for estimating 240 minute memory time scale would tend towards a higher *m* value → 0.6 in bimodal experiments. Whilst all bimodal data are predicted well by this approach, the 60 minute memoried bed of the unimodal data fails to be corrected effectively using this approach; review of Chapter 4 does not raise any definitive rationale for this.

More detailed evaluation of the data used to generate the EF of Table 6.2 and does, however, show that almost 100% data points of the memoried bed are possible to predict within the EF range. Given that prediction and performance evaluation in the current low flows of the present thesis is more challenging than in previous higher flow research which benchmarked the acceptable EF range, the use of $m = 0.2\text{-}0.6$ is therefore considered generally satisfactory as a method of accounting for memory effects as reflective of the associated enhanced selective transport. That said, this approach performs better for bimodal beds than unimodal beds and probably does not robustly present a generally applicable "graded" bed correction method. Also, as the distribution range of *m* values for a specific grade of bed are very small, this method appears only weakly sensitive to memory description.

A final point worthy of note is that from Table 6.2 and Table 6.3 it is obvious that high exponent values, say from 0.8 to 1.0 which are meant to provide bias towards equal mobility transport (Chapter 2, Section 2.5), provide the worst prediction in both beds (particularly in the bimodal mixture). As such, the many field studies where *m* values have been observed above 0.6 (Parker et al., 1982a; Ashworth and Ferguson, 1989; Kuhnle, 1992; Ashworth et al, 1992) differ with the calibrated *m* values applied in predicting bedload of the present thesis. Therefore, should the values from literature be erroneously assumed for memory bed, would yield a bedload under-prediction of 10 to 100 times for the 60 to 120 minute memory timescale data herein. Thus, the importance of low value *m* use in the present thesis (towards size selectivity) is most appropriate and strongly advocated for memory research. That said, it is important to conclude that even with using low *m* values the memory and grade specific trends in *m* are less sensitive than expected; such weakness in this mathematical approach therefore is the focus of Section 6.3.2.

6.3.2 Weakness of hiding function approach (*m*) for predicting sediment transport

In all graded transport formulae, the initial motion of each size class is determined using the hiding function (Chapter 2). Outwith the present thesis,

none of these functions explicitly include temporal water-working (although their effect might be unknowing in-built due to the data used). The hiding functions represent only an initial and constant state of bed structure; for example, in Wu's formula (hiding) P_{hi} and (exposure) P_{ei} remain constant in a given distribution irrespective of any applied temporal scale effect on the bed, such as memory stress. In the case of water working of bed prior to sediment motion, while the distribution in the bulk mix remains same, the hiding and exposure can change substantially due to changes in bed structure (Ockelford, 2011; Mao et al., 2011) and leads to different degrees of (im)mobility of fractions from beds of equivalent distribution (discussed in Chapters 4 and 5); this is schematically shown in Figure 6.1. The equations for calculating hiding (P_{hi}) and exposure (P_{ei}) probabilities are presented in Eq. 6.6 and 6.7 (see Wu, 2007). According to Eq.6.6 and 6.7 (or other hiding functions discussed in Chapter 2 in Section 2.5), the hiding and exposure probabilities (P_{hi} and P_{ei}) will be same for both beds as the size distribution is same in the two beds, and thus will calculate same set of entrainment threshold for individual size classes for these two scenarios. Thus, the variation of the exponent "*m*" in Eq. 6.1 has been investigated to explore the sensitivity of predicted transport to its value.

$$P_{hi} = \sum_{j=1}^{N} f_j \frac{D_j}{D_i + D_j} \qquad \text{Equation 6.6}$$

$$P_{ei} = \sum_{j=1}^{N} f_j \frac{D_i}{D_i + D_j} \qquad \text{Equation 6.7}$$

In Eq. 6.6 and 6.7, D_i and D_j are grain size for size class i and j, f_j is fractional proportion for grain class j; and N is total number of grain classes.

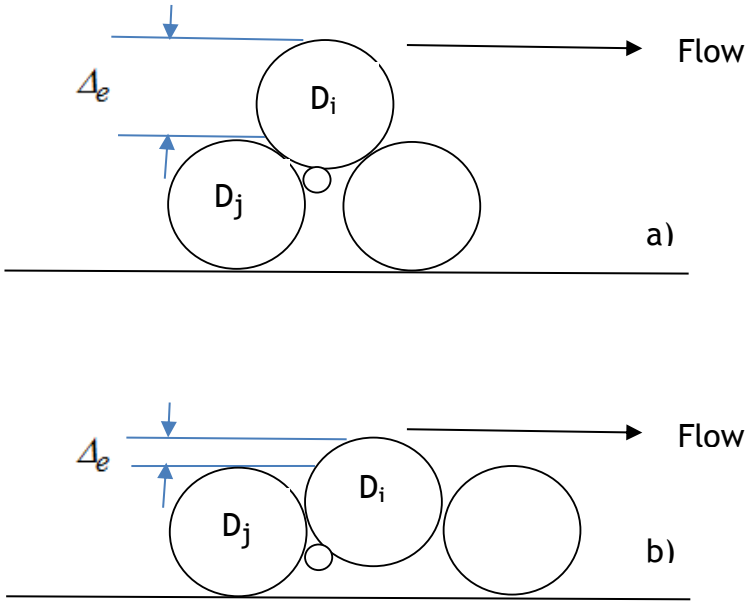

Figure 6.1: Two beds of invariant distribution of sediment, but different bed structure, yield same hiding and exposure according to Eq. 6.6 and 6.7 (and other hiding function equations in chapter 2: Eq. 2.28-2.34).

6.3.3 Memory incorporation via roughness scaling (*An*)

To overcome one of the weaknesses of using the hiding function scaling (*m*), the roughness scaling approach is better appropriate to considering a fractional (individual grain size) response to memory. Specifically, the roughness parameter is related to grain scale roughness (*n'* in Eq. 6.3) and, therefore, A_n, once it is related to grain size in Eq. 6.4 and 6.5. By modifying the parameter A_n in Eq. 6.5 to reflect improved packing arrangement due to memory (i.e. an increase in the value of A_n), a prediction of bedload has been made. The key inputs for each simulation in this framework for Wu's model are presented in

Table 6.4 indicating that only the A_n value is dependent upon memory time scale; the rest of the variables are common to all calculations. The detailed calculation sheet for the model run is presented in Appendix C (Table C.11). Analysis has used the same EF evaluation methodology as that used in Section 6.3.1, with data provided in Table 6.5 and Table 6.6.

Table 6.4: Key inputs in runs of Wu's et al. (2000) model for unimodal and bimodal bed of this thesis as appropriate to the roughness length framework (A_n) approach; scaling of the roughness parameter is the only variable input in this approach as shown in blue shaded row; other variables are same in all runs, such as: τ^*_{c50} , D_{50}; Manning's *n*; hiding function exponent; grain size used in the prediction requires conversion to metres (detailed calculation sheet presented in Appendix C)

Variables	Memory time scale in minutes					Comment
	10	30	60	120	240	
τ^*_{c50} *for* D_{50}	$\tau^*_{c50} = 0.03$					Same value in both grade of bed
D_{50} (mm)	4.8					-
Fractional size class (D_i) (mm)	1.2	1.7 9.5	2.4 13.4	3.3	4.7	6.7	Same in both grades of bed
Fractional contents (F_i) (-) for eight size classes	0.025	0.05 0.1	0.075 0.05	0.15	0.4	0.15	Unimodal: Table 3.2, Chapter 3
	0.05	0.1 0.1	0.2 0.04	0.12	0.08	0.31	Bimodal: Table 3.2, Chapter 3
Manning's *n* ($m^{-1/3}$.s)	0.017					-
Shear stress, τ (N/m^2)	See Table 4.2 (same for all runs)					Table 4.2
Hiding function exponent *"m"* (-)	m=0.6 m=06 is used as calibrated value by Wu (2007) for non-memoried bed					-
Grain scale roughness (A_n) ($m^{1/2}$. s^{-1})	A_n: 18 to 25 is varied for each memory experiment					-

Representing memory in terms of roughness length scale Eq. 6.4 and 6.5 and Tables 6.5-6 indicates sensitivity in A_n value, within a fairly tightly distributed range; between 18 and 22 for unimodal bed for memory timescales 10 to 240 minutes, and 19 and 25 for bimodal bed for memory timescales 10 to 120 minutes. The dependence of memory time scales with A_n values looks systematic, and also distinct between the two grades of bed. Between the two grades of sediment bed, the values shift by (approximately) a value of one for each memory time scale in the bimodal bed, possibly suggesting an appropriate method (and resolution) for mathematically quantifying/representing memory effects in this bed. The increases of A_n values with memory time scale are logical and in line with the improved hiding and compaction suggested by the

direct measurements during prolonged memory experiments by Ockelford and Haynes (2013). Results in Tables 6.5-6 show that 10 minutes memory timescale in both grades have A_n values 18 and 19 respectively; these values are similar to non-memoried bed values of A_n as stated in the wider literature (e.g., Strickler, 1923; Li and Liu, 1963; Zhang and Xie, 1993 and Wu and Wang, 1999).

Table 6.5: Unimodal bed: this thesis: Efficiency Factor (EF) of predicted load for different roughness scale with varying values of A_n

Experiment Identification Code	Efficiency (E) range for predicted load: q_b_Predicted /q_b_Observed load							
	An= 18	19	20	21	22	23	24	25
UM_SH_10	0.95	0.65	0.43	0.29	0.18	0.12	0.07	0.04
UM_SH_30	2.35	1.57	1.03	0.65	0.41	0.25	0.15	0.09
UM_SH_60	1.93	1.28	0.83	0.53	0.33	0.20	0.12	0.07
UM_SH_120	3.06	2.03	1.33	0.84	0.52	0.31	0.18	0.11
UM_SH_240	4.14	2.75	1.79	1.14	0.70	0.42	0.25	0.15

Table 6.6: Bimodal bed: this thesis: Efficiency Factor (EF) of predicted load for different roughness scale with varying values of A_n

Experiment Identification Code	Efficiency (E) range: Predicted /Observed load							
	An= 18	19	20	21	22	23	24	25
BM_SH_10	1.5	1.1	0.8	0.5	0.4	0.3	0.2	0.1
BM_SH_30	2.1	1.5	1.1	0.8	0.5	0.4	0.25	0.2
BM_SH_60	4.6	3.3	2.3	1.6	1.1	0.8	0.5	0.4
BM_SH_120	8.3	5.9	4.2	2.9	2.1	1.4	1.0	0.7

Table 6.5 and Table 6.6 illustrate that for bimodal beds the A_n values are more sensitive to memory stress time scales than unimodal bed; again, this supports the entrainment and bedload data of Chapters 4 and 5 in that the higher A_n values are an indication of a more stable and compact structured bed developing faster in bimodal sediment. With prolonged memory timeframes, values increase to 22 in unimodal and to 25 in bimodal bed; whilst these values are in line with the more compacted bed A_n values cited by Meyer-Peter and Muller (1948) and Patel and Ranga Raju (1996), the strongest support comes from validation (in next section) of previous memory researchers (Table 6.7); all of their memory bedload (see Section 6.3.4 on validation) requires to apply A_n values upto 22 for

satisfactory EF validation for 40 minutes memory time scales. Worthy of note is that Ockelford's "EF" indicates to require higher A_n values than those of the present thesis; this can be a facet of memory *per se* (which is unlikely due to the similarity in rate of change to the present study), but it is likely a cumulative effect of her different screeding and water-working process in her flume set-up. In particular, her analysis uses total bedload collected over the memory and stepped hydrograph period such that need of higher A_n values likely reflects overall water working of this cumulative timeframe (rather than just the memory period analysed here) representing a far more compact structure.

6.3.4 Validation of roughness scaling (A_n) model with other memory stress datasets

Two other memory stress transport datasets are available from Haynes and Pender (2007) and Ockelford (2011). As the bimodal bed was found more responsive for calibration of memory stress transport in scaling of the roughness parameter approach, these calibrated A_n values obtained in the present thesis has been applied to validate the other two bimodal datasets. It is now obvious from the calibration of the present thesis dataset that by adjusting A_n values, it is possible to calibrate sediment transport in a manner accounting for memory stress. Therefore, rather than undertaking separate calibration of other sets of data, it is more logical and robust to establish if the calibrated values (A_n) of the present thesis can be used to validate other memory stress datasets.

From Ockelford (2011), transport data for four memory time scales (10, 20, 40 and 60 minutes) are available for validation. From Haynes and Pender (2007), two memory time scales (30 and 60 minutes have been chosen for validation); although this latter study had two longer memory time scales (1440 and 5760 minutes); these fall outwith the range of calibration of the present thesis' dataset and are inappropriate for use herein. From both studies, the transport and shear stress from all five memory time scales are presented in Table 6.7.

Calibrated A_n values have been extracted from the different "Efficiency Factor" from Table 6.6 corresponding to the memory time scales of Haynes and Pender (2007), and Ockelford (2011). For example, for 60 minute memory time scale, the appropriate EF should be at A_n=22; the A_n values for other memory time

scales were deduced in a similar manner; see Table 6.6; then model validation runs were carried for the set of A_n values together with the respective physical data input of Table 6.4. Using this approach, the validated "EF" values are presented in Table 6.7.

Table 6.7: Validated bedload of memory dataset of Haynes and Pender (2007) and Ockelford (2011) in transport prediction by roughness scaling approach. For Ockelford's data *(*)* denotes a recognised outlier for the 60 minute memory experiment of her raw dataset

Researchers	Memory time scale (min)	Bed shear (N/m^2)	Total obs. Bedload (m3) (see note)	Predicted load (m^3)	A_n: taken from calibrated Model (This thesis)	"EF"
Ockelford (2011): bimodal bed (D_{50}: 4.8mm)	10	2.45	7.88E-04	1.74E-03	19	2.40
	20	2.5	7.76E-04	1.56E-03	20	2.00
	40	2.52	4.34E-04	1.15E-04	21	1.66
	*60**	*2.65*	*3.77E-05*	1.12E-03	22	18.50
Haynes and Pender (2007): bimodal bed (D_{50}=4.8mm)	30	3.54	6.98E-06	6.80E-6	20.2	0.98
	60	3.54	6.91E-06	3.87E-6	22	0.56

Overall, the EF data in Table 6.7 can be considered reasonably satisfactory in using the A_n approach for memory correction for both previous research studies, with data showing EF values of 0.56 – 2.40 (Ockelford's thesis notes 60 minute memory data as an outlier). This Section, whilst simplistic in approach and analysis, therefore concludes that satisfactory "EF" values are possible to achieve in graded beds, with consistent and strongly correlated grade dependent, and memory dependent A_n values.

However, the sensitivity to A_n values also demonstrates a range of uncertainty of under prediction for Ockelford's dataset, 2011 and Haynes and Pender, 2007 dataset in case of using inappropriate parameter values; this implicitly reflects the heterogeneity of structural changes a bed can undergo, yet also highlights the importance of parameter selection/estimation. Whilst this issue is explicitly teased out for discussion in Section 6.4, an example scenario warrants attention here. For example, in the unimodal bed erroneous use of a non-memoried A_n value (i.e. between 18 -20) for memoried beds of 60 to 240 minutes would lead

to bedload being over predicted 4-9 fold. Similarly, the converse is true in that erroneous use of high A_n values for a non-memoried would lead to bedload under-prediction. The response of A_n values for bimodal beds is higher than unimodal beds (for 30, 60 and 120 minutes memory time scales, see Figure 6.2), hence shows even greater sensitivity to such over/under-prediction of bedload.

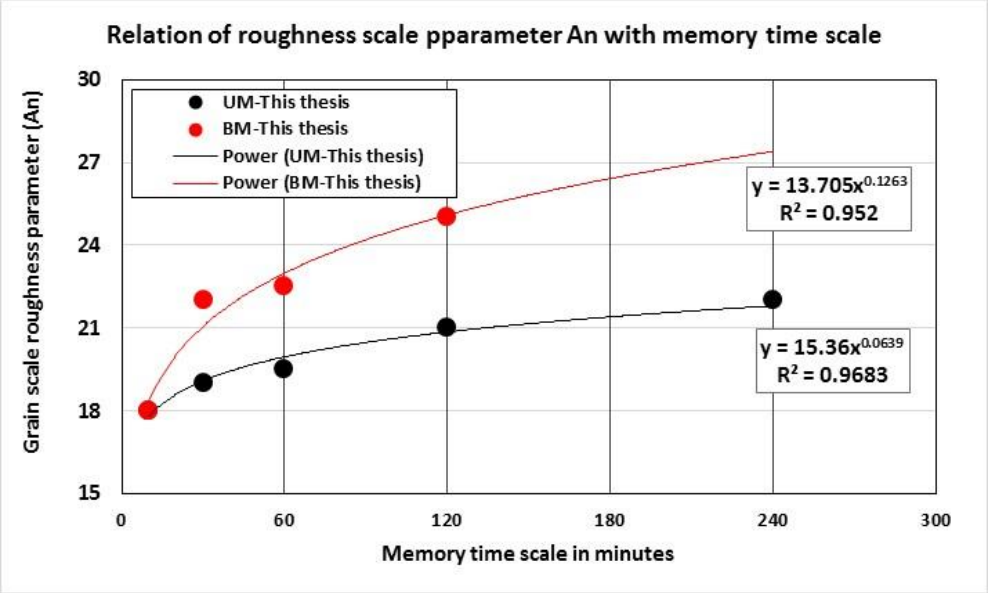

Figure 6.2: Range of A_n values from bedload prediction of unimodal and bimodal memory bed.

6.3.5 Testing the roughness scale frame work against field data of memory stress

Whilst Sections 6.3.3 and 6.3.4 have clearly demonstrated the viability of use of an A_n modified Wu et al. (2000a) bedload equation for incorporation of memory effects into laboratory-based data sets, there is merit in testing the viability of this approach in more complex field scenarios. Although long term bedload data appropriate to memory based analysis are rare, the Turkey Brook data (Reid and Frostick, 1986) of nine flood events (Chapter 2; Table 2.1) appears appropriate for trials. The data clearly show a relationship between memory and entrainment threshold being delayed to higher shear stress. Thus, this Section is

dedicated to testing the A_n based memory correction of Wu et al. (2000a) for predicting bedload in Turkey Brook. This compares and contrasts the measured bedload with the Wu's model predictions "with" and "without" A_n based memory correction.

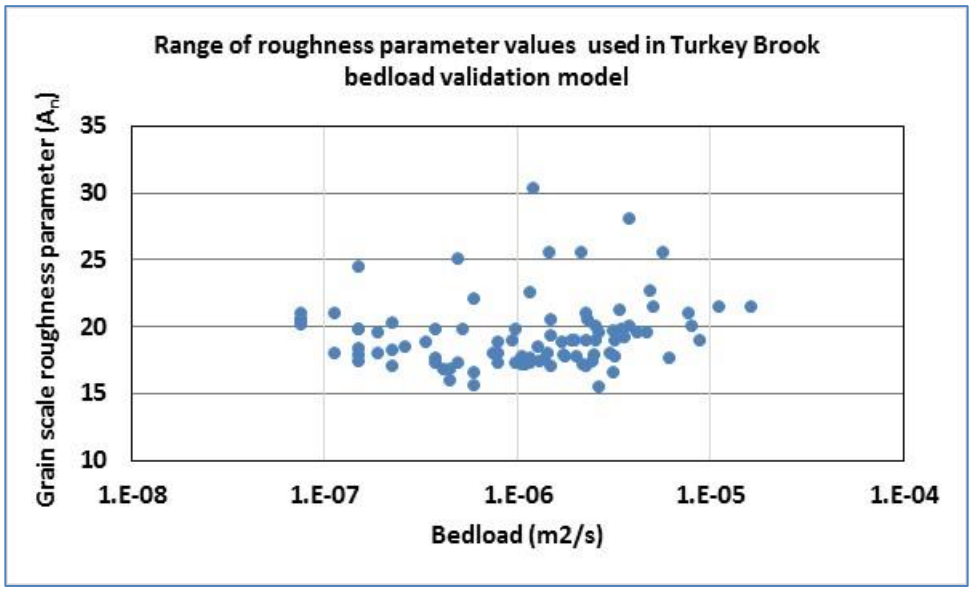

Figure 6.3: Range of grain scale roughness parameter value (A_n) used in Turkey Brook obtained by calibration of observed bedload in Wu et al. (2000a) model.

The distribution of calibrated A_n values required for the modelling of Turkey Brook transport regime reflects transport condition of both memoried and non-memoried bed (see Figure 6.3). For a satisfactory EF range, calibrated A_n values range were found approximately between 15.5 and 30. The lower values are representative of condition of transports where either the is memory erased away or for flood events of non-memoried bed (See Table 2.1 in chapter 2; and Appendix C for each flood event). The lower A_n values range between 15.5 and 20, which are very similar to the condition of non-memoried bed of laboratory data calibration and validation (Section 6.3.4). The higher A_n values representing memory condition range between 20 and 30. For higher memory in bed (representative of stronger bed packing and higher bed stability), the A_n values were categorically high, upto 30 as already mentioned above (all data in Appendix C); the relation of A_n on memory time scale is simplified with a linear relation in Figure 6.4. The sensitive transition of memoried bed is the gradual

erasing of memory and converging of transport condition towards non-memoried bed; then the A_n values slided towards non-memoried values, similar to the three memory stress laboratory data set; this sliding of the A_n values is more clearly clarified for two flood events, see Section 6.4; this adaptation time scale from memory to non-memory is further discussed in next section (Section 6.4).

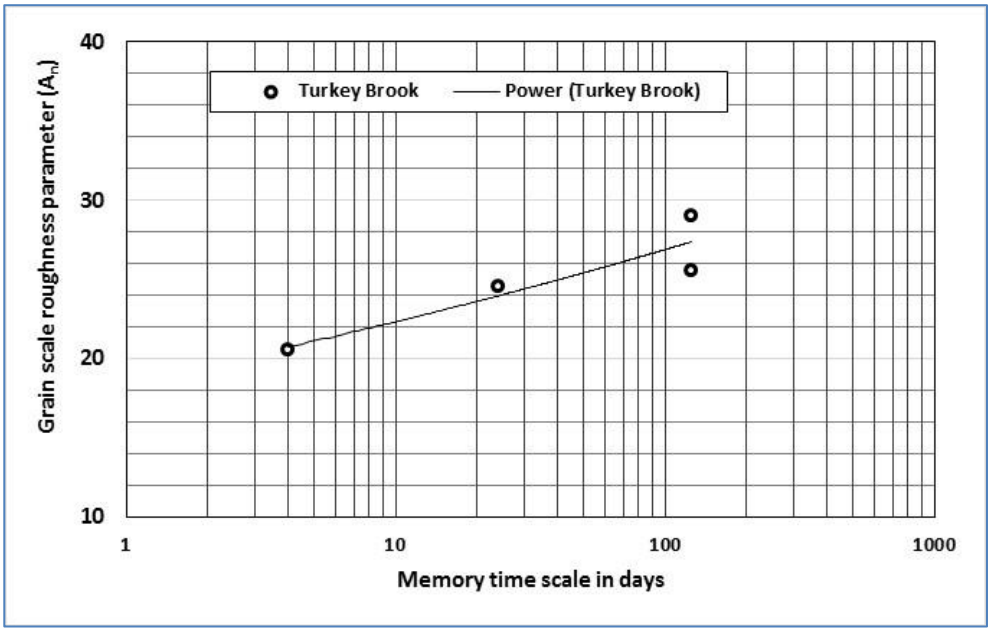

Figure 6.4: Turkey Brook dataset: roughness parameter A_n obtained for three flood events which experienced higher memory stress in bed; shown above relative to a less memory (or non-memoried) flood event, whose A_n value is around 20, similar to laboratory based research.

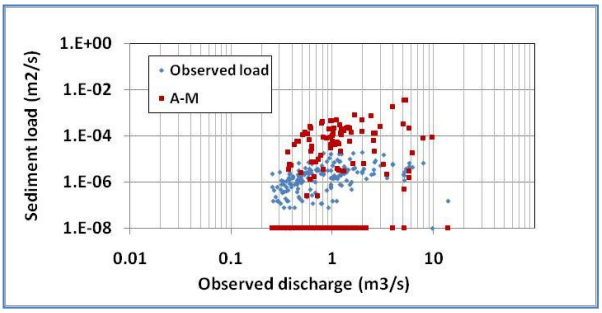

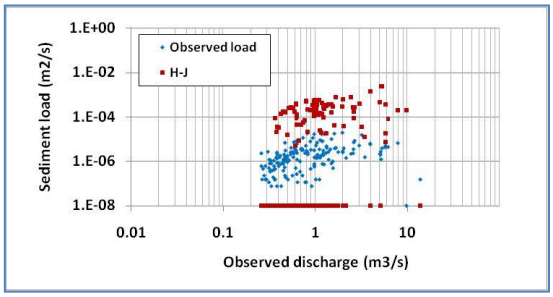

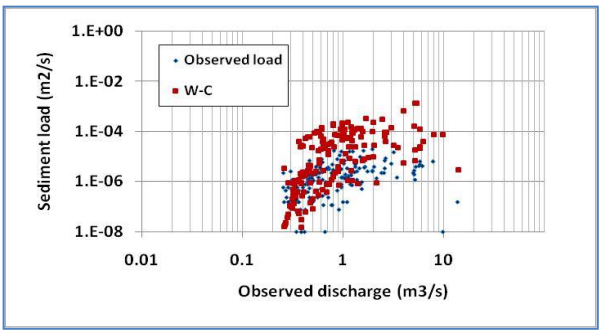

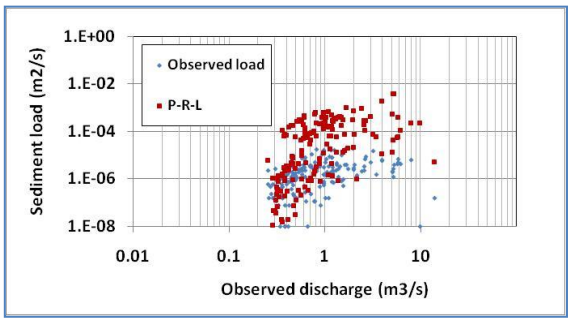

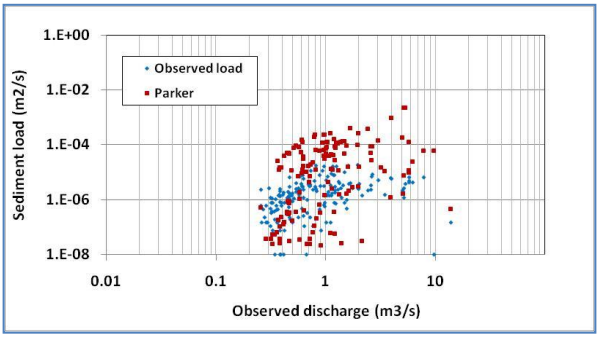

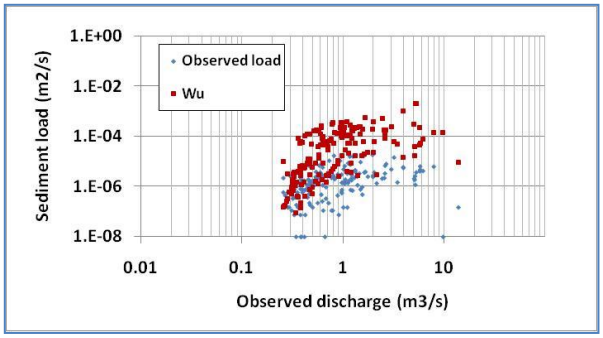

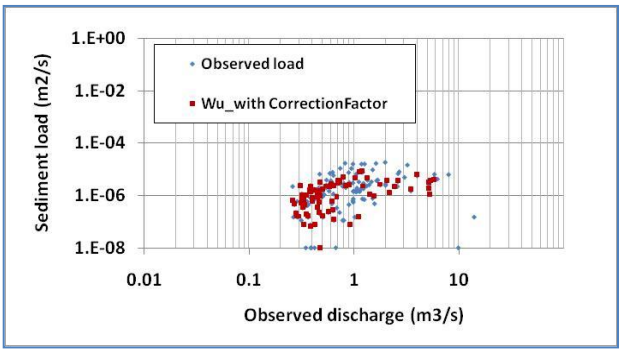

Figure 6.5: Predicted bedload transports in functions of graded sediment in "with" and "without" memory stress condition.

However, whereas the choice of appropriate model for application to low flows specific to the laboratory based data of Section 6.3.1 was limited to Wu et al. (2000a), the higher and more varied flows of Turkey Brook remove such constraint of model selection. As such, Wu's model (with and without A_n based memory correction) is also compared with other widely used non-memoried graded functions appropriate to the flow and sediment characteristics of Turkey Brook including: Ashida and Michiue (1972), Parker (1990a), Powell et al. (2001, 2003), Hunziker-Jaeggi (2002) and Wilcock-Crowe (2003). For each sediment transport formula, default parameter values (such as threshold shear stress, hiding function exponent, calibration parameter if there is any) were used without any change in the prediction; which is referred in Column 1 row 2 of Table 6.8 as "Graded sediment: original functions"; the objective was to demonstrate the predictive performance of these transport formulae for Turkey Brook. As it is known that Turkey Brook was affected by memory stress, then memory correction was imposed applying A_n which is different than the value Wu et al. (2000a) recommended for general application in his original formula; here the calibrated A_n values were obtained to match the EF range between 0.5 and 2.0. The summary of predicted bedload and their comparison against observed Turkey Brook data is presented in Figure 6.5 and analysed using the EF approach in Table 6.8.

Based on Figure 6.5, Wilcock-Crowe (2003), Parker (1990a), Powell et al. (2003) and Wu et al. (2000a) all suggest general similarity of bedload prediction. However, this prediction unequivocally improves visually for the A_n based memory correction approach of Wu; there is a fundamental difference between this memory correction with practices of calibration in research and industries for controlling over or under prediction; in the present thesis, it was emphasised (in Section 6.4) that once the memory stress erases, the A_n needs to adapted to normal transporting condition. Whereas in usual practice in industries, it often controlled by calibration parameter, such as roughness factor, and the parameter remains same even when the memory effect (or other unknown control) has disappeared (Barry et al., 2008; Muller et al., 2008 and Nitsche et al., 2011).

Quantifying this improvement using the EF data in Table 6.8 shows Wu's memory corrected function is able to predict 100% of the predicted data points with the

range of accepted EF. This is a clear advantage over the non-corrected formulae of Wu et al. (2000a) and other alternative models where only 2-18% of data fitted Turkey Brook's measured load. As such, the benefit of memory inclusion using an A_n based correction is demonstrated as a reasonable avenue for future research for both laboratory and field approaches.

Table 6.8: Efficiency Factor (EF) comparison of predicted bedload in functions of graded sediment with a correction factor for "with" and "without" memory stress condition

Sediment type	Functions	Total data number	Efficiency Factor (EE) range (Predicted /Observed load) : number of datasets in %			
			0> – 0.5	0.5 – 2.0	2.0 – 20	>20
Graded sediment: original functions	Parker	166	36	15	20	25
	A-M (Ashida and Michiue)	83	6	3	13	26
	W-C (Wilcock and Crowe)	166	13	18	38	27
	P-R-L (Powel et al.)	166	15	12	30	40
	H-J (Hunziker and Jaeggi)	81	0	2	11	33
	Wu (Wu et al.)	166	4	12	40	41
Graded sediment: with memory	Wu – with correction factor for memory stress	166	0	100	0	0

6.4 Discussion on predicted bedload

It is very clear from the evidence provided in this Chapter that none of the existing graded sediment formula, with the standard/recommended range of calibration parameters principally applicable for non-memoried bed, predict bedload adequately for memoried beds (Figure 6.5). Specifically, they suffer bedload over-prediction systematically for high discharges, yet individual equations show different sensitivity in bedload estimates for low flows. From the data provided, and rationale given in Section 6.1, development of Wu's equation for incorporation of memory effects does appear valid. Section 6.3 therefore appropriately concludes that memory effects can be incorporated via the roughness parameter A_n; this provides appropriate resolution to differentiate the responses to memory of both grade and time (as employed in the present thesis).

Detailed examination of the data from the present thesis and wider memory research of Haynes and Pender (2007), Ockelford (2011) and Turkey Brook field data (Reid and Frostick, 1986) strongly indicate smaller A_n values, typically of value range 16-18, for non-memoried beds in the laboratory, and up to 20 for the field data reported. This is supported by wider literature (Section 6.2) pertaining to loose beds; this reflects a lack of water-working of the structure, either due to laboratory set-up of artificial beds or where floods occur in quick succession to preclude 'recovery' of the bed to a more stable arrangement/structure. Conversely, for memoried bed, evaluated data suggest a range of A_n values generally between 19 and 25 in laboratory-based runs, and up to 30 for field data. There is a direct positive correlation between A_n values and memory timeframe; this appears to be a strong correlation of near-linear (field; Figure 6.5) or power relationship (laboratory; Figure 6.2). As such, there appears scope for using this type of relationship, i.e. where memory timeframe is known, to estimate the A_n values to be used in memory-corrected bedload equations. This is an important finding and, whilst the objectives of this thesis have been met, certainly warrants attention and review by future research.

The use of the A_n value approach to memory correction is clearly grade specific. In summary, the bimodal bed in the present thesis, and that of Haynes and Pender (2007), exhibits a stronger response of A_n values to increased memory duration, culminating in higher A_n values for a given memory duration. For the bimodal bed, the value range is 18-25 with increasing memory to 240 minutes in the present thesis, whilst only 18-23 for the equivalent unimodal beds. Because this scaling of the granular scale roughness by A_n offers varying magnitude of roughness, but from the bed of same sediment distribution, and thus, this supports the use of A_n values as reflective of bed restructuring to a more stable arrangement with higher resistance to entrainment, with a stronger bimodal process response (Chapter 5). Although the value range is very close in two beds, the subtle distinction is important as there is high sensitivity of the prediction of bedload to small changes in A_n (Section 6.3.4). As such, the sensitivity to A_n becomes an important point for extended discussion of its intended use, and forms the focus of the remainder of this discussion.

The sensitivity and applicability of an A_n correction approach to memory effects on bedload are worthy of discussion, particularly for two reasons: i) the sensitivity of bedload estimates to initial A_n value selection as specific to known inter-flood/antecedent memory duration, and ii) the progressive removal of memory effects, and hence related reduction of A_n, during a flood / transporting event. Whilst an introduction to the former problem is noted in Section 6.3.4, for clarity of discussion both issues have been discussed herein with reference to two flood events of the Turkey Brook data set.

Firstly, Table 6.8 has indicated the importance of correcting (increasing) the A_n value to account for memory effects. Also, calibrated A_n values in Table 6.5 and Table 6.6 indicate a method for calibration and selection of A_n values based on memory duration for the correction of bedload estimates. However, both failure to undertake the correction, or erroneous selection of the A_n value (even by a value of ±1) has important bearing on the total load. Consider the hydrograph as shown in Figure 6.7, this hydrograph had memory stress of 125 days in the bed (see Table 2.1 in Chapter 2) and had a duration of approximately 7 hours. According to the measured bedload, the total mass of sediment during this flood event is 945kg (Reid and Frostick, 1986) under this hydrograph. The implication of model prediction relative to this hydrograph is discussed below. Based on the analysis performed in this thesis, an A_n value of 25 can be correctly applied to Wu's memory modified approach to correct the bedload to that observed. Had the memory correction not been applied, and a lower value such as A_n = 20 used, then bedload would be dramatically over predicted, such that memory-related enhanced bed resistance would be ignored and bedload estimates would be 20 fold higher than that observed. Also, incorrect selection of the A_n value (Figure 6.6) would lead to notable errors of many tonnes. Where modelling is used for river engineering or management practices, such sensitivity may mean a significant difference to river siltation and erosion and thus may multiply uncertainties in flood risk assessment, planning and design of sediment and flow control structures.

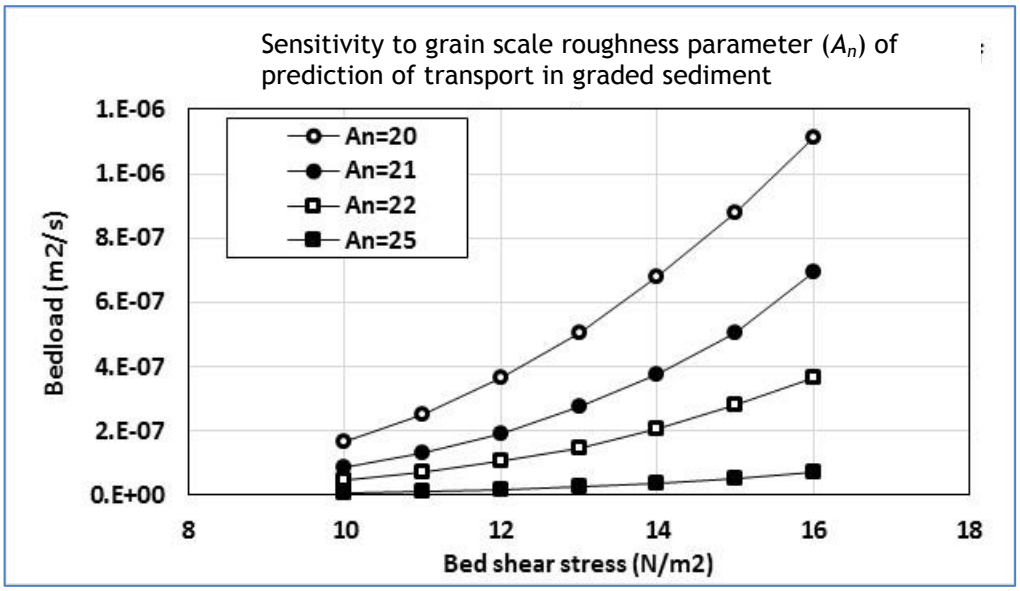

Figure 6.6: Sensitivity to grain scale roughness parameter (An) of prediction of transports in graded sediment bed is quantified here.

Secondly, the other implication is that during higher flow events sediment transport will increase and the memory of the bed will be progressively erased during the high flow event. In such an unsteady flow, the A_n values would therefore gradually reduce until the bed converges to a general transport condition where A_n values tend to those of a non-memoried condition. The memory erasing effect and timescale is shown in Figures 6.7-8 for two flood events of Turkey Brook; calibration of the A_n values has been undertaken against measured bedload (Reid and Frostick, 1986). As both flood events shown in Figure 6.8 experienced memory stress, the initial A_n values are 25 and 30. Over the flood duration, these values gradually reduce towards the values of non-memoried bed of A_n values of 18-20. In both flood events (Figure 6.8), the erasing time scale is about 2-3 hours to reach a value of A_n = 20. However, a period of 4 hours is required for the beds to reach a constant A_n value. The sliding scale of A_n over this early period of a flood event is important to bedload estimates, as erroneous use of the initial value of e.g., A_n = 25 (10th December 1978 event; Figure 6.7) as a constant over this 4 hour timeframe would have led to a total load many times higher than that measured; on average ~15 times higher than the observed data. This issue raises a further research question, as

to whether this 4 hour timeframe of memory erasing is fixed (and hence predictable). This appears unlikely, as the antecedent memory period between floods will vary and produce memory effects greater or less in the beds created. This is supported, to some degree, by comparison of Turkey Brook data with the laboratory data collected within this thesis; whilst the field data indicates 4 hours for memory erasing, the laboratory data was 40-55 minutes (Chapter 4 and 5). This is intuitive, in that the applied antecedent memory duration in the laboratory was only a few hours, whereas the field study had memory durations of weeks/months to produce a more resistant bed which took longer to break up. It would also be logical in explanation that, as memory effects stem from particle rearrangement / structure, the field beds were of wider grade and stronger bimodality; this would likely lead to Turkey Brook having longer timeframes for the erasing of memory (due to larger grains being present, which

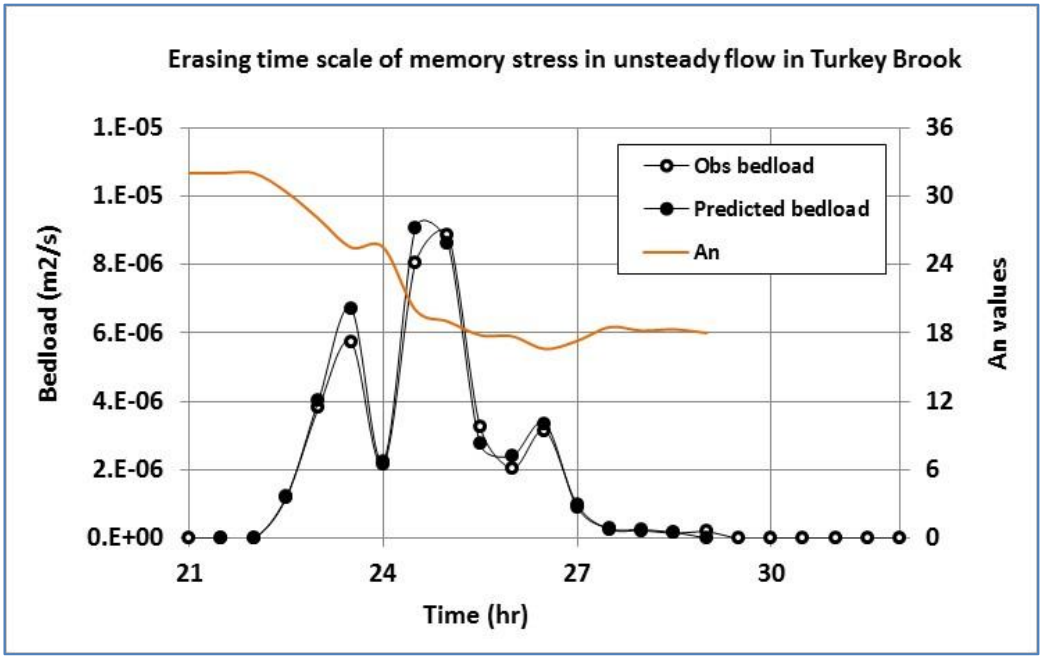

Figure 6.7: Time scale of erasing of memory stress: A_n values shown gradually adapting from memory condition towards non-memory condition (from Turkey Brook bedload validation model).

would require higher shear stresses for entrainment during the hydrograph rising limb). As such, the issue of memory erasing does appear to have mileage, in its

own right, regarding the sliding scale of A_n values to be applied during a flood or high flow event.

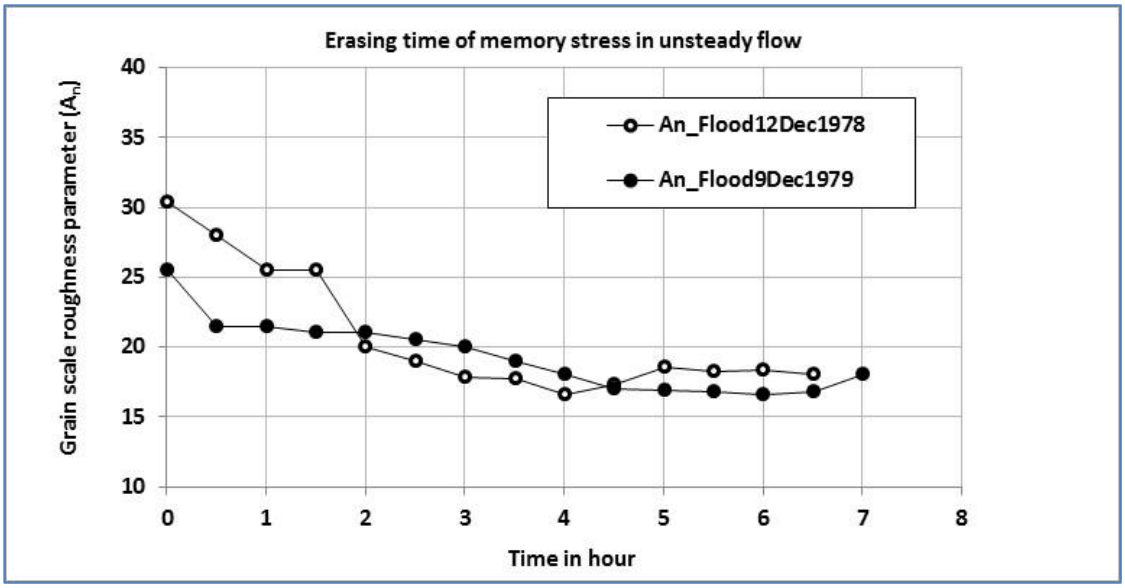

Figure 6.8: Time scale of erasing of memory stress: shown with gradual adaptation of grain scale roughness (A_n) from memory condition towards non-memory condition (from two flood events with higher memory stress in Turkey Brook bedload validation model).

6.5 Key outcomes

This Chapter has presented the first mathematical framework for accounting for memory effects on graded sediment transport. Based on Wu et al. (2000a) graded sediment transport formula (as appropriate to the low flow experiments of the present thesis), two novel approaches to its modification for memory were assessed. Firstly, a modified hiding function (m); secondly, a roughness length scaling (A_n). These approaches were tested against the flume data of Chapters 4 and 5, and the pros and cons of both approaches have been discussed at length. Preference towards the A_n based correction method has been justified and trialled in more detail against the wider memory data sets of Reid and Frostick (1986), Haynes and Pender (2007) and Ockelford (2011). Whilst the novelty of this Chapter's research dictates that it should be considered a "first approach", it clearly shows strong rationale in memory correction and provides

an appropriate methodology and framework for testing, calibration and validation.

Key outcomes from the above mathematically modelling are presented below:

- Use of a hiding function scaling for memory correction (m) appears limited in sensitivity to memory timeframe and grade effects. As such, the roughness length scaling (A_n) is advocated. This directly scales the total available shear stress (Eq. 6.5) and is sensitive to both memory timeframe and grade. Predicted bedload by scaling with the A_n values matches quite well with measured bedload; otherwise the prediction, e.g., for 120 minutes memory time scale, would have been 8 times higher than the observed load. More encouraging is that A_n values calibrated against several memory time scales of the laboratory data set of this thesis satisfactorily validated two other laboratory data set.

- Non-memoried beds appear adequately represented by A_n values of 18-20, in line with wider literature specific to loosely packed beds. As memory duration increases, the A_n value rises, representing an increase in packing density, imbrication and bed structure, and indicate a smoother compact bed with less roughness (lower value of n'). This does indicate the grain scale friction in planar bed is not solely dependent on the grain size, it is also dependent on the structure of the bed. Flume and field based evaluation of the range of A_n to be used for memory correction suggest up to a value of A_n = 30 may be appropriate.

- Caution is noted regarding the strong sensitivity of estimated bedload to the choice of A_n employed in Wu's equation. Failure to use a memory correction, or inappropriate use of A_n value may mean more than 20 fold variation of predicted load with measurement.

- During a high flow, sediment transporting event, it is essential that the A_n value is modified as appropriate to recognising the erasing of memory from the bed surface. Analysis of field and laboratory data indicates that this may take between 1-4 hours, depending on the type of bed and the antecedent memory timeframe.

Chapter 7: Conclusion and recommendation

7.1 Summary of key outcomes

This research thesis has distinctly quantified the effect of "memory stress" on sediment entrainment/transport in low flows. A large, flume-derived and novel time series of data on bed shear stress, total load and fraction load has been presented and analysed using a reference-transport based methodology, so as to quantify memory stress effects from 0-240 minute durations in unimodal and bimodal beds. Output data clearly illustrate that increased durations of applied memory stress increase the stability of the bed. This both delays the entrainment of sediment to higher shear stresses (up to 47%) and reduces the volume of subsequent sediment transport (up to 97%). Novel mathematical relations for predicting bedload after a range of memory stress durations have been determined and used to derive a correction factor as appropriate for use in existing graded sediment formulae. Key conclusions are provided below:

- A reference-based transport approach, employing a stepped discharge hydrograph, i.e. covering a range of shear stresses around the entrainment threshold (2.00-3.90 N/m^2) has been developed and employed specific to advancing memory stress research. This approach has been robustly defended against poorer alternative methodologies in the literature, and is proven essential to the development of the mathematical memory stress correction framework for use in existing sediment transport equations.

- Using Shvidchenko's (2000) reference based approach, the critical bed shear stress of entrainment threshold increases by up to 47% in bimodal beds, after 120 minutes of applied memory. However, the non-linear relationship between bed shear stress and bedload transport, yields greater sensitivity of bedload response to memory stress. Hence, the transported sediment volume decreases by up to 97% for the same applied memory stress timeframe. This order of magnitude response is generally supportive of earlier memory stress research and clearly shows memory stress control and significance over sediment transport processes.

- A size selective response of fractions to memory stress is shown, with end fractions most affected. For example, reduced mobility of the finer fractions was up to 95% in unimodal and 98% in bimodal bed, whilst the coarsest fractions stabilised by up to 40% (unimodal) and 90% (bimodal). This is in agreement with the detailed bed structure work of Ockelford and Haynes (2013) and indicates that memory stress increases the selectivity of transport in a graded bed.

- Memory stress effects are greatest at shear stresses close to the entrainment threshold (Shields number ~ 0.03 in this study). As the shear stress applied and associated transport increases, the influence of memory stress over bedload transport reduces. The effect of memory stress becomes insignificant at Shields number 0.05--0.06 where the transporting ability converges for memory and non-memoried beds. However, as the data show memoried beds to have lower cumulative transported loads (than non-memoried beds), memory effects do not have a legacy and are not 'erased' by over-compensation of subsequent bedload at higher shear stresses; this strengthens the case for long-term influence of memory on transported loads.

- The relationship between applied memory stress duration and delayed entrainment / reduced transport is non-linear. Short duration memory time scales were found more responsive, due to the loose packing structure permitting active rearrangement. At longer memory timescales, the rate of change gradually slows due to development of a stronger packing arrangement with less flexibility for continued restructuring. Memory influence in low transport regimes was found prevalent for $1x10^{-6} < q^* < 1x10^{-1}$). Review of the flume data generated herein does, however, indicate that use of the Shields entrainment threshold and reference transport approach ($q^* = 10^{-2}$, *and* $\tau_C^* = 0.06$), which is most commonly applied for assessment of bedload transport, is too high a value and inappropriate for capturing the smaller q^* values specific to the longer timeframe memory results. Therefore, for assessing memory effect on bedload transport, the reference transport of Shvidchenko et al. (2001,

q^* = 10^{-4}) and Parker et al. (1982a, q^* = 10^{-5}) appear more appropriate threshold conditions.

- Bed shear stress and bedload have been non-dimensionalised to form a generic bedload transport relation as the power function $q^* = C\,(\tau^*)^b$. Non-memoried beds yield exponent values equivalent to those available in the present day literature and practice; i.e., 12 < *b* > 16.2 (e.g., Paintal, 1971; Parker, 1990a). However, memoried beds indicate that both the exponent *"b"* and the coefficient *"C"* show sensitivity to memory timescale. The exponent (which is dependent on applied time average shear stress) increases with applied memory duration, rising from *b* = 16.2 to 21.5 for unimodal beds, and *b* = 12.0 to 25.5 for bimodal beds. Whilst the exponent increased due to memory stress by a factor of up to ~2, the coefficient (which parameterises the effect of structural changes on the bed) showed much higher sensitivity to memory timescales, increasing by nineteen orders of magnitude (10^{19}). This appears to be the first time that a set of non-dimensional bedload and shear stress equations have been analysed for relevance to memory.

- Correction factors have been proposed to include the effect of memory stress in Wu's graded sediment formula (Wu et al., 2000a) for improving the prediction of sediment transport; selection of this recent and widely accepted/adopted formula in current sediment transport research was specific to collaboration with the original authors and essential access to raw data. Two approaches have been developed and tested as appropriate to a memory-modified Wu's formula: i) by scaling the general power form of the hiding function, *m*, and ii) by scaling the roughness coefficient term, A_n, able to mirror the bed's structural development at the grain scale. Predicted data are calibrated and validated against present and past memory stress bedload datasets. Results show that it is almost impossible to make a useful prediction unless a memory correction is employed. Without memory correction, transport is severely over predicted in both of the above frameworks. However, with the use of memory correction approaches 100% of predicted results fall within the

accepted EF tolerance. Scaling of the roughness parameter (A_n) was found the more efficient method of accounting for memory correction. Here, the non-memoried bed yields A_n values between 17 and 19, while memoried beds increase this up to 30; the longer the memory time scale, the higher is the value of this parameter.

- The results of the memory study are consistent with over prediction of bedload transport by past researchers. Incorporation of memory is a possible means of correcting bedload transport calculations.

7.2 Recommendations

Given the applicability of the memory stress issue to all mobile-bed channels subjected to variable flow, future physical and mathematical modelling studies demand more variability and universality than could be tested in the present thesis. As such, the following future research priorities are identified from the key outcomes of the present thesis:

1. More detailed analysis of the significance of memory stress to hiding functions. All hiding functions are developed using relative size (D_i/D_{50}) effect; this is a crucial factor in representing and interpreting grain-scale structure, packing and tendency towards a particular transport mode (equal mobility versus selective transport). The regression of the available power functions (Chapter 2) showed wide range of exponent values from 0.33 to 1.0. However, mathematical modelling in Chapter 6 has clearly demonstrated that the effect of memory stress is implicit to the value of this hiding function. This brings significant difference to predictions of total load, particularly for the end fractions, and also brings universality of application of the function. As such, review of existing research for hiding function relationship to memory may help explain the range of values found in the literature. Similarly, future research is recommended (laboratory and field) to establish conclusively variability in the hiding function with temporal scaling.

2. Expanding research to validate the proposed bedload formula of memory stress. The empirical relations for unimodal and bimodal bed (Chapter 4 and 5) proposed in the present thesis are based on one experimental set-up (i.e. a

single bed slope, restricted grain size range, and a limited range of flows). Although the relation was transformed to a generic form by using non-dimensional parameters of bedload and shear stress, it is recommended to validate the relation via experiments encompassing a broader suite of set-up variables. In defence of this suggestion, the slope in natural gravel bed rivers varies by several order of magnitudes; e.g., Clearwater River of Idaho has a slope of 0.00048 (Emmett, 1976) yet Great Eggleshope of England has a slope of 0.01 (Carling and Reader, 1982). More-over, the proposed formula is for total bedload; given that the memory response is extremely sensitive to the end fractions, it might be challenging to expand the formula for each size fraction, but worth analysis via future research.

3. Effect of memory stress on transports in unsteady flow. Existing knowledge on memory stress is largely derived from steady-constant discharge (Haynes and Pender 2007) and quasi-steady constant stepped discharge (Peidra 2010; Ockelford, 2011 and present thesis), whereas natural flow is unsteady. Even magnitude variation in baseflow is sufficient to cause fluctuating turbulent intensity, hence such unsteadiness within the memory period itself will lead to sensitivity of packing density (Papanicolaou et al., 2002). Therefore, memory stress research should be expanded to unsteady flow conditions in a manner similar to that explored most recently by Mao (2012).

4. Climate change scenarios and associated modelling should be considered appropriate to choices and selection of memory timescales tested/modelled. In the UKCIP climate change scenarios, the summer will increasingly become drier whilst winter will become wetter. This will affect the baseflow and the duration between flood events in UK perennial rivers, which are considered the main drivers of memory stress development. Hence, this hydrological change may increase the stability of summer beds, delaying and reducing bedload transport rates; the opposite will be true for winter beds. If such memory forecasting can be embedded within sediment transport modelling, then sediment-related risk predictions (e.g., flood and erosion risk management) may become more robust and more widely employed.

5. The memory effect and initial motion data requires evaluation at higher Reynolds Numbers. Initial motion data at high Reynolds number (R_{e^*}) in rough turbulent flow are still scarce (Chapter 2); existing laboratory research on memory stress was carried out for similar gravel size range as that used in the present thesis; i.e. R_{e^*} values between 100 and 300. However, the field data set of Reid and Frostick (1986) is in the range of Re_* between 1400 and 4000. Whilst difficult to produce in some flume set-ups, the rarity of datasets specific to higher Reynolds numbers will strengthen the knowledgebase of memory effects, incipient motion and generally improve sediment transport prediction.

6. Memory stress correction with a focus on further validation for a wider range of formulae is required. Herein, the focus has been placed upon Wu's (Wu et al., 2000a) formulae. Although robust rationale is provided specific to this thesis, it is acknowledged that a range of formulae should be tested for both the proposed memory modification approach and further development of this framework.

Appendices

Appendix A: Unimodal sediment bed experimental programme in baseline and memory stress

Table A.1: List of unimodal bed experiments

Sediment bed:	Unimodal					
Median size (D_{50}), mm	4.8					
Size classes (D_i), mm	1.2	1.7 9.5	2.4 13.4	3.3	4.7	6.7
Fractional proportions (F_i)	0.025	0.05 0.1	0.075 0.05	0.15	0.4	0.15
Sorting parameter (σ_g)	1.65					
Flume length, working section (m)	7.0					
Flume width (m)	0.3					
Flume slope	0.005					
Sediment slot width (m)	0.15					

Experiment type	Exp. No.	Bedding in time (min)	Memory stress time scale (min)	Stability period (min)
Pump flow calibration and uniform flow set-up	1	3	-	-
	2	3	-	-
	3	3	-	-
	4	3	-	-
Pump flow and uniform flow verification, and primary runs for calculating baseline threshold motion to determine memory stress flow magnitude	5	3	-	-
	6	3	-	-
	7	3	-	-
	8	3	-	-
	9	3	-	-
Baseline experiment	10	3	0	64
	14	3	0	64
	15	3	0	64
	21	3	0	64
	24	3	0	64
	27	3	0	64
	32	3	0	64
	45	3	0	64
Memory experiment: 10 min. time scale	13	3	10	64
	30	3	10	64
	31	3	10	64
Memory experiment: 30 min. time scale	11	3	30	64
	17	3	30	64
	20	3	30	64
Memory experiment: 60 min. time scale	16	3	60	64
	19	3	60	64
	44	3	60	64
Memory experiment: 120 min. time scale	18	3	120	64
	22	3	120	64
	23	3	120	64
	43	3	120	64
Memory experiment: 240 min. time scale	26	3	240	64
	28	3	240	64
	29	3	240	64
	42	3	240	64

Appendix B: Bimodal sediment bed experimental programme in baseline and memory stress

Table B.1: List of bimodal bed experiments

Sediment bed:	Bimodal					
Median size (D_{50}), mm	4.8					
Size classes (D_i), mm	1.2	1.7 9.5	2.4 13.4	3.3	4.7	6.7
Fractional proportions (F_i)	0.05	0.1 0.1	0.2 0.04	0.12	0.08	0.31
Sorting parameter (σ_g)	1.93					
Flume length, working section (m)	7.0					
Flume width (m)	0.3					
Flume slope	0.005					
Sediment slot width (m)	0.15					
Experiment type	Exp. No.		Bedding in time (min)	Memory stress time scale (min)	Stability period (min)	
Pump flow calibration and uniform flow set-up	45		3	-	-	
	46		3	-	-	
	47		3	-	-	
	48		3	-	-	
Pump flow and uniform flow verification, and primary runs for calculating baseline threshold motion to determine memory stress flow magnitude	49		3	-	-	
	50		3	-	-	
	51		3	-	-	
	52		3	-	-	
Baseline experiment	53		3	0	64	
	54		3	0	64	
	57		3	0	64	
	66		3	0	64	
	69		3	0	64	
	73		3	0	64	
Memory experiment: 10 min. time scale	58		3	10	64	
	68		3	10	64	
	81		3	10	64	
	82		3	10		
Memory experiment: 30 min. time scale	56		3	30	64	
	59		3	30	64	
	71		3	30	64	
	72		3	30	64	
	79		3	30	64	
Memory experiment: 60 min. time scale	60		3	60	64	
	67		3	60	64	
	75		3	60	64	
	80		3	60	64	
	83		3	60	64	
Memory experiment: 120 min. time scale	74		3	120	64	
	76		3	120	64	
	82		3	120	64	
	77		3	120	64	
Memory experiment: 240 min. time scale	78		3	240	64	
	84		3	240	64	
	85		3	240	64	

Appendix C: Prediction of bed load for memory affected transports: calculation sheets

Turkey Brook parameters and prediction sheet

Parameter definitions for Kazi Hassan

1) Professor Gary Parker was helping in the computation in person in his office in Illinois
2) Professor Weiming Wu was helping in his Office in Mississippi for calculation with his formula

Calculation sheet for Ashida and Michiue (1972), Powell et al. (2003), Hanziker and Jaggei (2002), Wilcock and Crowe (2003) are presented below.

Parker's formula – his developed program was used, and available in Parker (1990b);

Table C.1: Turkey Brook grain statistics							
Ds50	surface median size				D50	substrate median size	
Dsm	surface arithmetic mean size				Dm	substrate arithmetic mean size	
Dsg	surface geometric mean size				Dg	substrate geometric mean size	
sigs	surface geometric standard deviation				sigsub	substrate geometric mean standard deviation	
You will find surface statistics for surface material with sand removed as well							
	Raw Grain Size Distribution Surface						
psi	Size mm		% Finer	Fraction in surf	For computing statistics		
	256		100				

7.5		181.02		0.0000	0.0000	0.0000	0.0000
	128		100				
6.5		90.51		0.0420	3.8014	0.2730	0.2206
	64		95.8				
5.5		45.25		0.2320	10.4991	1.2760	0.3873
	32		72.6				
4.5		22.63		0.4100	9.2772	1.8450	0.0350
	16		31.6				
3.5		11.31		0.1840	2.0817	0.6440	0.0922
	8		13.2				
2.5		5.66		0.0570	0.3224	0.1425	0.1663
	4		7.5				
1.5		2.83		0.0240	0.0679	0.0360	0.1760
	2		5.1				
0.5		1.41		0.0170	0.0240	0.0085	0.2337
	1		3.4				
-0.5		0.71		0.0340	0.0240	-0.0170	0.7536
	0.5		0				
-1.5		0.35		0.0000	0.0000	0.0000	0.0000
	0.25		0				
							2.0647
				1.0000		4.2080	1.4369
	Ds50		21.84		Dsg mm	18.481	
	Dsm	26.0979				sigs	2.707
	Fr sand	0.051					
	Fr gravel	0.949					

Table C.2: Turkey Brook grain statistics					
	Raw GSD Substrate		For computing statistics		
	% Finer	fi			
	100.000				
		0.000	0.000	0.000	0.000
	100.000				
		0.000	0.000	0.000	0.000
	100.000				
		0.122	5.521	0.671	0.475
	87.800				
		0.377	8.531	1.697	0.357
	50.100				
		0.238	2.693	0.833	0.000
	26.300				
		0.105	0.594	0.263	0.111
	15.800				
		0.054	0.153	0.081	0.222
	10.400				
		0.035	0.049	0.017	0.318
	6.933				
		0.069	0.049	-0.035	1.124
	0.000				
		0.000	0.000	0.000	
	0.000				

					2.607
		1.000		3.527	1.615
median, geom mean	D50	15.953	Dg	11.525	
arith mean	Dm	17.589		sigsub	3.062
fraction sand	Fr Sand	0.104			
Substrate statistics					

Table C.3: Turkey Brook Grain Size Distribution Surface Gravel Only

psi	Size mm		% Finer	Fi		
	256		100.00			
7.5		181.02		0.000	0	0
	128		100.00			
6.5		90.51		0.044	0.199399	0.187245
	64		95.57			
5.5		45.25		0.244	0.931987	0.273081
	32		71.13			
4.5		22.63		0.432	1.347583	0.001399
	16		27.92			
3.5		11.31		0.194	0.470376	0.172451
	8		8.54			
2.5		5.66		0.060	0.104082	0.226777
	4		2.53			
1.5		2.83		0.025	0.026294	0.219056
	2		0.00			

					3.079721	1.080008
		geom mean		Dsg	21.75233	1.039234
		geom std dev		sigg	2.055136	
		median		Ds50	22.80022	
		Surface statistics without sand				

Table C.4: Turkey Brook GSD			
Size mm	Surface	Surface Gravel	
256	100	100	
128	100	100	
64	95.8	95.57428872	
32	72.6	71.12750263	
16	31.6	27.92413066	
8	13.2	8.535300316	
4	7.5	2.528977871	
2	5.1	0	
1	3.4		
0.5	0		
0.25	0		

Table C.5: Definitions of key parameters in graded sediment transport formula						
Assume		R	1.65	Submerged specific gravity of sediment		
qi	gravel bedload transport rate, ith grain size range, m^2/s					
pGi	fraction of gravel bedload in the ith grain size range					
qG	gravel transport rate summed over all grain sizes, m^2/s					
DGg	geometric mean size of gravel					
ustar	shear velocity m/s					

Table C.6: Ashida-Michiue uses full surface grain size distribution, surface arithmetic mean size Dsm

	Dsm	26.0978971	mm			ustar	0.140648407	m/s		
	tsscm	0.05	critical Shields number							
	Di	Di/Dsm	taussi	tausci	qstari	Fi	qi	pGi		
7.5	181.019336	6.9361656	0.006751	0.018193826	0	0	0	0	0	0
6.5	90.50966799	3.4680828	0.013503	0.024714583	0	0.042	0	0	0	0
5.5	45.254834	1.7340414	0.027005	0.035490096	0	0.232	0	0	0	0
4.5	22.627417	0.8670207	0.054011	0.055222674	0	0.41	0	0	0	0
3.5	11.3137085	0.43351035	0.108022	0.09749604	0.002938763	0.184	2.61798E-06	0.6834794	2.392177779	0.115063617
2.5	5.656854249	0.21675518	0.216044	0.194459025	0.008744176	0.057	8.53164E-07	0.2227367	0.556841857	0.077454642

1.5	2.828427125	0.10837759	0.432087	0.38891805	0.024732266	0.024	3.59227E-07	0.0937839	0.140675838	0.237004246
0.5	1.414213562	0.05418879	0.864175	0.7778361	0.069953411	0	0			
-0.5	0.707106781	0.0270944	1.72835	1.5556722	0.197858126	0	0			
-1.5	0.353553391	0.0135472	3.4567	3.1113444	0.559627291	0	0			
								1		
					qT m^2/s		3.83037E-06			0.429522506
					qG m^2/s		3.83037E-06		3.089695474	0.655379665
					fr gravel		1	DGg	8.513164297	1.57503039

$$q_i^* = 17\left(\tau_{si}^* - \tau_{sci}^*\right)\left(\sqrt{\tau_{si}^*} - \sqrt{\tau_{sci}^*}\right)$$

$$\frac{\tau_{sci}^*}{\tau_{scm}^*} = F_{hc}\left(\frac{D_i}{D_m}\right) = \begin{cases} 0.843\left(\dfrac{D_i}{D_m}\right)^{-1} & for\ \dfrac{D_i}{D_m} \le 0.4 \\ \left[\dfrac{\log(19)}{\log\left(19\dfrac{D_i}{D_m}\right)}\right]^2 & for\ \dfrac{D_i}{D_m} > 0.4 \end{cases}$$

Table C.7: Powell, Reid and Laronne uses surface distribution with gravel removed										
Ds50 here refers to the median size of the surface material with gravel removed										
	Ds50	22.8002164								
	tssc50	0.03	Critical Shields number							
					ustar	0.085646799	m/s			
	Di	Di/Ds50	tssci	Fi	tssi	phii	Wsi	qi m^2/s	pGi	
	181.019336	7.93936922	0.006476	0	0.002503481	0.386602572	0	0	0	0
	90.50966799	3.96968461	0.010815	0.042	0.005006963	0.462948347	0	0	0	0
	45.254834	1.9848423	0.018064	0.232	0.010013925	0.554370787	0	0	0	0
	22.627417	0.99242115	0.030169	0.41	0.020027851	0.663847212	0	0	0	0
	11.3137085	0.49621058	0.050388	0.184	0.040055701	0.7949429	0	0	0	0
	5.656854249	0.24810529	0.084157	0.057	0.080111402	0.951927194	0	0	0	0
	2.828427125	0.12405264	0.140557	0.024	0.160222804	1.139912543	0.000890535	8.296E-10	1	1.5
	1.414213562									
	0.707106781									
	0.353553391									
									1	
							qG m^2/s	8.296E-10		1.5
							fr gravel	1	DGg	2.828427125

$$W_i^* = 11.2\left(1-\frac{1}{\phi}\right)^{4.5}, \quad \phi = \frac{\tau_{si}^*}{\tau_{sci}^*}$$

$$\frac{\tau_{sci}^*}{\tau_{sc50}^*} = F_{hc}\left(\frac{D_i}{D_{50}}\right) = \left(\frac{D_i}{D_{50}}\right)^{-0.74}, \quad \tau_{sc50}^* = \frac{\tau_{bs}}{\rho R g D_{50}} = 0.03$$

$$\phi = \frac{\tau_{s50}^*}{\tau_{sc50}^*}\left(\frac{D_i}{D_g}\right)^{-0.26}$$

Table C.8: Hunziker-Jaeggi uses arithmetic mean size of surface Dsm and arithmetic mean size of substrate Dsubm

						ustar	0.241264071	m/s	
	Dsm	26.0978971	mm			tausm	0.137792899		
	Dsubm	17.5890455	mm			tauscm	0.043895514		
						alpha	-0.08494357		
phii	Di	Di/Dsm	Fi		qstari	qi m^2/s	pGi		
7.5	181.019336	6.9361656	0		0.010079584	0	0	0	0
6.5	90.50966799	3.4680828	0.042		0.026099474	0.000120088	0.052853784	0.3435496	0.203809972
5.5	45.254834	1.7340414	0.232		0.067580423	0.000607271	0.26727537	1.4700145	0.248222269
4.5	22.627417	0.8670207	0.41		0.17498872	0.000982478	0.432413224	1.9458595	0.000569853
3.5	11.3137085	0.43351035	0.184		0.453105364	0.000403646	0.177654859	0.621792	0.190787478
2.5	5.656854249	0.21675518	0.057		1.17324403	0.000114473	0.050382333	0.1259558	0.208911673
1.5	2.828427125	0.10837759	0.024		3.037928179	4.41248E-05	0.019420429	0.0291306	0.179039472
0.5	1.414213562	0.05418879	0		7.866230205	0			
-0.5	0.707106781	0.0270944	0		20.36834776	0			
-1.5	0.353553391	0.0135472	0		52.740586	0			
									1.031340717
					qT m^2/s	0.002272081		4.5363021	1.015549466
					qG m^2/s	0.002272081	DGg	23.204008	2.021672722
					fr gravel	1			

$$q_i^* = 5\left(\frac{D_i}{D_m}\right)^{-3/2}\left[\left(\frac{D_i}{D_m}\right)^{-\alpha}\left(\tau_{sm}^* - \tau_{scm}^*\right)\right]^{1.5}$$

$$\tau_{sm}^* = \frac{\tau_{bs}}{\rho R g D_m}, \quad \tau_{scm}^* = \tau_{scmo}^*\left(\frac{D_{um}}{D_m}\right)^{0.33}, \quad \tau_{scmo}^* = 0.05$$

$$\alpha = 0.011\left(\tau_{sm}^*\right)^{-1.5} - 0.3$$

Table C.9: Wilcock-Crowe uses surface median size Ds50 and fraction sand in surface Frsand										
	Ds50	21.8381765	mm	surface		ustar	0.085646799	m/s		
	Frsand	0.051				tsrs50	0.02736586			
						taustar50	0.020751665			
phii	Di	Di/Ds50	b	fi	Wstari	Fi	qi m^2/s	pGi		
7.5	181.019336	8.28912324	0.689224	0.176516664	6.72998E-09	0	0	0	0	0
6.5	90.50966799	4.14456162	0.644236	0.303418499	3.91234E-07	0.042	6.37773E-13	3.242E-05	0.000210707	0.00033032
5.5	45.254834	2.07228081	0.44111	0.54986405	3.38093E-05	0.232	3.04442E-10	0.015474	0.085107147	0.07436057
4.5	22.627417	1.0361404	0.266389	0.751167007	0.000350869	0.41	5.58354E-09	0.2837972	1.277087233	0.40333667
3.5	11.3137085	0.5180702	0.188031	0.858119379	0.000952202	0.184	6.80029E-09	0.3456416	1.209745744	0.01276126
2.5	5.656854249	0.2590351	0.154745	0.934595428	0.001806336	0.057	3.99626E-09	0.20312	0.507799967	0.13256146

1.5	2.828427125	0.12951755	0.139754	1.009019132	0.003208978	0.024	2.98922E-09	0.1519348	0.227902149	0.4965733
0.5	1.414213562	0.06475878	0.132676	1.090323604	0.005738348	0	0			
-0.5	0.707106781	0.03237939	0.12924	1.181345486	0.010470037	0	0			
-1.5	0.353553391	0.01618969	0.127548	1.283076014	0.019454235	0	0			
						qT m^2/s	1.96744E-08		3.307852947	
						qG m^2/s	1.96744E-08	DGg	9.902912874	sgg
						fr gravel	1			

$$W_i^* = \frac{Rgq_i}{F_i u_{*s}^3} = G(\phi)$$

$$G = \begin{cases} 0.002\phi^{7.5} & for\ \phi < 1.35 \\ 14\left(1 - \dfrac{0.894}{\phi^{0.5}}\right)^{4.5} & for\ \phi \geq 1.35 \end{cases}$$

$$\phi = \frac{\tau_{s50}^*}{\tau_{ssr50}^*}\left(\frac{D_i}{D_{50}}\right)^{-b}$$

$$\tau_{ssr50}^* = 0.021 + 0.013\exp(-14F_s)$$

$$b = \frac{0.69}{1+\exp(1.5 - D_i / D_{50})}$$

Table C.10: Wu et al. (2000a) formula with Turkey Brook Data

	Theta_c	0.03		tau_b	16	tau_b and tau-b' is same				
	m	0.6	-0.6							
	n	0.030		n' and n is same		1.65	Submerged specific gravity of sediment			
	D50 (mm)	16				An	25			
psi	Di (or Dk)	Fraction	Pbk	Pek	Sum (Pbk+Pek)	n'	21.5	tau_ck	phibk	qb*k
	(mm)									
7.5	181.019	0.000	0.119	0.881	1	0.020	8.822	26.466	0	0
6.5	90.510	0.042	0.205	0.795	1	0.020	8.822	19.517	0	0
5.5	45.255	0.232	0.326	0.674	1	0.020	8.822	14.222	0	0
4.5	22.627	0.410	0.471	0.529	1	0.020	8.822	10.241	0	0
3.5	11.314	0.184	0.616	0.384	1	0.020	8.822	7.294	#NUM!	0
2.5	5.657	0.057	0.740	0.260	1	0.020	8.822	5.147	#NUM!	0
1.5	2.828	0.024	0.833	0.167	1	0.020	8.822	3.605	0.000523984	7.6094E-09
0.5	1.414	0.017	0.897	0.103	1	0.020	8.822	2.519	0.004526215	1.6461E-08
-0.5	0.707	0.034	0.939	0.061	1	0.020	8.822	1.772	0.018051017	4.6421E-08

-1.5	0.354	0.000	0.965	0.035	1	0.020	8.822	1.265	0.052885285	0
									qT (m2/s)	7.0491E-08
									qG (m2/s)	7.6094E-09

Table C.11: Wu et al. (2000a) formula applicable for laboratory data set of Haynes and Pender (2007), and Ockelford (2011) and this thesis; fractional contents and other input data need to vary according to author while applying this calculation sheet

	Theta_c	0.03		tau_b	3.540	tau_b and tau-b' is same				
	m	0.6	-0.6							
	n	0.017				An	21			
	D50 (mm)	4.8	Hiding and exposure function							
	Di (or Dk)	Fraction	Pbk	Pek	Sum (Pbk+Pek)	n'	taub_prime	tau_ck	phibk	qb*k
	181.019336	0	0.026	0.974	1	0.020	3.540	10.113	0	0
	90.50966799	0	0.051	0.949	1	0.020	3.540	7.620	0	0
	45.254834	0	0.096	0.904	1	0.020	3.540	5.714	0	0
	22.627417	0	0.170	0.830	1	0.020	3.540	4.252	0	0
	13.38656042	0.04	0.251	0.749	1	0.020	3.540	3.378	0.000343616	8.5633E-08
	9.465727653	0.1	0.316	0.684	1	0.020	3.540	2.892	0.001178023	4.364E-07
	6.693280212	0.31	0.388	0.612	1	0.020	3.540	2.470	0.002913028	1.9891E-06
	4.732863826	0.08	0.464	0.536	1	0.020	3.540	2.106	0.006106444	6.3983E-07
	3.346640106	0.12	0.541	0.459	1	0.020	3.540	1.794	0.011576808	1.0819E-06

	2.366431913	0.15	0.616	0.384	1	0.020	3.540	1.527	0.020492134	1.4234E-06
	1.673320053	0.1	0.687	0.313	1	0.020	3.540	1.302	0.034476134	9.4927E-07
	1.183215957	0.1	0.750	0.250	1	0.020	3.540	1.112	0.055741555	9.1259E-07
									qT (m2/s)	7.5182E-06
	V = 1/n * R^2/3* S^1/2								qG (m2/s)	7.5182E-06

Predicted sediment load from five functions of graded mix against field data of observed bedload

Table C.12: Predicted sediment load from five functions of graded mix against field data of observed bedload

Note: * Weiming Wu formula, but with no effect of An as n and n' considered equal

** Weiming WU formula, but An value obtained through calibration of individual flood events of Turkey Brook

Depth (m)	ustar, m/s	Observed discharge (m3/s)	Observed load (m2/s)	Predicted load (m2/s)						
				Ashida-Michiue	Powell, Reid and Laronne	Hunziker-Jaegg	Wilcock-Crowe	Weiming Wu*	Weiming Wu**	An values
0.62	0.24	5.186	1.20755E-06	3.51E-03	3.60E-03	2.27E-03	1.39E-03	2.03E-03	1.18E-06	30.35
0.63	0.24	5.303	3.81132E-06	3.48E-03	3.58E-03	2.26E-03	1.38E-03	2.01E-03	4.04E-06	28
0.55	0.21	3.953	5.73585E-06	1.68E-03	1.89E-03	1.32E-03	6.83E-04	1.03E-03	6.72E-06	25.5
0.44	0.19	2.437	2.15094E-06	6.96E-04	9.14E-04	7.25E-04	3.19E-04	5.08E-04	2.25E-06	25.5
0.31	0.15	1.173	8.03774E-06	4.26E-05	1.53E-04	1.36E-04	5.69E-05	1.07E-04	9.07E-06	20
0.30	0.14	1.122	8.86792E-06	3.83E-06	6.38E-05	2.40E-05	2.62E-05	5.41E-05	8.61E-06	19
0.27	0.12	0.891	3.24528E-06	0.00E+00	4.12E-06	0.00E+00	2.61E-06	7.91E-06	2.75E-06	17.8
0.26	0.11	0.826	2.03774E-06	0.00E+00	2.99E-06	0.00E+00	2.30E-06	6.39E-06	2.42E-06	17.7
0.24	0.11	0.725	3.13208E-06	0.00E+00	7.91E-07	0.00E+00	8.26E-07	2.63E-06	3.35E-06	16.6
0.23	0.10	0.678	9.81132E-07	0.00E+00	3.08E-07	0.00E+00	4.05E-07	1.51E-06	9.09E-07	17.3
0.22	0.10	0.624	2.64151E-07	0.00E+00	4.25E-07	0.00E+00	4.89E-07	1.80E-06	2.83E-07	18.5
0.21	0.10	0.562	2.26E-07	0.00E+00	2.03E-07	0.00E+00	2.91E-07	1.23E-06	2.51E-07	18.2
0.20	0.10	0.501	1.50943E-07	0.00E+00	1.24E-07	0.00E+00	2.13E-07	9.59E-07	1.72E-07	18.3
0.19	0.10	0.473	1.88679E-07	0.00E+00	7.07E-08	0.00E+00	1.45E-07	7.32E-07	0	18
0.16	0.14	0.376	1.50943E-06	3.28E-06	6.11E-05	2.02E-05	2.52E-05	5.24E-05		
0.18	0.15	0.465	6.75472E-06	5.40E-05	1.72E-04	1.55E-04	6.32E-05	1.18E-04		
0.20	0.16	0.541	0.000004	1.36E-04	2.91E-04	2.68E-04	1.03E-04	1.82E-04		
0.22	0.17	0.614	3.0566E-06	2.02E-04	3.74E-04	3.39E-04	1.31E-04	2.27E-04		
0.25	0.18	0.797	2.90566E-06	4.12E-04	6.14E-04	5.20E-04	2.13E-04	3.51E-04		
0.30	0.18	1.101	3.39623E-06	4.72E-04	6.79E-04	5.66E-04	2.36E-04	3.85E-04		
0.37	0.19	1.669	0.000004	7.59E-04	9.79E-04	7.67E-04	3.42E-04	5.42E-04		

0.40	0.18	1.982	2.83019E-06	4.83E-04	6.90E-04	5.74E-04	2.40E-04	3.91E-04		
0.42	0.16	2.569	2.26415E-06	1.22E-04	2.71E-04	2.51E-04	9.66E-05	1.72E-04		
0.43	0.15	2.607	7.01887E-06	2.02E-05	1.11E-04	8.73E-05	4.27E-05	8.31E-05		
0.44	0.13	1.982	2.49057E-06	0.00E+00	2.03E-05	0.00E+00	1.01E-05	2.34E-05		
0.45	0.13	1.623	3.77358E-06	0.00E+00	1.54E-05	0.00E+00	7.97E-06	1.92E-05		
0.45	0.12	1.326	3.96226E-06	0.00E+00	1.24E-05	0.00E+00	6.65E-06	1.66E-05		
0.46	0.13	1.144	1.73585E-06	0.00E+00	1.76E-05	0.00E+00	8.93E-06	2.12E-05		
0.48	0.13	1.053	1.96226E-06	0.00E+00	2.80E-05	0.00E+00	1.32E-05	2.95E-05		
0.44	0.12	0.973	5.66038E-07	0.00E+00	1.20E-05	0.00E+00	6.46E-06	1.62E-05		
0.40	0.12	0.885	4.5283E-07	0.00E+00	6.69E-06	0.00E+00	3.96E-06	1.09E-05		
0.36	0.11	0.792	1.13208E-07	0.00E+00	2.08E-06	0.00E+00	1.67E-06	5.01E-06		
0.33	0.11	0.771	1.13208E-07	0.00E+00	1.47E-06	0.00E+00	1.23E-06	3.95E-06		
0.30	0.11	0.72	2.26415E-07	0.00E+00	1.01E-06	0.00E+00	8.84E-07	3.08E-06		
0.28	0.11	0.678	3.39623E-07	0.00E+00	7.85E-07	0.00E+00	8.20E-07	2.61E-06		
0.165	0.14	0.397	6.03774E-07	4.92E-06	6.89E-05	3.11E-05	2.80E-05	5.74E-05	6.26E-07	22
0.178	0.15	0.446	1.16981E-06	5.77E-05	1.78E-04	1.62E-04	6.52E-05	1.21E-04	1.27E-06	22.5
0.216	0.17	0.609	4.90566E-07	2.45E-04	4.26E-04	3.80E-04	1.49E-04	2.54E-04	6.23E-07	25
0.25	0.18	0.786	4.9434E-06	3.40E-04	5.34E-04	4.62E-04	1.86E-04	3.10E-04	5.4E-06	22.7
0.287	0.16	1.012	5.0566E-06	9.77E-05	2.38E-04	2.20E-04	8.53E-05	1.54E-04	4.77E-06	21.4
0.329	0.14	1.318	4.67925E-06	2.90E-06	5.91E-05	1.75E-05	2.45E-05	5.11E-05	5.04E-06	19.5
0.418	0.11	2.152	1.39623E-06	0.00E+00	9.22E-07	0.00E+00	9.43E-07	2.90E-06	1.38E-06	17.5
0.549	0.12	3.935	6.15094E-06	0.00E+00	1.05E-05	0.00E+00	5.79E-06	1.48E-05	6.93E-06	17.6
0.616	0.12	5.108	1.92453E-06	0.00E+00	1.30E-05	0.00E+00	6.93E-06	1.71E-05	1.97E-06	19
0.648	0.14	5.751	4.18868E-06	1.54E-06	5.12E-05	7.17E-06	2.17E-05	4.59E-05	4.34E-06	19.5
0.618	0.14	5.147	2.67925E-06	4.66E-07	4.27E-05	0.00E+00	1.85E-05	4.01E-05	3.26E-06	19.6
0.519	0.14	3.452	1.50943E-06	2.13E-06	5.49E-05	1.18E-05	2.30E-05	4.83E-05	1.8E-06	20.5
0.456	0.16	2.594	3.43396E-06	6.01E-05	1.81E-04	1.65E-04	6.64E-05	1.23E-04	3.94E-06	21.2
0.407	0.14	2.034	3.81132E-06	6.13E-06	7.41E-05	3.84E-05	2.98E-05	6.06E-05	4E-06	20
0.38	0.13	1.763	2.56604E-06	0.00E+00	1.93E-05	0.00E+00	9.63E-06	2.26E-05	2.77E-06	19
0.356	0.12	1.543	9.81132E-07	0.00E+00	1.32E-05	0.00E+00	6.99E-06	1.72E-05	9.52E-07	19.8
0.338	0.11	1.39	1.16981E-06	0.00E+00	7.98E-07	0.00E+00	8.32E-07	2.64E-06	1.15E-06	17.6
0.314	0.11	1.212	2.18868E-06	0.00E+00	1.33E-06	0.00E+00	1.13E-06	3.70E-06	2.38E-06	17.2

0.3	0.11	1.103	1.50943E-07	0.00E+00	1.39E-06	0.00E+00	1.17E-06	3.81E-06	1.6E-07	19.8
0.28	0.11	0.908	7.54717E-08	0.00E+00	7.31E-07	0.00E+00	7.71E-07	2.50E-06	7.93E-08	20.1
0.17	0.11	0.423	7.54717E-08	0.00E+00	2.47E-06	0.00E+00	1.94E-06	5.62E-06	7.75E-08	21
0.18	0.12	0.465	2.26415E-07	0.00E+00	4.11E-06	0.00E+00	2.61E-06	7.89E-06	2.36E-07	20.2
0.18	0.12	0.469	3.01887E-06	0.00E+00	7.29E-06	0.00E+00	4.26E-06	1.15E-05	3.44E-06	18
0.18	0.12	0.465	1.69811E-06	0.00E+00	7.96E-06	0.00E+00	4.58E-06	1.22E-05	1.62E-06	18.8
0.18	0.12	0.462	5.28302E-07	0.00E+00	7.47E-06	0.00E+00	4.34E-06	1.17E-05	5.95E-07	19.8
0.18	0.12	0.446	3.77358E-07	0.00E+00	4.02E-06	0.00E+00	2.56E-06	7.79E-06	3.55E-07	19.8
0.17	0.11	0.397	7.92453E-07	0.00E+00	3.33E-06	0.00E+00	2.54E-06	6.87E-06	8.76E-07	18.8
0.16	0.11	0.38	2.45283E-06	0.00E+00	2.00E-06	0.00E+00	1.62E-06	4.88E-06	2.35E-06	17.4
0.16	0.11	0.373	1.43396E-06	0.00E+00	2.78E-06	0.00E+00	2.16E-06	6.08E-06	1.67E-06	18
0.15	0.11	0.359	1.50943E-07	0.00E+00	1.48E-06	0.00E+00	1.24E-06	3.97E-06	1.66E-07	19.8
0.15	0.11	0.346	1.88679E-07	0.00E+00	1.29E-06	0.00E+00	1.10E-06	3.62E-06	2.03E-07	19.5
0.15	0.11	0.33	7.54717E-08	0.00E+00	1.31E-06	0.00E+00	1.11E-06	3.66E-06	7.96E-08	20.5
0.14	0.11	0.32	3.39623E-07	0.00E+00	1.02E-06	0.00E+00	8.91E-07	3.09E-06	3.68E-07	18.8
0.14	0.10	0.314	1.16981E-06	0.00E+00	4.21E-07	0.00E+00	4.85E-07	1.79E-06	1.08E-06	17.3
0.14	0.10	0.317	7.92453E-07	0.00E+00	2.16E-07	0.00E+00	3.06E-07	1.26E-06	7.45E-07	17.3
0.14	0.10	0.324	1.09434E-06	0.00E+00	3.40E-07	0.00E+00	4.38E-07	1.59E-06	1.07E-06	17.2
0.15	0.11	0.33	7.92453E-07	0.00E+00	7.69E-07	0.00E+00	8.05E-07	2.58E-06	7.39E-07	18
0.16	0.11	0.38	7.54717E-08	0.00E+00	1.05E-06	0.00E+00	9.12E-07	3.15E-06	6.74E-08	20.5
0.18	0.11	0.469	1.0566E-06	0.00E+00	9.00E-07	0.00E+00	9.24E-07	2.85E-06	1.01E-06	17.8
0.21	0.11	0.581	2.26415E-06	0.00E+00	9.80E-07	0.00E+00	9.95E-07	3.02E-06	2.28E-06	17
0.22	0.12	0.638	1.13208E-07	0.00E+00	4.67E-06	0.00E+00	2.91E-06	8.59E-06	1.25E-07	21
0.24	0.13	0.704	3.25E-06	0.00E+00	2.71E-05	0.00E+00	1.28E-05	2.88E-05	3.21E-06	19
0.24	0.14	0.715	3.58491E-06	2.51E-07	4.02E-05	0.00E+00	1.76E-05	3.84E-05	3.67E-06	19.2
0.23	0.14	0.694	3.50943E-06	7.18E-06	7.80E-05	4.39E-05	3.12E-05	6.31E-05	4E-06	19.8
0.22	0.14	0.629	2.33962E-06	7.02E-06	7.75E-05	4.31E-05	3.10E-05	6.28E-05	2.42E-06	20.5
0.22	0.14	0.603	3.16981E-06	1.26E-06	4.93E-05	4.96E-06	2.10E-05	4.46E-05	2.98E-06	19.7
0.21	0.13	0.581	2.30189E-06	0.00E+00	1.45E-05	0.00E+00	7.57E-06	1.84E-05	2.24E-06	18.9
0.20	0.12	0.536	2.49057E-06	0.00E+00	4.31E-06	0.00E+00	2.72E-06	8.16E-06	2.37E-06	17.9
0.19	0.11	0.494	1.73585E-06	0.00E+00	2.71E-06	0.00E+00	2.11E-06	5.97E-06	1.8E-06	17.9
0.18	0.12	0.458	1.28302E-06	0.00E+00	3.89E-06	0.00E+00	2.49E-06	7.62E-06	1.3E-06	18.5

0.18	0.12	0.446	9.43396E-07	0.00E+00	4.43E-06	0.00E+00	2.79E-06	8.31E-06	8.83E-07	19
0.17	0.11	0.412	1.77358E-06	0.00E+00	2.19E-06	0.00E+00	1.75E-06	5.18E-06	1.73E-06	17.8
0.16	0.11	0.38	1.32075E-06	0.00E+00	8.25E-07	0.00E+00	8.56E-07	2.70E-06	1.43E-06	17.4
0.15	0.10	0.35	1.0566E-06	0.00E+00	2.89E-07	0.00E+00	3.85E-07	1.47E-06	1.09E-06	17.1
0.15	0.10	0.336	3.77358E-07	0.00E+00	1.61E-07	0.00E+00	2.58E-07	1.09E-06	4.45E-07	17.6
0.14	0.10	0.324	3.77358E-07	0.00E+00	6.39E-08	0.00E+00	1.36E-07	6.99E-07	3.87E-07	17.3
0.14	0.10	0.311	4.90566E-07	0.00E+00	1.25E-07	0.00E+00	2.14E-07	9.62E-07	5.5E-07	17.3
0.14	0.09	0.302	2.64151E-06	0.00E+00	4.36E-08	0.00E+00	1.07E-07	5.85E-07	2.43E-06	15.5
0.13	0.09	0.293	1.50943E-07	0.00E+00	4.48E-08	0.00E+00	1.09E-07	5.92E-07	1.63E-07	17.9
0.13	0.09	0.284	1.50943E-07	0.00E+00	1.10E-08	0.00E+00	5.06E-08	3.27E-07	1.63E-07	17.4
0.13	0.09	0.276	2.26415E-07	0.00E+00	5.85E-09	0.00E+00	3.81E-08	2.62E-07	2.08E-07	17
0.12	0.09	0.268	4.5283E-07	0.00E+00	1.46E-09	0.00E+00	2.31E-08	1.81E-07	5.04E-07	16
0.12	0.08	0.257	6.03774E-07	0.00E+00	4.26E-10	0.00E+00	1.67E-08	1.45E-07	6.59E-07	15.6
	0.15	0.363	1.50943E-07	1.93E-05	1.10E-04	8.51E-05	4.21E-05	8.21E-05		
	0.14	0.38	8.30189E-07	5.59E-06	7.18E-05	3.53E-05	2.90E-05	5.92E-05		
	0.15	0.422	7.54717E-07	3.91E-05	1.47E-04	1.29E-04	5.48E-05	1.04E-04		
	0.15	0.462	1.32075E-06	5.74E-05	1.77E-04	1.61E-04	6.50E-05	1.21E-04		
	0.16	0.515	1.09434E-06	1.11E-04	2.56E-04	2.38E-04	9.16E-05	1.64E-04		
	0.16	0.572	1.50943E-06	1.15E-04	2.62E-04	2.43E-04	9.36E-05	1.67E-04		
	0.16	0.595	3.77358E-06	6.35E-05	1.87E-04	1.71E-04	6.82E-05	1.26E-04		
	0.15	0.619	7.88679E-06	2.03E-05	1.12E-04	8.77E-05	4.28E-05	8.33E-05		
	0.14	0.814	1.76604E-05	3.28E-06	6.11E-05	2.02E-05	2.52E-05	5.24E-05		
	0.14	1.166	1.63774E-05	3.20E-06	6.07E-05	1.97E-05	2.51E-05	5.21E-05		
	0.15	1.491	9.84906E-06	5.33E-05	1.71E-04	1.54E-04	6.28E-05	1.17E-04		
	0.16	1.552	4.90566E-07	1.40E-04	2.97E-04	2.73E-04	1.05E-04	1.85E-04		
	0.17	1.491	7.92453E-07	2.13E-04	3.87E-04	3.49E-04	1.36E-04	2.33E-04		
	0.17	1.448	3.39623E-06	2.18E-04	3.94E-04	3.54E-04	1.38E-04	2.37E-04		
	0.17	1.382	2.60377E-06	2.06E-04	3.79E-04	3.42E-04	1.33E-04	2.29E-04		
	0.17	1.302	2.33962E-06	1.68E-04	3.32E-04	3.04E-04	1.17E-04	2.04E-04		
	0.16	1.217	1.84906E-06	1.23E-04	2.73E-04	2.53E-04	9.73E-05	1.73E-04		
	0.15	1.122	1.43396E-06	4.96E-05	1.65E-04	1.48E-04	6.08E-05	1.14E-04		
	0.15	1.067	1.4717E-06	3.84E-05	1.46E-04	1.28E-04	5.44E-05	1.03E-04		

	0.15	0.973	7.54717E-07	2.78E-05	1.27E-04	1.06E-04	4.79E-05	9.20E-05		
	0.15	0.967	6.41509E-07	4.15E-05	1.51E-04	1.33E-04	5.62E-05	1.06E-04		
	0.15	0.973	1.4717E-06	3.14E-05	1.33E-04	1.13E-04	5.02E-05	9.59E-05		
	0.15	1.006	1.50943E-07	5.43E-05	1.72E-04	1.56E-04	6.34E-05	1.18E-04		
	0.16	1.019	1.50943E-06	1.15E-04	2.62E-04	2.43E-04	9.35E-05	1.67E-04		
	0.17	1.033	1.39623E-06	1.98E-04	3.69E-04	3.34E-04	1.30E-04	2.24E-04		
	0.17	1.188	7.54717E-07	2.78E-04	4.64E-04	4.09E-04	1.62E-04	2.73E-04		
	0.16	1.24	7.16981E-07	1.06E-04	2.49E-04	2.31E-04	8.93E-05	1.60E-04		
	0.15	1.217	2.98113E-06	2.07E-05	1.12E-04	8.88E-05	4.31E-05	8.38E-05		
	0.12	0.257	2.26415E-06	0.00E+00	5.68E-06	0.00E+00	3.45E-06	9.79E-06		
	0.15	0.629	0.000006	3.48E-05	1.39E-04	1.21E-04	5.23E-05	9.95E-05		
	0.17	2.996	5.0566E-06	2.34E-04	4.13E-04	3.70E-04	1.45E-04	2.47E-04		
	0.17	5.772	4.83019E-06	2.02E-04	3.74E-04	3.38E-04	1.31E-04	2.26E-04		
	0.15	6.179	4.33962E-06	1.71E-05	1.05E-04	7.91E-05	4.05E-05	7.92E-05		
	0.17	5.05	2.15094E-06	3.08E-04	4.99E-04	4.35E-04	1.74E-04	2.91E-04		
	0.16	2.669	8.30189E-06	1.23E-04	2.74E-04	2.53E-04	9.75E-05	1.73E-04		
	0.14	1.605	1.7283E-05	6.27E-06	7.47E-05	3.92E-05	3.00E-05	6.10E-05		
	0.12	1.195	7.92453E-06	0.00E+00	4.37E-06	0.00E+00	2.75E-06	8.23E-06		
	0.18	0.98	1.4717E-06	4.24E-04	6.27E-04	5.29E-04	2.18E-04	3.58E-04		
	0.18	0.967	1.64906E-05	4.21E-04	6.23E-04	5.26E-04	2.16E-04	3.56E-04		
	0.17	0.935	1.10943E-05	1.94E-04	3.65E-04	3.31E-04	1.28E-04	2.21E-04		
	0.16	0.879	7.73585E-06	7.40E-05	2.03E-04	1.87E-04	7.36E-05	1.35E-04		
	0.15	0.769	2.30189E-06	1.38E-05	9.69E-05	6.92E-05	3.78E-05	7.46E-05		
	0.14	0.663	0	1.67E-06	5.21E-05	8.21E-06	2.20E-05	4.65E-05		
	0.14	0.563	2.56604E-06	2.48E-07	4.01E-05	0.00E+00	1.76E-05	3.83E-05		
	0.12	0.454	0.000002	0.00E+00	8.42E-06	0.00E+00	4.81E-06	1.27E-05		
	0.12	0.446	7.54717E-07	0.00E+00	4.02E-06	0.00E+00	2.56E-06	7.79E-06		
	0.10	0.408	1.50943E-06	0.00E+00	3.01E-07	0.00E+00	3.97E-07	1.49E-06		
	0.10	0.387	0	0.00E+00	1.87E-07	0.00E+00	2.74E-07	1.18E-06		
	0.09	0.363	4.5283E-07	0.00E+00	1.40E-08	0.00E+00	5.70E-08	3.60E-07		
	0.09	0.353	6.03774E-07	0.00E+00	1.90E-08	0.00E+00	6.68E-08	4.08E-07		
	0.09	0.353	4.15094E-07	0.00E+00	1.90E-08	0.00E+00	6.68E-08	4.08E-07		

	0.09	0.311	1.13208E-07	0.00E+00	3.36E-08	0.00E+00	9.17E-08	5.21E-07		
	0.14	0.49	1.39623E-06	2.54E-06	5.72E-05	1.49E-05	2.38E-05	4.99E-05		
	0.15	0.629	1.16981E-06	2.60E-05	1.23E-04	1.02E-04	4.68E-05	9.01E-05		
	0.16	0.82	2.45283E-06	8.65E-05	2.21E-04	2.05E-04	7.99E-05	1.45E-04		
	0.17	1.039	6.83019E-06	2.03E-04	3.75E-04	3.39E-04	1.32E-04	2.27E-04		
	0.17	1.248	1.65283E-05	1.92E-04	3.62E-04	3.29E-04	1.27E-04	2.20E-04		
	0.16	1.961	1.90943E-05	1.44E-04	3.01E-04	2.77E-04	1.07E-04	1.88E-04		
	0.14	3.19	1.51698E-05	5.53E-06	7.15E-05	3.49E-05	2.89E-05	5.91E-05		
	0.14	5.793	6.60377E-06	2.92E-06	5.92E-05	1.77E-05	2.46E-05	5.12E-05		
	0.16	7.891	6.49057E-06	8.01E-05	2.12E-04	1.96E-04	7.67E-05	1.40E-04		
	0.16	9.771	0	8.05E-05	2.12E-04	1.96E-04	7.69E-05	1.40E-04		
	0.12	13.842	1.50943E-07	0.00E+00	5.03E-06	0.00E+00	3.10E-06	9.03E-06		
	0.16	0.967	3.09434E-06	8.55E-05	2.20E-04	2.04E-04	7.94E-05	1.44E-04		
	0.14	0.731	1.12075E-05	9.28E-06	8.48E-05	5.32E-05	3.36E-05	6.73E-05		
	0.12	0.581	7.20755E-06	0.00E+00	9.32E-06	0.00E+00	5.23E-06	1.36E-05		
	0.10	0.536	0.000002	0.00E+00	3.15E-07	0.00E+00	4.13E-07	1.53E-06		
	0.09	0.494	9.0566E-07	0.00E+00	2.93E-08	0.00E+00	8.48E-08	4.91E-07		
	0.09	0.416	0	0.00E+00	1.83E-08	0.00E+00	6.55E-08	4.02E-07		
	0.09	0.383	0	0.00E+00	3.45E-09	0.00E+00	3.09E-08	2.23E-07		
	0.08	0.383	2.07547E-06	0.00E+00	3.21E-10	0.00E+00	1.57E-08	1.39E-07		
	0.08	0.343	0	0.00E+00	1.84E-12	0.00E+00	8.16E-09	8.77E-08		
	0.11	0.284	6.03774E-07	0.00E+00	1.02E-06	0.00E+00	8.93E-07	3.10E-06		
	0.09	0.262	1.50943E-07	0.00E+00	8.30E-10	0.00E+00	1.97E-08	1.62E-07		

Appendix D:

Experimental data on bedload transport from Unimodal and bimodal bed experiments in different memory time scales

Q (l/s)	Tao (N/m2)	Baseline	UM_SH_10	UM_SH_30	UM_SH_60	UM_SH_120	UM_SH_240
		bedload (m3/s/m)	bedload (m3/s/m)	bedload (m3/s/m)	bedload (m3/s/m)	bedload (m3/s/m)	bedload (m3/s/m)
7.5	2.36	3.44E-08	9.78E-08	5.67E-09	6.18E-08	1.38E-08	4.17E-09
8.75	2.55	1.06E-07	7.31E-08	1.12E-08	8.25E-08	3.78E-08	3.89E-08
10	2.74	2.44E-07	1.73E-07	1.19E-07	2.93E-07	3.85E-08	8.32E-08
11.25	2.93	6.63E-07	4.16E-07	4.79E-07	7.08E-07	3.32E-07	3.68E-07
12.5	3.03	1.71E-06	6.42E-07	1.24E-06	1.77E-06	1.87E-06	8.66E-07
13.75	3.23	3.84E-06	1.98E-06	1.69E-06	3.59E-06	4.44E-06	1.74E-06
15	3.41	5.18E-06	3.77E-06	4.41E-06	6.69E-06	7.05E-06	2.22E-06
16.25	3.58	8.28E-06	6.42E-06	6.13E-06	1.05E-05	9.13E-06	4.25E-06
17.5	3.74	9.88E-06	8.32E-06	9.52E-06	1.72E-05	1.30E-05	6.38E-06
18.75	3.86	1.00E-05	8.31E-06	1.29E-05	4.13E-06	1.13E-05	6.48E-06

Q (l/s)	Tao (N/m2)	Cumulative sediment load (m3/m); at each step, load is integrated over 6 minutes period, and cumulative load is sum of all steps)					
		Baseline	UM_SH_10	UM_SH_30	UM_SH_60	UM_SH_120	UM_SH_240
7.5	2.36	1.2E-05	3.5E-05	2.0E-06	2.2E-05	1.9E-06	1.5E-06
8.75	2.55	5.1E-05	6.2E-05	6.1E-06	5.2E-05	1.4E-05	1.6E-05
10	2.74	1.4E-04	1.2E-04	4.9E-05	1.6E-04	4.9E-05	4.5E-05
11.25	2.93	3.8E-04	2.7E-04	2.2E-04	4.1E-04	1.9E-04	1.8E-04
12.5	3.03	9.9E-04	5.0E-04	6.7E-04	1.1E-03	6.6E-04	4.9E-04
13.75	3.23	2.4E-03	1.2E-03	1.3E-03	2.3E-03	1.6E-03	1.1E-03
15	3.41	4.2E-03	2.6E-03	2.9E-03	4.8E-03	2.8E-03	1.9E-03
16.25	3.58	7.2E-03	4.9E-03	5.1E-03	8.5E-03	5.3E-03	3.4E-03
17.5	3.74	1.1E-02	7.9E-03	8.5E-03	1.5E-02	7.6E-03	5.7E-03
18.75	3.86	1.4E-02	1.1E-02	1.3E-02	1.6E-02	1.1E-02	8.1E-03

Size Class Range (mm)	Size class mean (mm)	Di/D50	Fractional sediment load (m3/m); at each step, load is integrated over 6 minutes period, and cumulative load is sum of all steps)					
			Baseline	UM_SH_10	UM_SH_30	UM_SH_60	UM_SH_120	UM_SH_240
1 - 1.4	1.2	0.25	1.07E-05	7.79E-06	3.96E-06	4.63E-06	2.38E-06	1.71E-06
1.4 - 2	1.7	0.35	8.45E-05	5.89E-05	4.81E-05	4.75E-05	1.48E-05	5.42E-06
2- 2.8	2.4	0.50	5.88E-04	3.72E-04	4.62E-04	4.64E-04	3.13E-04	9.22E-05
2.8 - 4	3.4	0.71	2.51E-03	1.53E-03	2.13E-03	2.37E-03	2.07E-03	1.15E-03
4 - 5.6	4.8	1.00	8.68E-03	6.06E-03	7.38E-03	7.93E-03	6.35E-03	5.61E-03
5.6 - 8	6.8	1.42	2.84E-03	1.91E-03	2.19E-03	2.56E-03	2.10E-03	2.09E-03
8 - 11.2	9.6	2.00	1.34E-03	8.27E-04	8.58E-04	1.13E-03	7.85E-04	1.11E-03
11.2 - 16	13.6	2.83	1.87E-04	1.11E-04	8.81E-05	2.00E-04	4.84E-05	1.87E-04

Q (l/s)	Tao (N/m2)	Baseline	BM_SH_10	BM_SH_30	BM_SH_60	BM_SH_120	BM_SH_240
		bedload (m3/s/m)	bedload (m3/s/m)	bedload (m3/s/m)	bedload (m3/s/m)	bedload (m3/s/m)	bedload (m3/s/m)
8.75	2.55	3.22E-07	2.25E-08	6.45E-08	-	2.11E-08	,-
10	2.74	4.35E-07	3.23E-08	6.37E-08	1.18E-08	4.98E-09	4.36E-08
11.25	2.93	4.72E-07	2.57E-07	1.93E-07	3.47E-08	1.01E-08	9.64E-08
12.5	3.03	1.34E-06	4.82E-07	2.23E-07	9.10E-08	1.55E-08	3.89E-07
13.75	3.23	4.44E-06	9.42E-07	7.91E-07	1.85E-07	3.30E-08	3.41E-07
15	3.41	4.92E-06	3.22E-06	2.97E-06	5.17E-07	6.54E-08	2.08E-06
16.25	3.58	4.66E-06	6.93E-06	4.27E-06	2.87E-06	3.16E-07	4.84E-06
17.5	3.74	4.84E-06	8.02E-06	4.72E-06	5.36E-06	1.41E-06	7.81E-06
18.75	3.86	3.03E-06	7.97E-06	1.13E-06	2.09E-06	6.80E-06	6.31E-06

Q (l/s)	Tao (N/m2)	Cumulative sediment load (m3/m); at each step, load is integrated over 6 minutes period, and cumulative load is sum of all steps)					
		Baseline	BM_SH_10	BM_SH_30	BM_SH_60	BM_SH_120	BM_SH_240
8.75	2.55	1.2E-04	0.0E+00	2.3E-05	0.0E+00	7.6E-06	0.0E+00
10	2.74	2.7E-04	9.8E-06	4.6E-05	4.2E-06	9.4E-06	1.6E-05
11.25	2.93	4.4E-04	1.7E-05	1.2E-04	1.7E-05	1.3E-05	5.0E-05
12.5	3.03	9.3E-04	3.2E-05	2.0E-04	5.0E-05	1.9E-05	1.9E-04
13.75	3.23	2.5E-03	1.4E-03	4.8E-04	1.2E-04	3.0E-05	3.1E-04
15	3.41	4.3E-03	3.3E-03	1.5E-03	3.0E-04	5.4E-05	1.1E-03
16.25	3.58	6.0E-03	5.0E-03	3.1E-03	1.3E-03	1.7E-04	2.8E-03
17.5	3.74	7.7E-03	6.7E-03	4.8E-03	3.3E-03	6.8E-04	5.6E-03
18.75	3.86	8.8E-03	8.3E-03	5.2E-03	4.0E-03	3.1E-03	7.9E-03

Size Class (mm)	Size class mean (mm)	Di/D50	Fractional sediment load (m3/m); at each step, load is integrated over 6 minutes period, and cumulative load is sum of all steps)					
			Baseline	BM_SH_10	BM_SH_30	BM_SH_60	BM_SH_120	BM_SH_240
1 - 1.4	1.2	0.25	2.56E-04	1.56E-04	9.34E-05	6.29E-05	5.67E-06	1.60E-04
1.4 - 2	1.7	0.35	1.28E-03	1.15E-03	6.54E-04	5.74E-04	1.83E-04	1.23E-03
2- 2.8	2.4	0.50	1.98E-03	2.34E-03	8.86E-04	7.64E-04	5.00E-04	1.77E-03
2.8 - 4	3.4	0.71	9.00E-04	1.08E-03	4.40E-04	3.74E-04	3.13E-04	7.68E-04
4 - 5.6	4.8	1.00	9.80E-04	1.28E-03	5.23E-04	4.67E-04	5.03E-04	9.67E-04
5.6 - 8	6.8	1.42	2.75E-03	3.49E-03	1.82E-03	1.47E-03	1.45E-03	2.57E-03
8 - 11.2	9.6	2.00	5.18E-04	4.96E-04	3.19E-04	2.74E-04	1.60E-04	3.55E-04
11.2 - 16	13.6	2.83	9.81E-05	2.87E-05	3.32E-05	2.66E-05	8.17E-06	4.70E-05

List of References

Aberle, J. and Nikora, V. (2006), Statistical properties of armored gravel bed surfaces, Water Resources Research, Vol. 42, DOI: 10.1029/2005WR004674

Ackers, P. and White, W. R. (1973), Sediment transport: New approach and analysis, Journal of Hydraulic Engineering, ASCE, Vol. 99, No. 11, 2041-2060

Almedeij, J. H. and Diplas, P. M. (2003), Bedload Transport in Gravel-Bed Streams with Unimodal Sediment, Journal of Hydraulic Engineering, ASCE, Vol. 129, No. 11, 896–904

Almedeij, J., Diplas, P. and Al-Ruwaih, F. (2006), Approach to separate sand from gravel for bed-load transport calculations in streams with bimodal sediments, Journal of Hydraulic Engineering, ASCE, Vol. 132, No. 11, 1176-1185

Alonso, C. V. (1 980), Selecting a Formula to Estimate Sediment Transport Capacity in Non-vegetated Channels, CREAMS A Field Scale Model for Chemicals, Runoff, and Erosion from Agricultural Management System, edited by W.G. Knisel, U.S.D.A. Conservation Research Report No. 26, Chapter 5, pp. 426-439

ASCE (2007), Manual of Practice 110, Sedimentation Engineering: Processes, Measurements, Modeling and Practice, Prepared by the ASCE Task Committee to Expand and Update Manual 54 of the Sedimentation Committee of the Environmental and Water Resources Institute of ASCE

American Society of Civil Engineers (1982), Task Committee on Relations Between Morphology of Small Stream and Sediment Yield, Relationships Between Morphology of Small Streams and Sediment Yield, Journal of the Hydraulics Division, ASCE, Vol. 108, No. 11, 1328-1365

Andrews, E. D. (1983), Entrainment of gravel from naturally sorted riverbed material, Geol. Soc. Am. Bull., 94, 1225–1231

Andrews, E. D. and Erman, D. C. (1986), Persistence in the size distribution of surficial bed material during an extreme snowmelt flood, Water Resources Research, Vol. 22, No.2, 191–197

Andrews, E. D. and Parker, G. (1987), Formation of a coarse surface layer as the response to gravel mobility, in Sediment Transport in Gravel-Bed Rivers, edited by C. R. Thorne, J. C. Bathurst, and R. D. Hey, pp. 269-300, John Wiley, New York

Ashworth, P. J. and Ferguson, R. I. (1989), Size-selective entrainment of bed load in gravel bed streams, Water Resources Research, Vol. 25, No. 4, 627–634

Ashworth, P. J., Ferguson, R. I., Ashmore, P. E., Paola, C., Powell, D. M. and Prestegaard, K. L. (1992), Measurements in a braided river chute and lobe:

2. Sorting of bedload during entrainment, transport and deposition, Water Resources Research, Vol. 28, No.7, 1887–1896

Ashida, K. and Michiue, M. (1971), An investigation of river bed degradation downstream of a dam, Proceedings, 14th Congress, International Association of Hydraulic Research, Société Hydrotechnique de France, Paris, Fornel, 3, 247–256

Ashida, K. and Michiue, M. (1972), Study on hydraulic resistance and bedload transport rate in alluvial streams, Transactions, Japan Society of Civil Engineering, 206, 59–69 (in Japanese)

Babaeyan-Koopaei, K., Ervine, D. A., Carling, P. A. and Cao, Z. (2002), Velocity and turbulence measurements for two overbank flow events in River Severn, Journal of Hydraulic Engineering, ASCE, Vol. 128, No. 10, 891–900

Bagnold, R. A. (1941), The Physics of Blown Sand and Desert Dunes, William Marrow and Co., New York, pp. 265

Bagnold, R. A. (1956), Flow of cohesionless grains in fluids, Royal Society of London, Philos. Trans., 249, pp. 235-297

Bagnold, R. A. (1980), An empirical correlation of bed load transport rates in flumes and natural rivers, Proc. Royal Society of London, Vol. 372, No. 1751, 453-473

Bathurst, J. C. (1985), Flow resistance estimation in mountain rivers, Journal of Hydraulic Engineering, ASCE, Vol. 111, No. 4, 625–643

Bathurst, J. C. (2013), Critical conditions for particle motion in coarse bed materials of nonuniform size distribution, Geomorphology, Vol. 197, 170–184

Bathurst, J. C., Graf, W. and Cao, H. (1987), Bed load discharge equations for steep mountain rivers, In C. R. Thorne, J. C. Bathurst and R. D. Hey (Eds.), Sediment Transport in Gravel-Bed Rivers, New York, pp. 453–477, John Wiley

Barry, J. J., Buffington, J. M., Goodwin, P., King, J. G. and Emmett, W. W. (2008), Performance of Bed-Load Transport Equations Relative to Geomorphic Significance: Predicting Effective Discharge and Its Transport Rate, Journal of Hydraulic Engineering, ASCE, Vol. 134, No. 5, 601–615

Bauer, B. O., Sherman, D. J. and Wolcott, J. F.(1992), Sources of Uncertainty in Shear Stress and Roughness Length Estimates Derived from Velocity Profiles, The Professional Geographer, Vol. 44, No. 4, 453-464

Beschta, R. L. and Jackson, W. L. (1979), The intrusion of fine sediment into a stable gravel bed, Journal of Fisheries Resource Board, Canada, Vol. 36, No. 2, 204-210

Bisal, F. and Nielsen, K. F. (1962), Movement of soil particles in saltation, Canadian Journal of Soil Science, Vol. 42, No.1, 81–86

Biron, P. M., Lane, S. N., Roy, A. G., Bradbrook, K. F. and Richards, K. (1998), Sensitivity of bed shear stress estimated from vertical velocity profiles: The problem of sampling resolution, Earth Surface Processes and Landforms, Vol. 23, No. 2, 133-139

Biron, P. M., Robson, C., Lapointe, M. F. and Guskin, S. J. (2004), Comparing different methods of bed shear Stress estimates in simple and complex flow fields, Earth Surface Processes and Landforms, Vol. 29, No. 11, 1403-1415

Blinco, P. H. and Partheniades, E. (1971), Turbulence Characteristics in Free Surface Flows over Smooth and Rough Boundaries, Journal of Hydraulic Research, Vol. 9, No. 8, 43-69

BMT-WBM (2014), TUFLOW FV User Manual Flexible Mesh Modelling 2014 (Build 2014)

Bonneville, R. (1963), essais de synthese des lois debut d'entrainment des sediment sous l'action d'um currant en regime uniform, Chatou: Belletin Du CREC, No. 5

Brownlie, W. R. (1981), Prediction of flow depth and sediment discharge in open channels, *Report* No. KH-R-43A, W. M. Keck Laboratory of Hydraulics and Water Resources, California Institute of Technology, Pasadena, California, USA, pp. 232

Brown, A. and Willetts, B. (1997), Sediment flux, grain sorting and the bed condition, in Environmental and Coastal Hydraulics: Protecting the Aquatic Habitat, ASCE, Vol. 2, 1469-1474, New York

Buffington, J. M. (1999), The legend of A. F. Shields., Journal of Hydraulic Engineering, ASCE, Vol. 125, No. 4, 376-387, Discussion by Marcelo H Garcia (2000), Member, ASCE, Journal of Hydraulic Engineering, 718

Buffington, J. M., Dietrich, W. E. an d Kirchner, J. W. (1992), Friction angle measurements on a naturally formed gravel streambed, Implications for critical boundary shear stress, Water Resources Research, Vol. 28, No. 2, 411-425

Buffington, J. M. and Montgomery, D. R. (1997), A systematic analysis of eight decades of incipient motion studies, with special reference to gravel-bedded rivers, Water Resources Research, Vol. 33, No. 8, 1993-2029

Bunte, K., Abt, S. R., Potyondi, J. P. and Ryan, S. E.(2004), Measurement of coarse gravel and coble transport using portable bedload traps, Journal of Hydraulic Engineering, ASCE, Vol. 130, No. 9, 879–893

Bunte, K., Abt, S. R., Swingle, K. W., Cenderelli, D. A. 3 and Johannes M. Schneider, J. M. (2013), Critical Shields values in coarse-bedded steep streams, Water Resources Research, Vol. 49, 7427–744

Camenen, B., Holubová, K. Lukač, M., Coz, J. L. and Paquier, A. (2011), Assessment of Methods Used in 1D Models for Computing Bed-Load Transport in a Large River: The Danube River in Slovakia, Journal of Hydraulic Engineering, ASCE, Vol. 137, No. 10, 1190-1199

Carling, P. A. (1983), Threshold of coarse sediment transport in broad and narrow natural streams, Earth Surface Processes and Landforms, Vol. 8, No. 1, 1–18

Carling, P. A. and Glaister, M. S. (1987), Rapid deposition of sand and gravel mixture downstream of a negative step: the role of matrix infilling and particle over-passing in the process of bar-front accretion, Journal of the Geological Society, Vol. 144, No. 4, 543-551

Carling, P. A., and Reader, N. A. (1982), Structure, composition and bulk properties of upland stream gravels, Earth Surface Processes and Landforms, Vol. 7, No. 4, 349–365

Carson, M . A. and G. A. Griffiths (1987), Bedload transport in gravel channels, Journal of Hydraulic (New Zealand), 26(1), 1-151, 1987

Casey, H. J. (1935a), Uber Geschiebebewegung, Mitteilungen der Preussischen Versuchsanstalt fur Wasserbau und Schiffbau, Heft 19, Berlin (in German)

Casey, H. J. (1935b), Uber Geschiebebewegung, Doktors-Ingenieurs dissertation, Hochschule, Berlin (in German)

Chepil, W. S. (1945), Dynamics of wind erosion: II. Initiation of soil movement, J. Soil Sci., Vol. 60, No. 5, 397–411

Chepil, W. S. (1959), Equilibrium of soil grains at the threshold of movement by wind, Soil Sci. Soc. Proc., Vol. 23, No. 6, 422–428

Chow, V. T. (1959), Open Channel Hydraulics, McGraw-Hill Book Company, NY

Church, M. and Rood, K. (1983), Catalogue of alluvial river data, Report, Department of Geography, University of British Columbia, Vancouver, B. C., Canada

Church, M., Wolcott, J. F., and Fletcher, W. K. (1991), A test of equal mobility in fluvial sediment transport: Behavior of the sand fraction, Water Resources Research, Vol. 27, No. 11, 2941–2951

Church, M., Hassan, M. A. and Wolcott, J. F. (1998), Stabilizing self-organized structures in gravel-bed stream channels: Field and experimental observations, Water Resources Research, Vol. 34, No. 11, 3169-3179

CIRIA (2002), Manual on scour at bridges and other hydraulic structures, May, R. W. P., Ackers, J. C. and Kirby, A. M., London

CIRIA (2013), Land use management effects on flood flows and sediments – guidance on prediction, Edited by Neil McIntyre, Imperial College, London, Colin Thorne, University of Nottingham

Cooper, J. R. and Frostick, L. E. (2009), The difference in the evolution of the bed surface topography of gravel and gravel-sand mixtures, 33rd IAHR Congress: Water Engineering for a Sustainable Environment, International Association of Hydraulic Engineering and Research, Vancouver, Canada

Cooper, J. R. and Tait, S. J. (2008), Water worked gravel beds in laboratory flumes- a natural analogue?, Earth Surface Processes and Landforms, Vol. 34, No. 3, 384-397

Coulthard, T. J. and Macklin, M. G. (2001), How sensitive are river systems to climate and land-use changes? A model based evaluation, Journal of Quaternary Science, Vol. 16, No. 4, 346–351

Coulthard, T. J., Macklin, M. G. and Kirkby, M. J. (2002), A Cellular Model of Holocene Upland River Basin And Alluvial Fan Evolution, Earth Surface Processes and Landforms, Vol. 27, No. 3, 269–288

Coulthard, T. J., Ramirez, J., Fowler, H. J. and Glenis, V. (2012), Using the UKCP09 probabilistic scenarios to model the amplified impact of climate change on drainage basin sediment yield, Hydrology and Earth System Sciences, Vol. 16, 4401-4416

Cranfield University (1999), Waterway bank protection: a guide to erosion assessment and management, Environmental Agency R and D Publication 11, Environmental Agency

Dancey, C. L., Diplas, P., Papanicolaou, A. and Bala, M. (2002), Probability of individual grain movement and threshold condition, Journal of Hydraulic Engineering, ASCE, Vol. 128, No. 12, 1069–1075

Day, T. J. (1980), A study of the transport of graded sediments, Report IT 190, Hydraulics Research Station, Wallingford, Wallingford, UK

Death, R. G. (1996), The effect of patch disturbance on stream invertebrate community structure: the influence of disturbance history, Oceologia, 108, 567–576

Defra (2015), Flood and Coastal Erosion Risk Management in England, Department for Environment, Food and Rural Affairs, UK

Dey, S. and Raikar, R. V. (2007), Characteristics of loose rough boundary streams at near-threshold, Journal of Hydraulic Engineering, ASCE, Vol. 133, No. 3, 288-304

DHI (2014), MIKE11 by DHI: A modelling System for Rivers and Channels, Release 2014, DHI, Denmark

Dietrich, W. E., Kirchner, J. W., Ikeda, H. and Iseya, F. (1989), Sediment supply and the development of the coarse surface layer in gravel-bedded rivers, Nature, 340, 215–217

Diplas, P. (1987), Bedload transport in gravel-bed streams, Journal of Hydraulic Engineering, ASCE, Vol. 113, No. 3, 277-291

Diplas, P., Dancey, C. L., Celik, A. O., Valyrakis, M., Greer, K. and Akar, T. (2008), The Role of Impulse on the Initiation of Particle Movement Under Turbulent Flow Conditions, Science, Volume 322, 717-720

Egashira, S. and Ashida, K. (1990), Mechanism of armoring phenomena, International Journal of Sediment Research, Vol. 5 No. 1, 49–55

Effenberger, M., Sailer, G., Townsend, C. R. and Matthaei, C. D. (2006), Local disturbance history and habitat parameters influence the micro distribution of stream invertebrates, Freshwater Biology, Vol. 51, No. 2, 312–332

Egiazaroff, I. V. (1965), Calculation of non-uniform sediment concentrations, Journal of Hydraulic Engineering, ASCE, Vol. 91, No. 4, 225–248

Einstein, H. A. (1942), Formulas for the transportation of bed load, Trans., ASCE, Vol. 107, 561–573

Einstein, H. A. (1950), The bed-load function for sediment transportation in open channel flows, Technical Bulletin 1026, U.S. Dept. of the Army, Soil Conservation Service, U.S. Department of Agriculture, Washington, D.C.

Ekström, M., Fowler, H. J., Kilsby, C. G. and Jones, P. D. (2005), New estimates of future changes in extreme rainfall across the UK using regional climate model integrations. 2. Future estimates and use in impact studies, Journal of Hydrology, Vol. 300, No. 1-4, 234-251

Emmett, W. W. (1976), Bedload transport in two large gravel bed rivers, Idaho and Washington Proceedings, Third Federal Inter-Agency Sedimentation Conference, Denver, Colorado, March 22–26, U.S. Government Printing Office, Washington, D.C.

Engelund, F. and Hansen, E. (1967), A monograph on sediment transport in alluvial streams, Teknisk Vorlag, Copenhagen

Environment Agency (1999), Waterway Bank Protection: A guide to erosion assessment and management, Environment Agency, Bristol, pp. 235

Espinosa, M. B., Osterkamp, W. R. and Vicente, L. L. (2003), Bedload Transport in Alluvial Channels, Journal of Hydraulic Engineering, ASCE, Vol. 129, No. 10, 783–795

Evans, E. P., Simm, J. D., Thorne, C. R., Arnell, N. W., Ashley, R. M., Hess, T. M., Lane, S. N., Morris, J., Nicholls, R. J., Penning-Rowsell, E. C., Reynard, N. S., Saul, A. J., Tapsell, S. M., Watkinson, A. R. and Wheater, H. S.

(2008), An update of the Foresight Future Flooding 2004 qualitative risk analysis, An Independent Review by Sir Michael Pitt

Fenton, J. D. and Abbott, J. E. (1977), Initial movement of grains on a stream bed: The effect of relative protrusion, Proc. Royal Society of London, Vol. 352, No. 1671, 523–537

Ferguson, R. I., Prestegaard, K. L. and Ashworth, P. J. (1989), Influence of sand on hydraulics and gravel transport in a braided gravel bed river, Water Resources Research, Vol. 25, No. 4, 635-643

Fowler, H. J. and Ekström, M. (2009), Multi-model ensemble estimates of climate change impacts on UK seasonal precipitation extremes, International Journal of Climatology, Vol. 29, No. 3, 385-416

Fredsoe, J. and Deigaard, R. (1994), Mechanics of coastal sediment transport, Marine Geol. 21(3-4), Elsevier Science, Amsterdam, The Netherlands, 336

Frostick, L. E., Lucas, P. M. and Reid, I. (1984), The infiltration of fines into coarse-grained alluvial sediments and its implications for stratigraphical interpretation, Journal of the Geological Society of London, Vol. 141, No. 6, 955-965

Galay, V. J. (1983), Causes of river bed degradation, Water Resources Research, Vol. 19, No. 5, 1057–1090

Garcia, M. (2000), Discussion on “The Legend of Shields” by Garcia, Journal of Hydraulic Engineering, ASCE, Vol. 125, No. 4

Gerbersdorf, S. U., Jancke, T. and Westrich, B. (2005), Physico-chemical and biological sediment properties determining erosion resistance of contaminated riverine sediments—temporal and vertical pattern at the Lauffen reservoir/River Neckar, Germany, Limnologica, Vol. 35, No. 3, 132–144

Gessler, J. (1966), Geschiebetrieb bei mischungen untersucht an naturlichen, abpflasterungserscheinungen in kanalen. Nr. 69, Mitteilungen der Versuchsanstalt f€ur Wasserbau und Erdbau, ETH Zurich, Germany

Gessler, J. (1967), The beginning of bedload movement of mixtures investigated as natural armouring channel, PhD Thesis, Swiss Federal Institute of Technology

Gibbins, C., Vericat, D. and Batalla, R. J. (2007), When is stream invertebrate drift catastrophic? The role of hydraulics and sediment transport in initiating drift during flood events, Freshwater Biology, Vol. 52, No. 12, 2369–2384

Gilbert, G. K. (1914), The transportation of debris by running water, Prof. Paper. 86, pp. 263, U.S. Geol. Survey, Washington D. C.

Gomez, B. (1983), Temporal variations in bedload transport rates: The effect of progressive bed armouring, Earth Surface Processes and Landforms, Vol. 8, No. 1, 41–54

Gomez, B. and Church, M. (1989), An assessment of bed load sediment transport formulae for gravel bed rivers, Water Resources Research, Vol. 25, No. 6, 1161–1186

Graf, W. H. (1998), Fluvial hydraulics, Flow and transport processes in channels of simple geometry, J Wiley and Sons, Chichester, UK

Grass, A. J. (1970), Initial instability of fine bed sand, Journal of Hydraulic Engineering, ASCE, Vol. 96, No. 3, 619–632

Hassan, M. A. and Church, M. (2000), Experiments on surface structure and partial sediment transport on a gravel bed, Water Resources Research, Vol. 36, No. 7, 1885-1895

Haywood, O. G. (1940), Flume experiments on the transportation by water of sand and light-weight materials, PhD thesis, Mass. Inst. of Tech., Cambridge

Haynes, H. and Pender, G. (2007), Stress history effects on graded bed stability, Journal of Hydraulic Engineering, ASCE, Vol. 133, No. 49, 343-349

Haynes, H. and Ockelford, A. (2009), A Comparison of Time-Induced Stability Differences Between a Framework-Supported and a Matrix-Supported Gravel: Sand Mixture, 33rd IAHR Congress: Water Engineering for a Sustainable Environment. International Association of Hydraulic Engineering and Research, Vancouver, Canada

HEC-RAS Version 4.1 (2015), HEC-RAS River Analy. System, US Army Corps of Engineers, Hydrologic Engineering Center, USA

Hirano, M. (1971), On riverbed variation with armouring, Proceedings, Japan Society of Civil Engineering, 195, 55–65 (in Japanese)

Hoey, T. B., Pender, G. and Fuller, C. (1997), Bedload grains-size distributions in degradational armouring experiments, International Association for Hydraulic Research, Madrid, Spain, 1451-1456

Hughes, N., Coats, J. S. and Petts, G. E. (1995), Local variability of gold in active stream sediments, Journal of Geochemical Exploration, Vol. 54, No. 2, 137-148

Peng, Hu, Cao, Z., Pender, G., and Liu, H. (2014), Numerical modelling of riverbed grain size stratigraphic evolution, International Journal of Sediment Research, in press (SCI)

Hunziker, R. and Jaeggi, M. N. R. (2002), Grain sorting processes, Journal of Hydraulic Engineering, ASCE, Vol. 128, No. 12, 1060–1068

Ikeda, S. (1982), Incipient motion of sand particles on side slopes, Journal of Hydraulic Engineering, ASCE, Vol. 108, No. 1, 95–114

Ikeda, H. and Iseya, F. (1988), Experimental study of heterogeneous sediment transport, Environmental Research Centre Paper 12, University of Tsukuba, Japan

ISIS (2015), ISIS Version 3.7, CH2M HILL, England

Jackson, W. L. and Beschta, R. L. (1984), Influences of increased sand delivery on the morphology of sand and gravel channels, Journal of the American Water Resources Association, Vol. 20, No. 4, 527–533

Jenkins, G. J., Perry, M. C. and Prior, M. J. (2008), UKCP2009, Scientific Report, the Climate of the United Kingdom and recent trends, Met Office/Hadley Centre, UK

Kay, A. L., Jones, R. G. and Reynard, N. S. (2006), RCM rainfall for UK flood frequency estimation II, Climate change results, Journal of Hydrology, Vol. 318, No. 1-4, 163-172

Kim, S-C, Friedrichs, C. T., Maa, JP-Y, Wright, L. D. (2000), Estimating bottom stress in tidal boundary layer from Acoustic Doppler velocimeter data, Journal of Hydraulic Engineering, ASCE, Vol. 126, No. 6, 399–406

Kirchner, J. W., Dietrich, W. E., Iseya, F. and Ikeda, H. (1990), The variability of critical shear stress, friction angle, and grain protrusion in water worked sediments, Sedimentology, Vol. 37, No. 4, 647–672

Kleinhans, M. G. (2010), Sorting out river channel, Progress in Physical Geography, Vol. 34, No. 3, 287-326

Kleinhans, M. and van Rijn, L. C. (2002), Stochastic prediction of sediment transport in sand-gravel bed rivers, Journal of Hydraulic Engineering, ASCE, Vol. 128, No. 4, 412-25

Klingeman, P. C. and Emmett, W. W. (1982), Gravel bedload transport processes, in Gravel-bed Rivers, edited by R. D. Hey, J. C. Bathurst, and C. R. Thorne, pp. 141-179, John Wiley and Sons, New York

Komar, P. D. (1987a), Selective gravel entrainment and the empirical evaluation of flow competence, Sedimentology, Vol. 34, No. 6, 1165– 1176

Komar, P. D. (1987b), Selective grain entrainment by a current from a bed of mixed sizes: A reanalysis, Journal of Sedimentary Research, Vol. 57, No. 2, 203–211

Komar, P. D. and Li, Z. (1986), Pivoting analysis of the selective entrainment of sediments by shape and size with application to gravel threshold, Sedimentology, Vol. 33, No. 3, 425–436

Kondolf, G. M. (1988), Salmonid spawning gravels: a geomorphic perspective on their size distribution, modification by spawning fish, and criteria for gravel, PhD thesis, The Johns Hopkins Univ., Baltimore, Maryland

Kondolf, G. M. (1994), Geomorphic and environmental effects of instream gravel mining, Landscape and Urban Planning, Vol. 28, No. 2-3, 225-243

Kondolf, G. M. (1997), Hungry water: Effects of dams and gravel mining on river channels, Environmental Management, Vol. 21, No. 4, 533-551

Kondolf G. M. and Wolman, M. G. (193), The Sizes of Salmonid Spawning Gravels, Water Resources Research, Vol. 29, No. 7, 2275-2285

Kramer, H. (1935), Sand mixtures and sand movement in fluvial models, Transactions of ASCE, Vol. 100, No. 1, 798–838

Krogstad, P. A., Antonia R. A., and Browne, L. W. B. (1992), Comparison between rough and smooth wall turbulent boundary layers, J. Fluid Mech., Vol. 245, 599-617

Kuhnle, R. A. (1992), Fractional transport rates of bedload on Goodwin Creek, Dynamics of gravel-bed rivers, P. Billi, R. D. Hey, C. R. Thorne, and P. Tacconi, eds., Wiley, New York, 141–155

Kuhnle, R. A. (1993a), Fluvial transport of sand and gravel mixtures with bimodal size distributions, Sedimentary Geology, Vol. 85, No. 1-4, 17-24

Kuhnle, R. A. (1993b), Incipient motion of sand-gravel sediment mixtures, Journal of Hydraulic Engineering, ASCE, Vol. 119, No. 12, 1400–1415

Kuhnle, R. A. (1994), Incipient Motion of Sand-Gravel Sediment Mixtures, Journal of Hydraulic Engineering, ASCE, Vol. 119, No. 12, 1400-1415

Lamarre, H. and Roy, A. (2005), Reach scale variability of turbulent flow characteristics in a gravel-bed river, Geomorphology, Vol. 68, No. 1-2, 95–113

Lamb, M. P., Dietrich, W. E. and Venditti, J. G. (2008), Is the critical Shields stress for incipient sediment motion dependent on channel-bed slope, Journal of Geophysical Research, Vol. 113, F02008, doi:10.1029/2007JF000831

Langendoen, E. J. (2001), Evaluation of the effectiveness of selected computer models of depth-averaged free surface flow and sediment transport to predict the effects of hydraulic structures on river morphology, Rep., WES Vicksburg, National Sedimentation Laboratory, Agricultural Research Service, U.S. Department of Agriculture

Li, C.H. and Liu, J. M. (1963), Resistance of alluvial rivers', Nanjing Hydraulic Research Institute, China (in Chinese)

Lisle, T. E. (1995), Particle size variations between bed load and bed material in natural gravel bed channels, Water Resources Research, Vol. 31, No. 4, 1107–1118

Lisle, T.E., Nelson, J. M., Pitlick, J., Madej, M. A. and Barkett, B. L. (2000), Variability of bed mobility in natural gravel-bed channels and adjustments to sediment load at the local and reach scales, Water Resources Research, Vol. 36, No. 12, 3743 – 3755

Luque, F. R., and van Beek, R. (1976), Erosion and transport of bedload sediment, Journal of Hydraulic Research, Vol. 14, No. 2, 127–144

Madsen, O. S. and Grant, W. D. (1976), Sediment Transport in the Coastal Environment, Tech. Rep. 204, R. M. Parson Laboratory, Mass. Inst. of Tech., Cambridge, MA

Mao, L. (2012), The effect of hydrographs on bed load transport and bed sediment spatial arrangement, Journal of Geophysical Research, Vol. 117, F03024, doi:10.1029/2012JF002428, 2012

Mao, L., Cooper, J. R. and Frostick, L. E. (2011), Grain size and topographical differences between static and mobile layers, Earth Surface Processes and Landforms, Vol. 36, No. 10, 1321-1334

Marion, A., Tait, S. J. and McEwan, I. K. (1997), On the competitive effects of particle rearrangement and vertical sorting, Proceedings of the 27th IAHR Congress, International Association for Hydraulic Research, Madrid, Spain, 2, 1493–1498

Marion, A., Tait, S. J. and McEwan, I. K. (2003), Analysis of small-scale gravel bed topography during armouring, Water Resources Research, Vol. 39, No. 12, 1334-1345

Measures, R. and Tait, S. J. (2008), Quantifying the role of bed surface topography in controlling sediment stability in water worked gravel deposits, Water Resource Research, Vol. 44, No. 4, 4413-4430

Meidema, S. A. (2010), Constructing the Shields curve, a new theoretical approach, and its applications, WODCON XIX, Beijing China

Melville, B. W. and Coleman, S. E. (2000), Bridge Scour, Water Resources Publications, LLC, Colorado, U.S.

Meyer-Peter, E., Favre, H. and Einstein, A. (1934), Neuere Versuchsresultate uber den Geschiebetried, Schweiz Bauzeitung, Vol. 103, No. 13

Meyer-Peter, E. and Müller, R. (1948), Formulas for bed-load transport, Proceedings, 2nd Congress International Association for Hydraulic Research, Stockholm, Sweden, International Association of Hydraulic Engineering and Research, Madrid, Spain, 39–64

Milhous, R. T. (1973), Sediment transport in a gravel-bottomed stream, PhD thesis, Oregon State University, Corvallis, Ore.

Miller, R. T. and Byrne R. J. (1966), The angle of repose for a single grain on a fixed rough bed, Sedimentology, Vol. 6, No. 4, 303–314

Miller, M. C., McCave, I. N. and Komar, P. D. (1977), Threshold of sediment motion under unidirectional currents, Sedimentology, Vol. 24, No. 4, 507–527

Misri, R. L., Garde, R. J. and Raju, G. R. (1983), Experiments on bedload transport of non uniform sands and gravels in proceedings of the second international symposium on river sedimentation, 440-450, Water Resource and Electrical Power Press, Beijing, China

Misri, R. L., Garde, R. J. and Ranga Raju, K. G. (1984), Bed load transport of coarse nonuniform sediment, Journal of Hydraulic Engineering, ASCE, Vol. 110, No. 3, 312-328

MIT OpenCourseWare, chapter 9, Mixed Sediments (http://ocw.mit.edu/courses/earth-atmospheric-and-planetary-sciences/12-090-special-topics-an-introduction-to-fluid-motions-sediment-transport-and-current-generated-sedimentary-structures-fall-2006/lecture-notes/)

MIT OpenCourseWare, chapter 14, Mixed Sediments (http://ocw.mit.edu/courses/earth-atmospheric-and-planetary-sciences/12-090-special-topics-an-introduction-to-fluid-motions-sediment-transport-and-current-generated-sedimentary-structures-fall-2006/lecture-notes/)

Monteith, H. (2005), Experimental investigation into the effect of antecedent flow conditions on the stability of graded sediment beds; stress history, Unpublished PhD Thesis, Department of Civil Engineering, Heriot-Watt University

Monteith, H. and Pender, G. (2005), Flume investigation into the influence of shear stress history, Water Resources Research, Vol. 41, doi: 10.1029/2005WR004297

Moores, A. J. and Rees, J. G. (eds.) (2011), UK Flood and Coastal Risk Management Research Strategy, Living with Environmental Change

Mueller, E. R., Pitlick, J. and Nelson J. M. (2005), Variation in the reference Shields stress for bed load transport in gravel-bed streams and rivers, Water Resources Research, Vol. 41, W04006, doi:10.1029/2004WR003692

Mueller, E., Batalla, R., Garcia, C. and Bronstert, A. (2008), Modeling Bed-Load Rates from Fine Grain-Size Patches during Small Floods in a Gravel-Bed River, Journal of Hydraulic Engineering, ASCE, Vol. 134, No. 10, 1430–1439

Murphy, J. M., Sexton, D. M. H., Jenkins, G. J., Booth, B. B. B., Brown, C. C., Clark, R. T., Collins, M., Harris, G. R., Kendon, E. J., Betts, R. A., Brown, S. J., Humphrey, K. A., McCarthy, M. P., McDonald, R. E., Stephens, A., Wallace, C., Warren, R., Wilby, R. and Wood, R. A. (2009), UK Climate Projections Science Report: Climate change projections, Met Office Hadley Centre, Exeter

Nakagawa, H., Tsujimoto, T., and Nakano, S. (1982), Characteristics of sediment motion for respective grain sizes of sand mixture, Bulletin, Disaster Prevention Research Institute, Kyoto University, 32, 1–32

Nezu, I. and Nakagawa, H. (1993), Turbulence in open channel flows, Balkema, Rotterdam, The Netherlands

Nikuradse, J. (1933), Stromungsgesetz in rauhren rohren, vdi-forschungsheft 361. (English translation: Laws of flow in rough pipes), 1950. Technical report, NACA Technical Memo 1292, National Advisory Commission for Aeronautics, Washington, DC

Neill, C. R. (1967), Mean-velocity criterion for scour of coarse uniform bed material, in Proceedings of the 12th Congress of the International Association of Hydraulic Research, Vol. 3, 46–54, IAHR, Delft, Netherlands

Neill, C. R. (1968), A re-examination of the beginning of movement for coarse granular bed materials, Report INT 68, Hydraulics Research Station, Wallingford, UK

Neill, C. R. and Yalin, M. S. (1969), Quantitative definition of beginning of bed movement, Journal of Hydraulic Engineering, ASCE, Vol. 95, No. 1, 585–588

Nikora, V. I., Goring, D. G. and Biggs, B. J. F. (1998), On gravel-bed roughness characterization, Water Resources Research, Vol. 34, No. 3, 517–527

Nitsche et al. (2011), Evaluation of bedload transport predictions using flow resistance equations to account for macro-roughness in steep mountain streams, Water Resources Research, Vol. 47, No. 10

Ockelford, A. (2011), The impact of stress history on non-cohesive sediment bed stability and bed structure, PhD thesis, School of Engineering, University of Glasgow, UK

Ockelford, A. and Haynes, H. (2008), The Effect of Grain Size Distribution Modality on the Relationship Between Stress History and Entrainment Threshold, 4th International Association of Hydraulic Research River Flow Conference, Cesme-Izmir, Turkey

Ockelford, A. and Haynes, H. (2013), The impact of stress history on bed structure, Earth Surface Processes and Landforms, Vol. 38, No. 7, 717-727

Oertel, H., Prandtl, L., Böhle, M., and Mayes, K. (2004), Prandtl's Essentials of Fluid Mechanics, Springer, 2004, pp. 723

Paintal, A. S. (1971), Concept of critical shear stress in loose boundary open channels, Journal of Hydraulic Research, Vo. 9, No. 1, 91–113

Paphitis, D. and Collins, M. B. (2005), Sand grain threshold, in relation to bed stress history: an experimental study, Sedimentology, Vol. 52, No. 4, 827-838

Papanicolaou, A. N., Diplas, P., Dancey, C. and Balakrishnan, M. (2001), Surface roughness effects in near bed turbulence: implications to sediment entrainment, J Eng Mech, Vol. 127, No. 3, 211–218

Papanicolaou, A. N., Diplas, P., Evaggelopoulos, N, and Fotopoulos, S. (2002), Stochastic incipient motion criterion for spheres under various bed packing conditions, Journal of Hydraulic Engineering, ASCE, Vol. 128, 369–380

Parker, G. (1980), Armored versus paved gravel beds, Discussion, Journal of Hydraulic Engineering, ASCE, Vol. 106, No. 11, 1120-1121

Parker, G. (1990a), Surface-based bedload transport relation for gravel rivers, Journal of Hydraulic Research, Vo. 28, No. 4, 417– 436

Parker, G. (1990b), The ACRONYM series of PASCAL programs for computing bedload transport in gravel rivers, External Memorandum M-200, St. Anthony Falls Laboratory, University of Minnesota, Minneapolis, Minn

Parker, G. (1991), Selective sorting and abrasion of river gravel. I: Theory, Journal of Hydraulic Engineering, ASCE, Vol. 117, No. 2, 131–149

Parker, G. (2006), eBook, Gary Parker's Morphodynamic Web Page

Parker, G., Klingeman, P. C. and McLean, D. G. (1982a), Bedload and size distribution in paved gravel-bed stream, Journal of Hydraulic Engineering, ASCE, Vol. 108, No. 4, 544-571

Parker, G., Dhamotharan, S., and Stefan, S. (1982b), Model experiments on mobile, paved gravel bed streams, Water Resources Research, Vol. 18, No. 5, 1395–1408

Parker, G., and Klingeman, P. C. (1982), On why gravel bed streams are paved, Water Resources Research, Vol. 18, No. 5, 1409–1423

Parker, G. and Toro-Escobar, C. M. (2002), Equal mobility of gravel in streams: The remains of the day, Water Resources Research, Vol. 38, No. 11, 1264, doi:10.1029/2001WR000669

Parker, G., Toro-Escobar, C. M., Ramey, M. and Beck, S. (2003), The effect of floodwater extraction on the morphology of mountain streams, Journal of Hydraulic Engineering, ASCE, Vol. 129, No. 11, 885-895

Patel, P.L. and Ranga Raju, K.G. (1996), Fractionwise calculation of bed load transport, Journal of Hydraulic Research, International Association for Hydraulic Research, Vol. 34, No. 3, 363–379

Patel, P. L. and Ranga Raju, K, G. (1999), Critical tractive stress of non-uniform sediments, Journal of Hydraulic Research, Vol. 37, No. 1, 39–58

Pender, G., Li, Q. and Rijn, V. (1995), Comparison of two hiding function formulations for non uniform sediment transport calculations, Proceedings of the Institute of Civil Engineers, Water, Maritime and Energy, Vol. 112, No. 2, 127-135

Pender, G., Hoey, T. B., Fuller, C. and Mcewan, I. K. (2001), Selective bedload transport during the degradation of a well sorted graded sediment bed, Journal of Hydraulic Research, Vol. 39, No. 3, 269-277

Pender, D., Patidar, S. and Haynes, H. (2015), Incorporating River Bed Level Changes into Flood Risk Modelling, E-proceedings of the 36th IAHR World Congress, The Hague, the Netherlands

Piedra, M., Haynes, H., Hoey, T. B. and Ervine, A. (2009), Review of approaches to estimating bed shear stress from velocity profile measurements, 33rd IAHR Congress Water Engineering for a Sustainable Environment, Vancouver, Canada

Piedra, M. M. (2010), Flume investigation of the effects of sub-threshold rising flows on the entrainment of gravel beds, PhD thesis, School of Engineering, Department of Civil Engineering, University of Glasgow, UK

Piedra, M. M., Haynes, H. and Hoey, T. B. (2012), The spatial distribution of coarse surface grains and the stability of gravel river beds, Sedimentology, Vol. 59, No. 3, 1014–1029, doi:10.1111/j.1365-3091.2011.01290

Pokrajac, D., Finnigan, J. J., Manes, C., McEwan, I. and Nikora, V. (2006), On the definition of the shear velocity in rough bed open channel flows, In Ferreira, Alves, Leal and Cardoso (eds.), Proc. Int. Conf. Fluvial Hydraulics River Flow 2006, Taylor and Francis Group, London, 89-98

Pope, N. D., Widdows, J., and Brinsley, V. (2006), Estimation of bed shear stress using the Turbulent Kinetic Energy approach—A comparison of annular flume and field data, Continental Shelf Res., Vol. 26, No. 4, 959-970

Powell, D. M. (1998), Patterns and processes of sediment sorting in gravel-bed rivers, Progress in Physical Geography, Vol. 22, No. 1, 1-32

Powell, D. M., Reid, I. and Laronne, J. B. (2001), Evolution of bedload grain-size distribution with increasing flow strength and the effect of flow duration on the 281rmouri of bedload sediment yield in ephemeral gravel-bed rivers, Water Resources Research, Vol. 37, No. 5, 1463–1474

Powell, D. M., Laronne, J. B. and Reid, I. (2003), The dynamics of bedload sediment transport in low-order, upland, ephemeral gravel-bed rivers, Advances in Environmental Monitoring and Modelling, Vol. 1, No. 2, http://www.kcl.ac.uk/advances

Prandtl, L. (1925), 282rmour über Untersuchungen zur ausgebildeten Turbulenz. Z. Angew. Math, Meth., 5, 136-139

Proffitt, G. T. (1980), Selective transport and 282rmouring of nonuniform alluvial sediments, Research Report 80/22, Department of Civil Engineering, University of Canterbury, New Zealand

Proffitt, G. T. and Sutherland, A. J. (1983), Transport of non-uniform sediments, Journal of Hydraulic Research, Vol. 21, No. 1, 33–43

Qian, H., Cao, Z., Pender, G., Liu, H. and Peng, H. (2015), Well-balanced numerical modelling of non-uniform sediment transport in alluvial rivers, International Journal of Sediment Research (in press)

Rakoczi, L. (1975), Influence of grain-size composition on the incipient motion and self-pavement of bed materials, Proc., 26th IAHR Congress, 2, International Association for Hydraulic Research, Sao Paulo, Brazil, 150-157

Reid, I. and Frostick, L.E. (1984), Particle interaction and its effects on the thresholds of initial and final bedload motion in coarse alluvial channels, Sedimentology of Gravels and Conglomerates. In Koster, E.H and Steel, R.J.S. (Eds). Canadian Society of Petroleum Geologists Memoir, 10, 61-68

Reid, I. and Frostick, L. E. (1985), Role of settling, entrainment and dispersive equivalence and of interstice trapping in placer formation, Journal of Geological Society of London, Vol. 142, No. 5, 739-746

Reid, I. and Frostick, L. E. (1986), Dynamics of bedload transport in Turkey Brook, a coarse-grained alluvial channel, Earth Surface Processes and Landforms, Vol. 11, No. 2, 143-155

Reid, I., Frostick, L.E. and Layman, J. T. (1985), The incidence and nature of bedload transport during flood flows in coarse-grained alluvial channels, Earth Surface Processes and Landforms, Vol. 10, No. 1, 33-44

Reid, I., Laronne, J. B. and Powell, D. M. (1995), The Nahal Yatir bedload database: Sediment dynamics in a gravel-bed ephemeral stream, Earth Surface Processes and Landforms, Vol. 20, No. 9, 845–857

Recking, A. (2009), Theoretical development on the effects of changing flow hydraulics on incipient bed load motion, Water Resources Research, Vol. 45, No. 10 W04401, doi:10.1029/2008WR006826.

Recking, A. (2010), A comparison between flume and field bed load transport data and consequences for surface-based bed load transport prediction, Water Resources Research, Vol. 36, No. 10, 1-16

Rice, S. P., Buffin-Bélanger, T., Lancaster, J. and Reid, I. (2008), Movements of a macroinvertebrate (Potamophylax latipennis) across a gravel bed substrate: effects of local hydraulics and micro-topography under increasing discharge. In Gravel-bed Rivers: From Process Understanding to

River Restoration. Edited by Habersack, H., Hoey, T., Piegay, H. and Rinaldi, M. Elsevier, Amsterdam, The Netherlands. pp. 637–660

Rickenmann, D. (1990), Bedload transport capacity of slurry flows at steep slopes, Mit- teilung 103 der Versuchsanstalt für Wasserbau, Hydrologie Glaziologie, ETH Zürich

Rinaldi, M., Wyzga, B. and Surian, N (2005), Sediment mining in alluvial channels: physical effects and management perspectives, River Research and Application, Vol. 21, No. 7, 805-828

Rollinson, G. K. (2006), Bed structure, pore spaces and turbulent flow over gravel beds, Unpublished PhD Thesis, Department of Civil Engineering, The University of Hull

Rovira, A., Batalla, R. J. and Sala, M (2005), Response of a river sediment budget after historical gravel mining (the lower Tordera, NE Spain), River Research and Applications, Vol. 21, No. 17, 829-847

Rivers and Fisheries Trusts of Scotland (2010), Aquaculture Planning Training Meeting – 30'th Sept 2010, Managing Director - Assn Of Salmon Fishery Boards Rivers and Fisheries Trusts of Scotland

Robert, A. (1990), Boundary roughness in coarse-grained channels. Progress in Physical Geography, Vol. 14, No. 1, 42-70

Rouse, H. (1937), Modern Conceptions of the Mechanics of Fluid Turbulence, Transactions, ASCE, Vol. 102, Paper No. 1965, pp. 463-543

Ryan, S. E. (1998), Sampling bedload transport in coarse-grained transport mountain channel using portable samplers, Proc., Federal Interagency Workshop, Sediment Technology for the 21st Century, St. Petersburg, Fla (http://wwwrvares.er.usgs/osw/sedtech21/ryan.html

Ryan, S. E. and Emmett, W. W. (2002), The Nature of Flow and Sediment Movement in Little Granite Creek Near Bondurant, Wyoming, General Technical Report RMRS-GTR-90, USDA Forest Service, Rocky Mountain Research Station

Rouse, H. (1939), An analysis of sediment transportation in the light of fluid turbulence, U. S. Department of Agriculture, Soil Conservation Service, SCS-TR 25, Washington D.C

Saadi, Y. (2002), The influence of different time varying antecedent flows on the stability of mixed grain size deposits, PhD thesis, Department of Civil and Structural Engineering, University of Sheffield

Saadi, Y. (2008), Fractional critical shear stress at Incipient Motion in a Bimodal Sediment, Civil Engineering Dimension, Vol. 10, No. 2, 89-98

Samaga, B. R., Ranga Raju, K. E., and Garde, R. J. (1986), Suspended load transport of sediment mixtures, Journal of Hydraulic Engineering, ASCE, Vol. 112, No. 11, 1019–1035

SEPA (2008), Bank Protection: Rivers and Lochs, Engineering in the Water Environment Good Practice Guide, Document reference WAT-SG-23, Scottish Environment Protection Agency, pp. 48

SEPA (2010), Engineering in water environment, good practice guide, Environment Agency, Scotland

Sear, D. A. (1992), Sediment transport processes in riffle-pool sequences and the effects of river regulation for hydro-electric power within the North Tyne, PhD thesis, University of Newcastle upon Tyne, Departments of Civil Engineering/Geography

Sear, D. A., Newson, M. D. and Thorne, C. R. (2003), Guidebook of applied fluvial morphology, Defra/Environment Agency Flood and Coastal Defence R&D Programme, R&D Technical Report FD1914, Defra

Shields, A. (1936), Application of similarity principles and turbulence research to bedload movement, (English translation), Hydrodynamics Laboratory, California Institute of Technology, Publication 167, pp. 36

Shvidchenko, A. B. (2000), Incipient motion of streambeds, PhD thesis, University of Glasgow, UK

Shvidchenko, A. B. and Pender, G. (2000), Flume study of the effect of relative depth on the incipient motion of coarse uniform sediments, Water Resources Research, Vol. 36, No. 2, 619-628

Shvidchenko, A. B., Pender, G. and Hoey, T. B. (2001), Critical shear stress for incipient motion of sand/gravel streambeds, Water Resources Research, Vol. 37, No. 8, 2273-2283

Smart, G. M. (1984), Sediment transport formula for steep channels, Journal of Hydraulic Engineering, ASCE, Vol. 110, No. 3, 267-276

Smart, G. M. (1999), Turbulent velocity profiles and boundary shear in gravel bed rivers, Journal of Hydraulic Engineering, ASCE, Vol. 125, No. 2, 106-116

Smart, G. M. and Jaeggi, M. N. R. (1983), Sediment transport on steep slopes, Mitteilungen 64 der Versuchsanstalt für Wasserbau, Hydrologie und Glaziologie, ETH Zurich, Zurich, Switzerland, 19–76

Song, T. and Chiew, Y. M. (2001), Turbulence measurement in non-uniform open channel flow using acoustic Doppler velocimeter (ADV), Journal of Engineering Mechanics, Vol. 127, No. 3, 219-232

Soulsby, R. and Whitehouse, R. (1997), Threshold of sediment motion in coastal environment, Proceedings Pacific Coasts and Ports, pp. 149-154, Christchurch, New Zealand, University of Canterbury

Strickler, A. (1923), Beiträge zur Frage der Geschwindigkeitsformel und der Rauhigkeitszahlen für Ströme, Kanäle und geschlossene Leitungen. Mitteilungen des Amtes für Wasserwirtschaft 16

Sutherland, A. (1991), Hiding functions to predict self armouring, Proceedings, International Grain Sorting Seminar, ETH Zürich, 117, 273-298

Tait, S. J., Willetts, B. B. and Maizels, J. K. (1992), Laboratory observations of bed armouring and changes in bedload composition, In Dynamics of Gravel-bed Rivers. Billi, P., Hey, R. D., Thorne, C. R. and Tacconi, P, (Eds). Wiley, Chichester, 205-225

Taylor, B. D. (1971), Temperature effect in low-transport, flat-bed flows, PhD thesis, Report No. KH-R-27, W. M. Keck Laboratory of Hydraulics and Water Resources, Division of Engineering and Applied Science, California Institute Of Technology, Pasadena, California

Taylor, B. D. and Vanoni, V. A. (1972), Temperature effect in low-transport, flat-bed flows, Journal of Hydraulic Engineering, ASCE, Vol. 98, No. 8, 1427-1445

Thompson, C. E. L., Amos, C. L., Jones, T. E. R. and Chaplin, J. (2003), The manifestation of fluid-transmitted bed shear stress in a smooth annular flume – A comparison of methods, Journal of Coastal Research, Vol. 19, No. 4, 1094-1103

Tsujimoto, T. (1999), Sediment transport processes and channel incision: mixed size sediment transport, degradation and armouring, Incised River Channels, Darby, S. E. and A. Simon, eds., John Wiley and Sons

Tsujimoto, T. and Motohashi, K. (1990), Static armoring and dynamic pavement, Journal of Hydroscience and Hydraulic Engineering, Vol. 8, No. 1, 55–67

USWES (1935), Study of river bed material and their use with special reference to the Lower Mississippi River, Paper 17, U.S. Waterways Experiment Station, Vicsburg, Miss.

Vanoni, V. A. (1964), Measurements of critical shear stress for entraining fine sediments in a boundary layer, KH-R-7, pp. 47, W. M. Keck Lab., Hydraul. Water Resour. Div. Eng. Appl. Sci., California Institute of Technology, Pasadena

Van Rijn, L. C. (1984), Sediment transport. I: Bedload transport, Journal of Hydraulic Engineering, ASCE, Vol. 110, No. 10, 1613–1641

Vignaga, E, Haynes, H, and Sloan, W. T. (2011), Quantifying The Tensile Strength of Microbial Mats Grown Over Non Cohesive Sediments, Biotechnology and Bioengineering, doi: 10.1002/bit.24401

Wathen, S. J., Ferguson, R. I., Hoey, T. B. and Werrity, A. (1995), Unequal mobility of gravel and sand in weakly bimodal river sediments, Water Resources Research, Vol. 31, No. 8, 2087–2096

WEWS (2003), Water Environment and Water Services (Scotland) Act 2003

White, C. M. (1940), The equilibrium of grains on the bed of a stream, Proc. Royal Society of London, A. 174, 322–338

White, W. R., and Day, T. J. (1982), Transport of graded gravel bed material, Gravel-bed rivers, R. D. Hey, C. R., Thorne, and J. Bathurst, eds., Wiley, New York, 181–223

White, W. R., Milli, H. and Crabe, A. D. (1975), Sediment Transport Theories: A Review, Proceedings of the Institute of Civil Engineers, London, Part 2, No. 59, pp. 265-292

Wiberg, P. L. and Smith, J. D. (1987), Calculations of the critical shear stress for motion of uniform and heterogeneous sediments, Water Resources Research, Vol. 23, No.8, 1471–1480

Wiberg, P. L. and Smith, J. D. (1989), Model for calculating bedload transport of sediment, Journal of Hydraulic Engineering, ASCE, Vol. 115, No. 1, 101-123

Wilcock, P. R. (1988), Methods for estimating the critical shear stress of individual fractions in mixed-size sediment, Water Resources Research, Vol. 24, No. 7, 1127–1135

Wilcock, P. R. (1992a), Experimental investigation of the effect of mixture properties on transport dynamics, in Dynamics of Gravel-bed Rivers, edited by P. Billi, R. D. Hey, C. R. Thorne, and P. Tacconi, pp. 109–139, John Wiley, New York

Wilcock, P. R. (1992b), Flow competence: A criticism of a classic concept, Earth Surface Processes and Landforms, Vol. 17, No. 3, 289–298

Wilcock, P. R. (1993), Critical shear stress of natural sediments, Journal of Hydraulic Engineering, ASCE, Vol. 119, No. 4, 491-505

Wilcock, P. R. (1996), Estimating local bed shear stress from velocity observations, Water Resources Research, Vol. 32, No. 11, 3361-3366

Wilcock, P. R. (1997a), The components of fractional transport rate, Water Resources Research, Vol. 33, No. 1, 247–258.

Wilcock, P. R. (1997b), Entrainment, displacement and transport of tracer gravels, Earth Surface Processes and Landforms, Vol. 22, No. 12, 1125–1138

Wilcock, P. R. (1998), Two-fraction model of initial sediment motion in gravel-bed rivers, Science, Vol. 280, No. 5362, 410-412

Wilcock, P. R. (2001), Toward a practical method for estimating sediment-transport rates in gravel-bed rivers, Earth Surface Processes and Landforms, Vol. 26, No. 13, 1395-1408

Wilcock, P. R., Kenworthy, S. T. and Crowe, J. C. (2001), Experimental study of the transport of mixed sand and gravel, Water Resources Research, Vol. 37, No. 12, 3349–3358

Wilcock, P. R. and Crowe, J. C. (2003), Surface-based transport model for mixed-size sediment, Journal of Hydraulic Engineering, ASCE, Vol. 129, No. 2, 120–128

Wilcock, P. R, and McArdell, B. W. (1993), Surface based fractional rates: Mobilization thresholds and partial transport of a sand-gravel sediment, Water Resources Research, Vol. 25, No. 7, 1629– 1641

Wilcock, P. R. and McArdell, B. W. (1997), Partial transport of a sand/gravel sediment, Water Resources Research, Vol. 33, No. 1, 235–245

Wilcock, P. R. and Southard, J. B. (1988), Experimental study of incipient motion in mixed-size sediment, Water Resources Research, Vol. 24, 1127-1135

Wilcock, P.R. and Southard, J. B. (1989), Bedload transport of mixed size sediment: fractional transport rates, bed forms, and the development of a coarse bed surface layer, Water Resources Research, Vol. 25, 1629 –1641

Williams, E., and Simpson, J. H. (2004), Uncertainties in estimates of Reynolds stress and TKE production rate using the ADCP variance method, J. Atmospheric and Oceanic Technology, Vol. 21, No. 2, 347-357

Willetts, B. B., Maizels, J. K. and Florence, J. (1988), The simulation of stream bed armouring and its consequences, Proceedings of the Institute of Civil Engineering, Vol. 84, No. 3,, 615-617

Wu B., Molinas, A. and Julien, P. Y. (2004), Bed-material load computations for non-uniform sediments, Journal of Hydraulic Engineering, ASCE, Vol. 130, No.10, 1002-1012

Wu, F. C. and Chou, Y. J. (2003), Rolling and lifting probabilities for sediment entrainment, Journal of Hydraulic Engineering, ASCE, Vol. 129, 110–119

Wu, W. (2007), Computational River Dynamics, Taylor and Francis, Taylor and Francis Group, London / Leiden / New York / Philadelphia / Singapore

Wu, W. and Wang, S. S. Y. (1999), Movable bed roughness in alluvial rivers, Journal of Hydraulic Engineering, ASCE, Vol. 125, No. 12, 1309–1312

Wu, W., Wang , S. S.Y. and Yafei, J. (2000a), Non-uniform sediment transport in alluvial rivers, Journal of Hydraulic Research, Vol. 38, No. 6

Wu, W., Wang, S. S. Y. and Yafei, J. (2000b), Nonuniform sediment transport in alluvial rivers, Journal of Hydraulic Research, IAHR, Vol. 38, No. 6, 427–434

Yalin, M. S. (1963), An expression for bedload transportation, Journal of the Hydraulic Division, ASCE, Vol. 89, No. 3, 221-250

Yalin, M. S. (1972), Mechanics of Sediment Transport, Pergamon, New York

Yalin, M. S. (1977), Mechanics of Sediment Transport, Pergamon, Tarrytown, N. Y.

Yang, C. T. (1973), Incipient Motion and Sediment Transport, Journal of the Hydraulic Division, ASCE, Vol. 99, No. 10, 1679-1704

Yang, C. T. (1976), Minimum Unit Stream Power and Fluvial Hydraulics, Journal of the Hydraulics Division, ASCE, Vol. 102, No. 7, 919-934

Yang, C. T. (1984), Unit Stream Power Equation for Gravel, Journal of Hydraulic Engineering, ASCE, Vol. 110, No. 12, 1783-17 97

Yang, C.T. and Huang, C. (2001), Applicability of Sediment Transport Formulas, International Journal of Sediment Research, Vol. 16, No. 3, 335-343, Beijing, China

Yang, S. and Wang, X. (2006), Incipient motion of coarse particles in high gradient rivers, International Journal of Sediment Research, Vol. 21, No. 3, 220–229

Young, W. J and Warburton, J. (1996), Principles and practice of hydraulic modelling of braided gravel-bed rivers, Journal of Hydrology (NZ), Vol. 35, No. 2, 175-198

Zanke, U. C. E. (2003), On the influence of turbulence on the initiation of sediment motion, International Journal of Sediment Research, Vol. 18, No. 1, 17-31

Zhang, R.J. and Xie, J. H. (1993), Sedimentation Research in China, Systematic Selections, Water and Power Press, Beijing, China